

Development of An Economically Viable H₂O₂-based, Liquid-Phase Ethylene Oxide Technology: Reactor Engineering and Catalyst Development Studies

by

Madhav Ghanta

Bachelor of Technology in Chemical Engineering,
Osmania University, Hyderabad, India, 2006
Masters of Science in Chemical and Petroleum Engineering
University of Kansas, Lawrence, KS, 2008

Submitted to the graduate program in Chemical and Petroleum Engineering and the Graduate Faculty of the University of Kansas in partial fulfillment of the requirements for the degree of
Doctor of Philosophy

Committee Members:

Prof. Bala Subramaniam (Chair)

Prof. Daryle H. Busch

Prof. R. V. Chaudhari

Dr. Darryl Fahey

Prof. Susan M. Williams

Date Defended: 05/03/2012

The Dissertation Committee for Madhav Ghanta certifies
that this is the approved version of the following dissertation

**Development of An Economically Viable H₂O₂-based, Liquid-Phase Ethylene
Oxide Technology: Reactor Engineering and Catalyst Development Studies**

Committee Members:

Prof. Bala Subramaniam (Chair)

Prof. Daryle H. Busch

Prof. R. V. Chaudhari

Dr. Darryl Fahey

Prof. Susan M. Williams

Date Approved: 05/07/2012

Abstract

Ethylene Oxide (C_2H_4O , abbreviated as EO), a high volume chemical intermediate is used as a raw material for a variety of consumer products, such as plastic bottles, anti-freeze, sports gear, detergents and paints. In 2009, approximately 19 million metric tons of EO were produced and its demand is projected to grow at an average rate of 3-4% per year over the next decade. Currently, EO is manufactured by the silver catalyzed ethylene epoxidation process which is highly energy intensive and wasteful because much of the ethylene (feedstock) and EO (product) burns to form carbon dioxide, a greenhouse gas. Worldwide, commercial production of EO releases 3.4 million metric tonnes of CO_2 each year making it the second largest emitter of CO_2 among all chemical processes. Furthermore, loss of ethylene feedstock to burning represents a loss of \$1.1 billion per year worldwide.

In this dissertation, an alternative liquid phase ethylene epoxidation technology (henceforth referred to as CEBC EO process) has been demonstrated with both homogeneous Re-based and heterogeneous Ce- and W-based catalysts. In this process, the ethylene gas is compressed under pressure (50 bars) and dissolved in a liquid reaction medium containing the oxidant 50 wt% H_2O_2/H_2O , promoter pyridine N-oxide and catalyst (methyl trioxorhenium or W-KIT-6 or W-KIT-5). The ensuing catalytic reaction produces EO with near complete selectivity with no CO_2 detected in either the liquid or gas phases. Methanol is employed as a co-solvent to enhance the ethylene solubility in the liquid phase. At the operating conditions ($P = 50$ bars, $T = 20-40$ °C), the volumetric expansion studies reveal that the liquid reaction phase (methanol+ H_2O_2/H_2O) is expanded by up to 12% by compressed ethylene. The corresponding ethylene solubility is 22 mole %, converting ethylene from being the limiting reactant in the liquid phase at ambient pressure to an excess reactant at the higher pressures. Fundamental engineering studies

(volumetric expansion, mass transfer and conversion studies) essential for achieving pressure-intensification established the optimum agitation speed for Re-catalyzed ethylene epoxidation to be 1200 rpm. Operating at conditions that enhanced the ethylene solubility and eliminated interphase mass transfer limitations maximized the EO productivity (1.61-4.97 g EO/h/g metal) on MTO catalyst, rendering it comparable to the conventional silver-catalyzed process. Further, intrinsic kinetic parameters, estimated from fixed time semi-batch reactor studies, disclosed the moderate activation energy (57 ± 2 kJ/mol).

Based on a plant-scale simulation of the CEBC EO process using Aspen HYSYS[®], preliminary economic and environmental assessments of the process are performed, both of which are benchmarked against the conventional silver-catalyzed ethylene epoxidation process. The capital costs for both processes lie within prediction uncertainty. The EO production cost for the conventional process is estimated to be 71.6 ¢/lb EO. The CEBC process has the potential to be competitive with the conventional process if the MTO catalyst remains active, selective and stable for at least six months at a leaching rate of approximately 0.11 lb MTO/h (or 5 ppm Re in the reactor effluent). Comparative cradle-to-gate life cycle assessments (LCA) reveal that the overall environmental impacts on air quality, water quality and greenhouse gas emissions are similar for both processes given the uncertainties involved in such predictions. The LCA results implicate sources outside the EO production plants as the major contributors to potential environmental impacts: fossil fuel-based energy required for natural gas processing (used for producing ethylene, hydrogen and methanol) in both processes and to the significant requirements of coal-based electrical power for compressing large volumes of recycled ethylene and other gases in the conventional process.

These results of the economic analysis prompted the evaluation of alternative catalysts that are inexpensive and exhibit the best performance metrics (high activity, near complete selectivity towards desired product and high stability). These evaluation studies identified tungsten and cerium based catalysts as possible alternatives. W-based catalysts formed EO with near complete selectivity and recycle studies established catalyst durability. Further, the EO productivity with these catalysts (0.3-3.2 g EO/h/g W) is of the same order of magnitude as the Re-based and Ag-based catalysts.

Acknowledgement

I would like to thank my advisor, Professor Subramaniam, who provided me with the opportunity, training, feedback, constant support and encouragement that allowed me to complete this work. I thank him for introducing me to the realm of *gas-expanded liquids* and its application to ethylene epoxidation and also for providing me the opportunity to apply fundamental engineering knowledge (thermodynamic, mass transfer and modeling) and the concept of sustainability to process development (new CEBC-EO process). Furthermore, his inputs have been instrumental in the improvement of my soft skills. One such example is tremendous improvement in my presentation skill.

I would like to thank Professor Busch for his valuable comments and help in understanding the chemistry in my research work. I would like to thank Professor R.V. Chaudhari for providing useful inputs on modeling, process development, aiding in the design of key experiments and providing me career advice. I would like to thank Dr. Fahey for his valuable guidance on process simulation, economic and environmental analysis, tips on improving my writing and presentation skill and providing me with career advice. Also, I would like to thank Professor Susan Williams for the willingness to serve on my committee.

I would like to thank Dr. Claudia Bode for her friendship and valuable guidance on improving my presentation (oral and poster) and writing skill. I would like to thank Dr. Anand for synthesis and characterization of catalysts and providing me guidance on the interpretation of data. I would like to thank Dr. Kirk, Dr. Feng, Ed Atchison and Alan Walker for their help with equipment problem solving.

I would like to thank Dr. Debdut Roy, Dr. Swarup Maiti, Dr. Bibhas Sarkar and Dr. Christopher Lyon for their friendship and insightful discussions. I would like to thank current

and alumni of the Subramaniam group especially Dr. Chad, Dr. Bhuma, Dr. Venu, Dr. Sagar, Shirley and Meng for their friendship and insightful discussions. I would like to thank Mark, Brandon, Karthik and Sommer for their friendship.

I would like thank my parents, brother and sister in law for their unconditional love, enduring support and financial aid for my higher level education.

I would like to acknowledge CEBC for providing the financial support under the National Science Foundation Engineering Research Center Grant and National Science Foundation Accelerating Innovation Research Grant for providing the necessary funding to carry out my research.

Table of Contents

Title Page		
Acceptance Page	ii	
Abstract	iii	
Acknowledgement	vi	
Table of Contents	viii	
List of Figures	xiii	
List of Tables	xvii	
Chapter 1	Ethylene Oxide Technology: Current Status, Technological Barriers and a Greener Process Concept	
1.	Introduction	1
1.1	Conventional Silver-Catalyzed Ethylene Oxidation Process	2
1.1.1	Safety Considerations	5
1.2	Desired Attributes for an alternate EO technology	7
1.3	Liquid Phase Epoxidation of Light Olefins	7
1.3.1	CEBC-PO Process	7
1.3.2	CEBC-EO Process	9
1.3.3	Solvent Engineering	10
1.3.4	Reaction Engineering Aspects	12
1.4	Catalysts for Selective Ethylene Epoxidation	13
1.4.1	Rhenium-based Catalysts	13
1.4.1.1	Immobilization of Rhenium-based Catalysts	14
1.4.2	Tungsten-based Catalysts	14
1.5	Continuous CEBC-EO Process Concept	17
1.6	Life Cycle Assessment	17
1.7	Dissertation Goals and Objectives	18
References		21
Chapter 2	Highly Selective Homogeneous Ethylene Epoxidation in Gas (Ethylene)-Expanded Liquid: Transport and Kinetic Studies	

2.1	Introduction	27
2.2	Experimental	31
	2.2.1 Materials	31
	2.2.2 Apparatus and Procedure	31
2.3	Results and Discussion	35
	2.3.1 Volumetric Expansion Studies	35
	2.3.2 Mass Transfer Studies Involving Gas-Expanded Phases	39
	2.3.3 Kinetic Analysis	45
	2.3.4 Comparison with Conventional Process	50
2.4	Conclusion	52
	Notation	53
	References	55
Chapter 3	Is Ethylene Oxide from Ethylene and Hydrogen Peroxide More Economical and Greener compared to Conventional Silver-Catalyzed Process?	
3.1	Introduction	60
3.2	Methodology	62
	3.2.1 Simulation Package, Specifications and Assumptions	62
3.3	Process Description	63
	3.3.1 Conventional Vapor Phase Process	63
	3.3.2 CEBC-EO Process	68
	3.3.3 Direct Hydrogen Peroxide Process	72
	3.3.4 Anthraquinone Process	72
3.4	Capital Costs	73
3.5	Production Costs	74
3.6	Environmental Impact Analysis	74

3.6.1	Basis	76
3.6.2	Raw Material Sources	77
	3.6.2.1 Production of Ethylene Oxide and Hydrogen Peroxide	77
	3.6.2.2 Production of Ethylene	82
	3.6.2.3 Production of Hydrogen	86
3.7	Results and Discussion	89
3.7.1	Economic Assessment	89
	3.7.1.1 Total Capital Investment	89
	3.7.1.2 Production Costs	91
	3.7.1.3 Comparison of the CEBC-EO (Case 1) and Conventional Silver-Catalyzed Ethylene Epoxidation Process	97
	3.7.1.4 Comparison of the Case 1 and Case 2 of the CEBC-EO Process	99
3.7.2	Environmental Impact Analysis	103
	3.7.2.1 Conventional and CEBC-EO Process	103
	3.7.2.2 Anthraquinone and Direct H ₂ O ₂ Process	110
	3.7.2.3 Ethylene Production	112
	3.7.2.4 Hydrogen Production	120
	3.7.2.5 Energy Production	123
3.8	Conclusions	132
	References	136

Chapter 4	Tungsten Incorporated Mesoporous Silicates as Epoxidation Catalyst	
4.1	Introduction	148
4.2	Experimental	149
4.2.1	Materials	149
4.2.2	Catalyst Testing	150
4.3	Results and Discussion	150
4.3.1	Catalyst Characteristics	150
4.3.2	Ethylene Epoxidation	152
4.4	Conclusions	164
References		165
Chapter 5	Comparative Economic and Environmental Assessment of Propylene Oxide Production by the PO/TBA, HPPO and CEBC-PO Processes	
5.1	Introduction	168
5.2	Methodology	169
5.2.1	Simulation Package	169
5.3	Process Description	170
5.3.1	PO/TBA Process	170
5.3.2	Hydrogen Peroxide/Propylene Oxide (HPPO) Process	175
5.3.3	CEBC-PO Process	179
5.4	Capital Costs	182
5.5	Production Costs	182
5.6	Environmental Assessment	183
5.6.1	Basis	183
5.6.2	Raw Material Sourcing	184
5.7	Results and Discussion	187
5.7.1	Economic Assessment	187

5.7.1.1	Part I: Comparison of LyondellBasell PO/TBA process and CEBC-PO Process	187
A.	Total Capital Investment	188
B.	Production Costs	190
5.7.1.2	Part II: Comparison of the HPPO and CEBC-PO Process	194
A.	Total Capital Investment	194
B.	Production Costs	195
5.7.2	Environmental Impact Assessment	198
5.8	Conclusions	205
References		207
Chapter 6	Conclusions and Recommendations	
6.1	Conclusions	214
6.2	Recommendations	218
References		221
Appendix A-	Volumetric Expansion of Liquid Phase by Propylene	223
Appendix B-	Analytical Procedure	227
Appendix C-	Economic Analysis	230
Appendix D-	Estimation of Allocation Factors for Environmental Assessment	232
Appendix E-	Estimation of Transport Limitations	235

List of Figures

Figure No.	Description	Page No
1-1	Global ethylene oxide production	1
1-2	Ethylene oxide uses and their applications	2
1-3	Ethylene oxide manufacturers and their capacities	2
1-4	Schematic of the silver-catalyzed ethylene epoxidation	3
1-5	Enhanced ethylene oxide yield due to improved catalyst design	4
1-6	Flammability envelope of ethylene+O ₂ mixture at 1 bar in presence of CO ₂	5
1-7	Flammability envelope of EO+O ₂ mixture at 1 bar in presence of N ₂	6
1-8	Schematic of the proposed CEBC-PO process	8
1-9	Vapor-liquid equilibrium of EO + methanol at 10 °C and 25 °C	11
1-10	Vapor-liquid equilibrium of EO + methanol at 10 °C and 25 °C	12
1-11	Schematic of the proposed continuous CEBC-EO process	17
2-1	Schematic of CEBC expanded-phase EO process	28
2-2	Schematic of the Jurgeson cell	32
2-3	Schematic of stirred semi-batch mixer unit to measure the ethylene transport rates into the liquid phase	33
2-4	Schematic of the experimental setup for ethylene epoxidation in gas-expanded liquid phase	34
2-5A	Volumetric expansion ratios of ethylene + methanol binary system upon pressurization by ethylene. The size of the plotted data point represents the experimental uncertainty	36
2-5B	Volumetric expansion of ethylene + methanol + 50 wt% H ₂ O ₂ /H ₂ O system upon pressurization by ethylene. Initial composition of liquid phase: 0.748 mol methanol + 0.134 mol H ₂ O ₂ + 0.253 mol H ₂ O. Initial volume = 15 mL. The size of the plotted data point represents the experimental uncertainty	37
2-5C	Volumetric expansion of ethylene + t-butyl alcohol + 50 wt% H ₂ O ₂ /H ₂ O system upon pressurization by ethylene. Initial composition: 0.21 mol t-	38

	butyl alcohol + 0.08 mol H ₂ O ₂ + 0.11 mol H ₂ O. Initial volume = 15 mL.	
	The size of the plotted data point represents the experimental uncertainty	
2-6	Effect of stirring speed on the uptake of compressed ethylene by the liquid phase. P = 50 bar; T = 25 °C; Initial composition of the liquid phase: 0.748 mol methanol + 0.134 mol H ₂ O ₂ + 0.253 mol H ₂ O	40
2-7	Regressed ethylene uptake profiles at various stirring speeds using first-order model. Slopes provide the mass transfer coefficients	43
2-8	Variation of volumetric mass transfer coefficient with stirring speed. P = 50 bars; T = 25 °C; Initial composition of the liquid phase: 0.748 mol methanol + 0.134 mol H ₂ O ₂ + 0.253 mol H ₂ O	43
2-9	EO yield in the presence and absence of mass transfer limitations Ethylene P = 50 bars; T = 40 °C; MTO amount = 0.361 mmol; methanol = 0.748 mol; H ₂ O ₂ = 0.116 mol; H ₂ O = 0.220 mol; acetonitrile = 0.0191 mol; pyridine N-oxide = 2.19 mmol; batch time = 5 h; agitation speed	45
2-10	EO yield in the absence of mass transfer limitations. Ethylene P = 50 bars; T = 40 °C; agitation speed = 1200 rpm; MTO amount = 0.361 mmol; methanol = 0.748 mol; H ₂ O ₂ = 0.116 mol; H ₂ O = 0.220 mol; acetonitrile = 0.0191 mol; pyridine N-oxide = 2.19 mmol; batch time = 5 h	47
2-11	Regression of temporal EO yields based on a pseudo first order kinetic model. P = 50 bars; T = 40 °C; agitation speed = 1200 rpm; MTO amount = 0.361 mmol; methanol = 0.748 mol; H ₂ O ₂ = 0.116 mol; H ₂ O = 0.220 mol; acetonitrile = 0.0191 mol; pyridine N-oxide = 2.19 mmol; batch time = 5 h	48
2-12	Arrhenius plot for EO formation via the CEBC EO process. P = 50 bars; T = 40 °C; agitation speed = 1200 rpm; MTO amount = 0.361 mmol; methanol = 0.748 mol; H ₂ O ₂ = 0.116 mol; H ₂ O = 0.220 mol; acetonitrile = 0.0191 mol; pyridine N-oxide = 2.19 mmol; batch time = 5 h	49
3-1	Process flow diagram for the conventional vapor phase EO process. Table 3-2 lists the simulation parameters employed in this simulation	64

	and the compositions of the recycle (R_{1-5}) and purge streams	
3-2	Process flow diagram: (A) Hydrogen Peroxide production; (B) CEBC-EO process. Table 3-3 lists the simulation parameters and mass flow-rates of the various components entering and leaving the H_2O_2 and EO reactor	68
3-3	Boundaries of the conventional vapor phase EO process considered in the cradle-to-gate LCA	78
3-4	Boundaries of the CEBC-EO process considered in the cradle-to-gate LCA	79
3-5	Boundaries of the direct H_2O_2 process considered in the cradle-to-gate LCA	80
3-6	Boundaries of the Anthraquinone Process considered in the cradle-to-gate LCA	80
3-7	System boundaries for the production of ethylene from crude oil	83
3-8	System boundaries for the production of ethylene from natural gas	85
3-9	System boundaries for the production of ethylene from corn	86
3-10	System boundaries for the production of hydrogen from methane	87
3-11	Comparison of the total capital investment for the simulated conventional and CEBC-EO processes	90
3-12	Comparison of the total production cost for the conventional vapor phase and CEBC-EO processes. (*) The catalyst life and leaching rate are assumed to be 1 year and 2.2 lbs MTO/year; (#) 50% of the unreacted H_2O_2 is destroyed in the PFD, thus there is a significant incentive to push H_2O_2 conversion to a much higher level; (^) "Other" includes costs for, research, plant overhead, materials and supplies for operation and maintenance, and labor.	93
3-13	Effect of catalyst durability and leaching rate on the net profitability of the CEBC process	96
3-14	Comparison of the total capital investment for the simulated conventional process and two cases of the CEBC process	98

3-15	Comparison of the total production cost for the simulated conventional process and the two cases of the CEBC process	98
3-16	Effects of catalyst durability and leaching rate on the net profitability of the CEBC process	101
3-17	Comparison of the profitability for the case 1 and case 2 of the CEBC process	102
4-1	Representative Transmission Electron Microscopy of W-KIT-6	151
4-2	Sample gas chromatogram of the ethylene epoxidation products for W-catalyzed reaction	152
5-1	Process flow diagram for the PO/TBA process	171
5-2	Process flow diagram for the HPPO process	175
5-3	Process flow diagram for the CEBC-PO process	179
5-4	Boundaries of the cradle-to-gate LCA of the PO/TBA process	184
5-5	Boundaries of the cradle-to-gate LCA of the HPPO process	185
5-6	Boundaries of the cradle-to-gate LCA of the CEBC-PO process	186
5-7	Comparison of the total capital investment for PO/TBA, HPPO and CEBC-PO processes	188
5-8	Comparison of the total production costs for the PO/TBA, HPPO and CEBC-PO processes	190
5-9	The effect of catalyst durability and leaching rate on the net profitability of the CEBC-PO process	197

List of Tables

Table No.	Description	Page No.
2-1	Volumetric mass transfer coefficients for ethylene + methanol binary and ethylene + 0.748 mol methanol + 0.134 mol H ₂ O ₂ + 0.253 mol H ₂ O and ethylene + 0.21 mol t-butyl alcohol + 0.08 mo H ₂ O ₂ + 0.11 mol H ₂ O quaternary mixtures	44
2-2	Effect of catalyst loading on H ₂ O ₂ consumption and product yields. P= 50 bars; T= 40 °C; agitation speed = 1200 rpm; methanol = 0.748 mol; H ₂ O ₂ = 0.116 mol; H ₂ O = 0.22 mol; acetonitrile = 0.0191 mol; pyridine N-oxide = 2.19 mmol; batch time = 5 h	46
2-3	Rate constants for the liquid phase CEBC-EO process (P= 50 bars)	50
2-4	Comparison of key parameters and performance metrics in the conventional and CEBC-EO processes	50
3-1	Assumptions common to simulations of the conventional and CEBC-EO processes	63
3-2	Simulation parameters for the conventional vapor phase process. Mass flow rates of various components entering and leaving the reactor and in the purge and recycle streams (R ₁₋₅) (in lbs/h) for the conventional vapor phase EO process obtained from HYSYS [®] simulation	65
3-3	Simulation parameters for direct H ₂ O ₂ and CEBC-EO processes. Mass flow rates of various components entering and leaving the hydrogen peroxide and ethylene epoxidation reactor (in lbs/h) for the CEBC-EO process obtained from HYSYS [®] simulation	70
3-4	Impact categories considered in cradle-to-gate LCA	76
3-5	Costs of various raw material and products	92
3-6	Comparison of the environmental emissions obtained from toxic release inventory data for BASF's Geismar, LA ethylene oxide facility and that predicted by the GaBi [®] software	104
3-7	Environmental impact (cradle-to-gate) of manufacturing 200,000 tonnes of ethylene oxide by the conventional process and CEBC process	106

3-8	Major adverse environmental impacts in the conventional process and their percentage contributions	107
3-9	Major adverse environmental impacts in the CEBC process and their percentage contributions	107
3-10	Environmental impact (cradle-to-gate) analysis for producing 220,000 tonnes of H ₂ O ₂ using Anthraquinone process and direct H ₂ O ₂ process	111
3-11	Qualitative comparison of the environmental impacts associated with production of ethylene and that obtained from the toxic release inventory data submitted by Total Petrochemical Inc. (unknown capacity) for their Port Arthur, TX facility and for the ethylene cracker operated by ExxonMobil (unknown capacity) at their Baytown facility to USEPA	114
3-12	Environmental impact (cradle-to-gate) of manufacturing 400,000 metric tonnes/yr of ethylene from corn, crude oil and natural gas	115
3-13	Environmental impact (cradle-to-gate) of manufacturing 100,000 metric tonnes/yr of hydrogen from light gases (methane, ethane), naphtha and Chlor-Alkali plant	120
3-14	Gate-to-gate analysis for the mining of coal to produce 1000 MJ of energy. Cradle-to-Grave environmental impact assessment for the producing 1000 MJ of energy from coal. Comparison of the emissions for the production of energy to that reported by the Lawrence Energy Center to USEPA	125
3-15	Gate-to-gate environmental impact assessment for extracting natural gas to produce 1000 MJ of energy and cradle-to-grave environmental impact of producing 1000 MJ from natural gas. Comparison of the predicted emissions for the production of energy to that reported by Astoria Generating Station to USEPA	128
3-16	Gate-to-gate environmental impact assessment for the production of fuel oil to produce 1000 MJ of energy and the cradle-to-grave environmental impact assessment for the production of 1000 MJ of energy from heavy fuel oil and light fuel oil	129

3-17	Cradle-to-grave environmental impact assessment of producing energy from hard coal (anthracite), lignite coal, heavy fuel oil, light fuel oil and natural gas	131
4-1	Catalyst loading, %H ₂ O ₂ conversion and EO Yield for W-KIT-6 catalyst (sodium tungstate) at various metal loadings. The initial reaction mixture contained 0.748 mol methanol + 0.134 mol H ₂ O ₂ + 0.253 mol H ₂ O. Agitation speed = 1600 rpm, T = 35 °C, P = 50 bars, reaction time = 6 h.	154
4-2	Catalyst loading, %H ₂ O ₂ conversion and EO Yield for W-KIT-6 catalyst (tungstic acid) at various metal loadings. The initial reaction mixture contained 0.748 mol methanol + 0.134 mol H ₂ O ₂ + 0.253 mol H ₂ O. Agitation speed = 1600 rpm, T = 35 °C, P = 50 bars, reaction time = 6 h.	156
4-3	Catalyst loading, %H ₂ O ₂ conversion and EO Yield for W-KIT-5 catalyst (sodium tungstate) at various metal loadings. The initial reaction mixture contained 0.748 mol methanol + 0.134 mol H ₂ O ₂ + 0.253 mol H ₂ O. Agitation speed = 1600 rpm, T = 35 °C, P = 50 bars, reaction time = 6 h.	158
4-4	Catalyst loading, %H ₂ O ₂ conversion and EO Yield for W-KIT-5 catalyst (tungstic acid) at various metal loadings. The initial reaction mixture contained 0.748 mol methanol + 0.134 mol H ₂ O ₂ + 0.253 mol H ₂ O. Agitation speed = 1600 rpm, T = 35 °C, P = 50 bars, reaction time = 6 h.	160
4-5	Catalyst loading and EO Yield for W-incorporated support. The initial reaction mixture contained 0.748 mol methanol + 0.134 mol H ₂ O ₂ + 0.253 mol H ₂ O. Agitation speed = 1600 rpm, T = 35 °C, P = 50 bars, reaction time = 6 h.	161
4-6	Catalyst loading, %H ₂ O ₂ conversion and EO yield and productivity for unsupported catalysts. The initial reaction mixture contained 0.748 mol methanol + 0.134 mol H ₂ O ₂ + 0.253 mol H ₂ O. Agitation speed = 1600 rpm, T = 35 °C, P = 50 bars, reaction time = 6 h.	162
5-1	Assumptions made common to the simulations of the PO/TBA HPPO and CEBC-EO Processes	170
5-2	Simulation parameters for the PO/TBA process obtained from literature.	174

	Input/Output stream flow rates (lb/h) from the TBHP and PO reactor obtained from HYSYS [®] simulation	
5-3	Simulation parameters for the Hydrogen Peroxide/Propylene Oxide (HPPO) process. Input/Output stream flow rates (lb/h) for the H ₂ O ₂ and PO reactor obtained from HYSYS [®] simulation	178
5-4	Simulation parameters for the CEBC-PO process. Input/Output stream flow rates (lb/h) for the H ₂ O ₂ and PO reactor obtained from the HYSYS [®] simulation	181
5-5	Costs of various raw material and products used in the analysis	191
5-6	The cost of various utilizes in the LyondellBasell PO/TBA, HPPO and CEBC-PO processes	192
5-7	Comparison of the environmental impact (gate-to-gate) estimated from the toxic release inventory data submitted by the PO/TBA for their Bayport, Texas facility and that predicted by the GaBi [®] software	199
5-8	Comparative cradle-to-gate environmental impact assessment for producing propylene oxide by the PO/TBA, HPPO and CEBC-PO processes	201
5-9	Major adverse environmental impacts in the production of propylene oxide by the PO/TBA process	202
5-10	Major adverse environmental impacts in the production of propylene oxide by the HPPO and CEBC-PO processes	202

Chapter 1

Ethylene Oxide Technology: Current Status, Technological Barriers and a Greener Process Concept

1. Introduction

The chemical industry needs cleaner, energy efficient manufacturing processes. Towards this goal, this dissertation research targets the process for manufacturing one of the world's largest bulk chemical intermediates ethylene oxide (EO), which is currently made by a wasteful and energy intensive technology. The current annual demand for EO is greater than 19 million tonnes (Figure 1-1¹) and is predicted to grow at approximately 2-3% over the next decade, primarily because of increasing standards of living in highly populated areas like China, India and South America.¹

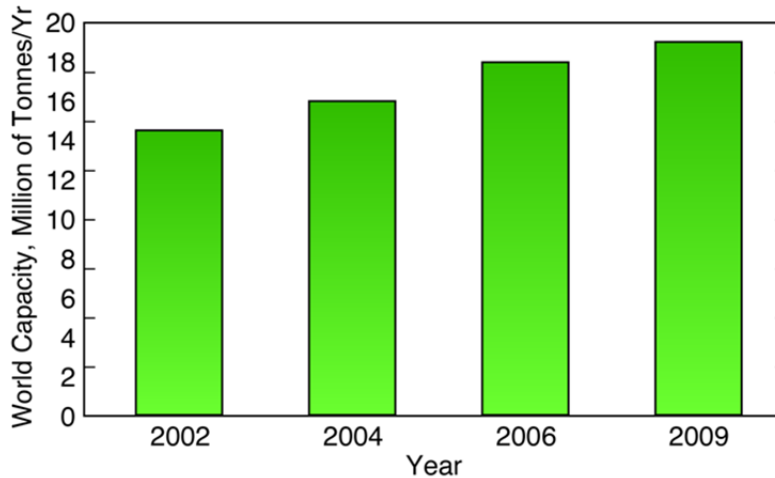


Figure 1-1: Global ethylene oxide production has grown at a rate of 3-4% since 2002.

Examples of everyday products made with EO as raw material are shown in Figure 1-2. A majority of EO is processed to ethylene glycol (EG) for antifreeze and poly(ethylene terephthalate) (PET), which is used in beverage bottles, clothes, sports gear, *etc.*¹ Surface active agents used in detergents and soaps are also derived from EO.

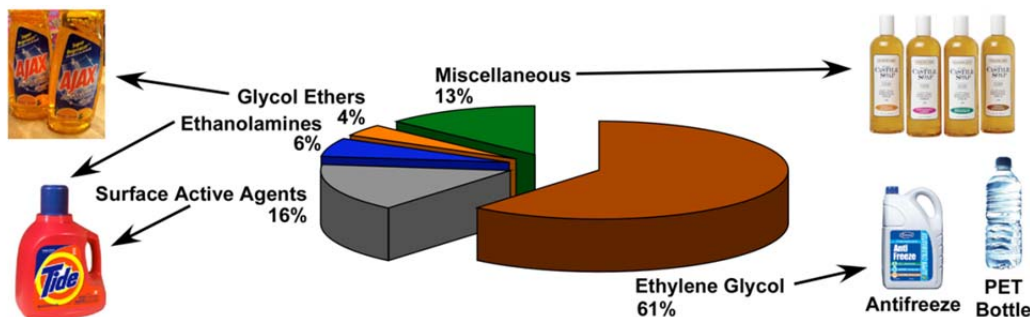


Figure 1-2: Ethylene oxide uses and their applications

1.1 Conventional Silver-Catalyzed Ethylene Oxidation Process

The conventional ethylene epoxidation technology was originally developed in 1931 by T. E. Lefort and first commercialized by Union Carbide Chemicals.² The major producers of EO today are shown in Figure 1-3.³

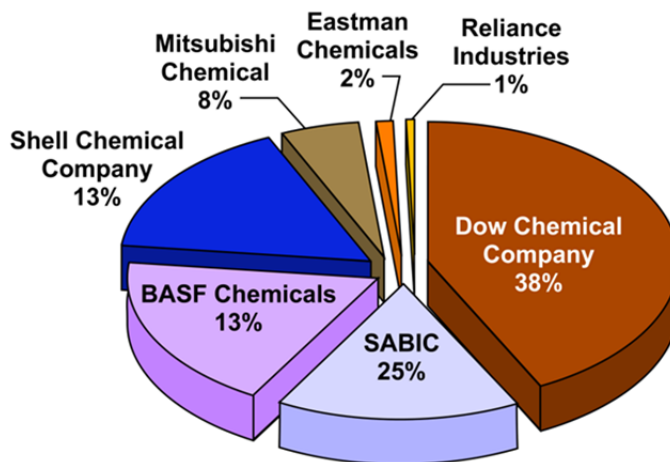


Figure 1-3: Ethylene oxide manufacturers and their capacities

For the past 70 years, various manufacturers have significantly improved the process for making EO. Currently, silver-catalyzed ethylene epoxidation is the predominant process for making EO. The major licensors of EO process technology are Scientific Design-Shell Chemical Company and Dow Chemical Company. Shell licenses two versions of their EO/EG technology based on their proprietary catalyst: (a) the Shell MASTER process uses the high-selectivity EO catalyst; and (b) the Shell OMEGA process, which is based on high selectivity EO catalyst and produces monoethylene glycol (EG).⁴

Dow Chemical Company licenses the former Union Carbide EO process known as the Meteor EO/EG process.⁵ This technology is based on a simple single reactor design and the proprietary Dow EO catalyst, which is highly active and selective.⁶

The description of the conventional silver-catalyzed EO process technology provided here is obtained from patents and published literature.⁷⁻¹⁰ Typically, ethylene is oxidized by either air or oxygen at 200-260 °C in the presence of an alumina-supported silver catalyst.^{2, 7} In addition to EO, a significant quantity of CO₂ is formed as byproduct, primarily attributed to the burning of ethylene and EO (Figure 1-4).

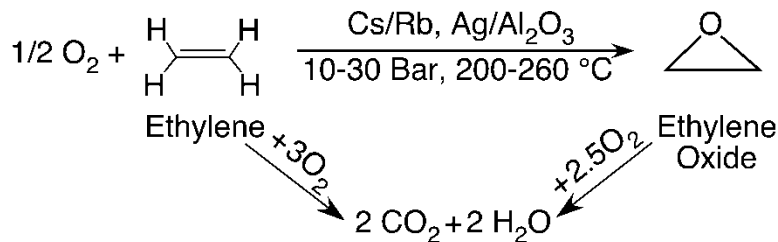


Figure 1-4: Schematic of the silver-catalyzed ethylene epoxidation showing the CO₂ byproduct.²

Catalyst selectivity toward EO has been improved over the years by impregnating promoters such as cerium, rubidium, tin, antimony, barium and lithium onto the surface of the support.¹¹⁻¹³ These catalyst modifications have resulted in marked enhancement in EO selectivity from 45% in 1945 to 90% (selectivity of fresh catalyst) in 1995, as shown in Figure 1-5.^{2, 7, 12} Despite these improvements, significant gains are still needed to eliminate the CO₂ byproduct formation and improve process efficiency.

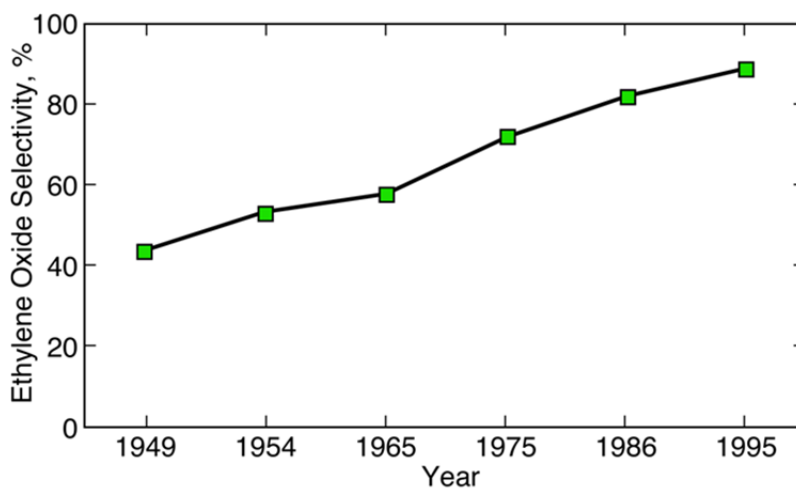


Figure 1-5: Enhanced ethylene oxide yield due to improved catalyst design

To minimize the unwanted burning of ethylene and EO to CO₂ in the conventional silver-catalyzed EO process, the ethylene conversion per pass is maintained at 4-8% by employing a high ethylene gas hourly space velocity.^{7, 14, 15} However, despite catalyst and process improvements, the burning of ethylene and EO to carbon dioxide still accounts for 10-15% yield loss. This means that globally, approximately 3.4 million tonnes of CO₂ are emitted each year (roughly equivalent to emissions from nearly a million cars each year), making this process the second largest emitter of CO₂ byproduct among all chemical processes.

In addition to greenhouse gas emissions, the 15% yield loss due to burning translate into a feedstock loss of US \$1.1 billion/year globally (assuming an ethylene cost of 32 ¢/lb). The loss of potential value addition of this ethylene to EO amounts to approximately US \$200 million/yr. In comparison, the worldwide profit associated with the production of 19 million tonnes of EO/yr is US \$2 billion. Thus, there is a tremendous economic incentive to minimize the EO yield loss due to the burning of ethylene (feedstock) and EO (product).

1.1.1 Safety Considerations

Ethylene and EO can form highly flammable mixtures in a vapor phase that also contains O₂, the oxidant in the conventional process.^{2, 7} The ethylene flammability envelope extends from 3 mol% (lower flammability limit, LFL) to 37 mol% (upper flammability limit, UFL) ethylene in O₂ (Figure 1-6).¹⁶

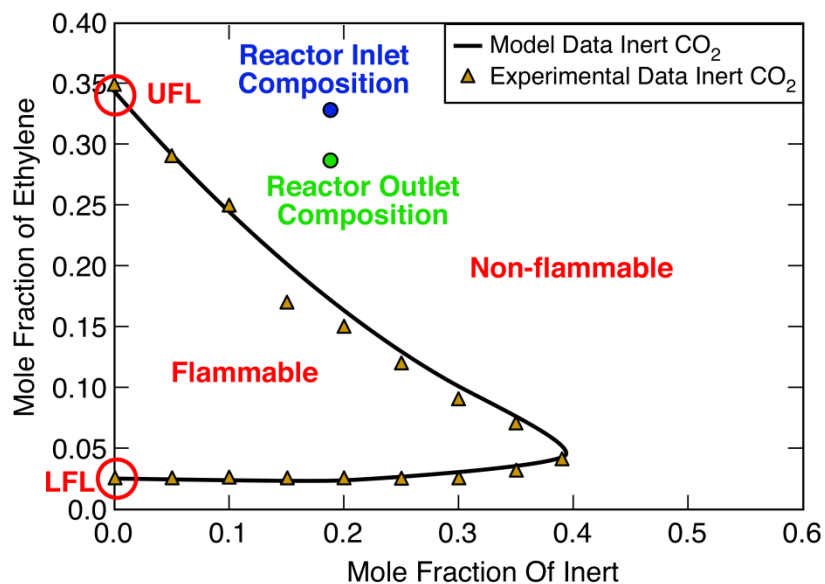


Figure 1-6: Flammability envelope of ethylene+O₂ mixture at 1 bar in presence of CO₂.¹⁶

In contrast, as shown in Figure 1-7, EO has a much wider flammability envelope extending from 3 mol% (LFL) to pure EO (UFL).^{10, 16-18} In fact, pure EO by itself can undergo spontaneous decomposition in the vapor phase *via* a free radical mechanism.¹⁷ These flammability concerns necessitate elaborate safety precautions in reactor design/operation and storage equipment to prevent explosions. To either shrink or eliminate the flammability envelope, CH₄ (due to its high heat capacity) and inerts such as Ar, CO₂ and N₂ are used to dilute the vapor phase and to absorb the heat of reaction, thereby preventing thermal runaway reactions.

Note from Figures 1-6 and 1-7 that beyond approximately 45 mol% inerts for ethylene+O₂ and 60 mol% inerts for EO+O₂ mixtures, the vapor phase mixture lies outside the flammability envelope.¹⁶ CO₂ has higher heat capacity than N₂ and hence generally causes a greater reduction in the flammability envelope for a fixed inert concentration. In practice, the ethylene concentration in the vapor phase of the reactor is maintained outside the flammability envelope by diluting the vapor phase with N₂, Ar, CO₂ and CH₄. The EO concentration in the reactor outlet stream is held to 3.5 mol% by limiting ethylene conversion to 4-8% per pass.^{17, 18}

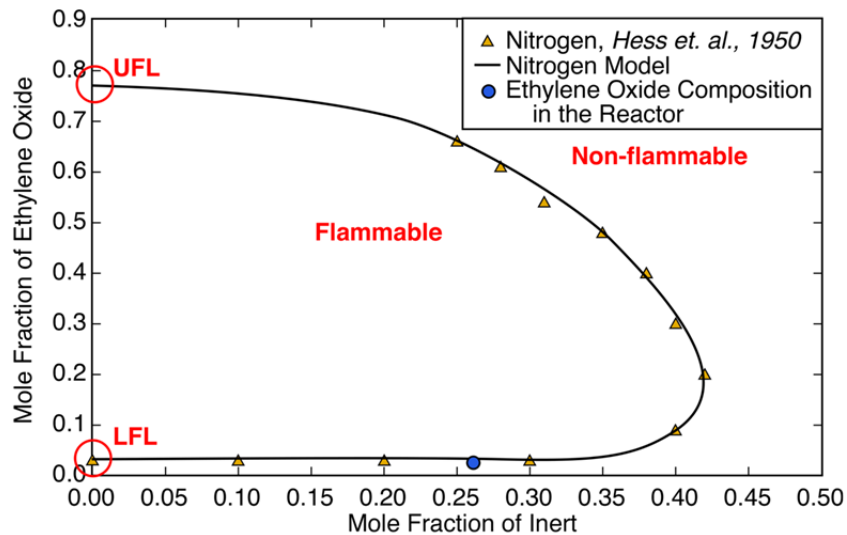


Figure 1-7: Flammability envelope of EO+O₂ mixture at 1 bar in presence of N₂.^{10, 16-18}

1.2 Desired Attributes for an alternate EO technology

The major drawbacks of the current silver-catalyzed ethylene epoxidation technology are as follows: (a) the burning of ethylene and EO results in a significant financial loss, which is accompanied by an increase in greenhouse gas emissions; (b) safety concerns due to the presence of flammable ethylene/EO/O₂ mixtures in the vapor phase necessitate the use of inerts as feed diluents and operation at low ethylene conversions, requiring cumbersome downstream separation steps to recover and recycle large amounts of unreacted ethylene and diluents. The challenges facing the development of an alternate technology are as follows: (a) selectively epoxidize ethylene to its corresponding epoxide, completely eliminating the burning of ethylene and EO; (b) eliminate the possibility of flammable vapors making the process inherently safe; and (c) be economically competitive with reduced environmental footprint.

1.3 Liquid Phase Epoxidation of Light Olefins

1.3.1 CEBC-Propylene Oxide Process (CEBC-PO Process)

In 2007, investigators at the Center for Environmentally Beneficial Catalysis (CEBC), University of Kansas (KU) reported an alternative approach to selectively epoxidize propylene to propylene oxide (PO), a chemical intermediate with an annual demand of 4 million tonnes/year.^{16, 19-21} A schematic of the CEBC-PO process is shown in Figure 1-8.

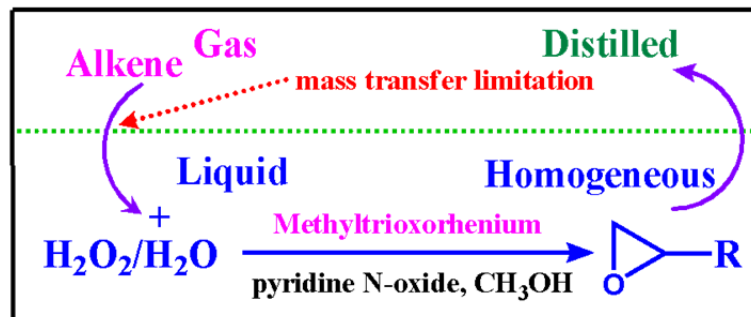


Figure 1-8: Schematic of the proposed CEBC-PO process

In this process, propylene is transported from the gas phase into the liquid phase where it reacts with the oxidant, hydrogen peroxide (H_2O_2), in the presence of homogeneous catalyst, methyltrioxorhenium (abbreviated as MTO, CH_3ReO_3) and promoter, pyridine N-oxide (PyNO). The propylene epoxidation reaction occurs under mild reaction conditions of $40\text{ }^\circ\text{C}$ and 50 bar. The MTO catalyst transfers an oxygen atom from H_2O_2 to propylene, selectively forming propylene oxide.^{16, 22} The solubility of propylene in $\text{H}_2\text{O}_2/\text{H}_2\text{O}$ mixture is low and a co-solvent is employed to enhance the solubility of propylene in the liquid phase.¹⁹ The CEBC-PO process is similar to a process recently developed by Dow and BASF called the Hydrogen Peroxide/Propylene Oxide (HPPO) process. Both processes employ the same oxidant (H_2O_2), solvent (methanol), and operating conditions (near-ambient temperature and tens of bars of propylene pressure). The key difference between the two processes is the catalyst: the CEBC-PO process uses an MTO a novel catalyst²⁰ and the HPPO process uses titanium silicate (TS-1). This prompted CEBC investigators to search for an alternative application of their greener process concept. While TS-1 catalyst used to epoxidize propylene does not work for ethylene epoxidation, CEBC researchers discovered that their MTO-based homogeneous catalyst system does indeed selectively epoxidize ethylene as it does propylene.

1.3.2 CEBC-Ethylene Oxide Process Concept (CEBC-EO Process)

The conceptual design of the CEBC-EO process is identical to what was previously demonstrated for the PO process shown in Figure 1-8. In the CEBC-EO process, ethylene is transported from the gas phase into the liquid phase where it reacts with the oxidant (H_2O_2) in the presence of the catalyst (MTO) and promoter (pyridine N-oxide) to selectively form the product EO, with water as the byproduct.²³ At the operating temperature of 20-40 °C, the oxidant H_2O_2 is stable and the vapor phase is devoid of oxygen. Furthermore, in this temperature range, the EO product dissolves completely in the liquid phase at a pressure greater than 2 bar.²⁴

To test the system, we initially performed the reaction in a variable-volume phase equilibrium cell (used as a batch reactor) where only gentle stirring of the liquid phase was possible. The products were sampled at the end of the run and analyzed by GC. In addition to the reactant (ethylene), solvent (methanol) and the internal standard (acetonitrile), only an ethylene oxide (product) peak was detected, demonstrating the high selectivity of the CEBC-EO process. The absence of CO_2 and O_2 in the vapor phase was confirmed by GC analysis of vapor phase samples.¹⁶

The low reaction rates reported from the first runs were attributed to gas-liquid mass transfer limitations under the gentle stirring conditions used in the reactor. To better understand mass transfer effects, a systematic investigation of the effect of stirring on ethylene mass transfer rates, and therefore on epoxidation rates, was undertaken. For reliable interpretation and modeling of mass transfer and kinetics data, accurate knowledge of the thermodynamic volumetric expansion (*i.e.*, ethylene solubility in the liquid phase) of the liquid phase was obtained. Clearly, estimations of reliable mass transfer coefficients and intrinsic kinetic parameters are essential not

only to assess the intrinsic activity/productivity of the investigated catalysts in batch conversion studies but also for rational reactor design, plant scale simulation and economic analysis.

1.3.2 Solvent Engineering

Ethylene epoxidation by H_2O_2 in the presence of a homogenous catalyst is a gas-liquid reaction and a gas-solid-liquid reaction when using supported catalysts. In either case, the solubility of the substrate gas in adequate amounts in the liquid phase containing the oxidant and catalyst is of paramount importance.^{25, 26} The solubility of olefins in $\text{H}_2\text{O}_2/\text{H}_2\text{O}$ mixtures is on the order of 10^{-3} M at 20 °C, 1 atm.²⁷ To improve this solubility, methanol is employed as a co-solvent, the high propylene oxide yields obtained in the CEBC-PO process is the basis for the choice.^{16, 19} The mole fraction of ethylene in pure methanol at 20 °C and 1 bar is 5.2 mol% (shown in Figure 1-9).

Ethylene, when compressed to its critical pressure in the vicinity of its critical temperature ($P_c = 51.2$ bar; $T_c = 9.1$ °C), dissolves appreciably in methanol (22 mol% at 25 °C and 50 bars, as shown in Figure 1-9).²⁸ The solubility parameter (d) correspondingly increases upon compression and the density becomes liquid-like beyond the critical pressure (P_c).²⁹ The ethylene solubility in methanol increases exponentially (rather than linearly when Henry's law applies) as the critical pressure is approached and results in a significant swelling or volumetric expansion of the liquid phase forming an ethylene-expanded liquid phase. Beyond 50 bars, phase separation is observed and this region should generally be avoided to prevent interphase transport limitations. Given that the epoxidation temperatures (0-40 °C) of this study are in the vicinity of the critical temperature of ethylene ($T_c=9.1$ °C), it should be possible to enhance the availability

of ethylene in a methanol-containing liquid phase by simple pressure-tuning around the critical pressure of ethylene.^{16, 22}

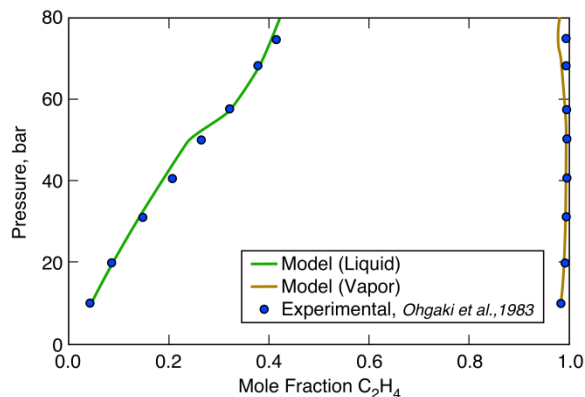


Figure 1-9: Vapor-liquid equilibrium of C₂H₄ + methanol at 25 °C²⁸

As shown in Figure 1-7, EO forms highly flammable mixtures in vapor phases containing O₂. In the conventional process, safety concerns necessitate the use of diluents and operation at low ethylene conversions. Despite these precautions, EO burning remains an issue. In the CEBC-EO process concept, almost all the EO formed remains dissolved in the liquid phase at the reactor operating pressure and temperature.²⁴ The virtual absence of O₂ and EO in the vapor phase of the CEBC-EO process makes the process inherently safe and eliminates the limitations on ethylene converted per pass.

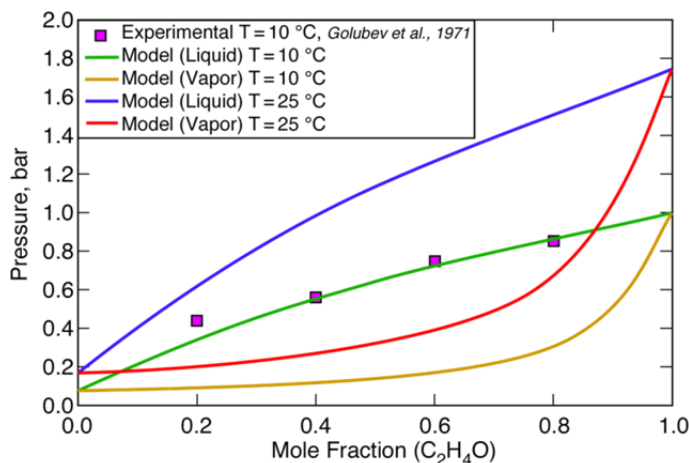


Figure 1-10: Vapor-liquid equilibrium of Ethylene Oxide+ methanol binary at 25 °C²⁴

1.3.3 Reaction Engineering Aspects

For a gas-liquid-solid (three phase) catalytic epoxidation reaction, several interphase mass transfer steps must occur before the gas phase (ethylene) and liquid phase (H₂O₂) react on the catalyst to form the desired product. These steps include: (a) transport of ethylene from the gas to the gas-liquid interphase; (b) transport of ethylene from the gas-liquid interphase to bulk liquid; (c) transport of ethylene and H₂O₂ from the bulk liquid phase to the catalyst surface; (d) intra-particle diffusion of ethylene and H₂O₂ through the pores of catalyst; (e) adsorption of H₂O₂ on the active sites; (f) epoxidation of C₂H₄ at the active site and; (g) product desorption from the active sites.

In the case of a homogeneous catalyst only steps (a) and (b) need to occur prior to the reaction. The high solubility of ethylene in the liquid phase results in the formation of a gas-expanded liquid. Mass transfer limitations in gas-expanded liquid is not well understood, and there are no known empirical correlations for estimating these transport limitations. A systematic

study has been performed as part of this dissertation research to explore the effect of transport limitations on reaction rates.

1.4 Catalysts for Selective Ethylene Epoxidation by H₂O₂

The goal of this study is to identify active metals that are economically competitive and abundantly available, and also exhibit desirable performance metrics such as high catalytic activity, near complete selectivity towards desired EO product, and durability over extended periods of time.

1.4.1 Rhenium-based catalysts

Methyltrioxorhenium is a homogeneous catalyst that catalyzes the epoxidation of alkenes by H₂O₂ at relatively mild temperatures.^{30, 31} Herrmann *et al.*³² demonstrated the catalytic activity of methyltrioxorhenium for the selective epoxidation of various olefins by H₂O₂ and reported high epoxide yields. In addition, H₂O₂-based methyltrioxorhenium-catalyzed epoxidation of various terminal and internal olefins, aromatics and sulfonated compounds have been extensively reported in literature.³²⁻³⁴

With the exception of propylene and 2-butene, all the substrates reported in the literature are high boiling olefins; hence, their epoxidation is a liquid-liquid reaction. Herrmann *et al.*³² performed the epoxidation of propylene at the low temperature of -10 °C to dissolve sufficient quantity of the light gases into the liquid phase. Low propylene conversions were reported.³² Further, in addition to propylene oxide, 1,2 propanediol, the hydrolysis product of propylene oxide, was also detected. The ring opening hydrolysis reaction of the propylene oxide is primarily attributed to the acidic nature of the reaction mixture.³²

1.4.1.1 Immobilization of Rhenium-based Catalysts

Despite its high activity and selectivity, the industrial application of methyltrioxorhenium catalyst has been hindered by its exorbitant cost. Further, the build-up of water in the system affects the catalyst activity and separation strategies such as distillation employed to remove water may destroy the catalyst complex. Thus, there is incentive to develop a heterogenized version of the MTO catalyst.

Saladino *et al.*³⁵ heterogenized MTO onto poly(4-vinylpyridine) and polystyrene. The heterogenized catalyst selectively epoxidizes terpenes to their corresponding epoxides. Recycle runs established the durability of the catalyst. The true heterogeneity of the catalyst was established by conducting hot filtration tests. Similarly, MTO microencapsulated in polystyrene was found to be highly active and selective for the epoxidation of olefins such as styrene, α -methyl styrene, and *cis*- β -methyl styrene by H₂O₂. The use of protic solvents enhanced the catalytic activity and selectivity.³⁶ In additional examples, Bracco *et al.*³⁷ and Ferraudi *et al.*³⁸ were able to immobilize rhenium onto poly(vinyl pyridine). Efforts are currently underway at CEBC to immobilize methyltrioxorhenium onto a soluble poly(4-vinyl-pyridine) aimed at developing an active, selective and easily separable version of the rhenium catalyst.

1.4.2 Tungsten-based catalysts

At a market price of \$154-\$182 per ton,³⁹ tungsten is much less expensive compared to rhenium. Tungsten has a wide range of industrial applications. It is used to make wear resistant alloy parts and coatings, filament in a bulbs, superalloys for turbine blades, heavy metal alloys for armaments, heat sinks, and as catalysts.^{39, 40} A homogeneous tungsten catalyst have been reported to be highly active for epoxidation.⁴⁰ However, for heterogenized tungsten catalysts,

low activity and leaching of the active metal species from the solid support have been reported as major problems.⁴⁰ Strukul *et al.*⁴¹ reported on a series of mesoporous mixed tungsten/silica oxides prepared by sol-gel method, and demonstrated their activity for the selective epoxidation of allylic alcohols by H₂O₂. The catalytic activity of the synthesized material was attributed to the presence of highly dispersed framework-incorporated tungsten. Furthermore, the calcination temperature was found to have a significant influence on the activity and selectivity of the catalyst.

Koo *et al.*⁴² obtained nanosized WO₃ particles supported on mesoporous MCM-48. The synthesized heterogeneous catalysts were highly efficient and selective for the epoxidation of both internal and terminal olefins by H₂O₂. Gao *et al.*⁴³ incorporated WO₃ into the framework of the meso cellular foam (MCF). The catalytic activity and recyclability of the synthesized material was tested for the epoxidation of cycloocta-1,5-diene by H₂O₂. The catalytic activity was mainly attributed to the presence of isolated tungsten species anchored onto the support through W-O-Si covalent bonds. Further, the ultra-large pores of the support alleviated substrate diffusion limitations enhancing epoxide yield.

Jacobs *et al.*⁴⁴ introduced tungsten catalysts into macroreticular resins or siliceous material *via* ion exchange. The grafted catalyst epoxidized norbornene, geraniol and cyclohexene by H₂O₂ selectively. Liu *et al.*⁴⁵ incorporated a tungsten peroxo compound onto the surface of hexagonal molecular sieves (HMS). The synthesized material epoxidized propylene with near complete selectivity to propylene oxide but the activity of the synthesized material was found to be low.

Gelbard *et al.*⁴⁶ immobilized peroxo tungstic species onto a aminophosphorylated polymethacrylate. The resulting material demonstrated significant activity for the epoxidation of cyclohexene. Recycle studies established the durability of the catalyst. Mizuno *et al.*⁴⁷

immobilized a dinuclear peroxotungstate anion on a silica support modified by dihydroimidazolium-based ionic liquid. The catalyst was highly stable and demonstrated catalytic activity towards the epoxidation of octene, hexene, norbornene, cycloheptene, geraniol, and 4-methyl-3-penten-2-ol by H_2O_2 .

Zhang *et al.*⁴⁸ incorporated tungsten into the framework of MCM-41 and reported that crystalline WO_3 was not observed up to a tungsten loading of 5.6 wt%. The high activity for the hydroxylation (a chemical process to introduce hydroxyl group onto an organic compound) of cyclohexene and selectivity towards *trans*-1,2-cyclohexanediol and glycol monoacetate established the catalytic activity of the synthesized material.

Dai *et al.*⁴⁹ doped tungsten into MCM-41 and reported a critical Si/W value of 30, beyond which the formation of extraframework WO_3 was reported. The synthesized material was found to be highly active compared to crystalline WO_3 and WO_3/SiO_2 prepared by incipient wetness impregnation method. The synthesized material epoxidizes cyclopentene to glutaraldehyde with a selectivity of 71%, but, the leaching of metal was reported.

Much of the research involving epoxidation of olefins by H_2O_2 in the presence of tungsten incorporated catalyst was performed using model compounds such as hexene, cyclooctene, octene, geraniol, and cyclopentene *etc.* Extensive leaching of tungsten metal from the support surface has been reported as a major drawback for tungsten-incorporated mesoporous material such as W-MCM-41, W-MCM-48. The low cost of tungsten coupled with significant catalytic activity, has encouraged CEBC researchers to attempt the incorporation of tungsten into the framework of other mesoporous supports such as KIT-5 and KIT-6.⁵⁰ In this dissertation, we have tested the catalytic activity of such W-KIT-6 and W-KIT-5 materials for ethylene epoxidation.

1.5 Continuous CEBC-EO Process Concept

The CEBC-EO process is envisioned to operate in a continuous mode in a stirred flow-through reactor fitted with a nano-filtration membrane, as shown in Figure 1-11. In the case of MTO, it is assumed that the catalyst is suitably modified by binding to a soluble polymer. This dissolved catalyst-polymer complex is retained in the reactor by the size-exclusivity of the nanofiltration membrane that allows the passage of small molecules such as EO (product), methanol (solvent) and unreacted reactant (ethylene) to pass through. The reactor effluents are separated by a train of distillation columns. This catalyst retention strategy and the reactor configuration are similar to that recently demonstrated by CEBC researchers for homogeneous hydroformylation.⁵¹ In the case of heterogeneous catalysts, the CEBC-EO process would occur in a continuous mode either in a continuous stirred tank reactor (CSTR) fitted with a coarse membrane or in a trickle bed reactor.

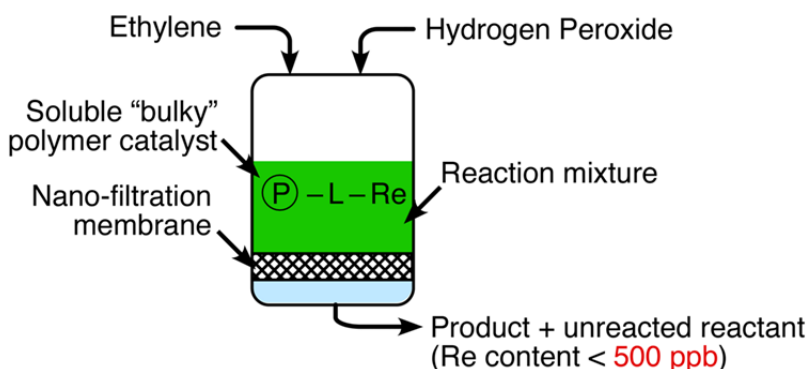


Figure 1-11: Schematic of the proposed continuous CEBC-EO process

1.6 Life Cycle Assessments

The purpose of a life cycle assessment (LCA) is to provide a quantitative assessment of the environmental impact for a product or a process. By performing a comparative cradle-to-gate

LCA of the alternative (CEBC-EO process) and the conventional silver-catalyzed ethylene epoxidation process, we identify the major environmental impact drivers (hot spots) and their percentage contributions relative to the overall impact in each impact category. This quantitative information is vital to establish the relative greenness of a process or product.

1.7 Dissertation Goals and Objectives

The goal of this dissertation is to better understand the practical viability of the CEBC-EO technology concept by performing fundamental engineering studies and quantitative sustainability (both economic and environmental impact) analyses. Specific objectives are to:

- Perform experimental and modeling investigations into the dissolution (i.e., volumetric expansion) of water/methanol based liquid phases by compressed ethylene in the expected range of operating conditions;
- Experimentally obtain mass transfer coefficients for ethylene dissolution into the self-expanded liquid phase containing methanol and water;
- Measure intrinsic kinetic parameters for the methyltrioxorhenium-catalyzed ethylene epoxidation
- Benchmark the liquid phase ethylene epoxidation process against the conventional silver catalyzed ethylene epoxidation process and perform comparative economic and cradle-to-gate life cycle assessments to identify key economic drivers and identify the major environmental impact drivers in both the processes.
- Similarly benchmark the liquid phase propylene epoxidation process against the PO/TBA and HPPO processes and perform comparative economic and cradle-to-gate life cycle

assessment (LCA) to identify the major economic drivers and hot spots in the PO technologies.

- Evaluate tungsten-based heterogeneous catalysts as inexpensive alternatives for ethylene epoxidation by establishing the activity, selectivity and durability of these catalysts.

This dissertation is composed of four chapters in addition to the introduction (Chapter 1) and conclusions/recommendations (Chapter 6). In Chapter 2, results of the fundamental engineering studies that led to significant improvements in the productivity of the CEBC-EO process are presented. The results pertaining to the volumetric expansion, mass transfer and kinetic studies are vital for the rational reactor design, plant scale simulation and economic analysis.

In Chapter 3, plant-scale simulations of the conventional silver-catalyzed ethylene epoxidation process (based on process data from the patent literature) and CEBC-EO process (based on lab-scale experimental data obtained as part of this dissertation research) are presented. The total capital investments and total production costs for both the processes are compared and major economic drivers governing the feasibility of both the processes are presented. Further, the comparative cradle-to-gate life cycle assessments (LCA) of the two processes are presented and the major sources of adverse environmental impact are presented.

Chapter 3 also presents the results of the comparative cradle-to-gate LCA for producing ethylene (raw material involved in both conventional and CEBC processes) and hydrogen (additional raw material involved in the CEBC-EO process for producing hydrogen peroxide) from diverse feedstocks (such as natural gas, crude oil and corn). The relative environmental impacts from these sources are compared. Furthermore, the environmental impacts based on the cradle-to-grave LCA for the production of energy from coal (hard coal, lignite), fuel oil (heavy and light fuel oil) and natural gas are presented.

Chapter 4 presents results of the evaluation of tungsten-incorporated mesoporous silicas (KIT-5 and KIT-6) as novel heterogeneous catalysts for ethylene epoxidation. The results of the catalyst performance metrics (activity, selectivity and stability) are presented and compared for various tungsten metal sources used in the preparation of these heterogeneous catalysts.

In Chapter 5, HYSYS-based process flow diagrams for the CEBC-PO, PO/TBA and HPPO processes were developed using published literature and patents. Total capital and total production costs for the three processes were calculated and compared to identify the major factors that influence process economics. The results from the HPPO process (which has a similar oxidant and operating conditions as the CEBC-EO process) help assess the key economic drivers with regard to the profitability of the commercial PO process and the proposed CEBC-EO process. Furthermore, the quantitative results of the comparative cradle-to-gate life cycle assessment used in the identification of the major environmental hot spots are presented.

References

1. SRI Consulting. <http://chemical.ihs.com/WP/Public/Reports/eo/> (Accessed February 1st, 2012),
2. Weissermel, K.; Arpe, H.-J., *Industrial Organic Chemistry*. 4th ed.; Wiley-VCH: Washington D.C., 2003.
3. ICIS. <http://www.icis.com/chemicals/channel-info-chemicals-a-z/> (Accessed June 15th, 2010),
4. Ethylene Oxide/Ethylene Glycol (EO/EG) Processes. http://www.shell.com/home/content/globalsolutions/refinery_chemical_licensing/petrochemical_technology/ethylene_oxide_processes/ (April 3rd),
5. Coleman, H. J. *PERP Program-Ethylene Oxide/Ethylene Glycol*; White Plains, New York, 2006.
6. Dow Technology Licensing-METEOR Ethylene Oxide/Glycol Process Technology. <http://www.dow.com/licensing/offer/meteor.htm> (April 3rd),
7. Buffum, J. E.; Kowaleski, R. M.; Gerdes, W. H. Ethylene Oxide Catalyst. US 5145824, 1992.
8. McCain, J.; Naumann, A. W.; Wang, W. Y. Thermal Process for Removal of Contaminants From Process Streams. US 5563282, 1996.
9. Rebsdatt, S.; Mayer, D., Ethylene Oxide. In *Ullmann's Encyclopedia of Industrial Chemistry*, 6th ed.; Hawkins, S.; Russey, W. E.; Pilkart-Muller, M., Eds. Wiley-VCH: New York, 2005; Vol. 13, p 23.
10. Zabetakis, M. G., *Flammability Characteristics of combustible gases and vapor*. 1st ed.; U.S. Department of Interior, US Bureau of Mines: 1939.

11. Evans, W. E.; Chipman, P. I. Process for Operating the Epoxidation of Ethylene. US 2003/0139633 A1, 2003.
12. Rizkalla, N. Process For Preparing Silver Catalyst For Ethylene Epoxidation. 5374748, December 20th, 1994.
13. Rase, H. F., *Handbook of Commercial Catalysts Heterogeneous Catalysts*. CRC Press: New York, 2000; p 487.
14. Rizkalla, N. Process for preparing silver catalyst for ethylene epoxidation. US 5374748, 1994.
15. Cavitt, S. B. Silver Catalyst for Ethylene Epoxidation. US 4102820, 1978.
16. Lee, H. J.; Ghanta, M.; Busch, D. H.; Subramaniam, B., Towards a CO₂-free ethylene oxide process: Homogeneous ethylene oxide in gas-expanded liquids. *Chemical Engineering Science* **2010**, 65, (1), 128-134.
17. Hess, L. G.; Tilton, V. V., Ethylene Oxide - Hazards and Methods of Handling. *Industrial and Engineering Chemistry* **1950**, 42, (6), 1251-1258.
18. Jones, G. W.; Kennedy, R. E., Extinction of ethylene oxide flames with carbon dioxide. *Industrial and Engineering Chemistry* **1930**, 22, 146-147.
19. Lee, H. J.; Shi, T. P.; Busch, D. H.; Subramaniam, B., A greener, pressure intensified propylene epoxidation process with facile product separation. *Chemical Engineering Science* **2007**, 62, (24), 7282-7289.
20. Busch, D. H.; Subramaniam, B.; Lee, H. J.; Shi, T. P. Process for Selective Oxidation of Olefins to Epoxides. US 7649101 B2, 2010.
21. Subramaniam, B.; Busch, D. H.; Lee, H. J.; Ghanta, M.; Shi, T.-P. Process for Selective Oxidation of Olefins to Epoxides. US 8080677 B2, 2011.

22. Ghanta, M.; Lee, H. J.; Busch, D. H.; Subramaniam, B., Highly Selective Homogeneous Ethylene Epoxidation in Gas (Ethylene)-Expanded Liquid: Transport and Kinetic Studies. *AIChE Journal (in press)* **2011**.
23. Sheldon, R. A., Catalysis: The Key to Waste Minimization. *J. Chem. Tech. Biotechnol.* **1997**, 68, 8.
24. Golubev, Y. D.; Dement'eva, L.; VLasov, G. M., The Solubility of ethylene oxide in C1-4 alcohols. *Soviet Chemical Industry* **1971**, (8), 3.
25. Danckwerts, P. V., *Gas-Liquid Reactions*. 1st ed.; McGraw-Hill Book Company: New York, 1970.
26. Doraiswamy, L. K.; Sharma, M. M., *Fluid-Fluid-Solid Reactions*. 1st ed.; John Wiley & Sons: 1984; Vol. 2.
27. Bradbury, E. J.; McNulty, D.; Savage, R. L.; Mcsweeney, E. E., Solubility of Ethylene in Water - Effect of Temperature and Pressure. *Industrial and Engineering Chemistry* **1952**, 44, (1), 211-212.
28. Ohgaki, K.; Nishii, H.; Saito, T.; Katayama, T., High-Pressure Phase-Equilibria for the Methanol-Ethylene System at 25 C and 40 C. *Journal of Chemical Engineering of Japan* **1983**, 16, (4), 263-267.
29. Busch, D. H.; Subramaniam, B., Catalytic Oxidation Reactions in Carbon Dioxide-Expanded Liquids Using Green Oxidants Oxygen and Hydrogen Peroxide. In *Gas Expanded Liquids and Near Critical Media Green Chemistry and Engineering*, Hutchenson, K. W.; Scurto, A. M.; Subramaniam, B., Eds. Oxford University Press: 2009; p 353.

30. Hermann, W. A.; Marz, D. W.; Wagner, W.; Kuchler, J.; Weichselbaumer, G.; Fischer, R. W. use of organorhenium compounds for the oxidation of multiple C-C bonds oxidation processes based thereon and novel organorhenium compounds. US 5155247, 1992.
31. Crocco, G. L.; Shum, W. F.; Zajacek, J. G.; Kesling, H. S. J. Epoxidation Process. US 5166372, Nov 24th, 1992, 1992.
32. Herrmann, W. A.; Fischer, R. W.; Marz, D. W., Methyltrioxorhenium as catalyst for olefin epoxidation. *Angewandte Chemie International Edition in English* **1991**, 30, (12), 2.
33. Adam, W.; Mitchell, C. M., Methyltrioxorhenium (VII) Catalyzed Epoxidation of Alkenes with the Urea/Hydrogen Peroxide Adduct. *Angewandte Chemie International Edition in English* **1996**, 35, (5), 533-535.
34. Gansauer, A., A Novel Methyltrioxorhenium (MTO) Catalyzed Epoxidation of Olefins: An Impressive Example of Simplicity, Selectivity, and Efficiency. *Angewandte Chemie International Edition in English* **1997**, 36, (23), 2591-2592.
35. Saladino, R.; Neri, V.; Pelliccia, A. R.; Mincione, E., Selective epoxidation of monoterpenes with H₂O₂ and polymer-supported methylrhenium trioxide systems. *Tetrahedron* **2003**, 59, 7403-7408.
36. Vezzosi, S.; Ferre, A. G.; Crucianelli, M.; Crestini, C.; Saladino, R., A novel and efficient catalytic epoxidation of olefins with adducts derived from methyltrioxorhenium and chiral aliphatic amines. *Journal of Catalysis* **2008**, 257, (2), 262-269.
37. Bracco, L. L. B.; Juliarena, M. P.; Ruiz, G. T.; Feliz, M. R.; Ferraudi, G. J.; Wolcan, E., Resonance energy transfer in the solution phase photophysics of -Re(CO)₃L⁺ pendants

- bonded to poly(4-vinylpyridine). *Journal of Physical Chemistry B* **2008**, 112, (37), 11506-11516.
38. Wolcan, E.; Ferraudi, G., Photochemical and Photophysical Properties of Fac-Re(I) Tricarbonyl Complexes: A Comparison of Monomer and Polymer Species with - ReI(CO)₃Phen Chromophores. *The Journal of Physical Chemistry A* **2000**, 104, (41), 9281-9286.
39. Shedd, K. B. *Tungsten*; United States Department of Interior: Washington D. C., 2011; p 20.
40. Shylesh, S.; Jia, M. J.; Thiel, W. R., Recent Progress in the Heterogenization of Complexes for Single-Site Epoxidation Catalysis. *European Journal of Inorganic Chemistry* **2010**, (28), 4395-4410.
41. Somma, F.; Strukul, G., Oxidation of geraniol and other substituted olefins with hydrogen peroxide using mesoporous, sol-gel-made tungsten oxide-silica mixed oxide catalysts. *Journal of Catalysis* **2004**, 227, (2), 344-351.
42. Koo, D. H.; Kim, M.; Chang, S., WO₃ nanoparticles on MCM-48 as a highly selective and versatile heterogeneous catalyst for the oxidation of olefins, sulfides, and cyclic ketones. *Organic Letters* **2005**, 7, (22), 5015-5018.
43. Gao, R.; Yang, X.; Dai, W.-L.; Le, Y.; Li, H.; Fan, K., High-activity, single-site mesoporous WO₃-MCF materials for the catalytic epoxidation of cycloocta-1,5-diene with aqueous hydrogen peroxide. *Journal of Catalysis* **2008**, 256, (2), 259-267.
44. Hoegaerts, D.; Sels, B. F.; de Vos, D. E.; Verpoort, F.; Jacobs, P. A., Heterogeneous tungsten-based catalysts for the epoxidation of bulky olefins. *Catalysis Today* **2000**, 60, (3-4), 209-218.

45. Liu, Y.; Murata, K.; Inaba, M., Epoxidation of propylene with molecular oxygen in methanol over a peroxy-heteropoly compound immobilized on palladium exchanged HMS. *Green Chemistry* **2004**, 6, 510-515.
46. Gelbard, G.; Breton, F.; Quenard, M.; Sherrington, D. C., Epoxidation of cyclohexene with polymethacrylate-based peroxotungstic catalysts. *Journal of Molecular Catalysis a-Chemical* **2000**, 153, (1-2), 7-18.
47. Yamaguchi, K.; Yoshida, C.; Uchida, S.; Mizuno, N., Peroxotungstate immobilized on ionic liquid-modified silica as a heterogeneous epoxidation catalyst with hydrogen peroxide. *Journal of the American Chemical Society* **2005**, 127, (2), 530-531.
48. Zhang, Z.; Suo, J.; Zhang, X.; Li, S., Synthesis, characterization, and catalytic testing of W-MCM-41 mesoporous molecular sieves. *Applied Catalysis A: General* **1999**, 179, (1), 11-19.
49. Dai, W. L.; Chen, H.; Cao, Y.; Li, H. X.; Xie, S. H.; Fan, K. N., Novel economic and green approach to the synthesis of highly active W-MCM41 catalyst in oxidative cleavage of cyclopentene. *Chemical Communications* **2003**, (7), 892-893.
50. Ramanathan, A.; Subramaniam, B.; Badloe, D.; Hanefeld, U.; Maheswari, R., Direct incorporation of tungsten into ultra-large-pore three-dimensional mesoporous silicate framework: W-KIT-6. *J. Porous Mater.* **2012**.
51. Fang, J.; Jana, R.; Tunge, J. A.; Subramaniam, B., Continuous homogeneous hydroformylation with bulky rhodium catalyst complexes retained by nano-filtration membranes. *Applied Catalysis A: General* **2011**, 393, 294-301.

Chapter 2

Highly Selective Homogeneous Ethylene Epoxidation in Gas (Ethylene)- Expanded Liquid: Transport and Kinetic Studies

2.1 Introduction

Ethylene oxide (EO), a bulk chemical intermediate, has a worldwide demand that is growing at 6-7%/year and is currently at nearly 20 million tonnes/year.¹ Commercially, EO is produced by the vapor phase oxidation of ethylene with oxygen over a supported silver catalyst in fixed bed reactors. The ethylene conversion per pass is maintained at 4-8% to minimize the burning of ethylene and EO, and to avoid the formation of flammable vapors. Further, diluent gases such as CH₄, Ar, N₂ and CO₂ are deployed to reduce the flammability envelopes associated with ethylene/EO/Air mixtures.²⁻⁵ Despite advances in the heterogeneous silver-based catalyst formulations, the selectivity towards EO is reported to be around 85% with the byproducts being CO₂.⁵ The CO₂ emitted as byproduct in the conventional EO process is approximately 3.4 million metric tons/year, making it the second largest emitter of CO₂ among all chemical processes. More importantly, the selectivity loss as CO₂ translates into an ethylene feedstock loss of approximately \$1.1 billion/year assuming an ethylene feedstock price of 32 ¢/lb. Increases in ethylene price, predicted to double within the next decade,⁶ will only exacerbate this loss. The rising cost of ethylene¹ and the expansion of EO demand prompted researchers at the Center for Environmentally Beneficial Catalysis (CEBC) to develop an alternative process that conserves the ethylene feedstock and is more energy efficient.^{4, 6, 7}

In the proposed process concept (henceforth, referred to as the CEBC EO process) (Figure 2-1), EO is produced by the selective oxidation of ethylene with hydrogen peroxide (H₂O₂) using a

homogeneous catalyst, methyltrioxorhenium, MTO. Compressed ethylene gas (roughly 40-50 bar) is mixed with a liquid-phase reaction mixture containing water, methanol, hydrogen peroxide (oxidant), MTO and a promoter, pyridine N-oxide (PyNO) in the 20-40°C range (*t*-butyl alcohol can serve as an alternative solvent to methanol).^{4, 6} The MTO transfers an oxygen atom from H₂O₂ to ethylene, selectively forming EO. The elimination of burning conserves feedstock and reduces the carbon footprint. Also, H₂O₂ is stable at these operating conditions such that the vapor phase is devoid of oxygen as confirmed by gas chromatographic analysis. Also, the EO product, which is flammable in the gas phase, remains dissolved in the liquid phase at the operating pressure. The virtual elimination of O₂ and EO from the vapor phase makes the process *inherently safe*.

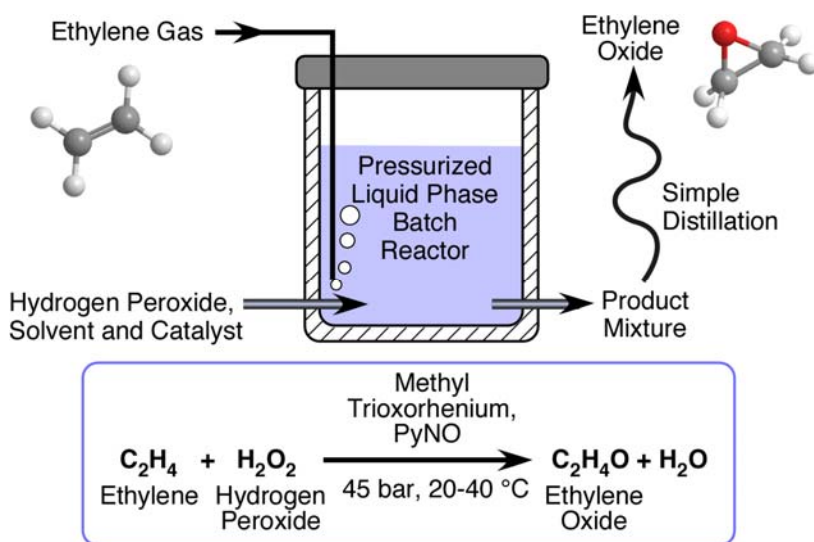


Figure 2-1: Schematic of CEBC expanded-phase EO process

It must be noted that in the CEBC-EO process, the reaction occurs in a gas-expanded liquid phase wherein the substrate (ethylene itself) is used as the expansion gas to increase its

availability in the liquid phase. The concept is similar to how propylene (the reactive substrate) was exploited as the expansion medium in our earlier work.⁵ This work is thus complementary to the H₂O₂-based olefin epoxidation in supercritical CO₂ or CO₂-expanded liquid phases that have been previously reported.^{2, 5, 7-9}

A number of similarities exist between the CEBC EO process and the Dow/BASF Hydrogen Peroxide/Propylene Oxide (HPPO) process.¹¹ (i) methanol is employed as the co-solvent; (ii) H₂O₂ is the oxidant; and (iii) the operating pressures (tens of bars) and temperatures (25-40 °C) in both processes are similar.^{2, 5, 10} Under the reaction conditions, ethylene and propylene are both relatively close to their critical points ($P_c = 50.76$ bars, $T_c = 9.5^\circ\text{C}$), ($P_c = 46.1$ bars; $T_c = 91^\circ\text{C}$), respectively. Hence their solubilities in the methanol-containing liquid phase are substantial,¹² actually resulting in the formation of gas-expanded liquids (GXLs). The economic viability of the HPPO process is in major part due to the relatively high profit margins enjoyed by PO and the relatively inexpensive catalyst (Ti-based), factors that effectively offset the cost of using H₂O₂ as oxidant. In contrast, the rhenium-based catalyst is expensive making and the economic viability of the CEBC EO process more challenging. However, recent developments in the cost-effectiveness and greener syntheses of both H₂O₂ and the MTO catalyst provide justification for continued investigations aimed at improving the commercial viability of this technology.

Conventionally, H₂O₂ has been produced by the standard anthraquinone process, a highly energy intensive technology.¹⁰⁻¹² In recent years, significant advances in the development of alternative H₂O₂ processes have been reported to lower the cost of H₂O₂ production.¹³ Solvay commercialized the high productivity amylanthraquinone technology,¹⁴ and the direct H₂O₂ process has been demonstrated at the pilot plant scale by a joint venture between Headwaters Inc.

and Evonik.¹⁵ The MTO catalyst is a highly versatile epoxidation catalyst and is known to catalyze a broad spectrum of oxygen transfer reactions.¹⁶⁻¹⁸ The mechanism of oxygen transfer in the MTO/H₂O₂ system has been extensively studied.^{19, 20} In the presence of excess H₂O₂ the catalyst MTO remains in the highly active diperoxo form. Yin and Busch recently reported that the conversion of simple MTO into the mono-peroxide complex facilitates the primary pathway for the destruction of MTO catalyst.²¹ Consequently, in the presence of excess H₂O₂, the preferred active species (diperoxo complex) has the potential to be indefinitely stable. Recently, Hermann *et al.* reported a greener, process for the synthesis of MTO that has the potential to reduce the cost of the catalyst.²²

For rational development and economic assessment of the CEBC EO process, fundamental engineering data are essential. This paper is focused on understanding the thermodynamics, mass transfer rates, and intrinsic epoxidation kinetics associated with the dissolving of ethylene and its subsequent conversion in its self-expanded liquid phase. Herein, the volumetric expansion of the liquid reaction phase by pressurized ethylene is quantitatively established. Based on the measured ethylene dissolution rates into the liquid phase at constant pressure and temperature but different agitation speeds, gas-liquid mass transfer coefficients were estimated from a mathematical model of the stirred semi-batch system. The ethylene epoxidation reactions were re-investigated in the absence of mass transfer limitations to quantify the enhancement of EO yield and also obtain intrinsic kinetic parameters from temporal conversion and selectivity profiles.

2.2 Experimental

2.2.1 Materials

Ethylene was purchased from Matheson Tri-Gas Co. (Ultra high purity grade). The MTO (71.0-76.0 wt.% Re), oxidant (50 wt% H₂O₂ in H₂O), methanol (HPLC grade, ≥ 99.99%), *t*-butyl alcohol (ACS reagent, >99.7%), ferroin indicator solution, acetonitrile (HPLC grade ≥ 99.9%) and pyridine-N-oxide (95%) were purchased from Sigma-Aldrich and used without further purification. Ceric sulfate (0.1 N) was purchased from Fisher Scientific. Trace metal grade sulfuric acid (99.9 wt%) purchased from Fisher Scientific was diluted to 5% (v/v) H₂SO₄ solution. Hydranal composite 5, one component reagent for volumetric titration of H₂O is purchased from Riedel-de-Haen. Ethylene oxide and anhydrous ethylene glycol standards were purchased from Supelco Analytical and Sigma-Aldrich, respectively.

2.2.2 Apparatus and Procedure

Volumetric Expansion Studies The high solubility of compressed ethylene in methanol leads to the formation of ethylene-expanded liquids. Volumetric expansion studies were conducted in a 50 cm³ high-pressure Jurgeson gauge cell designed to withstand a pressure of 400 bar at 100 °C shown in Figure 2-2.²³ Either methanol (solvent) or methanol+50%H₂O₂/H₂O or *t*-butyl alcohol+50% H₂O₂/H₂O mixture is loaded into the Jurgeson gauge cell and immersed in a constant temperature bath. Ethylene is charged into the cell from an external reservoir through a two-stage pressure regulator, maintaining the Jurgeson cell at a constant pressure. The attainment of equilibrium is facilitated by mixing the gas and liquid phases with the aid of a piston that can be moved vertically within the cell across the two phases and a magnetic stirrer bar in the liquid

phase. The volume of the ethylene-expanded liquid phase at equilibrium is measured visually on a calibrated linear scale attached to the view cell.²⁴

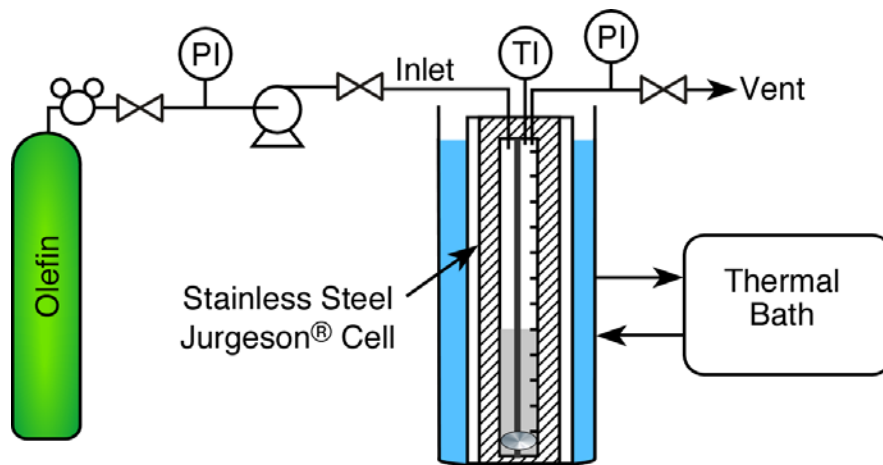


Figure 2-2: Schematic of the Jurgeson cell

Mass Transfer Investigations These studies were conducted in a 50 mL Parr reactor setup (Figure 2-3). The pressure and temperature in the reactor are monitored using LabView 7.0[®] data acquisition software. Ethylene is charged into the reactor from an external reservoir at ambient temperature through a two-stage pressure regulator that maintains the reactor pressure constant at 50 bars. The decrease in the external reservoir pressure, a direct measure of ethylene uptake in the Parr reactor, is also logged by the LabView 7.0[®] software.

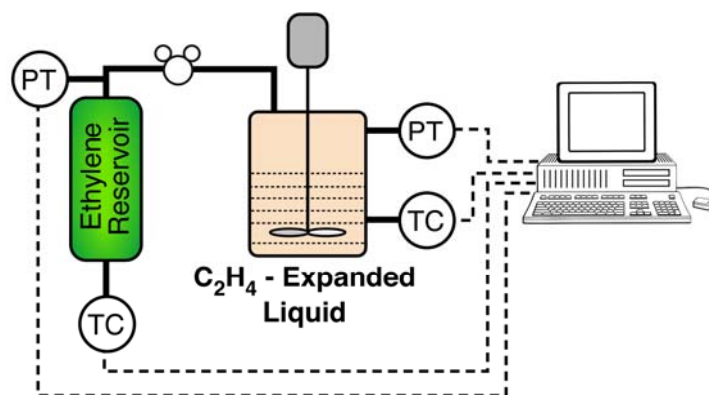


Figure 2-3: Schematic of stirred semi-batch mixer unit to measure the ethylene transport rates into the liquid phase

Kinetic Studies in Gas-Expanded Liquid Phase The schematic of the reactor setup for the epoxidation studies is shown in Figure 2-4. Ethylene epoxidation reactions were conducted in a semi-continuous mode in a 50-mL Parr reactor equipped with a magnetically driven stirrer, a pressure transducer and a thermocouple. The reactor temperature is controlled between 20-40 °C by a circulating water bath. The impeller speed is maintained at 1200 rpm to ensure the absence of mass transfer resistances. A micropump (model# 415A) circulates the reaction mixture at a flow rate of approximately 30 mL/min to facilitate the sampling of the ethylene-expanded liquid phase for analysis. A solution containing 50% H₂O₂/H₂O (0.268 mol), pyridine N-oxide (1.82 mmol), and MTO (0.18-0.54 mmol) dissolved in CH₃OH (30 mL) and internal standard CH₃CN (1 mL) was charged into the reactor and ethylene was injected from an external reservoir pressurizing the reactor up to 50 bars.⁴ The ethylene epoxidation reaction is not impacted by the presence of acetonitrile which is confirmed experimentally. The reactor pressure was maintained constant by continuously replenishing the consumed ethylene from the external ethylene reservoir. Isothermal, constant pressure semi-batch reactions lasting up to 5 h were carried out at

several temperatures in the 20-40 °C range. The gas-expanded liquid phase was sampled at regular time intervals. The H₂O₂ and H₂O contents of the liquid phase were quantified by ceric sulfate and Karl Fischer titrations, respectively.²⁵⁻²⁸ Details of the GC analysis, ceric sulfate titration and Karl Fischer titration are provided in Appendix B1-B3.

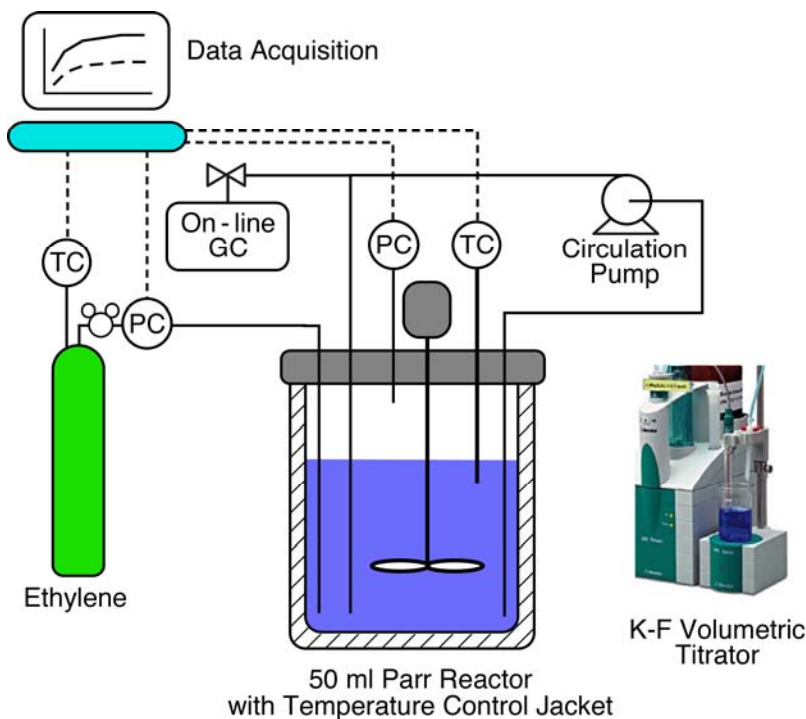


Figure 2-4: Schematic of the experimental setup for ethylene epoxidation studies in gas-expanded liquid phase

In the presence of a molar excess of H₂O₂ (with respect to the catalyst), the MTO catalyst is present as the highly active di(peroxo) rhenium complex that selectively transfers an oxygen atom from H₂O₂ to ethylene to form EO.^{17, 20} The reaction order with respect to catalyst concentration was established by varying the catalyst amount (from 0.180-0.542 mmol). The intrinsic kinetic parameters (k' , E) for ethylene epoxidation were estimated from the temporal

concentration profiles (of EO, H₂O₂ and H₂O) at different temperatures by regression with a pseudo-first order kinetic model based on conversion of the limiting reactant (H₂O₂) to EO in the presence of excess ethylene and constant catalyst concentration.

2.3 Results and Discussion

2.3.1 Volumetric Expansion Studies

Reliable estimation of interphase gas-liquid mass transfer coefficients is vital for rational process development. Unlike conventional liquid phases, gas-expanded liquid phases are compressible depending on the extent of gas dissolution into the liquid phase. The volumetric expansion data are essential to accurately account for the dilution caused by the enhanced ethylene dissolution in the liquid phase and therefore to reliably interpret conversion and selectivity data used to obtain kinetic parameters.

The volumetric expansion ratio is defined as the equilibrium volume of the expanded liquid phase at temperature T and pressure P , relative to the volume (V_o) of the unexpanded phase at 1 atm and the same T .²⁴

$$\frac{V(T,P)}{V_o(T,P_o)} \tag{1}$$

In the 20-40 °C temperature range, the solubility of ethylene in the liquid phase is substantial at pressures in the vicinity of the critical pressure of ethylene ($P_c = 50.76$ bar). As shown in Figures 2-5A and 2-5B, the volume of the initial liquid phase, containing either methanol alone or a representative reaction mixture containing 0.748 mol methanol + 0.134 mol H₂O₂ + 0.253 mol H₂O, increases with increasing ethylene pressure.

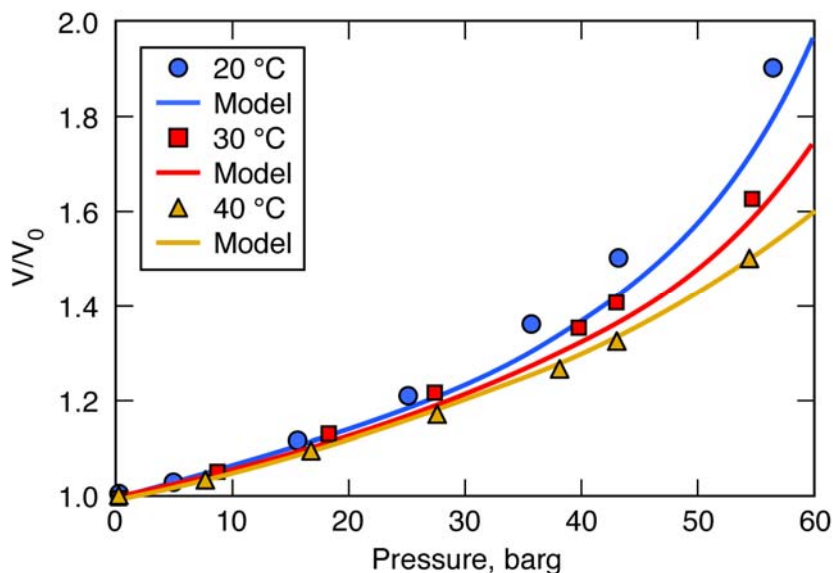


Figure 2-5A: Volumetric expansion ratios of ethylene+methanol binary system upon pressurization by ethylene. The size of the plotted data point represents the experimental uncertainty

For the ethylene+methanol system, the expansion shows the characteristic exponential dependence as the critical pressure of ethylene is approached. At a fixed pressure, the volumetric expansion of the liquid phase decreases with increasing temperature due to the lower gas solubility at higher temperatures. The maximum volumetric expansion ratios for the ethylene+methanol system at approximately 50 bars and at 20, 30 and 40 °C are 1.89, 1.62 and 1.50, respectively, signifying substantial increases in the liquid phase volume upon ethylene addition. The corresponding mole fractions (x_E) of ethylene in the liquid phase are 0.309, 0.216 and 0.163 respectively. These values are consistent with the reported VLE behavior of this binary system and previously predicted values.²⁹ In comparison, the ethylene mole fraction in methanol phase at 20°C and 1 bar is 0.052.

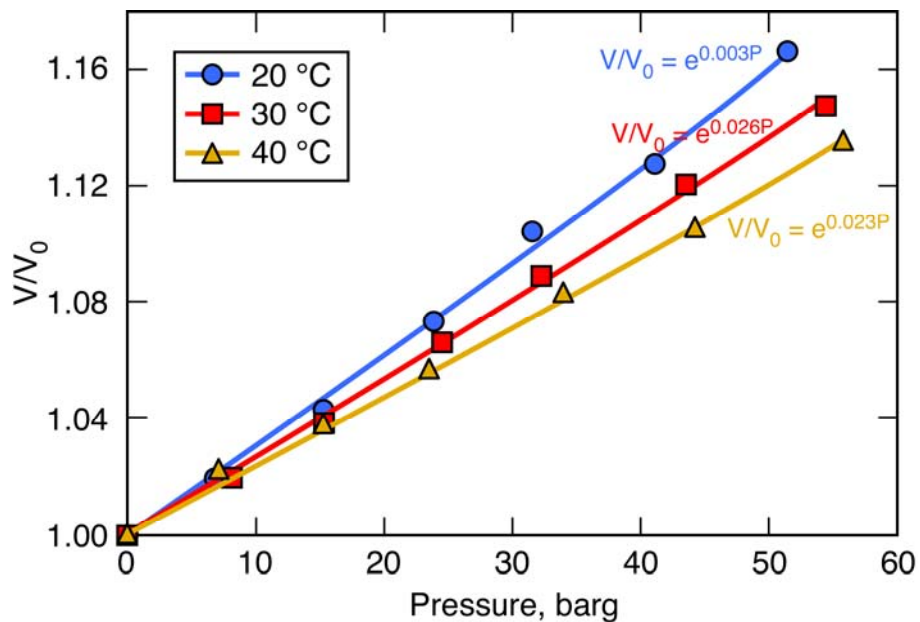


Figure 2-5B: Volumetric expansion of ethylene+methanol+50 wt% H₂O₂/H₂O system upon pressurization by ethylene. Initial composition of liquid phase: 0.748 mol methanol + 0.134 mol H₂O₂ + 0.253 mol H₂O. Initial volume = 15 mL. The size of the plotted data point represents the experimental uncertainty.

The expansion ratios in the ternary mixture (containing methanol, H₂O₂ and H₂O) at similar conditions are comparatively lower, albeit significant, being 1.17, 1.15 and 1.13, respectively. Further, the volumetric expansion profile is linear in the pressure range reflecting the fact that ethylene is less soluble in the presence of water. The corresponding mole fractions of ethylene are 0.0216, 0.017 and 0.0141. In comparison, the ethylene mole fraction in water at 20°C and 50 bars is $1.96(10^{-3})$.

Figure 2-5C shows the volumetric expansion of a mixture containing 0.21 mol *t*-butyl alcohol + 0.08 mol H₂O₂+ 0.11 mol H₂O by ethylene. At a fixed temperature, the volumetric expansion

of the liquid phase increases with increasing pressure. The volumetric expansion of the liquid phase decreases with increasing temperature due to lower gas solubility. The maximum volumetric expansion at 50 bars and at 20, 30 and 40 °C are 1.42, 1.32 and 1.25, respectively, signifying substantial increases in the liquid phase volume upon ethylene addition. The corresponding mole fractions of ethylene are 0.209, 0.169 and 0.142, respectively.

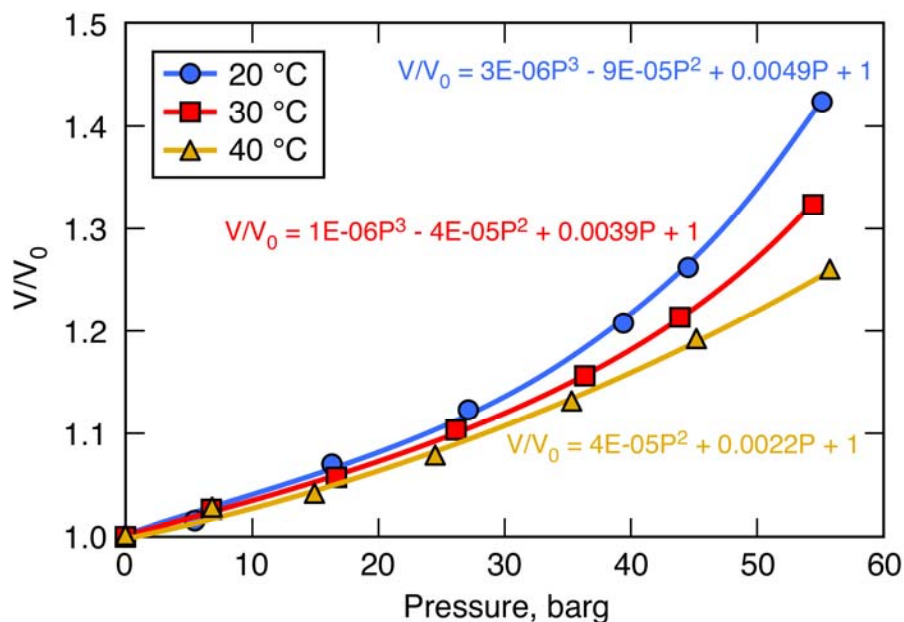


Figure 2-5C: Volumetric expansion of ethylene+t-butyl alcohol+50 wt% H₂O₂/H₂O system upon pressurization by ethylene. Initial composition of liquid phase: 0.21 mol *t*-butyl alcohol + 0.08 mol H₂O₂+ 0.11 mol H₂O. Initial volume = 15 mL. The size of the plotted data point represents the experimental uncertainty.

It must be noted that the minor components (MTO catalyst and PyNO_x promoter) are soluble in the reaction mixture but constitute less than 0.005 wt% of the initial reaction mixture. To avoid reaction, MTO and PyNO were not included in the aforementioned volumetric expansion

studies. Further, EO was also not included in the expansion studies since the EO formed during the reaction constitutes only 4.5 wt% of the reaction mixture even at the highest conversion (at the catalyst loading of 0.54 mmol), remaining mostly in the liquid phase at typical reaction conditions.³⁰ Volumetric expansion studies of methanol, and ternary mixtures of methanol + H₂O₂ + H₂O *t*-butyl alcohol + H₂O₂ + H₂O by propylene is shown in Appendix A.^{31, 32}

2.3.2 Mass Transfer Studies Involving Gas-Expanded Phases

The volumetric mass transfer coefficient is experimentally determined by conducting ethylene uptake experiments as explained in the Experimental section. The transient pressure profiles from the reservoir provide a direct measure of the rate at which ethylene dissolves into the liquid phase. At 25 °C and 50 bars, the rate of ethylene dissolution into the liquid phase increases with stirring indicating the presence of gas-liquid mass transfer limitations (Figure 2-6). The ethylene uptake by the liquid phase reaches equilibrium asymptotically at sufficiently high stirring rates (>1000 rpm). Beyond 1200 rpm, there is no observed change in the slope of the pressure profiles indicating that interphase mass transfer limitations are no longer significant. Further, at stirrer speeds exceeding 1200 rpm, approximately 99% of the equilibrium solubility is attained within 100 s. At 50 bars and 25 °C, the measured equilibrium mole fraction of ethylene in the liquid phase is 0.21 which closely matches the published value.²⁹ Using this technique, the equilibrium mole fractions of ethylene in the ternary mixture (0.748 mol methanol+0.1344 mol H₂O₂+0.253 mol H₂O) at 50 bars were found to be 0.108 and 0.0405 at 25 °C and 35 °C, respectively. In comparison, the equilibrium mole fraction of ethylene in water at 35 °C and 50 bar ethylene pressure is $1.96(10^{-3})$.³³ This solubility enhancement by more than an order of magnitude in methanol-based reaction mixtures under moderate compression renders ethylene as

the stoichiometrically excess reactant in the gas-expanded liquid phase. For reference, the corresponding mole fractions of H_2O_2 in the ethylene-expanded liquid phase at 50 bars are 0.061 at 25°C and 0.0615 at 40°C .

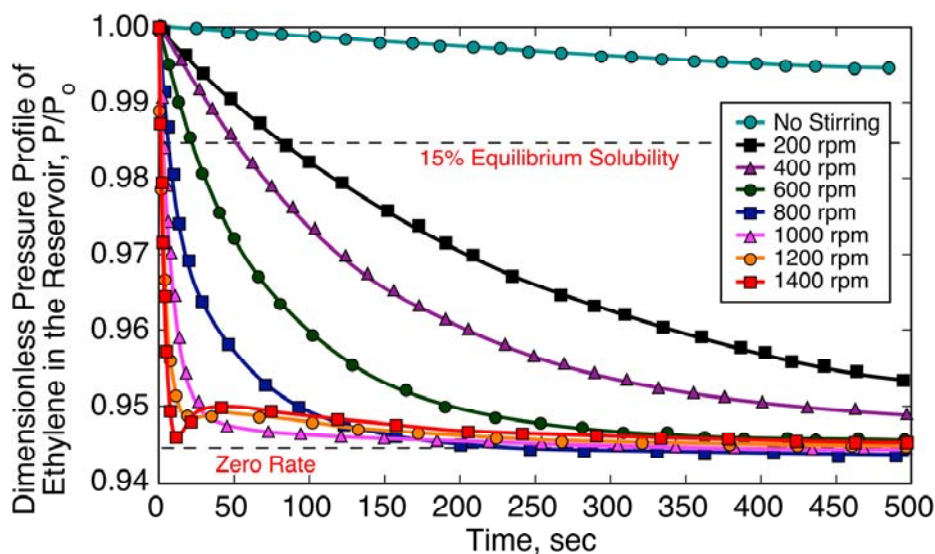


Figure 2-6: Effect of stirring speed on the uptake of compressed ethylene by the liquid phase. $P = 50$ bar; $T = 25^\circ\text{C}$; Initial composition of the liquid phase: 0.748 mol methanol + 0.134 mol H_2O_2 + 0.253 mol H_2O .

Ethylene uptake by the liquid phase (0.21 mol *t*-butyl alcohol + 0.08 mol H_2O_2 + 0.11 mol H_2O) reaches equilibrium solubility at a high stirrer speed of 1200 rpm. At these agitation speed 99% of the equilibrium solubility is achieved within 100 s. The equilibrium mole fraction of ethylene in the liquid phase at 50 bars and 25°C is 0.06 which is an order of magnitude greater than the equilibrium solubility of ethylene in 50 wt% $\text{H}_2\text{O}_2/\text{H}_2\text{O}$.

A mathematical model was developed to estimate the mass transfer coefficient (k_{La}) of the system. The model assumes instantaneous equilibrium at the *gas-liquid interface* for the

solubility of ethylene in either methanol or the ternary mixtures (73.6 wt% methanol+13.2 wt% H₂O₂+13.2 wt% H₂O and 76 wt% *t*-butyl alcohol+13.4 wt% H₂O₂+9.7 wt% H₂O). At constant pressure, the depletion of ethylene in the external reservoir equals the rate at which ethylene dissolves into the gas phase. A differential mass balance for ethylene in the isothermal, constant pressure semi-batch mixer yields:

$$-\left(\frac{V_R}{RT}\right)\left(\frac{dP_g}{dt}\right) = k_i a (C_E^* - C_{EL}) V_L \quad (2)$$

The equilibrium concentration of ethylene at the gas-liquid interface (C_{E^*}) is estimated by equating the fugacities of ethylene in the gas and liquid phases (eq. 3).

$$y_E \phi_i P = x_{E^*} \gamma_i P_s; \text{ where } x_{E^*} = C_{E^*} V_m \quad (3)$$

$$C_E^* = \left(\frac{\phi P}{P_s \gamma_i V_m}\right) \quad (4)$$

The gas phase (ϕ) fugacity coefficient is estimated using the following equations (5)³⁰

$$\ln \phi = \frac{B_i}{B} (Z - 1) - \ln(Z - B) + \frac{A}{2.828B} \left[\frac{B_i}{B} - \frac{2}{a\alpha} \sum_j y_j (a\alpha)_{ij} \right] \times \ln \left[\frac{Z + 2.414B}{Z - 0.414B} \right] \quad (5)$$

The liquid phase fugacity coefficient is estimated by the Universal quasi-chemical equation (UNIQUAC) equation (6) developed by Abrams and Prausnitz.³¹

$$\ln \gamma_1 = \ln \frac{\phi_1}{x_1} + \frac{z}{2} q_1 \ln \frac{\theta_1}{\phi_1} + \phi_2 \left(l_1 - \frac{r_1}{r_2} l_2 \right) - q_1' \ln(\theta_1' + \theta_2' \tau_{21}) + \theta_2' q_1' \left(\frac{\tau_{21}}{\theta_1' + \theta_2' \tau_{21}} - \frac{\tau_{12}}{\theta_2' + \theta_1' \tau_{12}} \right) \quad (6)$$

The saturation vapor pressure of ethylene P_s , is estimated using the Antoine equation (7) as follows:

$$\ln P_s = A - \frac{B}{T + C} \quad (7)$$

The ethylene concentration in the liquid phase (C_{EL}) is obtained from knowing the ethylene transferred from the external reservoir as follows

$$C_{EL} = \left(\frac{P_{g,I} - P_g}{RT} \right) \frac{V_R}{V_L} \quad (8)$$

Substituting eqs. 3, 4 and 8 into eq. 1 and rearranging, we obtain eq. 9.

$$-\left(\frac{dP_g}{dt} \right) = k_l a \left[\frac{\phi P R T V_L}{P_s \gamma_i V_m V_R} - P_{g,I} + P_g \right] \quad (9)$$

Integrating the equation using the initial condition ($t = 0, P_g = P_{g,I}$) yields

$$\ln \left[\frac{\frac{\phi P R T V_L}{P_s \gamma_i V_m V_R} - P_{g,I} + P}{\frac{\phi P R T V_L}{P_s \gamma_i V_m V_R}} \right] = k_l a t \quad (10)$$

Solution of the equation results in the following linearized equation.³⁴

$$\ln \left[\frac{\frac{\phi P R T V_L}{P_s \gamma_i V_m V_R} - P_{g,I} + P_g}{\frac{\phi P R T V_L}{P_s \gamma_i V_m V_R}} \right] = k_l a t \quad (11)$$

Reliable estimations of $k_l a$ were obtained by regressing the transient ethylene pressure profiles corresponding to low uptake values (up to 15% of equilibrium values) where the differences in mass transfer rates at various stirring speeds are easily discerned. Further, at these levels of ethylene uptake, the volumetric expansion is low (< 2%) and hence the assumption of constant liquid phase volume is valid. By plotting the observed P_g vs. t values according to equation (4), linear plots are obtained (Figure 2-7), confirming the first-order nature of the mass transfer process. As shown in Figure 2-8, the $k_l a$ values (slopes of the plot in Figure 2-7) increase with stirring and reach an asymptotic value beyond 1200 rpm.

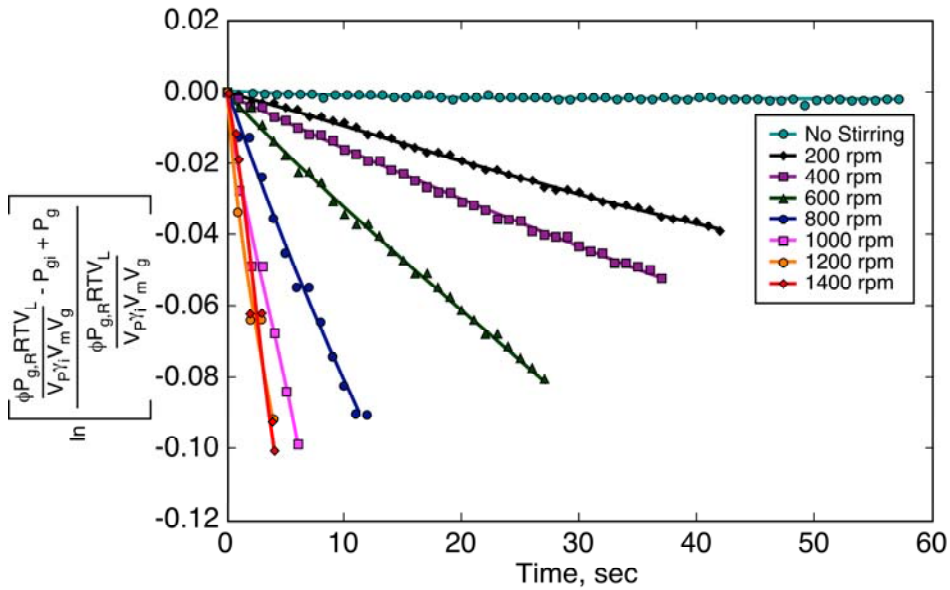


Figure 2-7: Regressed ethylene uptake profiles at various stirring speeds using first-order model. Slopes provide the mass transfer coefficients

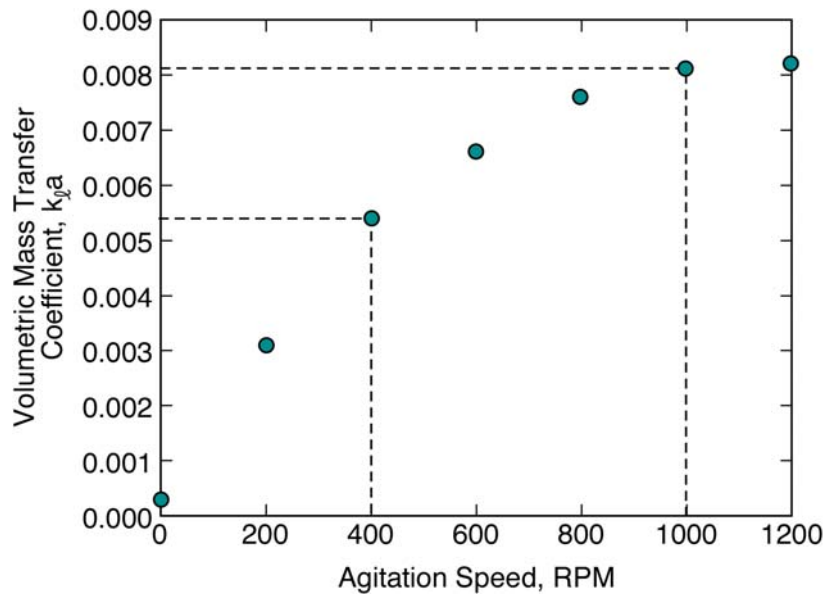


Figure 2-8: Variation of volumetric mass transfer coefficient with stirring speed. $P = 50$ bars; $T = 25$ °C; Initial composition of the liquid phase: 0.748 mol methanol + 0.134 mol H_2O_2 + 0.253 mol H_2O

The values of the volumetric mass transfer coefficients ($k_{l,a}$) for the ethylene+methanol (binary), ethylene + 0.748 mol methanol + 0.1344 mol H₂O₂ + 0.253 mol H₂O (quaternary) and ethylene + 0.21 mol *t*-butyl alcohol + 0.08 mol H₂O₂+ 0.11 mol H₂O (quaternary) systems are summarized in Table 2-1. At 1200 rpm, the $k_{l,a}$ values for these systems are 0.0135 s⁻¹, 0.0082 s⁻¹ and 0.0355 s⁻¹ respectively. It must be noted that when increasing the stirring speed from 400 rpm to 1200 rpm, the volumetric mass transfer coefficient increases by threefold for the binary system, and by a factor of 1.6 and 2.9 for the quaternary systems. Consequently, enhanced EO yields were observed in the absence of mass transfer limitations. As seen in Figure 2-9, the temporal EO yields at 40 °C and 50 bars are enhanced several-fold at 1200 rpm compared to operation at 400 rpm. At the end of 5 h, the EO yield obtained at 1200 rpm (0.049 mol) is more than an order of magnitude greater than that obtained at 400 rpm.

Table 2-1: Volumetric mass transfer coefficients for ethylene+methanol binary and ethylene+0.748 mol methanol +0.134 mol H₂O₂+0.253 mol H₂O and ethylene + 0.21 mol *t*-butyl alcohol + 0.08 mol H₂O₂+ 0.11 mol H₂O quaternary mixtures

Agitation speed (rpm)	Volumetric Mass Transfer Coefficient (s ⁻¹), (10 ³)		
	Ethylene+Methanol	Ethylene+Methanol +H ₂ O ₂ /H ₂ O	Ethylene+ <i>t</i> -butyl alcohol +H ₂ O ₂ /H ₂ O
0	0.49	0.32	0.3
200	1.81	5.12	5.52
400	4.92	5.42	11.7
600	7.31	6.32	19.1
800	10.21	7.61	25.5
1000	12.12	8.12	31.4
1200	13.21	8.21	35.0
1400	13.22	8.22	35.1

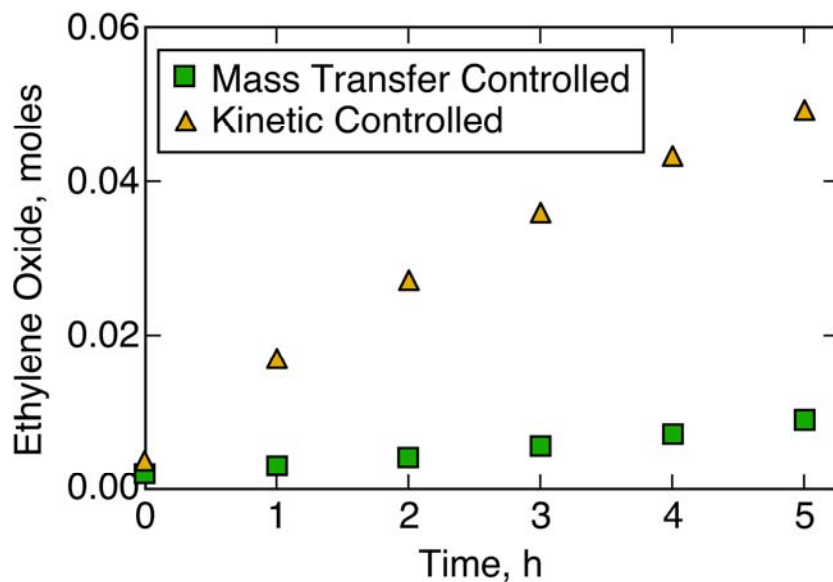


Figure 2-9: EO yield in the presence and absence of mass transfer limitations. Ethylene P= 50 bars; T= 40 °C; MTO amount = 0.361 mmol; methanol = 0.748 mol; H₂O₂ = 0.116 mol; H₂O = 0.220 mol; acetonitrile = 0.0191 mol; pyridine *N*-oxide = 2.19 mmol; batch time = 5 h; agitation speed

2.3.3 Kinetic Analysis

The temporal conversion and selectivity measurements for estimating kinetic parameters were obtained from fixed-time semi-batch studies, ensuring that interphase mass transfer limitations are eliminated. The effect of catalyst concentration on EO yield was first investigated by varying the catalyst concentration in the liquid phase. As shown in Table 2-2, the moles of EO formed, H₂O₂ consumed and H₂O formed are within 5-10% in most cases, consistent with the reaction stoichiometry. Further, the EO yield increases nearly linearly with catalyst loading (0.180-0.54 mmol) suggesting first order dependence with respect to catalyst concentration. In the presence of excess H₂O₂ (molar oxidant/catalyst ratio >10), the MTO catalyst is present as the highly active diperoxo complex.²⁰ In our experiments, the molar oxidant (H₂O₂)/catalyst

(MTO) ratio ranges from 34-102. The enhanced epoxidation rates at higher catalyst loadings are therefore attributed to the greater concentration of the active diperoxo species.

Table 2-2: Effect of catalyst loading on H₂O₂ consumption and product yields. P = 50 bars; T = 40 °C; agitation speed = 1200 rpm; methanol = 0.748 mol; H₂O₂ = 0.116 mol; H₂O = 0.220 mol; acetonitrile = 0.0191 mol; pyridine *N*-oxide= 2.19 mmol; batch time = 5 h

Catalyst, mmol	EO yield, mol	H ₂ O ₂ consumed, mol	H ₂ O produced, mol
0.180	0.0248	0.0278	0.0234
0.361	0.0493	0.0478	0.0507
0.542	0.0697	0.0710	0.0698

Kinetic measurements were performed with a fixed catalyst loading of 0.36 mmol at 50 bars and in the 20-40 °C temperature range. At these conditions, the ethylene concentration in the liquid phase is typically in excess. Continuous ethylene replenishment in the reactor to maintain constant pressure ensures that the ethylene excess is maintained throughout the reaction. At these conditions, the end-of-run (~5 h) EO yield increases from 0.015 mol to 0.049 mol as the reaction temperature is increased from 20 to 40 °C (Figure 2-10). The EO yield and selectivity at 40 °C and 50 bars are 50% (based on H₂O₂ converted) and 98+%, respectively.

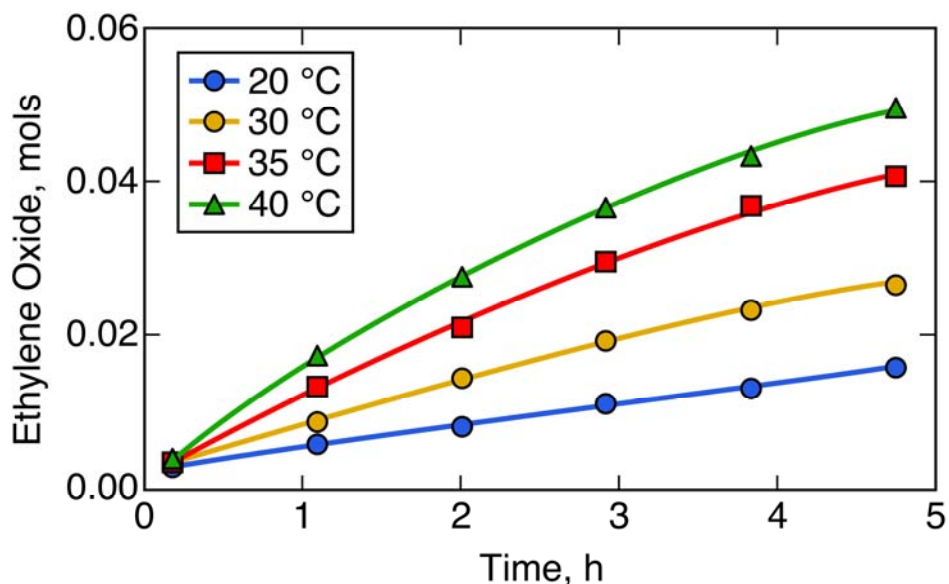


Figure 2-10: EO yields in the absence of mass transfer limitations. Ethylene P = 50 bars; T = 40 °C; agitation speed = 1200 rpm; MTO amount = 0.361 mmol; methanol = 0.748 mol; H₂O₂ = 0.116 mol; H₂O = 0.220 mol; acetonitrile = 0.0191 mol; pyridine *N*-oxide = 2.19 mmol; batch time = 5 h

For the kinetic analysis, the rate of EO formation is assumed to be first order with respect to the concentrations of ethylene (C_{EL}), hydrogen peroxide ($C_{H_2O_2}$) and the catalyst (C_{cat}). Given that the catalyst and ethylene concentrations in the liquid phase are maintained constant, the EO yield vs. time data were regressed with a simple constant-density, pseudo first order model for EO formation as follows.

$$\left(\frac{dC_{EO}}{dt}\right) = k' C_{H_2O_2,t} \quad (12)$$

where $k' = k C_{EL} C_{cat}$

Recognizing that the moles of EO formed should equal the moles of H₂O₂ converted

$$C_{H_2O_2,t} = C_{H_2O_2,0} - C_{EO,t} \quad (13)$$

Substituting eq. (6) into eq. (5) yields

$$\left(\frac{dC_{EO}}{dt}\right) = k'(C_{H_2O_2,0} - C_{EO,t}) \quad (14)$$

Initial condition: $t=0, C_{EO}=0$

$$-\ln\left[\frac{C_{H_2O_2,0} - C_{EO,t}}{C_{H_2O_2,0}}\right] = k't \quad (15)$$

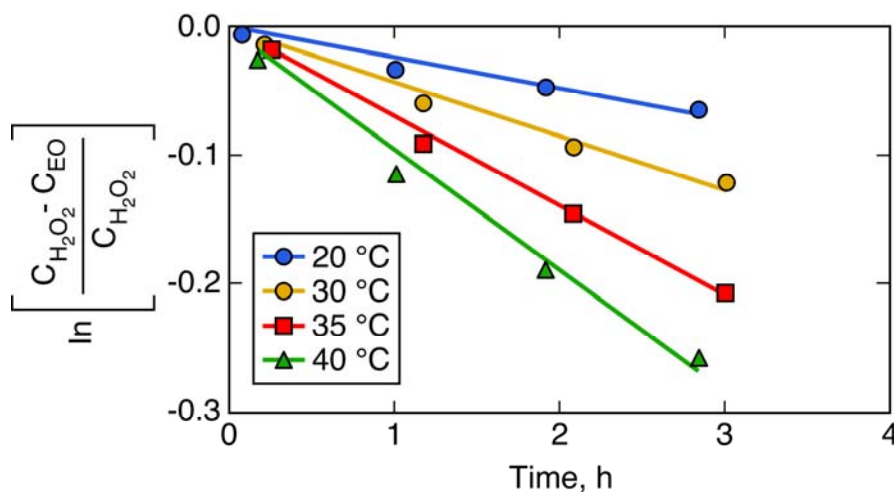


Figure 2-11: Regression of temporal EO yields based on a pseudo-first-order kinetic model. P = 50 bars; T= 40 °C; agitation speed = 1200 rpm; MTO amount = 0.361 mmol; methanol = 0.748 mol; H₂O₂ = 0.116 mol; H₂O = 0.220 mol; acetonitrile = 0.0191 mol; pyridine *N*-oxide = 2.19 mmol; batch time = 5 h

The pseudo first-order rate constant for the ethylene epoxidation system is estimated from temporal conversion and selectivity data, where the H₂O₂ conversion (and thus EO yield) is less than 15%. As inferred from Figure 2-11, the linearity of the data at each temperature, plotted

according to eq. (15), validates the assumption of pseudo-first order kinetics. The pseudo-first-order rate constants (k'), estimated from the slopes, are tabulated in Table 2-3. Arrhenius plot of these rate constants yields moderate activation energy of 57 ± 2 kJ/mol (Figure 2-12) with a pre-exponential factor of $3.8 (10^7) \text{ s}^{-1}$.

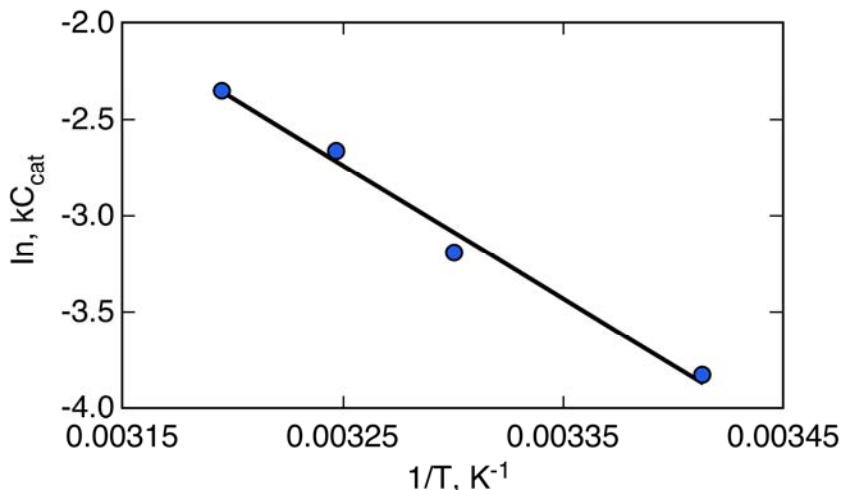


Figure 2-12: Arrhenius plot for EO formation via the CEBC EO process. P= 50 bars; T= 40 °C; agitation speed= 1200 rpm; MTO amount= 0.361 mmol; methanol=0.748 mol; H₂O₂= 0.116 mol; H₂O=0.220 mol; acetonitrile= 0.0191 mol; pyridine *N*-oxide= 2.19 mmol; batch Time = 5 h

At 50 bars and 40 °C, the volumetric mass transfer coefficient ($k_l a$) and the epoxidation rate constant (k') under the operating condition are 0.0082 s^{-1} (Table 2-2) and $2.64(10^{-5}) \text{ s}^{-1}$ (Table 2-3), respectively. The ratio of the observed reaction rate (R_{EO} , estimated from the slope of the temporal EO formation profile at early time) and the estimated reaction rate under mass transfer limitations (i.e., the product of the volumetric mass transfer coefficient and maximum

concentration of H₂O₂ in the liquid phase) is 3.21(10⁻³). This value is significantly less than the empirical criterion for the elimination of mass transfer limitations shown in eq. (16).³⁵

$$\alpha = \frac{R_{EO}}{k_l a C_{H_2O_2}} < 0.1 \quad (16)$$

Table 2-3: Rate constants for the liquid phase CEBC-EO process (P= 50 bars)

Temperature, °C	Rate constant k' , s ⁻¹
20	6.2 (10 ⁻⁶)
30	1.18 (10 ⁻⁵)
35	1.85 (10 ⁻⁵)
40	2.64 (10 ⁻⁵)

2.3.4 Comparison with Conventional Process

Table 2-4 compares the CEBC-EO process to the conventional vapor phase ethylene epoxidation process.

Table 2-4: Comparison of key parameters and performance metrics in the conventional and CEBC-EO processes

	Conventional Process	CEBC Process
Pressure, bars	10-20	50
Temperature, °C	200-300	20-40
*Conversion	10% per pass	50% per batch
EO Selectivity	80-90%	99+%
CO ₂ byproduct	10-20%	No CO ₂ detected
Productivity, g EO/h/g of active metal	2.2-4.1	1.61-4.97

*Conversion in the conventional process is based on ethylene whereas in the CEBC Process is based on H₂O₂.

The ethylene separation and recompression costs in the conventional process are suspected to be rather high due to the rather low (4-8%) per pass conversion, necessitated by the propensity of ethylene and EO to form highly flammable vapors in the presence of air. The lower flammability limit (LFL) and upper flammability limit (UFL) of ethylene in air are 3 mol% and 35 mol%.^{2, 3} The corresponding values for EO range from 3 mol% to pure EO.^{2, 36, 37} To reduce the flammability envelope, a number of diluents are employed despite these advantages burning of ethylene and EO has been observed. The build-up of CO₂ is known to adversely impact selectivity of the reaction.⁴ Thus, in the conventional process, the CO₂ concentration in the recycle stream must be minimized. In other words, the net cost of ethylene entering the reactor will be substantially more than the cost of the makeup feedstock entering the reactor. In contrast, the vapor phase in the CEBC-EO process contains no O₂, since at the operating temperature, the oxidant H₂O₂ is stable. Further, EO remains substantially dissolved in the liquid phase at the operating conditions such that EO levels in the vapor phase are below the lower flammability limit. The absence of flammable vapor in the gas phase makes the process inherently safe.

For CEBC process, the EO yield and selectivity at 40 °C and 50 bars are 50% (based on H₂O₂ converted) and 98+%, respectively. The process conditions (50 bars, 20-40 °C) in the proposed CEBC-EO process are moderate and the EO productivity 1.61-4.91 (g EO/h/g metal) is comparable to that observed in the conventional process 2.2-4.1 (g EO/h/g metal).⁵ Further, the CEBC process is highly selective towards the desired product EO and no CO₂ is detected as byproduct in either the gas or liquid phases. The efficient utilization of ethylene feedstock has the potential to make the CEBC-EO process economically favorable. However, H₂O₂ is more expensive than O₂ as oxidant and this cost must be offset by not only the savings from better utilization of feedstock but also reduced operating expenses. Further, there are no limitations on

the ethylene conversion per pass in the CEBC-EO process, which should significantly lower the ethylene purification and recycle costs. These avenues for cost savings are being investigated via comparative economic analyses of the CEBC-EO process and the conventional process. The results of the cradle-to-gate life cycle assessment are presented in Chapter 3, enabling us to assess if the savings in CO₂ emissions (as byproduct), achieved in the CEBC-EO process, are offset by CO₂ emissions resulting from either increased power consumption or from the use of other reagents that produce CO₂ as byproduct (such as H₂O₂ production). Such analyses are essential to establish quantitative performance metrics for the CEBC-EO process to be sustainable.

2.4 Conclusion

A liquid-phase homogenous catalytic process for selective ethylene epoxidation that operates at mild process³⁸ conditions uses benign reagents and completely eliminates ethylene and/or burning to CO₂ has been characterized with respect to the underlying thermodynamics, mass transfer rates and intrinsic kinetics. The activation energy for ethylene epoxidation by methyltrioxorhenium catalyst using H₂O₂ as oxidant and PyNO as promoter is moderate (+57±2 kJ/mol). These fundamental investigations have helped optimize operating conditions (P, T, stirring speed) to enhance the ethylene solubility and its rate of dissolution in the liquid phase, and thereby to maximize the EO productivity. The EO productivity in the CEBC-EO process is comparable to that in the conventional EO process.

The complete utilization of ethylene to produce EO and the inherently safe nature of the CEBC-EO process provide a stimulus for identifying the major economic drivers and establishing performance benchmarks (such as catalyst life and durability, H₂O₂ cost, reduction

in CO₂ emissions, etc.) for economic viability. Indeed, successful commercialization of such processes is needed to promote sustainability in the chemical industry.

Notation

a_{ij}	interaction parameter for the UNIQUAC model, J gmol
b_i	van der Waals co-volume of component i
C_E^*	concentration of ethylene at the gas-liquid interface (mol L ⁻¹)
C_{EL}	concentration of ethylene in the liquid phase at any time (mol L ⁻¹)
$C_{EO,t}$	concentration of ethylene oxide at time t (mol L ⁻¹)
$C_{H_2O_2,0}$	initial ($t = 0$) concentration of hydrogen peroxide in the liquid phase (mol L ⁻¹)
$C_{H_2O_2,t}$	concentration of hydrogen peroxide at time t (mol L ⁻¹)
E	activation energy (kJ mol ⁻¹)
ka	gas-liquid mass transfer coefficient (s ⁻¹)
k	intrinsic rate constant for epoxidation reaction (L mol ⁻¹ s ⁻¹)
k'	kC_E , pseudo first order rate constant (s ⁻¹)
l_1	van der Waals surface area parameter of component 1
P	reactor pressure held constant at a predetermined value (bar)
P_g	pressure in the external ethylene reservoir at time t (bar)
$P_{g,1}$	initial ethylene pressure in the external reservoir (bar)
P_s	saturation vapor pressure of ethylene at reactor pressure and temperature (bar)
q_l	molecular surface area contribution for each functional group
r_1	van der Waals volume parameter of component 1
r_{EO}	rate of ethylene oxide formation (mol L ⁻¹ s ⁻¹)

R	universal gas constant, $0.082057 \text{ L bar}^{-1} \text{ mol}^{-1} \text{ K}^{-1}$ or $1.985(10^{-3}) \text{ Kcal mol}^{-1} \text{ K}^{-1}$ (or) $0.08314(10^{-3}) \text{ KJ mol}^{-1} \text{ K}^{-1}$
T	reactor temperature ($^{\circ}\text{C}$ or K)
t	elapsed time from the start of an experiment (s^{-1})
V_L	liquid phase volume at time t (L)
V_m	molar volume of the liquid phase (mol L^{-1})
V_R	volume of the external ethylene reservoir (L)
V_0	initial ($t = 0$) volume of the liquid phase in the reactor (L)
x_E	mole fraction of ethylene in the liquid phase
y_E	mole fraction of ethylene in the gas phase
y_j	mole fraction of component i in the gas phase
Z	compressibility factor in PREOS and co-ordination number in UNIQUAC model ($Z=10$)

Greek Letters

α	scaling factor for the mixture
ϕ	gas phase fugacity coefficient of ethylene (details in supplementary material)
γ	liquid phase activity coefficient of ethylene (details in supplementary material)
τ_{ij}	energy parameters in UNIQUAC equation
θ, θ'	area fractions

References

1. ICIS. <http://www.icis.com/chemicals/channel-info-chemicals-a-z/> (Accessed June 15th, 2010),
2. Lee, H. J.; Ghanta, M.; Busch, D. H.; Subramaniam, B., Towards a CO₂-free ethylene oxide process: Homogeneous ethylene oxide in gas-expanded liquids. *Chemical Engineering Science* **2010**, 65, (1), 128-134.
3. Zabetakis, M. G., *Flammability Characteristics of combustible gases and vapor*. 1st ed.; U.S. Department of Interior, US Bureau of Mines: 1939.
4. Rebsdatt, S.; Mayer, D., Ethylene Oxide. In *Ullmann's Encyclopedia of Industrial Chemistry*, 6th ed.; Hawkins, S.; Russey, W. E.; Pilkart-Muller, M., Eds. Wiley-VCH: New York, 2005; Vol. 13, p 23.
5. Lee, H. J.; Shi, T. P.; Busch, D. H.; Subramaniam, B., A greener, pressure intensified propylene epoxidation process with facile product separation. *Chemical Engineering Science* **2007**, 62, (24), 7282-7289.
6. The Cost of Ethylene will double in the next decade. In 2010.
7. Hancu, D.; Green, H.; Beckman, E. J., H₂O₂ in CO₂/H₂O biphasic systems: Green synthesis and epoxidation reactions. *Industrial & Engineering Chemistry Research* **2002**, 41, (18), 4466-4474.
8. Hancu, D.; Green, J.; Beckman, E. J., H₂O₂ in CO₂: Sustainable production and green reactions. *Accounts of Chemical Research* **2002**, 35, (9), 757-764.
9. Nolen, S. A.; Lu, J.; Brown, J. S.; Pollet, P.; Eason, B. C.; Griffith, K. N.; Glaser, R.; Bush, D.; Lamb, D. R.; Liotta, C. L.; Eckert, C. A.; Thiele, G. F.; Bartels, K. A., Olefin epoxidations using supercritical carbon dioxide and hydrogen peroxide without added

- metallic catalysts or peroxy acids. *Industrial & Engineering Chemistry Research* **2002**, 41, (3), 316-323.
10. Pujado, P. R.; Hammerman, J. I. Integrated Process For The Production Of Propylene Oxide. US 5599956, 1997.
 11. Durst, R. A.; Bates, R. G., Hydrogen Peroxide In *Kirk-Othmer Encyclopedia of Chemical Technology*, 5th ed.; Eul, W.; Moeller, A.; Steiner, N., Eds. Wiley: 2007; Vol. 14, p 32.
 12. Goor, G.; Glenneberg, J.; Jacobi, S., Hydrogen Peroxide. In *Ullmann's Encyclopedia Of Industrial Chemistry*, 6th Edition ed.; Hawkins, S.; Russey, W. E.; Pilkart-Muller, M., Eds. Wiley VCH: New York, 2007; Vol. 18, p 35.
 13. Cost of Hydrogen Peroxide. In 2010.
 14. ChemSystems.
http://www.chemsystems.com/about/cs/news/items/PERP%200708_3_Hydrogen%20Peroxide.cfm (Accessed July 27th, 2010),
 15. Zhou, B.; Rueter, M.; Parasher, S. Supported Catalysts Having a Controlled Coordination Structure and Methods For Preparing Such Catalysts. US 7011807 B2, 2006.
 16. Sharpless, B. K.; Yudin, A. K. Epoxidation of Olefins. US 6271400 B2, August 7th, 2001, 2001.
 17. Espenson, J. H.; AbuOmar, M. M., Reactions catalyzed by methylrhenium trioxide. *Electron Transfer Reactions* **1997**, 253, 99-134.
 18. Romao, C. C.; Kuhn, F. E.; Herrmann, W. A., Rhenium(VII) oxo and imido complexes: Synthesis, structures, and applications. *Chemical Reviews* **1997**, 97, (8), 3197-3246.
 19. Owens, G. S.; Aries, J.; Abu-Omar, M. M., Rhenium oxo complexes in catalytic oxidations. *Catalysis Today* **2000**, 55, (4), 317-363.

20. AbuOmar, M. M.; Hansen, P. J.; Espenson, J. H., Deactivation of methylrhodium trioxide-peroxide catalysts by diverse and competing pathways. *Journal of the American Chemical Society* **1996**, 118, (21), 4966-4974.
21. Yin, G.; Busch, D. H., Mechanistic Details to Facilitate Applications of an Exceptional Catalyst, Methyltrioxorhenium: Encouraging Results from Oxygen-18 Isotopic Probes. *Catalysis Letters* **2009**, 130, (1-2), 52-55.
22. Tosh, E.; Mitterpleininger, J. K. M.; Rost, A. M. J.; Veljanovski, D.; Herrmann, W. A.; Kuhn, F. E., Methyltrioxorhenium revisited: improving the synthesis for a versatile catalyst. *Green Chemistry* **2007**, 9, (12), 1296-1298.
23. Jin, H.; Subramaniam, B., Homogeneous catalytic hydroformylation of 1-octene in CO₂-expanded solvent media. *Chemical Engineering Science* **2004**, 59, (22-23), 4887-4893.
24. Laird, B.; Houndonougbo, Y.; Jin, H.; Rajagopalan, B.; Wong, K.; Kuczera, K.; Subramaniam, B., Phase equilibria in carbon dioxide expanded solvents: Experiments and molecular simulations. *Journal of Physical Chemistry B* **2006**, 110, (26), 13195-13202.
25. Determination of Hydrogen Peroxide Concentration (0.1% to 5%). <http://www.solvaychemicals.us/static/wma/pdf/6/6/2/5/XX-122.pdf> (June 10th),
26. Hurdis, E. C.; Romeyn, H., Accuracy of Determination of Hydrogen Peroxide by Cerate Oxidimetry. *Analytical Chemistry* **1954**, 26, (2), 320-325.
27. Margolis, S. A., Sources of systematic bias in the measurement of water by the coulometric and volumetric Karl Fischer methods. *Analytical Chemistry* **1997**, 69, (23), 4864-4871.

28. Margolis, S. A., Source of the difference between the measurement of water in hydrocarbons as determined by the volumetric and coulometric Karl Fischer methods. *Analytical Chemistry* **1999**, 71, (9), 1728-1732.
29. Ohgaki, K.; Nishii, H.; Saito, T.; Katayama, T., High-Pressure Phase-Equilibria for the Methanol-Ethylene System at 25 C and 40 C. *Journal of Chemical Engineering of Japan* **1983**, 16, (4), 263-267.
30. Golubev, Y. D.; Dement'eva, L.; VLasov, G. M., The Solubility of ethylene oxide in C1-4 alcohols. *Soviet Chemical Industry* **1971**, (8), 3.
31. Ogaki, K.; Takata, H.; Washida, T.; Katayama, T., Phase Equilibria for four binary systems containing propylene. *Fluid Phase Equilibria* **1988**, 43, (1), 105-.
32. Azarnoosh, A.; Mcketta, J. J., Solubility of Propylene in Water. *Journal of Chemical Engineering Data* **1959**, 4, (3), 2.
33. Bradbury, E. J.; McNulty, D.; Savage, R. L.; Mcsweeney, E. E., Solubility of Ethylene in Water - Effect of Temperature and Pressure. *Industrial and Engineering Chemistry* **1952**, 44, (1), 211-212.
34. Chaudhari, R. V.; Gholap, R. V.; Emig, G.; Hofmann, H., Gas-Liquid Mass-Transfer in Dead-End Autoclave Reactors. *Canadian Journal of Chemical Engineering* **1987**, 65, (5), 744-751.
35. Doraiswamy, L. K.; Sharma, M. M., *Fluid-Fluid-Solid Reactions*. 1st ed.; John Wiley & Sons: 1984; Vol. 2.
36. Hess, L. G.; Tilton, V. V., Ethylene Oxide - Hazards and Methods of Handling. *Industrial and Engineering Chemistry* **1950**, 42, (6), 1251-1258.

37. Jones, G. W.; Kennedy, R. E., Extinction of ethylene oxide flames with carbon dioxide. *Industrial and Engineering Chemistry* **1930**, 22, 146-147.
38. Abu Omar, M. M.; Hansen, P. J.; Espenson, J. H., Deactivation of methylrhenium trioxide-peroxide catalysts by diverse and competing pathways. *Journal of the American Chemical Society* **1996**, 118, (21), 4966-4974.

Chapter 3

Is Ethylene Oxide from Ethylene and Hydrogen Peroxide More Economical and Greener compared to Conventional Silver-Catalyzed Process?

3.1 Introduction

Ethylene oxide (EO), a bulk chemical intermediate, is produced industrially by the vapor-phase oxidation of ethylene over silver-based catalysts as shown in Figure 1-5.¹ This process employs high temperatures (200-260 °C) and moderate pressures (10-30 bar), and the selectivity towards EO is 85%.² The per-pass ethylene conversion is maintained at 4-8% to minimize side reactions, mainly the burning of ethylene (feed) and ethylene oxide (product) to carbon dioxide and to avoid flammable vapor phase mixtures.³⁻⁵ Research over the years has resulted in a dramatic enhancement in the selectivity to EO from 40% in 1949 to 85% in 2005.² Despite process advances, the burning of ethylene feedstock represents a loss of approximately \$1.1 B/yr in feedstock (based on an ethylene price of 32 ¢/lb) and approximately \$200 M/yr in potential value addition (based on an EO price of 79 ¢/lb). In addition, the CO₂ emissions (~3.4 million tonnes/yr) as byproduct pose environmental concerns.

Investigators at the Center for Environmentally Beneficial Catalysis (CEBC) have reported an alternative ethylene epoxidation technology that produces ethylene oxide with almost total EO selectivity based on converted ethylene.⁶⁻⁸ The CEBC-EO process uses hydrogen peroxide (H₂O₂) as oxidant and methyltrioxorhenium (CH₃ReO₃, abbreviated as MTO) as a homogeneous catalyst. The process is conducted in an aqueous phase containing dissolved oxidant, catalyst, a small amount of pyridine-N-oxide as catalyst promoter, and methanol as co-solvent. Ethylene

gas at 5-6 MPa is introduced into the liquid-phase reaction mixture at 20-40 °C. Because this temperature is close to the critical point of ethylene ($P_c = 5$ MPa, $T_c = 9$ °C), the compressed ethylene dissolves substantially into the liquid phase enhancing the reaction rate.⁶ The intrinsic productivity of the active metal catalyst in the Re-based CEBC-EO (1.61-4.97 g EO/h/g metal) process is comparable to that reported for the Ag catalyst-based vapor phase process (0.7-4.4 g EO/h/g metal).⁹ In the CEBC process, the EO product remains completely dissolved in the liquid-phase and the oxidant (H_2O_2) does not decompose. The absence of O_2 and EO in the gas phase eliminates vapor phase flammability and makes the reactor operation inherently safe.⁹

The present work compares economic and environmental impact analyses of the conventional silver-catalyzed process (hereafter referred to as the conventional process) and the CEBC-EO process (hereafter referred to as the CEBC process). Quantitative economic analysis during the early stages of technology development is essential to identify the major economic drivers and to set quantitative performance benchmarks (such as catalyst lifetime and leaching rate, oxidant/catalyst ratio, cooling, temperature, pressure etc.) that must be met for the new technology to be economically viable.¹⁰ Similarly, comparative cradle-to-gate life cycle assessment (LCA) of the conventional and CEBC processes will enable the identification of the major adverse environmental impacts in both processes and establish whether or not the new technology is more sustainable than the existing process. Cradle-to-gate LCA for the production of H_2O_2 by the anthraquinone and direct H_2O_2 processes to identify the major environmental impact drivers in both the processes is performed. We also perform a sensitivity analysis on the sourcing of ethylene and hydrogen from various sources to identify feedstocks with the least environmental impact. The approach to such comparative analyses is similar to the methodology previously reported by CEBC researchers for evaluating alternative hydroformylation¹¹ and

solid-acid catalyzed alkylation processes.¹²

3.2 Methodology

3.2.1 Simulation Package, Specifications and Assumptions

Aspen HYSYS[®] 2009.7.1 software was employed to perform process simulations.¹³ The software provides stream information for mass and energy flows that are utilized in the design specifications and cost estimations for various process equipment such as pumps, heat exchangers and distillation columns.¹⁴⁻¹⁷ A tray sizing utility, an optimization tool embedded in the software, aids in the energy-efficient design of distillation columns and strippers.¹³ The catalyst synthesis and regeneration section in both the processes are neglected due to the low capital costs compared to other unit operations. The physical properties of the catalysts and other solids utilized in the production of the EO and their interaction with the other components of the reaction mixture are estimated using the solid property estimator tool embedded in Aspen HYSYS[®]. UNIQUAC model is employed to estimate thermodynamic properties such as activity, compressibility, fugacity and volume. The electricity obtained from U.S. power grid is produced by a portfolio of fuel sources, and steam is produced from natural gas. Specifications and assumptions common to the PFD simulations of the two processes are summarized in Table 3-1.

Table 3-1: Assumptions common to the simulations of the conventional and CEBC-EO processes

PFD Specification	Description
Plant Capacity	200,000 tonnes/yr
Direct Costs	Installation (8.3-10%), Instrumentation and control (9.2-12%), Piping (7.3-10%), Electrical (4.6-6%), Building (4.6%), Land (1.5%), Yard (1.8%)
Indirect Costs	Engineering and Supervision (18-25%), Construction Expenses (17-20%), Legal Expenses (3%), Contractors Fees (6%) ¹⁴
Utility Costs	Steam (\$10/1000 lbs), Electricity (0.0655 \$/KWh), Cooling Water (\$0.10/1000 gal), Refrigeration (-50 °C, \$60/GJ & -30 °C, \$30/GJ) ^{14, 18}
Labor Costs	Skilled Labor (46.9 \$/person/h), Unskilled Labor (35.6 \$/person/h) ^{19, 20}
Miscellaneous Costs	Distribution, Marketing, Research and Development (10% of production cost), Depreciation Rate (10% of purchased equipment), Tax Rate (25% of total fixed capital), Operating Supplies (10% of labor costs), Plant Overhead (80% of labor costs), Maintenance Material (3% of purchased cost) ¹⁴

3.3 Process Descriptions

3.3.1 Conventional Process

The conventional silver-catalyzed ethylene epoxidation process may be viewed in three sections (Figure 3-1).^{3, 21}

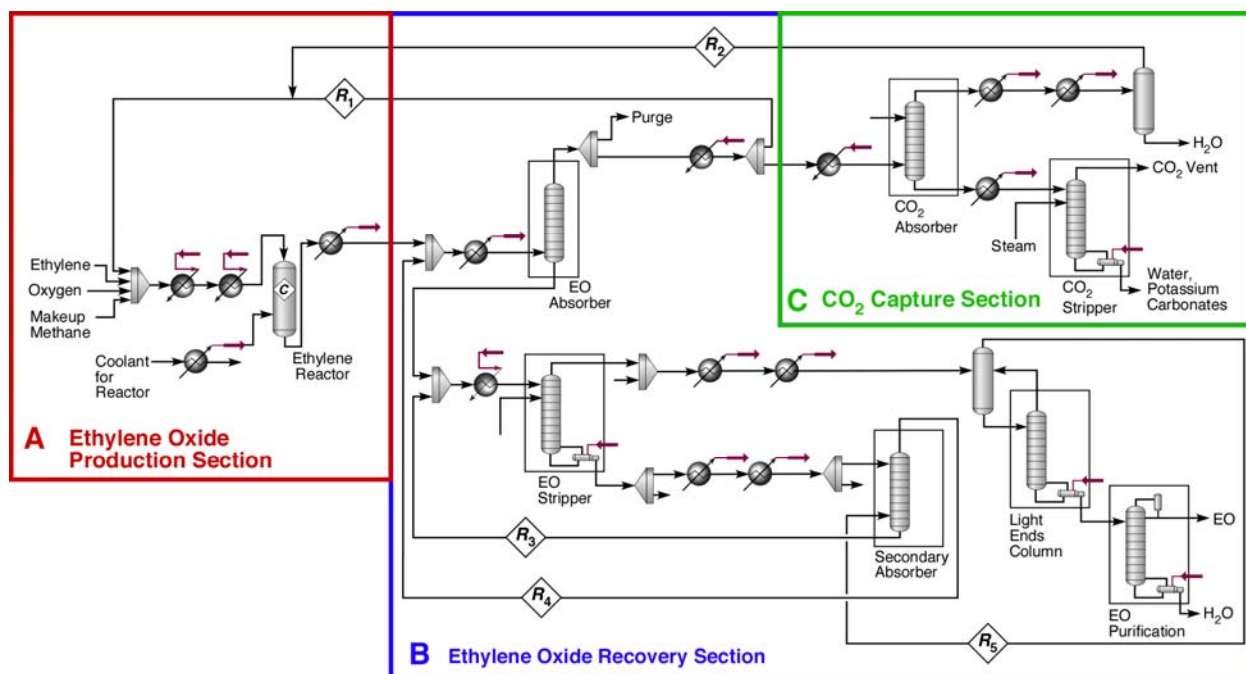


Figure 3-1: Process flow diagram for the conventional process. Table 3-2 lists the simulation parameters employed in this simulation and the compositions of the recycle (R₁₋₅) and purge streams.^{1, 22}

Ethylene epoxidation reactor (Section A): Table 3-2 summarizes simulation parameters that are unique to this process and the mass flow rates of the components entering and leaving the reactor. Along with ethylene (technical grade) and oxygen, recycled gases (N₂, Ar, CO₂ methane, and unreacted ethylene and oxygen, Table 3-2) are co-fed into three fixed-bed reactors (*volume* = 89 m³ each) in parallel. The ethylene epoxidation reaction is exothermic and sustained at 250 °C under steady operation. The gas hourly space velocity (GHSV) in the reactor is 3,300 h⁻¹. The ethylene is epoxidized to ethylene oxide over a silver-based catalyst (Ag doped with other promoting metals such as Cs, Re, and Li on a support).³ The relative feed rates, and thus the gas phase composition in the reactor, are chosen to prevent forming a flammable vapor mixture of ethylene and EO with oxygen.⁴ Reaction moderators (1.5 ppm each of ethyl chloride and vinyl

Table 3-2: Simulation parameters for the conventional process.^{3, 4, 21, 23} Mass flow rates of various components entering and leaving the reactor and in the purge and recycle streams (R₁₋₅) (in lbs/h) for the conventional process obtained from HYSYS[®] simulation

Reaction Conditions	Reactor: Fixed Bed Catalytic Reactor (three FBRs in parallel) P= 1.5 MPa; T= 250 °C; Conversion (C ₂ H ₄)= 8% per pass; Conversion (CH ₄)= 1.3% per pass GHSV (Gas Hourly Space Velocity)= 3300 h ⁻¹							
Catalyst	Ag-Cs-Re-Li on ring support							
Reaction Moderator	1.5 ppm ethyl chloride+1.5 ppm vinyl chloride							
Product Selectivity	EO=85%; Acetaldehyde=0.1%; Formaldehyde=0.01%							
Ethylene Epoxidation Reactor								
Reactants	Input	Output	Purge	R ₁	R ₂	R ₃	R ₄	R ₅
Methane	236140	233000	313	173580	58941	-	122	122
Nitrogen	1910	1910	3	1431	478	-	--	-
Ethane	6070	6070	8	4543	1516	-	-	-
Ethylene	288090	250780	332	187663	62567	-	440	440
Oxygen	92850	55710	-	41690	13903	-	28	29
Ethylene Oxide	0	50050	-	262	-	7330	33	6965
Argon	172230	172230	228	128885	42986	-	103	103
Acetaldehyde	0	51	0	0	0	0	0	0
Carbon Dioxide	69240	86690	115	64876	4330	-	1088	4
Water	3230	10380	3	9984	2102	50977	9	54

chloride) are also fed into the reactor to minimize the burning of hydrocarbons. Further, the per-pass ethylene conversion is limited to 8% to minimize side reactions.^{2, 4} The low conversions

allow the three fixed bed reactors to be approximated as a single differential reactor. A small amount of methane (1.3%) is converted to CO₂ as it passes through the reactor. The heat of reaction is recovered as medium-pressure steam that is utilized in the separation operations. The catalyst bed is reactivated by periodically taking the reactor offline to burn off the coke.

Separation of EO (Section B): The reactor effluent stream containing EO, unreacted ethylene and other feed components (CH₄, Ar, N₂, CO₂, O₂) are fed to an EO absorber (see Figure 3-1) maintained at approximately 2 MPa where the EO dissolves in water.²³ The EO absorber column is operated at a higher pressure compared to the reactor to maximize EO recovery (dissolution in the liquid phase). Ethylene glycol is added to EO absorbers and functions as an anti-foaming agent. At this absorber pressure, substantial amounts of EO are dissolved in the liquid phase. About 75% of the undissolved gases are recycled directly back to the reactor. The remaining 25% are sent to a CO₂ removal unit (described in Section C). In addition to EO, the liquid phase from the primary absorber also contains small but still significant amounts of dissolved gases. The EO along with these gases is separated from the water and ethylene glycol in a steam stripper. As shown in Figure 3-1, the overhead stream from the stripper containing EO, ethylene, CO₂, CH₄, and Ar is fed to a refrigerated light ends distillation column. Approximately 85% of the EO contained in this gas stream is separated in this column. Due to the closeness in the boiling points of acetaldehyde (20 °C) and EO (9 °C), and the presence of light gases, refrigeration is deployed to maximize EO recovery. The overhead gas stream from the light ends column contains the remaining EO and is sent to the secondary absorber, which is operated at a lower pressure. The bottom stream (R₃) from the secondary absorbers (containing dissolved EO) is sent to the steam stripper for EO recovery, while the overhead stream from the secondary absorber (R₄) is compressed and recycled back to the primary EO absorber. Thus the recovery of

EO from gaseous diluents entails EO absorption, stripping of the dissolved EO with steam, and a light ends column operated with refrigeration for EO purification. To prevent the build-up of nitrogen, a small purge stream is maintained near the overhead stream of EO absorber.

CO₂ capture for ethylene recovery (Section C): Approximately 75% of the vapor phase from the EO absorber is recycled directly back to the reactor (Table 3-2). The remaining 25% is sent to a CO₂ absorber as high CO₂ concentration in the reactor has an adverse impact on the activity and selectivity of the catalyst.²⁴ Aqueous potassium carbonate (K₂CO₃) in this absorber reacts with CO₂ in the stream to form potassium bicarbonate (KHCO₃).²¹ The vapor phase from the CO₂ absorber containing the diluents (Ar, CH₄, and N₂) and unreacted O₂ and ethylene is recycled back to the reactor. The KHCO₃ from the absorber is regenerated to K₂CO₃ by steam stripping. This process strategy moderates the CO₂ concentration recycled back to the reactor. The small quantity of CO₂ impurity present in the overhead stream of the EO stripper is separated in the light ends column.

3.3.2 CEBC-EO Process

The CEBC process consists of two production steps as shown in Figure 3-2.

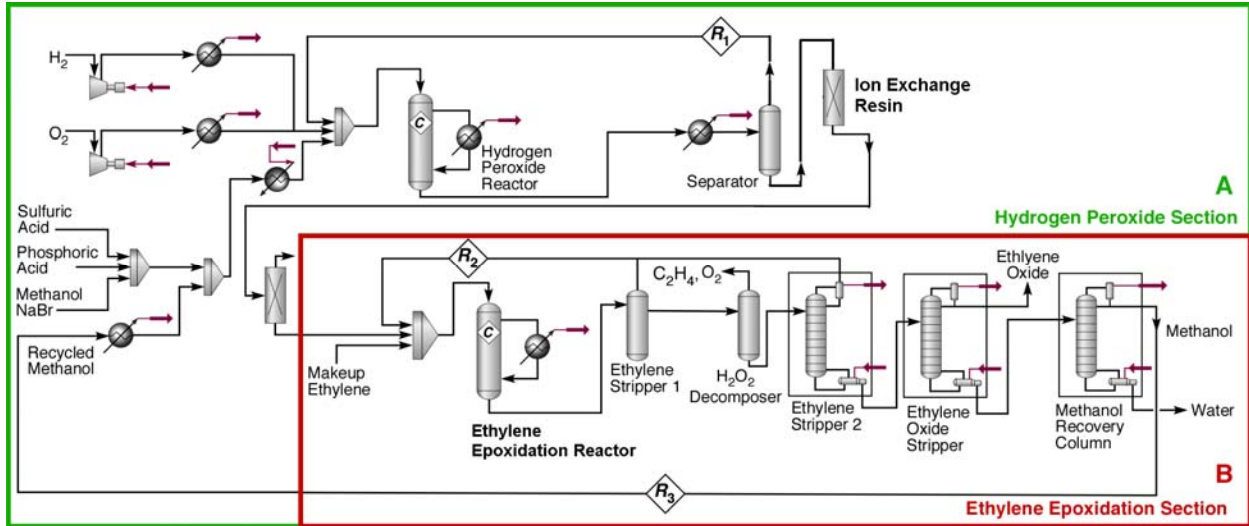


Figure 3-2: Process flow diagram: (A) Hydrogen Peroxide production; (B) CEBC ethylene epoxidation process. Table 3-3 lists the simulation parameters and mass flow-rates of the various components entering and leaving the H_2O_2 and EO reactor*

*The recirculation streams are modeled as recycle stream in the HYSYS software

Table 3-3 summarizes the simulation parameters and mass flow rates of various components entering and leaving the H_2O_2 and ethylene epoxidation reactors. In the first step (Section A), H_2O_2 is manufactured on-site by a direct route (see following section for process details). In the second step (Section B of Figure 3-2) ethylene (make-up as well as recycled), aqueous H_2O_2 , make-up catalyst and promoter, and methanol (99.99% purity) are co-fed with ethylene into a continuous stirred tank reactor (*total volume* = $341\ m^3$) fitted with a nano-filtration membrane. Mass transfer studies (Chapter 2) clearly established the importance of adequate mixing in maintaining high EO productivity in the CEBC process. Hence, for this preliminary economic analysis, we chose a CSTR equipped with a nanofiltration membrane. We assume that the total

volume is divided into three stirred reactors (114 m³) connected in parallel. The total cost of the three reactors is approximately \$10 million. The reactor pressure and temperature are 5 MPa and 40 °C, respectively. The liquid hourly space velocity (LHSV) is assumed to be 5 h⁻¹ with EO yield and selectivity values being 48% per pass and 99+% (based on ethylene) respectively.^{6, 8} It is also assumed that the MTO catalyst is bound to a soluble polymer support, and that the activity and selectivity of the catalyst are unchanged. Further, the catalyst is sufficiently bulky to be substantially retained in the reactor by the nanofiltration membrane. Only the smaller components of the reaction mixture (such as EO, unreacted ethylene, H₂O₂, methanol and H₂O) pass through the membrane. This catalyst retention strategy and reactor configuration are similar to those recently demonstrated by CEBC researchers for homogeneous hydroformylation.²⁵ The heat of reaction is removed by cooling water to maintain the reactor temperature at approximately 40°C. The oxidant (H₂O₂) is stable at the operating temperature. The absence of oxygen in the reactor gas phase eliminates the need to deploy inerts such as N₂ and Ar in the feed stream. Further, the absence of CO₂ formation obviates the CO₂ capture section required in the conventional process.⁹

Table 3-3: Simulation parameters for direct H₂O₂ and CEBC-EO processes^{6, 8, 9} Mass flow rates of various components entering and leaving the hydrogen peroxide and ethylene epoxidation reactor (in lbs/h) for the CEBC-EO process obtained from HYSYS[®] simulation

Direct H ₂ O ₂ Process							
Reaction Conditions	Reactor: Fixed Bed Catalytic Reactor (three FBR in parallel) <i>P</i> = 5.1 MPa; <i>T</i> =40 °C; Conversion (H ₂)= 76% LHSV (Liquid Hourly Space Velocity)= 5 h ⁻¹						
Catalyst	Palladium nitrate impregnated on alloy-steel monoliths prepared from mesh						
Product Selectivity	H ₂ O ₂ selectivity=82%; H ₂ O=18%						
CEBC-Liquid Phase EO Process							
Reaction Conditions	Reactor: CSTR (three CSTR in parallel) <i>P</i> = 5.0 MPa; <i>T</i> = 40 °C; Conversion (H ₂ O ₂)= 48% per batch LHSV (Liquid Hourly Space Velocity) = 5 h ⁻¹						
Catalyst	Methyl trioxorhenium (MTO)						
Product Selectivity	EO=99% (based on ethylene)						
Reactants	Hydrogen Peroxide		Ethylene Oxide		R ₁	R ₂	R ₃
	Input	Output	Input	Output			
Hydrogen	9262	20	-	-	20	-	-
Oxygen	381724	279158	-	-	-	-	-
Phosphoric Acid	1018	1018	-	-	-	-	-
Sulfuric Acid	254	254	-	-	-	-	-
Hydrogen Peroxide (H ₂ O ₂)	-	89360	89360	42800	-	-	-
Water	16388	20635	20635	41200	-	-	-
Methanol	1300190	1300190	1300190	1300190	-	-	1300190
Ethylene	-	-	67794	35224	-	35224	-
Ethylene Oxide	-	-	-	50250	-	-	-
MTO (catalyst)	-	-	2212	-	-	-	-

Reaction mixture is re-circulated through a series of coolers to remove the heat of reaction.

The recirculation streams are modeled as recycle stream in the HYSYS software.

Further, in addition to this base case two cases of the CEBC-EO process are benchmarked

against the conventional process and comparative economic and environmental assessment performed. In the first case (Case 1), (a) Hydrogen Peroxide oxidant is synthesized directly from hydrogen and oxygen; (b) the heat of reaction from the EO reactor is removed by refrigeration and (c) the unreacted H_2O_2 is recovered from the liquid phase by distillation. In the second case (Case 2), (a) the H_2O_2 is procured from an external supplier; (b) the heat of reaction from EO reaction is removed by cooling water (since the reaction T is $40\text{ }^\circ\text{C}$) and (c) the H_2O_2 is safely decomposed before the reactor effluent is sent for EO product recovery.

The bulk of the unreacted ethylene is recovered by simple depressurization from the reactor pressure of 5 MPa to 0.5 MPa in ethylene stripper 1. The presence of unreacted H_2O_2 in the reactor effluent streams poses safety concerns. For example, methanol and H_2O_2 in the vapor phase can lead to the formation of explosive mixtures in the distillation column. Hence, unreacted H_2O_2 is decomposed post-reaction at $50\text{ }^\circ\text{C}$ (below methanol boiling point) prior to secondary recovery of the remaining unreacted ethylene (in ethylene stripper 2). The effluent from this decomposer is a gaseous mixture of oxygen and ethylene whose composition lies below the lower flammability limit (LFL) of mixture.⁴ In the absence of H_2O_2 , the EO product and methanol solvent can be safely separated by distillation. It must be noted that the CEBC process is similar to the Dow/BASF (Hydrogen Peroxide/Propylene Oxide, HPPO) process in many respects.^{26, 27} Both processes use H_2O_2 as oxidant and methanol as solvent. Further, the operating pressures (a few MPa) and temperatures ($25\text{-}35\text{ }^\circ\text{C}$) are similar.

MTO catalyst synthesis and performance metrics: The high cost of rhenium ($3,000\text{ } \$/\text{lb}$)²⁸ necessitates the near complete recovery of the MTO catalyst. Recently, a green and improved route for MTO synthesis was reported by Herrmann et al.²⁹ Based on this reported procedure, the cost of fresh catalyst and the cost of periodically reconstituting the catalyst are assumed to be

\$5,000/lb and \$2,000/lb, respectively. Strategies for MTO immobilization on polymer supports have been reported by Saladino et al.^{30, 31} and Bracco et al.³¹

3.3.3 Direct Hydrogen Peroxide Process

Recently, new technologies for a H₂O₂ process, by direct synthesis from H₂ and O₂, have been reported by Headwaters Technology Innovation³², Evonik³³ and BASF.³⁴ Presently, H₂O₂ is manufactured commercially by the alkylanthraquinone route.³⁵ In the direct H₂O₂ process patented by BASF (Section A of Figure 3-2), the synthesis of H₂O₂ in methanol is facilitated by a Pd(NO₃)₂ catalyst supported on a steel monolith in a fixed bed reactors (*Volume* = 190 m³).^{27, 34} The liquid hourly space velocity (LHSV) is estimated to be 5 h⁻¹.³⁶ Under optimized conditions of 40 °C and 5.1 MPa, the reported conversion (based on H₂) and selectivity towards H₂O₂ are 76% and 82% respectively, with water as byproduct. Temperature control in the reactor is achieved by re-circulating a portion of the liquid stream through a series of heat exchangers to remove the heat of reaction. The unreacted H₂ is recovered and recycled (R₁) back to the reactor. The concentration of H₂O₂ in the reactor effluent stream is approximately 7 wt%.³⁴

3.3.4 Anthraquinone Process

Alkylanthraquinone (2-ethylanthraquinone) is dissolved in a suitable aromatic solvent and is catalytically hydrogenated to 2-ethylanthrahydroquinone in the presence of palladium metal supported on a silica support. The reaction mixture is filtered to recover the palladium catalyst from the hydroquinone solution. The degree of hydrogenation is maintained at 45-50% to minimize secondary reactions. The hydroquinone solution is non-catalytically oxidized with air at 30-40 °C at pressures of up to 5 bar, to obtain hydrogen peroxide and the resulting

anthraquinone is recycled for hydrogenation. The concentration of hydrogen peroxide in the product mixture is 7.0 wt%. The H₂O₂ is extracted from the reaction mixture using demineralized water in a liquid-liquid sieve tray column operated in counter-current mode. The difference in the density of the reaction mixture and extractant (water) is exploited to minimize the required surface area of the liquid-liquid contactor. Both, the hydrogenation and oxidation steps are highly exothermic and the heat of reaction is removed by conventional methods such as precooling of the reaction mixture and the deployment of cooling water jackets and internal cooling coils.^{37, 38} The hydrogen peroxide concentration in the reactor effluent stream is similar in both the standard anthraquinone and direct H₂O₂ process. Further, the palladium loading on the support is 0.7 wt% in both processes; the environmental impact of mining palladium for catalyst preparation is similar for both the technologies.

3.4 Capital Costs

Fixed capital investment includes the cost of purchased equipment, offsite installed capacity, direct and indirect installation costs.¹⁴ The total capital investment is estimated based on standard methods. The methodology to estimate the reactor cost is shown in Appendix C (Section C3). All costs were adjusted to 2010 dollars using Chemical Engineering Plant Cost Index (CEPCI).³⁹ *Direct costs* were estimated as a percentage of purchased equipment costs, and include all the expenses for the purchase and installation of piping, instrumentation and control, electrical, insulation and land use. *Indirect costs* were estimated as a percentage of direct costs, and include the cost of engineering and supervision, construction expenses, legal expenses, and contractor's fees. *Offsite* installed capacity includes water purification systems to remove dissolved salts from cooling and boiler feed water and refrigeration units for cooling the propane refrigerant.

Unscheduled Expenses and Contingency Fund expenses amount to 10% and 25%, respectively, of the fixed capital investment.¹⁴

3.5 Production Costs

Production costs include raw materials, labor and utility expenses. The costs of raw materials, products, catalysts and solvents are derived from a variety of sources including the Chemical Market Reporter.⁴⁰ In recent years, the market price of ethylene has varied between \$700/tonne in 2001 to \$1,700/tonne in 2008. The ethylene price in mid-2010 has been relatively stable at \$900/tonne.⁴⁰ Hence, the 2010 costs of raw materials and products were used in the economic analysis. *Utility costs* associated with cooling water, electricity and steam in both processes are estimated based on the energy balance calculations obtained from Aspen HYSYS[®]. The unit cost of various utilities was obtained from the Energy Information Administration, US Department of Energy.⁴¹ The analysis includes plant overhead costs related to research and development, distribution, marketing and administration. *Operating labor* expenses are determined by plant capacity and the number of principal processing steps. The U.S. Bureau of Labor and Engineering News Record provides average hourly wage and monthly labor indices for both skilled and unskilled labor.^{19, 20} *Annual depreciation and tax rates* are assumed to be 10% and 25%, respectively, for all processes. *Gross profit* is estimated as the difference between the revenue generated by the sale of products and byproducts less production costs. *Net profit* is estimated after deduction of tax.

3.6 Environmental Impact Analysis

Comparative cradle-to-gate life cycle assessments (LCA) were accomplished using GaBi

4.4[®] software developed by PE solutions.⁴² This software contains U.S. specific datasets (such as impacts arising from shale gas recovery, coal and natural gas based power generation, etc.) and incorporates TRACI (Tool for the Reduction and Assessment of Chemicals and Other Environmental Impacts), a computer database developed by the U.S. Environmental Protection Agency (USEPA) for conducting a U.S.-specific environmental assessment.⁴³ The impact assessment methodologies within TRACI are based on a midpoint characterization approach proposed by the International Panel of Climate Change (IPCC).⁴⁴ This LCA analysis incorporates all direct and indirect environmental impacts associated with raw material production and processing. Thus, the boundaries of this LCA analysis include raw material extraction, transport and processing. Quantitative information on the various mass and energy streams associated with the conventional and CEBC processes are obtained from Aspen HYSYS[®] simulations. The cumulative environmental impacts due to potential emissions from these streams per annum are compared with respect to various environmental impact categories such as acidification, global warming potential, ecotoxicity, human carcinogenic and non-carcinogenic effects, and eutrophication. Descriptions of the various impact categories are listed in Table 3-4. From these results, potential sources of significant environmental impacts are identified. The approach is similar to recently reported case studies and techno-economic analysis have been reported in literature.^{45, 46}

Table 3-4: Impact categories considered in cradle-to-gate LCA⁴³

Impact Category	Description
Global Warming Potential	Refers to the change in climate caused by the buildup of chemicals that trap heat from the reflected sunlight that would have otherwise passed out to earth's atmosphere
Acidification	Refers to the increase in acidity of water and soil systems
Ecotoxicity	Quantifies the potential ecological harm of unit quantity of chemical released into an evaluative (soil, water and air) environment
Eutrophication	Estimates the release of chemicals containing N or P to air or water
Human Health Cancer	Potential of a chemical released into an evaluative environment to cause human cancer effects
Human Health Non-Cancer	Potential of a chemical released into an evaluative environment to cause human non-cancer effects
Smog Air	Potential of a chemical to cause photochemical smog
Ozone Depletion Potential	Potential to destroy ozone based on chemical's reactivity and lifetime

3.6.1 Basis

A U.S.-specific life cycle assessment (cradle-to-gate) is made to quantify the environmental impacts of producing 50,050 lb/h (or ~200,000 tonnes/year) of ethylene oxide by both the conventional and the CEBC processes. The environmental impacts due to mining of rhenium, palladium and silver catalysts are not considered in this analysis due to the lack of information. Moreover, the actual amounts these metals used are small compared to the usage of the other raw materials. Because potassium carbonate and potassium bicarbonate datasets are not included in our GaBi database, we substitute the environmental impacts of processing these material with those associated with sodium carbonate and sodium bicarbonate. The similarity in extraction, processing and synthesis steps is the rationale behind this assumption. Further, we compare the environmental impact of producing 219,000 tonnes/yr of H₂O₂ using the standard anthraquinone and direct H₂O₂ technology. The palladium loading on the support is 0.7 wt% in both the processes; the environmental impact of mining palladium for catalyst preparation is similar for both the technologies. In our analysis, the post reaction separation and concentration steps are

neglected in the LCA of both the anthraquinone and direct H₂O₂ processes due to similar environmental impacts.

Given that ethylene, hydrogen and energy may be derived from various sources, the effects of their sourcing on the overall environmental impact of the CEBC process have been studied. The bases are taken as (i) *400,000 metric tonnes of ethylene/yr* produced from each of the following sources: crude oil, natural gas and corn. The process details for the simulation of an ethylene cracker were obtained from literature.⁴⁷; (ii) *100,000 metric tonnes of hydrogen/yr* produced from each of the following sources: methane, naphtha, light gases and as a byproduct from a Chlor-Alkali plant; (iii) *1000 MJ* of energy produced from each of the following sources: natural gas, coal (hard coal and lignite coal considered separately) and fuel oil (heavy fuel oil and light fuel oil considered separately). The assumptions and boundaries for ethylene and hydrogen production in the U.S. from the various feedstocks are described in the following section.

3.6.2 Raw Material Sources

3.6.2.1 Production of Ethylene Oxide and Hydrogen Peroxide

The mass flow rates of the various raw materials consumed during steady operation of these processes are shown in Figures 3-3, 3-4, 3-5 and 3-6.

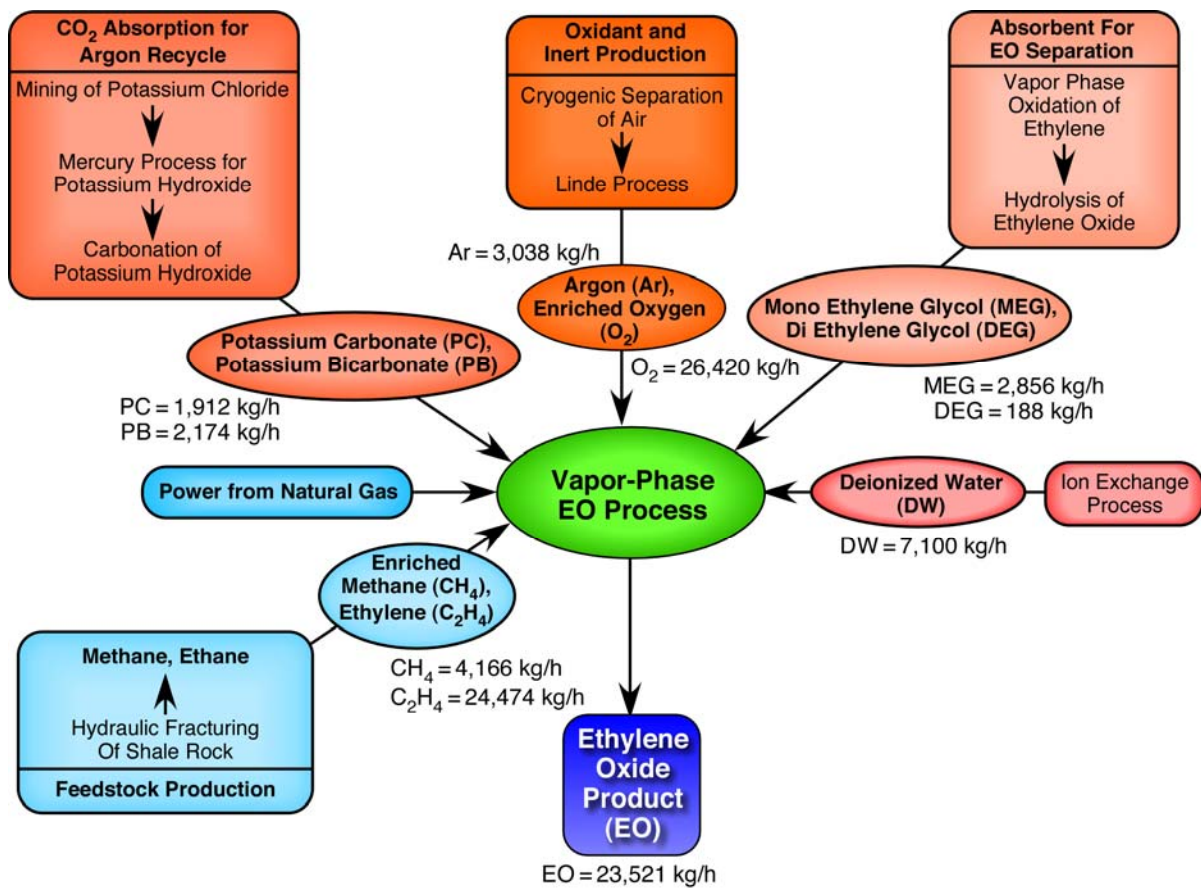


Figure 3-3: Boundaries of the conventional silver-catalyzed ethylene epoxidation process considered in the cradle-to-gate LCA.

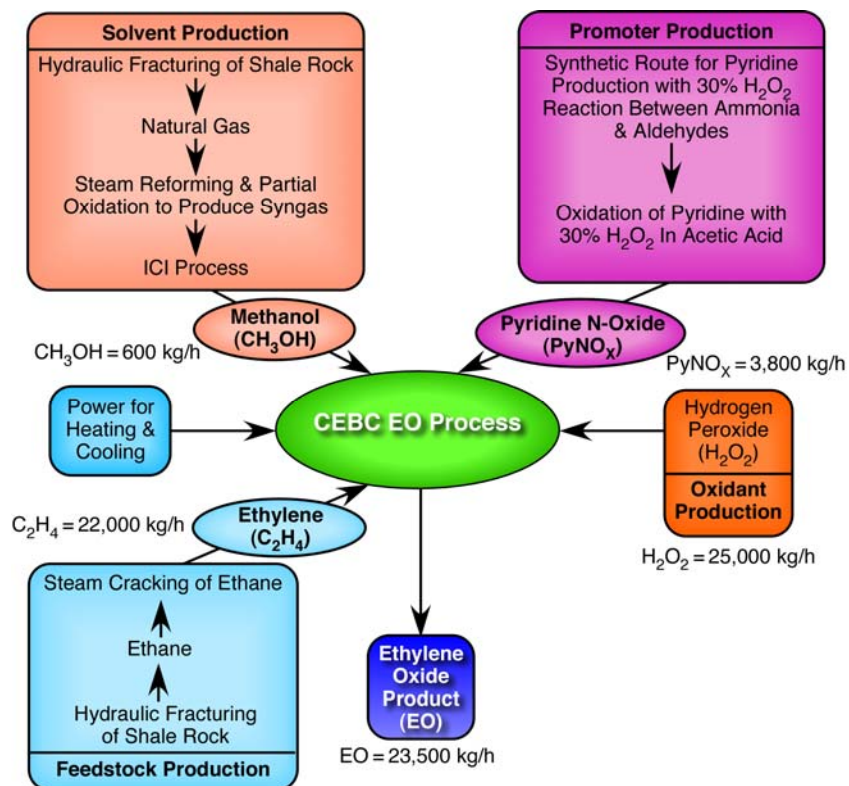


Figure 3-4: Boundaries of the CEBC-EO process considered in the cradle-to-gate LCA

Natural gas is a major raw material source for producing ethylene, hydrogen and methanol required in the two processes. Further, a small amount of methane is used as diluent in the conventional process. In the U.S., methane is recovered from natural gas either from conventional wells or by the hydraulic fracturing of shale rock.⁴⁸ Raw natural gas is a mixture of crude oil, hydrocarbons (methane, ethane, propane, butane and pentanes), water vapor, H₂S, CO₂, He and N₂. Oil and moisture are removed by simple depressurization followed by phase separation. The remaining water vapor is absorbed by glycols. The H₂S and CO₂ are removed by treatment with an amine solution. Finally, methane is separated from the other hydrocarbons by fractional distillation.⁴⁹

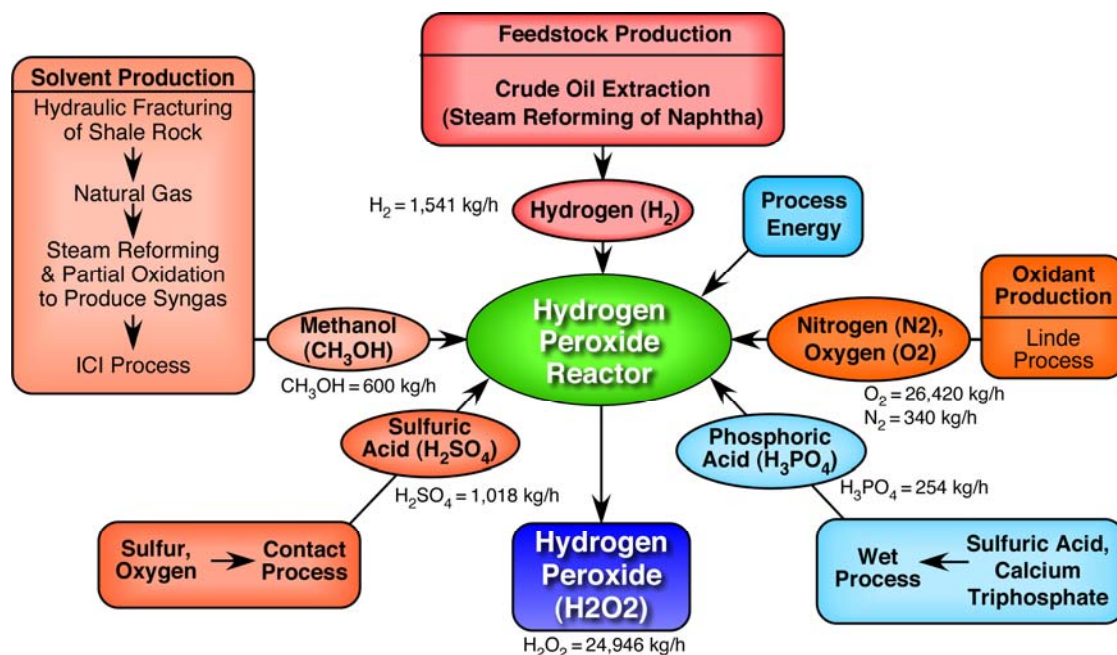


Figure 3-5: Boundaries of the direct H₂O₂ process considered in the cradle-to-gate LCA

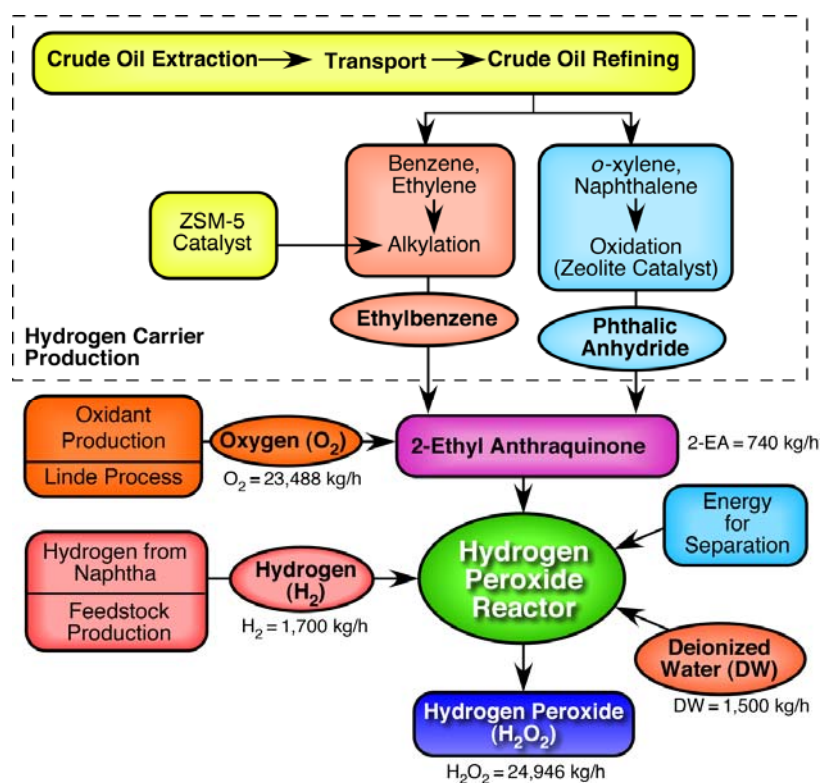


Figure 3-6: Boundaries of the Anthraquinone Process considered in the cradle-to-gate LCA.

Ethylene is produced by cracking ethane (obtained from natural gas) and is separated from unconverted ethylene by energy-intensive fractional distillation at low temperatures. The energy required to produce either 97.9% or polymer grade purity 99.99% ethylene is also considered in this environmental assessment.⁵⁰ *Hydrogen* is primarily produced by cracking of ethane to ethylene, by steam reforming of naphtha or of methane, or as a byproduct from chlor-alkali plants.⁵¹ Methanol is obtained via the ICI[®] process⁵² wherein methane is steam reformed to produce synthesis gas which is transformed to methanol. *Pure argon* and *oxygen* are produced by the cryogenic separation of air (Linde[®] process).⁵³

Pyridine-N-Oxide is prepared by the oxidation of pyridine with 30% H₂O₂ in acetic acid. Industrially, pyridine is produced by the reaction of acetaldehyde and formaldehyde with ammonia in the presence of solid-acid catalysts at high temperatures and space velocity.⁵⁴ *Sulfuric acid* and *phosphoric acid* are produced by the Contact[®] process⁵⁵ and Wet[®] process.⁵⁶

Potassium carbonate and potassium bicarbonate: Potassium chloride mined from solid ores is electrolyzed (via the Mercury[®] process) to produce potassium hydroxide in high purity which is further reacted with CO₂ to form potassium carbonate.⁵⁷ *Glycols (mono-ethylene and di-ethylene glycols)* are produced by EO hydrolysis in excess H₂O.⁵⁸ *Deionized water* is produced by purifying water in a mixed bed ion exchanger.⁵⁹

The environmental impacts associated with the production of all raw materials are taken into account. Further, as appropriate, the emissions associated with the transport of crude oil and natural gas from exporting nations to the U.S. and the desulfurization of crude oil are also considered.⁵¹

2-Ethylantraquinone, the hydrogen carrier, is prepared by the reaction of ethylbenzene and phthalic anhydride.⁶⁰ Ethylbenzene is synthesized by the alkylation of benzene, a refinery

product. Benzene is reacted with ethylene in the presence of H-ZSM-5, a stable recyclable catalyst (Mobil-Badger[®] process).⁶¹ Similarly, phthalic anhydride is manufactured by the catalytic oxidation of o-xylene (oxidation of o-xylene in presence of vanadium pentoxide with titanium trioxide-antimony trioxide catalyst), a refinery product and by the oxidation of naphthalene (vapor phase oxidation of naphthalene in air in presence of vanadium oxide catalyst).⁶²

3.6.2.2 Production of Ethylene

Ethylene from naphtha: This LCA analysis incorporates the environmental impacts due to the energy investment needed for the extraction of crude oil from the reservoirs, transportation to a refinery in the U.S. and further processing to produce ethylene. The transportation involves the pumping of the crude oil from the Middle Eastern source to the nearest seaport via pipeline, subsequent shipping in a tanker to the U.S. (distance is assumed to be 8000 km, typical of the distance from a Middle East destination), and delivery from the U.S. port of entry to the refinery *via* pipeline. Naphtha is a low boiling fraction obtained from the distillation of crude oil. Steam cracking of naphtha gives a mixture of olefins.⁶³ Natural gas is assumed to be the source of process energy for heating. Figure 3-7 shows the boundaries of the various processes considered in this analysis for the naphtha feedstock. A weighting factor of 0.058 (calculation shown in Appendix D) is allocated based on the proportional allocation method to estimate the environmental impacts associated with ethylene production from naphtha.

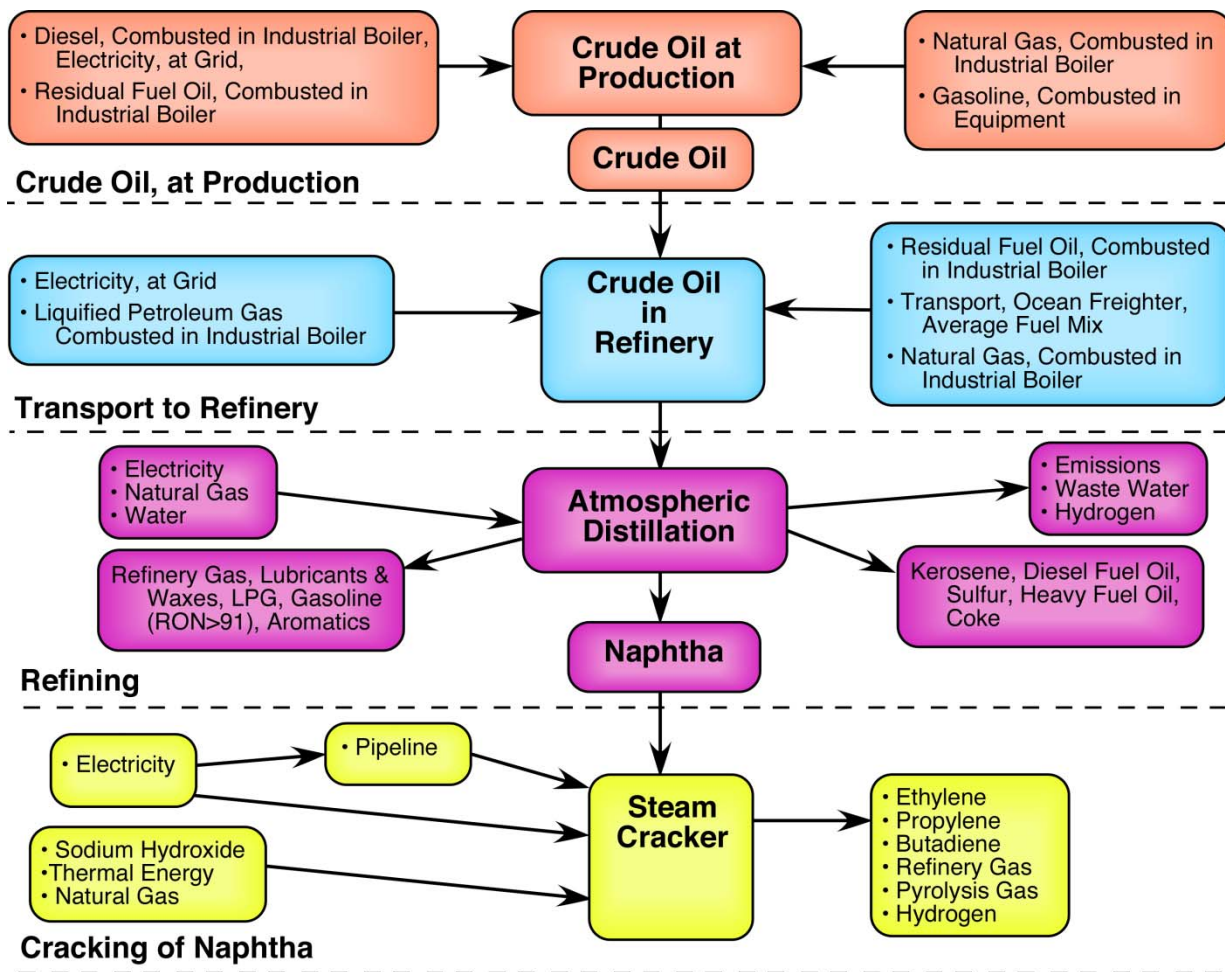


Figure 3-7: System boundaries for the production of ethylene from crude oil

Ethylene from natural gas: Natural gas obtained from shale rock is a mixture of hydrocarbons. Typical composition of natural gas is methane (70-90 mole%), light alkanes [ethane, propane, butane (0-20 mole%)], carbon dioxide (0-8 mole%), oxygen (0-0.2 mole%), nitrogen (0-5 mole%), hydrogen sulfide (0-5 mole%) and traces of rare gases such as argon, helium, neon and xenon.⁴⁹ The composition of the natural gas is based on the feed source and location. Natural gas processing entails the purification and separation of various hydrocarbon fractions. The natural gas is separated from oil by simple depressurization. The bulk of the water in the natural gas is removed by simple phase separation. However, the removal of remaining water vapor is

accomplished by dehydrating the natural gas either by adsorption using solid desiccant or glycol-based dehydrating agents. Due to the large affinity of water to glycols, the trapped water vapor in natural gas is easily absorbed by glycols upon contact.

Valuable hydrocarbons such as ethane, propane, butane are separated from methane by fractional distillation. In addition to water, oil and natural gas liquids, raw natural gas often contains hydrogen sulfide (H_2S) and CO_2 . In presence of water, CO_2 forms carbonic acid which is corrosive and also reduces the BTU value of the natural gas by 2% or 3%. Natural gas contains substantial quantities of H_2S that are extremely toxic and corrosive to equipment and pipelines. Sour natural gas is made virtually sulfur- and CO_2 -free by treatment with an amine solution. The amine solution is regenerated by recovering the absorbed H_2S and CO_2 .^{49, 51} Natural gas processing plants account for 15% of the total U.S. sulfur production. Figure 3-8 is a pictorial representation of the various processes considered in this analysis. Ethane so obtained is cracked to produce ethylene. Natural gas is also assumed to be the source of energy for all the above-mentioned steps. A weighting factor of 0.125 (calculation shown in Appendix D) is allocated based on the proportional allocation method to estimate the environmental impacts associated with ethylene production from natural gas.

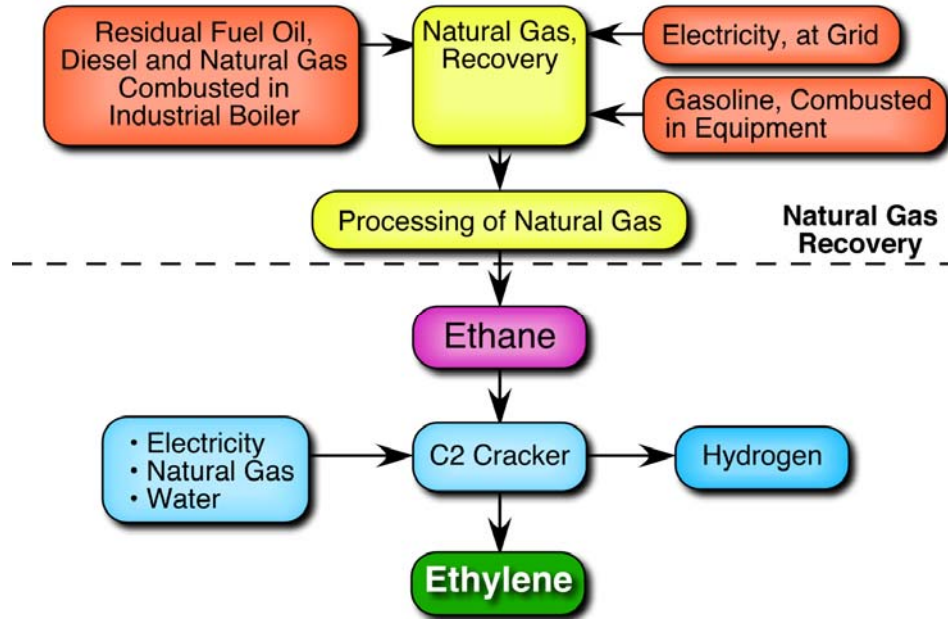


Figure 3-8: System boundaries for the production of ethylene from natural gas.

Ethylene from ethanol: The energy-consuming processes associated with ethanol production from corn include soil cultivation, planting, pesticide and fertilizer manufacture and its application, harvesting, transport to the refinery, fermentation, and distillation of ethanol to remove the water. The fertilizers used are urea, monoammonium phosphate, ammonium nitrate and NPK-15. The byproduct of corn processing is dried distillers grain seed (DDGS also referred to as dried laitance), which has economic value as either animal feed or as a solid fuel. Natural gas is assumed to be the source of energy for all the above-mentioned steps. The net calorific value of DDGS and ethylene serves as the basis for allocating the environmental impact of ethylene production from ethanol. A graphical representation of the various boundaries in this analysis is shown in Figure 3-9. A weighting factor of 0.63 (calculation shown in Appendix D) is allocated based on the proportional allocation method to estimate the environmental impacts associated with ethylene production.

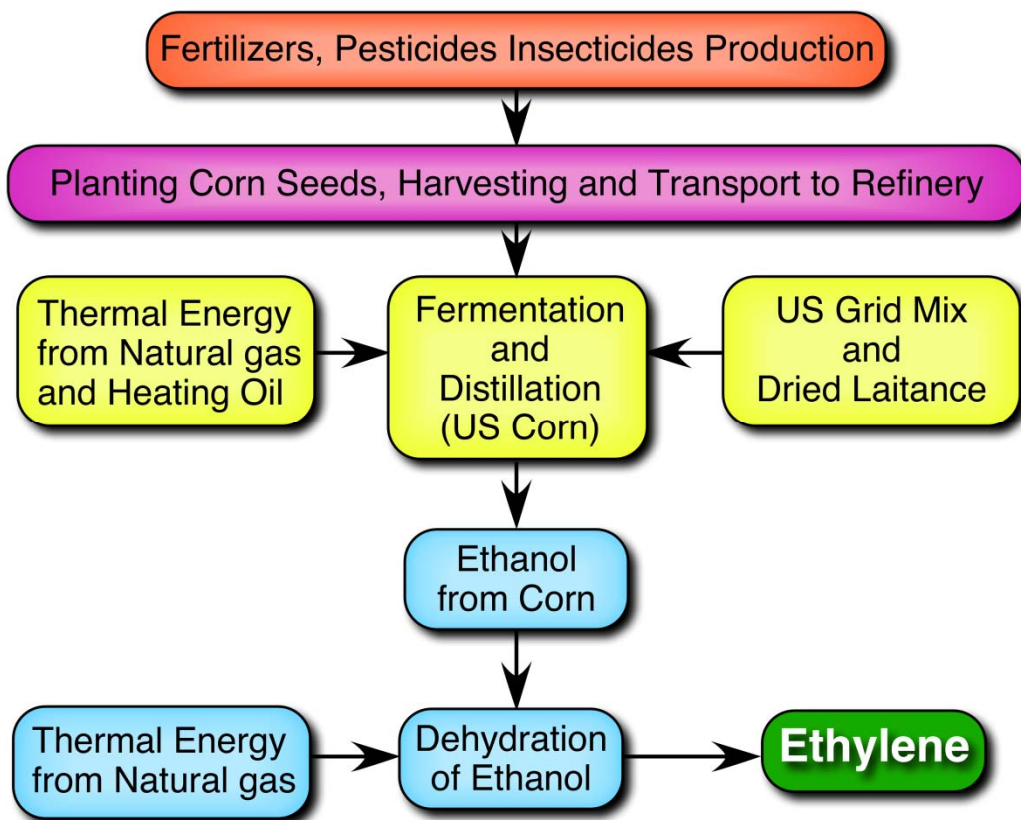


Figure 3-9: System boundaries for the production of ethylene from corn

3.6.2.3 Production of Hydrogen

Hydrogen from Methane: The recovery and processing of natural gas is described in the ethylene from natural gas section. Purified methane is transported via pipeline to a refinery where it is steam-reformed to produce synthesis gas, i.e., a mixture of CO and H₂. This mixture is further subjected to high temperature and low temperature water-gas shift to convert CO and H₂O to CO₂ and H₂. CO₂ is removed from the resulting CO₂+H₂ mixture by amine absorbers. The purity of H₂ produced by this method is 97-99%. H₂ may be further purified to 99.9% by pressure-swing adsorption.⁵¹ The boundaries considered in this analysis are shown in Figure 3-10. A weighting factor of 0.4 (calculation shown in Appendix D) is allocated based on the proportional

allocation method to estimate the environmental impacts associated with hydrogen production.

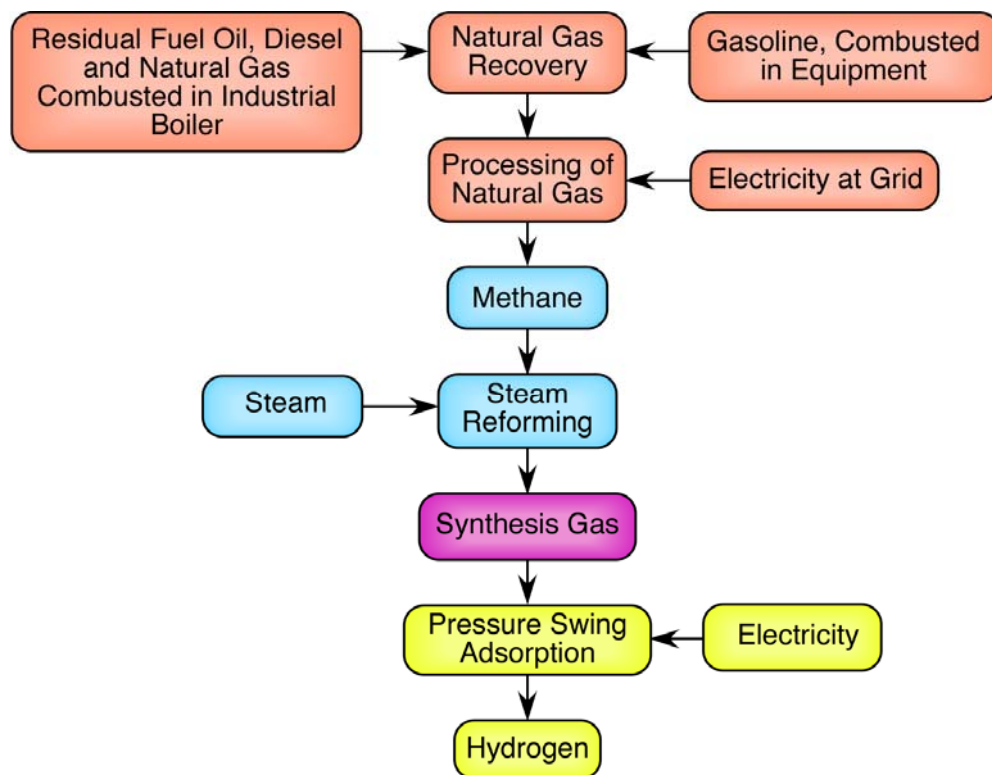


Figure 3-10: System boundaries for the production of hydrogen from methane

Hydrogen at Refinery: The environmental impact of crude oil extraction and transportation reflects the U. S. crude oil mix. The extracted crude oil is desalted and distilled at atmospheric pressure into various fractions. The desulfurized heavy naphtha fraction is reformed by catalytic transformation of aliphatic paraffins to iso-paraffins and cyclo-paraffins to aromatic compounds. These compounds are blended with gasoline to increase its octane number. H₂ is the byproduct of these processes. The sulfur content of the crude (sweetness of crude) dictates the net H₂ yield of a petroleum refinery. The average net H₂ yield obtained at a refinery in the U.S. during the reforming of naphtha is 2-3%.⁵¹ Figure 3-8 shows the boundaries of the various processes considered in this analysis for the production of H₂. A weighting factor of 0.165 (calculation

shown in Appendix D) is allocated based on the proportional allocation method to estimate the environmental impacts associated with hydrogen production.

Hydrogen from an Ethylene Cracker: In the U.S., significant portion of H₂ is produced by the cracking of natural gas liquids in the recovered natural gas and by the steam cracking of ethane, propane and butadiene. The impact of H₂ production in this cradle-to-gate LCA reflects the feedstock distribution from both these sources. The feed stream is diluted with steam and then led through a furnace, where it is heated rapidly to a high temperature. Temperature and residence time define the product yield. The product stream leaving the cracker is quenched to prevent further reactions.⁵¹ Figure 3-9 is a pictorial representation of the various processes considered in this analysis. A weighting factor of 0.165 (calculation shown in Appendix D) is allocated based on the proportional allocation method to estimate the environmental impacts associated with hydrogen production.

Hydrogen from Chlor-Alkali Plant: Sodium hydroxide is produced industrially by the electrolysis of sodium chloride and approximately, *389,000 metric tonnes of H₂/yr* are produced as co-product annually in this process.⁶⁴ The product distribution of this process is NaOH solution, Cl₂ and H₂ in the mass ratio 1:0.88:0.025, respectively.⁶⁵ The amalgam process is the dominant technology employed in the manufacture of sodium hydroxide. In this process, sodium hydroxide is produced from sodium amalgam and water over a graphite catalyst at 80-120 °C. The concentrated NaOH solution produced is very pure and can be sold without any further purification. A weighting factor of 0.13 (calculation shown in Appendix D) is allocated based on the proportional allocation method to estimate the environmental impacts associated with

hydrogen production.

Hydrogen Production in Germany: The effect of location on the environmental impact of H₂ production (from natural gas) is established by performing a Germany specific cradle-to-gate analysis. The bulk of its natural gas demand is met by imports via pipeline from The Netherlands, Norway, and Russia. Multiple valuable co-products (olefins, liquid fuels) are produced during H₂ production from all the feedstocks. The boundaries for this analysis are similar to that represented in Figure 3-9 but the distances and quality of natural gas (sulfur content and methane concentration) are specific to Germany. A weighting factor of 0.4 is allocated based on the proportional allocation method to estimate the environmental impacts associated with hydrogen production

3.7 Results and Discussion

3.7.1 Economic Assessment

Figure 3-11 compares the Total Capital Investment (TCI) and the relative costs of various unit operations for the simulated conventional and CEBC processes. The various categories are represented as designed bars and the relative areas of the designed bars reflect comparative costs.

3.7.1.1 Total Capital Investment

The total capital investments for the conventional and the base case of the CEBC processes (Figure 3-11) are both approximately \$120 million, the difference being within the predicted uncertainty of a preliminary economic analysis ($\pm 25\%$).

Reactors in the conventional process cost \$11 million compared to \$22 million for the CEBC

process. Material of construction for the reactors in the conventional process is carbon steel. In contrast, in the CEBC process, both the ethylene epoxidation and H₂O₂ synthesis reactor are constructed of stainless steel (SS-304) to minimize metal catalyzed decomposition of H₂O₂. Stainless steel is three times more expensive than carbon steel.

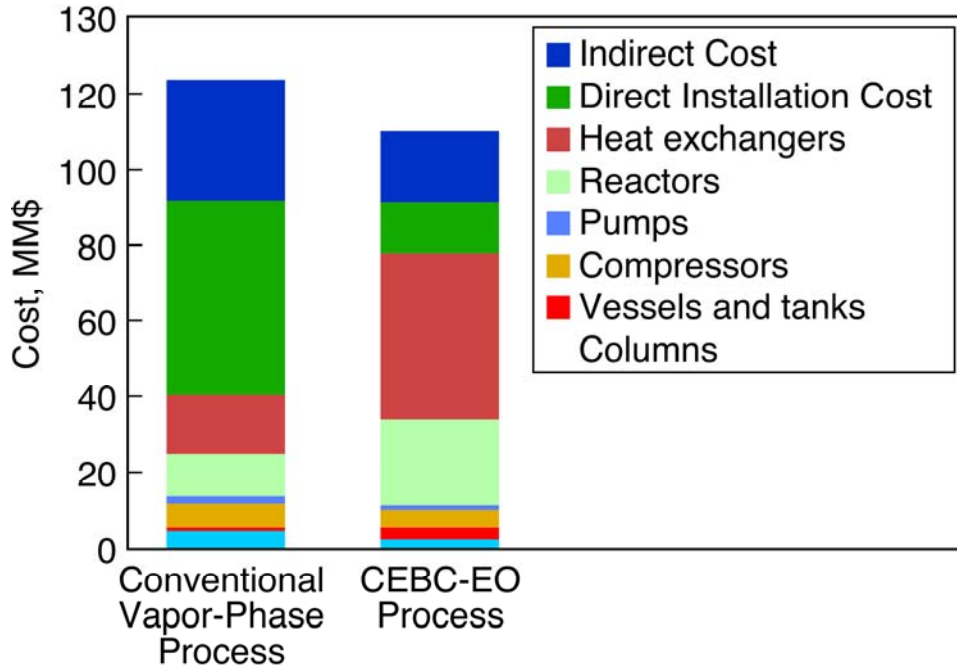


Figure 3-11: Comparison of the total capital investment for the simulated conventional and CEBC processes

As shown in Figure 3-11, the pump costs in both the processes are about \$1.9 million and \$1.2 million, respectively. The compressor cost for the conventional and CEBC processes are \$6 million and \$4 million, respectively. For the conventional process, in addition to ethylene and oxygen, large volumes of diluent gases are compressed to reactor pressure. While the CEBC process contains no diluents, the ethylene must be compressed to higher pressures escalating the compressor and pump costs. The estimated distillation equipment costs for the conventional

vapor phase process are approximately \$4.5 million compared to \$2.5 million for the CEBC process. *Heat Exchanger* costs in the conventional vapor phase process are \$15 million compared to the \$44 million for the CEBC process.

Direct installation costs for the conventional and CEBC processes are \$51 million and \$13 million, respectively. The use of a large volume of CH₄ and inert gases such as Ar, N₂ drastically increases the piping, installation, instrumentation and insulation costs in the conventional process. The bulk of the unreacted ethylene in the CEBC process is recovered by simple depressurization compared to the conventional process where large volume of reactants and diluents are processed.

3.7.1.2 Production Costs

The EO production cost in the conventional process is compared to the *base case* of the CEBC process. In this scenario, we assume a catalyst life of 1 year at a leaching rate of 2.2 lb MTO/h (i.e., 10 ppm Re in the reactor effluent). Further, we assume that 99% of the leached metal is recovered. The costs of various raw materials and products used in this analysis are summarized in Table 3-5. As shown in Figure 3-12, the costs of (a) ethylene feedstock, (b) EO separation and purification (c) operation of the CO₂ capture section and (d) recompression of recycled gases R₁ and R₂ are dominant in the conventional process. In contrast, the production cost in the CEBC-EO process is dominated by the cost of raw materials (C₂H₄, H₂O₂ and catalyst).

Table 3-5: Costs of various raw material and products⁴⁰

Commodity	Price,\$/lb
Ethylene	0.32
Mono-ethylene glycol (MEG)	0.65
Di-ethylene Glycol (DEG)	0.39
Oxygen	0.033
Methane	0.134
Potassium Carbonate	0.39
Hydrogen	0.088
Nitrogen	0.033
Argon	0.145
Methanol	0.94
Pyridine <i>N</i> -Oxide	1.35
Potassium Carbonate	0.18
Phosphoric Acid	0.204
Sulfuric Acid	0.033
Methyl trioxorhenium	5,000
Silver	455
Palladium Nitrate Catalyst	7,924
Ethylene Oxide	0.79

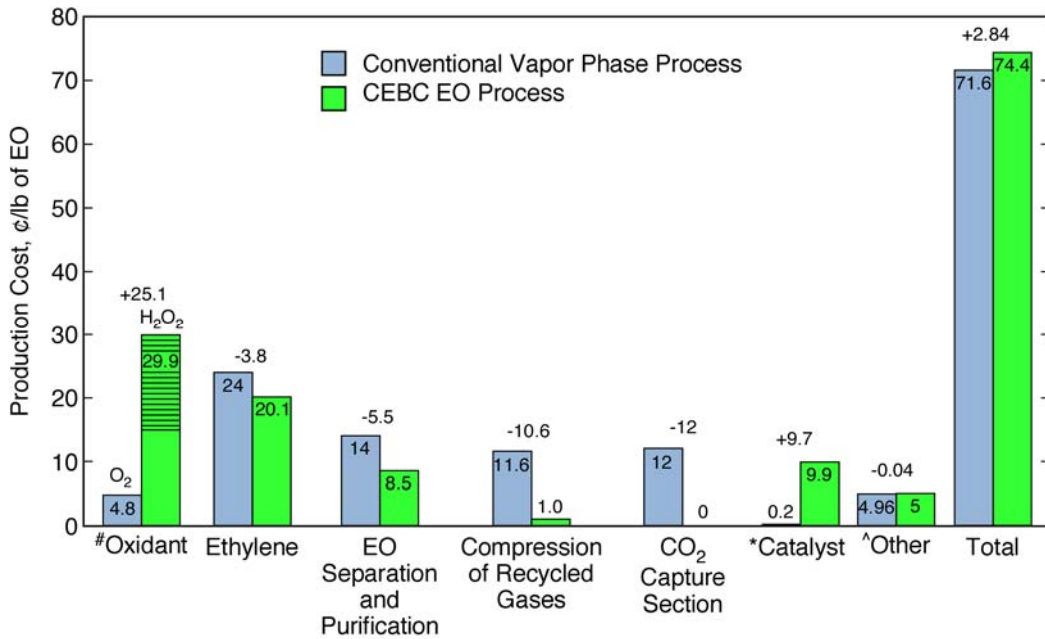


Figure 3-12: Comparison of the total production cost for the conventional and CEBC processes. (*) The catalyst life and leaching rate are assumed to be 1 year and 2.2 lbs MTO/h; (#)50% of the unreacted H₂O₂ is destroyed in the PFD, thus there is a significant incentive to push H₂O₂ conversion to a much higher level; (^) “Other” includes costs for, research, plant overhead, materials and supplies for operation and maintenance, and labor.

Oxidant: In the conventional process, the synthesis of 1 lb EO requires 1.45 lbs oxygen, which costs 4.8 ¢. In contrast, 1.76 lb of H₂O₂ (costing 29.9 ¢/lb) is used in making 1 lb EO via the CEBC process. This cost is estimated as follows. The cost of synthesizing H₂O₂ is 17 ¢/lb, assuming a H₂ price of 8.8 ¢/lb. The H₂O₂/catalyst ratio in the CEBC process is maintained at 143, which exceeds the value of 10 required for the catalyst to be in the active diperoxo form.⁶⁶ The H₂O₂ conversion (to EO) is 48% in the CEBC process. It is assumed that the unreacted H₂O₂ is decomposed prior to separation of other components. Thus, there is significant incentive to

enhance H₂O₂ utilization in order to save up to nearly 15 ¢ (the value of decomposed H₂O₂) for every lb of EO produced.

Ethylene: The cost of ethylene is assumed to be 32 ¢/lb for both polymer grade and technical grade ethylene (Table 3-5) due to the non-availability of pricing information for technical grade ethylene. The quantities of ethylene needed to synthesize 1 lb EO by the conventional vapor phase process and by the CEBC-EO process are 0.75 lb and 0.63 lb, resulting in an ethylene cost of 24 and 20.16 ¢/lb EO, respectively. In other words, for similar EO production capacity, the quantity of ethylene consumed is higher for the conventional process by 15%, reflecting the 15% burning of ethylene to CO₂. The elimination of burning in the CEBC-EO process results in a feedstock savings of 3.84 ¢/lb EO (Figure 3-12). Clearly, higher ethylene prices (for example, doubling of the ethylene price) will have a greater adverse effect on the economics of the conventional vapor phase process compared to the CEBC-EO process.

EO separation: The high operating pressure (2 MPa) of the primary EO absorber results in the dissolution of significant quantities of ethylene (1,400 lb/h), acetaldehyde (81 lb/h), CO₂ (1,544 lb/h), CH₄ (395 lb/h) and Ar (450 lb/h) in addition to EO (49,788 lb/h) in the liquid phase containing water, mono-ethylene glycol and di-ethylene glycol. EO is stripped from this stream using high-pressure steam (1 MPa, 253,000 lbs/h). Approximately 20% of the steam requirement is met with steam generated using the reaction exotherm. The net cost of process steam for EO stripping is 4.5 ¢/lb EO. The cost of EO separation (by refrigeration) in the light ends column is 2.75 ¢/lb EO. The total cost of utilities employed for EO separation, purification and recycle (Section B of Figure 3-1) is 14 ¢/lb EO.¹⁴

In the CEBC process, the *absence* of diluents (such as N₂, CO₂, CH₄ and Ar employed in the conventional process) and the high EO solubility in the liquid phase allow for the recovery of the

bulk (95%) of the unreacted ethylene by simple depressurization from the reactor operating pressure from 5 to 0.5 MPa. The ethylene stripper in the CEBC-EO process is cooled to $-30\text{ }^{\circ}\text{C}$ to recover the remaining ethylene. The rate of heat removal in the condenser of the ethylene stripper 2 is 30.5 GJ/h translating into a cost of 1.8 ¢/lb EO. Unlike the conventional process, the exothermic reactors of the CEBC process operate at near-ambient temperatures that are not conducive for producing process steam. Hence separate utilities are used for steam generation. The cost of process steam for EO separation in the CEBC process is 5.7 ¢/lb EO.

Compression costs: In the conventional process, the electricity costs for the recompression of recycle gases and make-up reactants to reactor pressure are 10 ¢/lb EO and 1.6 ¢/lb EO, respectively, totaling 11.6 ¢/lb EO. In contrast, the recycle volume is significantly lower in the CEBC process due to much higher per pass ethylene conversion and the absence of other diluent gases in the feed stream resulting in a relatively low compression cost of 1 ¢/lb EO.

Partial capture of CO₂ byproduct: Approximately, 260,000 lb/h of high-pressure steam is required to strip CO₂, costing 5.2 ¢/lb EO. Further, the electricity cost for the pumping and cooling of the CO₂ absorber effluent stream is 3.5 ¢/lb EO. Including the cost of the make-up absorbents, the total cost of utilities in the CO₂ removal section is 12 ¢/lb EO. If the recycle stream is vented and not recycled, the value of the feedstock (C₂H₄ = 62,000 lb/h, CH₄ = 58,500 lb/h, Ar = 42,000 lb/h and O₂ = 13800 lb/h) losses amounts to 68 ¢/lb EO.

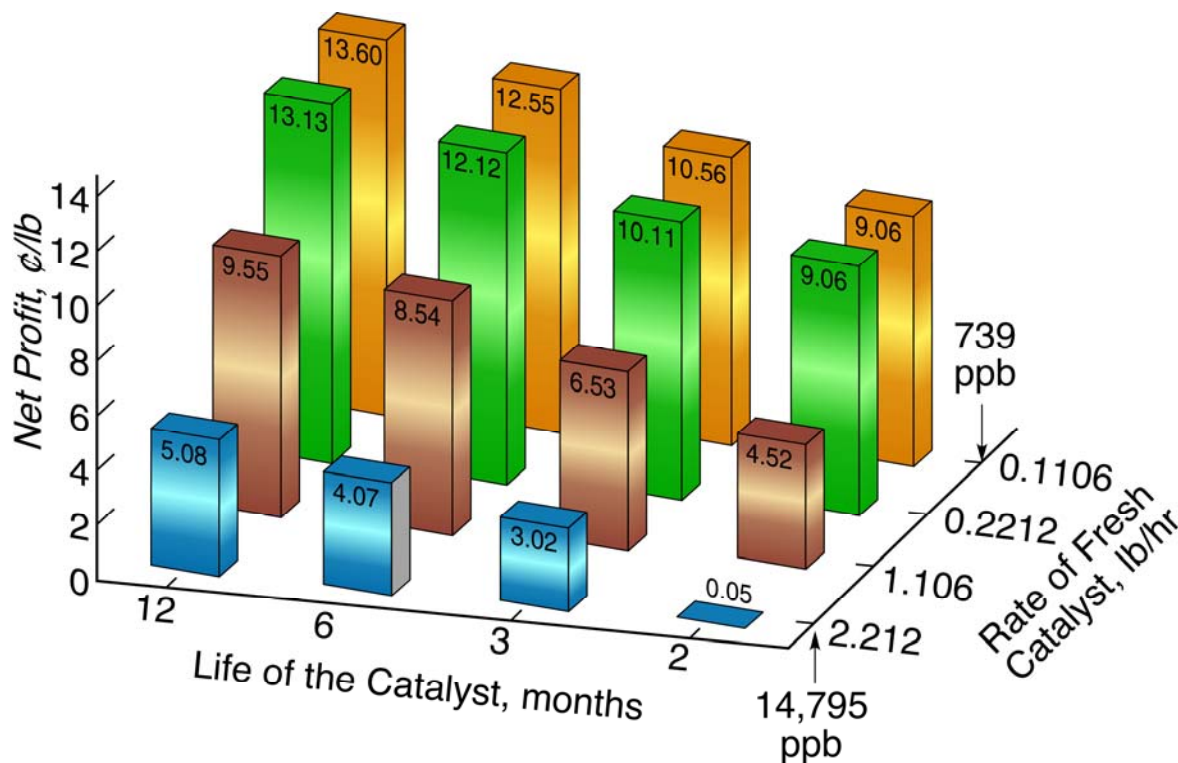


Figure 3-13: Effects of catalyst durability and leaching rate on the net profitability of the CEBC process.

MTO catalyst life and leaching rate: The cost of silver metal is \$455/lb. For the catalyst (silver/alumina/promoter) employed in the conventional process, approximately 6000 lbs of silver metal is impregnated onto the surface of the alumina support. In contrast, the cost of rhenium metal is \$3,000/lb and 2,212 lbs MTO is dissolved in the liquid phase of the ethylene epoxidation reactor. Hence, near-quantitative recovery of the catalyst is essential for economic viability of the CEBC process. Figure 3-13 shows the sensitivity of EO production costs in the CEBC process to variations in catalyst leaching rate and active lifetime. As expected, a low catalyst leaching rate and a long catalyst life are necessary to make the CEBC process economical. The CEBC process has the potential to achieve a profit margin of 13.6 ¢/lb EO provided the minimum catalyst life of the immobilized MTO is 1 year at a leaching rate of 0.11 lb MTO/h (i.e., makeup catalyst

addition rate). These performance benchmarks are guiding the design of the polymer-bound MTO catalyst for optimum catalyst retention and stability while maintaining the activity and selectivity.

Figure 3-12 provides a comparison of the production costs by categories in the conventional and CEBC processes. The increased production costs associated with the use of expensive H₂O₂ oxidant and Re-based catalyst in the CEBC process are offset by lower ethylene requirement, lower cost associated with EO separation, lower gas recycle and recompression costs, and the avoidance of CO₂ separation. The cost of various utilities (steam, refrigeration, electricity and cooling water) in both processes is provided in the Appendix C (Table C1). As shown in Figure 3-12, the EO production costs for the conventional process and the CEBC process (base case) are 71.6 and 74.4 ¢/lb EO, respectively. The 2009 market price of EO is 79 ¢/lb EO, making both processes profitable.⁴⁰ As can be inferred from Figure 3-12, steps to enhance H₂O₂ utilization in the CEBC process can save up to 15 ¢/lb EO and the development of catalysts that exceed the specified performance metrics has the potential to further improve the economics.

3.7.1.3 Comparison of the CEBC (Case 1) and Conventional Silver-Catalyzed Ethylene Epoxidation Process

Capital Costs:

Figure 3-14, compares the capital cost of the two additional cases of the CEBC process and the simulated conventional process. The cost of reactors, pumps, compressors for both the cases are similar to that of the base case. The deployment of refrigeration to remove the heat of reaction in the case 1 of CEBC process results in greater capital investment for the procurement of heat exchanger and refrigeration equipment (\$44 million) compared to the conventional process (\$15

million).

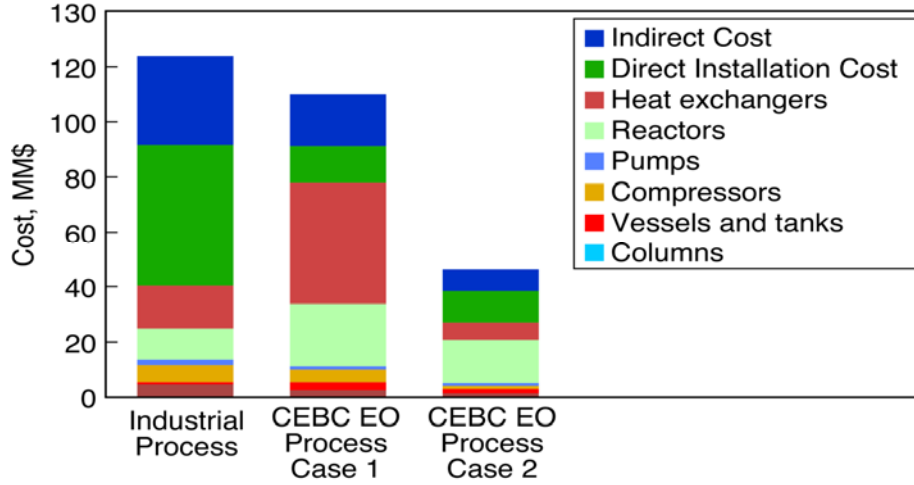


Figure 3-14: Comparison of the total capital investment for the simulated conventional process and two cases of the CEBC-EO process

Production Costs

Figure 3-15 compares the total production costs in the CEBC process (Cases 1 and 2) and simulated conventional process.

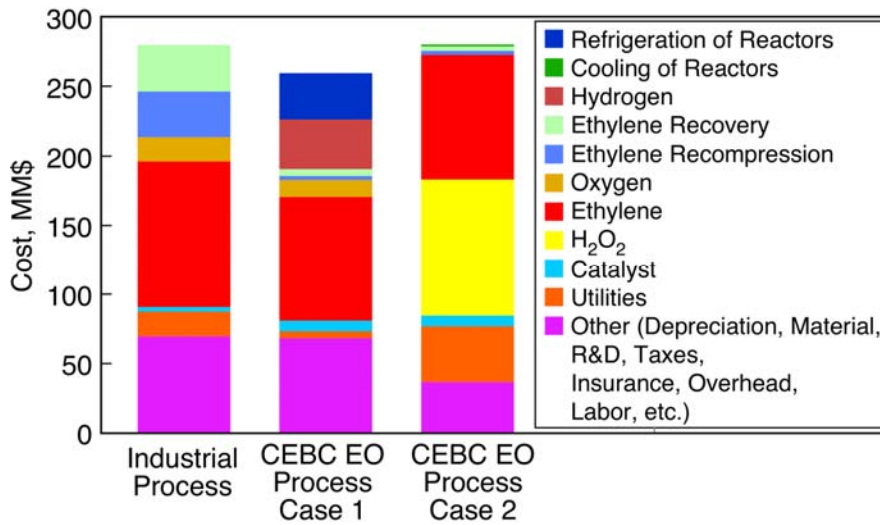


Figure 3-15: Comparison of the total production cost for the simulated conventional process and the two cases of the CEBC-EO process

The cost of ethylene, CO₂ capture, compression of gases and EO separation for this case 1 are similar to that of the base case of the CEBC process.

Oxidant: The cost of oxygen in the conventional process is 4.8 ¢/lb EO. In contrast, 0.85 lb of H₂O₂ (costing 14.4 ¢) is consumed for the synthesis of 1 lb EO *via* the CEBC process. The unreacted H₂O₂ is recovered and recycled back to the ethylene epoxidation reactor.

Utilities: The EO separation and recovery cost for the Case 1 of the CEBC process is similar to that of the base case. The heat of reaction in the H₂O₂ and EO reactor is removed by the deployment of refrigeration, an expensive utility amounting to a cost of 15 ¢/lb EO.

3.7.1.4 Comparison of the Case 1 and Case 2 of the CEBC Process

Capital Costs

The total capital investment for the case 1 and case 2 of the CEBC process is approximately \$120 million and \$45 million, respectively. Pump, compressor and column costs are similar in both the case 1 and case 2 of the CEBC process due to similarity in process parameters and stream compositions. Direct installation costs for case 1 and case 2 of the CEBC process are approximately \$11 million and \$13 million. The lower total capital investment for the case 2 of the CEBC process is attributed to the procurement of H₂O₂ from an external provider (compared to in-house synthesis) and deployment of cooling water to remove the heat of reaction from the ethylene epoxidation reactor.

Reactors: The cost of reactors in the case 1 and case 2 of the CEBC process are \$22 million and \$15 million, respectively. The procurement of H₂O₂ oxidant from an external supplier in the case 2 eliminates the H₂O₂ synthesis section hence reducing the overall cost of reactors. Cooling water is employed to remove the heat of reaction in case 2. The complex reactor design and large

surface requirement in case 2 increases the cost of the ethylene epoxidation reactor from \$11 million to \$15 million.

Heat Exchanger and Refrigeration equipment cost in cases 1 and 2 are \$44 million and \$6 million, respectively. The disparity in capital investment is mainly due to the procurement of H_2O_2 from an external supplier and cooling of the EO reactor with water in case 2 compared to onsite H_2O_2 production and the refrigeration of reactors in case 1.

Production Cost

From Figure 3-15, we can ascertain that EO production costs in case 2 are higher than the case 1 of the CEBC process. The raw material and utility expenses dominate the production costs in both the processes. The ethylene purity, feed composition, yield and selectivity towards EO recovery of unreacted ethylene are similar in both cases. The durability and leaching rate of the MTO catalyst will have a similar effect on the EO production cost in both cases of the CEBC process. For both cases the catalyst life and rate of addition of fresh catalyst (to offset catalyst loss) is assumed to be 1 year and 0.022 lb/h.

Synthesis of H_2O_2 oxidant: The molar ratio of H_2O_2 /ethylene in the liquid phase is 1.0:1.0 in both cases. The cost of synthesizing H_2O_2 by the direct H_2O_2 process and anthraquinone process are 17 ¢/lb and 27 ¢/lb, respectively. Further, the unreacted H_2O_2 is recovered in the case 1 compared to the case 2 where the H_2O_2 is safely decomposed. Thus, the net oxidant cost in the case 1 of the CEBC process is 14.4 ¢/lb EO compared to 27 ¢/lb EO in the case 2.

Utilities: The refrigeration costs in case 1 amounts to \$33 million. In case 2, temperature control is achieved by maintaining a cooling water circulation rate of 8000 gal/min through the jacket of the ethylene reactor. Though the cost of cooling water cost is only \$1.2 million, the electricity

costs associated with pumping of the large volumes of coolant amounts to 3.5 ¢/lb EO. The total utility cost in case 2 is less than that for case 1 by approximately \$ 4 million.

Sensitivity Analysis on the catalyst life and leaching rate: In this analysis, we also assume that 99% of the leached metal is recovered and the cost of fresh catalyst and reconstitution cost is 5,000 and 2,000 \$/lb. The CEBC process has the potential to be cost competitive provided the polymer bound MTO catalyst is active for 1 year and the rate of addition of fresh catalyst is less than 1.1 lb/h and higher profit margins can be achieved at lower catalyst leaching rates. Figure 3-16, shows the expected qualitative trend (i.e., an increase in catalyst leaching rate and low durability makes the CEBC process uneconomical) and that the profitability in the CEBC process is dependent on the near quantitative recovery and recycling of the leached catalyst.

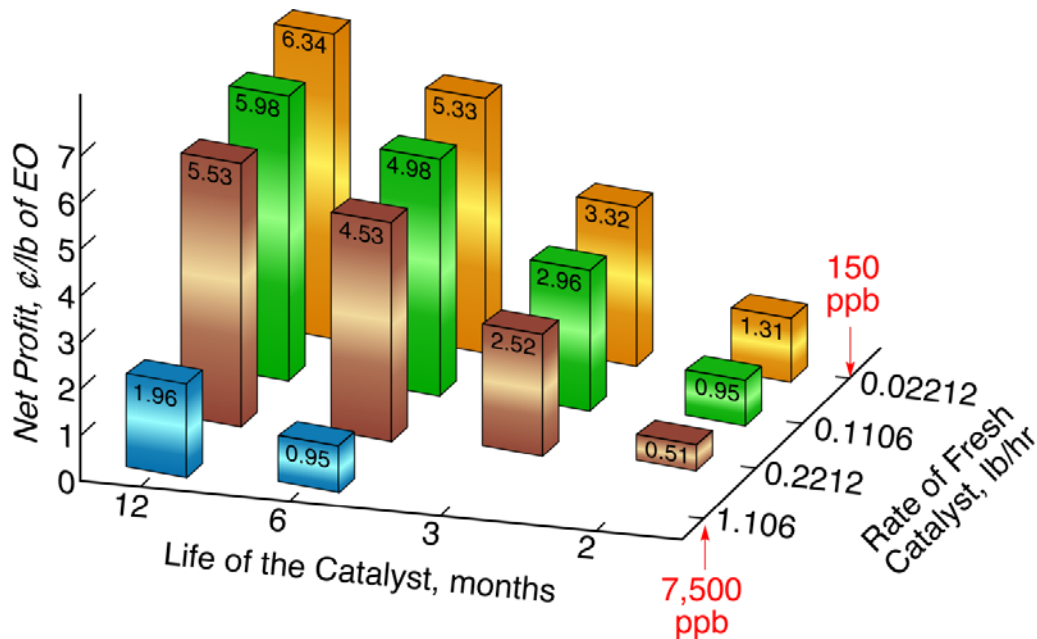


Figure 3-16: Effects of catalyst durability and leaching rate on the net profitability of the CEBC process

For similar performance metrics (catalyst life = 1 year, leaching rate = 0.022 lb/h and recovery of leached metal = 99%) the profit margin in case 2 of the CEBC-EO process is 8.2 ¢/lb EO compared to 6.3 ¢/lb in the case 1 of the CEBC-EO process (Figure 3-17).

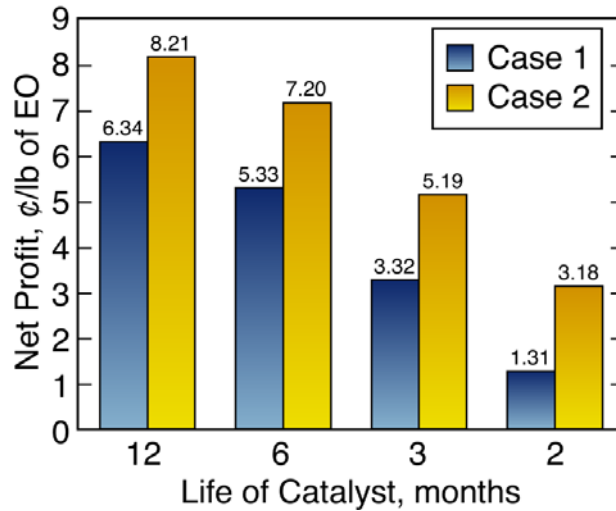


Figure 3-17: Comparison of the profitability for the case 1 and case 2 of the CEBC process

For a similar catalyst life and leaching rate the profit margin is highest for the base case of the CEBC process. For example, for a catalyst life of 1 year and leaching rate of 1.1 lb/h the profit margin for the case 1 and case 2 of the CEBC-EO process are lower compared to the base case of CEBC process. The deployment of refrigeration an expensive utility to remove the heat of reaction in the case 1 of the CEBC process offsets the savings achieved by the recycle of unreacted H₂O₂ resulting in lower profit margin compared to base case. The H₂O₂ production cost is higher for the anthraquinone process compared to direct H₂O₂ route. The additional costs partially offset the savings achieved by the use of cooling water to remove the heat of reaction resulting in a lower profit margin in the base case of the CEBC process.

3.7.2 Environmental Impact Analysis

3.7.2.1 Conventional and CEBC Process

Gate-to-gate analysis: The approach to estimate the environmental impact was assessed by first performing a *gate-to-gate* environmental impact assessment of the simulated conventional process and comparing the estimated emissions with those from a commercial plant of similar capacity (Table 3-6). The BASF facility in Geismar, LA has an EO production capacity of 215,000 tonnes EO/yr which is approximately similar to that used in this simulation (200,000 tonnes EO/yr). This BASF EO production facility uses the conventional Ag-catalyzed process and the emissions from this plant are taken from the annual toxic release inventory data reported to the United States Environmental Protection Agency (USEPA) for both emitted and treated waste at the facility.⁶⁷ The greenhouse gas emission data for this facility are obtained from “ghgdata”, a publication tool developed by the USEPA.⁶⁸ As shown in Table 3-6, the actual emissions from the BASF facility range from 1-10% of the total waste produced. The rest of the waste generated (90+%) is treated at the facility and disposed.

Table 3-6: Comparison of the environmental impacts estimated from the toxic release inventory data for BASF's Geismar, LA ethylene oxide facility and that predicted by the GaBi[®] software^{67, 68}

Environmental Impact	Units	Conventional Process		
		Toxic Release Inventory (gate-to-gate) EPA, millions Equivalent		GaBi [®] gate-to-gate, millions Equivalent
		Total Waste	Released Waste	
Acidification	[mol H ⁺ Eq.]	133.6	12.6	N/A
Global Warming Potential	[kg CO ₂ Eq.]	85.7	N/A	144
Ecotoxicity-Air	[kg 2,4- DCP Eq.]	1.29	0.08	7.86(10 ⁻⁶)
Ecotoxicity-Ground Surface Soil	[kg 2,4- Benzene Eq.]	0.04	0.003	N/A
Ecotoxicity-Water	[kg 2,4- DCP Eq.]	N/A	N/A	4.18
Eutrophication	[kg N- Eq.]	0.14	0.014	0.049
Human Health Cancer-Air	[kg Benzene Eq.]	0.21	0.004	13.3
HHC-Ground Surface Soil	[kg Benzene Eq.]	N/A	N/A	N/A
HHC-Water	[kg Benzene Eq.]	0.21	0.004	7.69
Human Health Criteria-Air Point	[kg PM-2,5 Eq.]	N/A	N/A	N/A
Human Health Non Cancer-Air	[kg Toluene Eq.]	596.4	6.95	745
HHNC-Ground Surface Soil	[kg Toluene Eq.]	3.35	0.33	N/A
HHNC-Water	[kg Toluene Eq.]	484	136	346
Ozone Depletion Potential	[kg CFC-11 Eq.]	N/A	N/A	N/A
Smog Air Potential	[kg NO _x Eq.]	0.93(10 ⁻³)	0.029(10 ⁻³)	3.4(10 ⁻³)

DCP: Dichlorophenoxyace, Eq.: Equivalent

N/A: Data not available to estimate the impact

As inferred from Table 3-6, the magnitudes of several of the total emissions reported by BASF (including those that cause global warming, eutrophication and impact human health) are of the same order of magnitude as those estimated with GaBi[®] software for the simulated conventional process, with the predicted emissions being greater in most cases. In the case of ecotoxicity-air, the estimated emissions were found to be order of magnitude lower than those reported for the Geismar BASF facility. The reason for this discrepancy is that metal emissions (zinc, cesium, rubidium, and nickel) during catalyst bed reactivation, the primary source of ecotoxicity (air), could not be considered due to the lack of publicly available information. Based on the results of the foregoing gate-to-gate analysis, we conclude that only differences that are greater than an order of magnitude can be considered reliable for making safe conclusions about the relative environmental impacts of competing processes. Nevertheless, the quantitative information generated by the cradle-to-gate life cycle assessment is useful to identify potential major polluters that contribute most to the adverse environmental impacts.

Cradle-to-Gate Life Cycle Assessment: Table 3-7 compares the cradle-to-gate environmental impacts of EO production by the conventional process and the various cases of the CEBC process. The estimated cradle-to-gate environmental impacts are generally one to two orders of magnitude greater than the gate-to-gate emissions (Table 3-6). The overall cradle-to-gate environmental impact of the CEBC process is of the same order of magnitude as the conventional process and any differences lie within prediction uncertainty. The potential hot spots in the two processes are discussed in the following sections. Tables 3-8 and 3-9 lists the major hot spots and their percentage contributions in the conventional and CEBC processes.

Table 3-7: Environmental impact (cradle-to-gate) of manufacturing 200,000 tonnes of ethylene oxide by the conventional process and CEBC process

Environmental Impact	Units	Conventional Process, millions	Base case CEBC Process, millions	Case 1 CEBC Process, million	Case 2 CEBC Process, million
Acidification	[mol H ⁺ Eq.]	300	284	1063.2	1198.5
Global Warming Potential	[kg CO ₂ Eq.]	1538	1159	4,850	5,687
Ecotoxicity-Air	[kg 2,4- DCP Eq.]	1.75	1.88	5.612	5.99
Ecotoxicity-Ground Surface Soil	[kg 2,4- Benzene Eq.]	0.015	0.012	0.042	0.049
Ecotoxicity-Water	[kg 2,4- DCP Eq.]	38.5	45.5	69.1	94.1
Eutrophication	[kg N- Eq.]	0.14	0.12	0.363	0.479
Human Health Cancer-Air	[kg Benzene Eq.]	0.53	0.54	2.14	2.40
HHC-Ground Surface Soil	[kg Benzene Eq.]	41(10 ⁻⁵)	36(10 ⁻⁵)	9(10 ⁻⁵)	11.1(10 ⁻⁵)
HHC-Water	[kg Benzene Eq.]	0.11	0.87	0.273	0.317
Human Health Criteria-Air Point	[kg PM2.5- Eq.]	1.77	1.75	6.42	7.30
Human Health Non Cancer-Air	[kg Toluene Eq.]	378	442	1085	1189.5
HHNC-Ground Surface Soil	[kg Toluene Eq.]	0.93	0.94	2.85	3.2
HHNC-Water	[kg Toluene Eq.]	2702.4	2465.9	8,193	9,699
Ozone Depletion Potential	[kg CFC-11 Eq.]	8.23(10 ⁻⁵)	8.05(10 ⁻⁵)	0.317(10 ⁻³)	0.35(10 ⁻³)
Smog Air Potential	[kg NO _x Eq.]	2.1(10 ⁻³)	9.0(10 ⁻³)	7.85(10 ⁻³)	9.06(10 ⁻³)

DCP: Dichlorophenoxyace, Eq.: Equivalent

N/A: Data not available to estimate the impact

Table 3-8: Major adverse environmental impacts in the conventional process and their percentage contributions

Major Impacts	Impact Category	% Contribution relative to similar impacts from other sources
Coal-based electrical power production	Acidification	66
	Global warming potential	51
	Human health non-cancer air	46
Natural gas-based energy for producing process steam	Ecotoxicity-water	49
Natural gas based energy (for ethane cracking to produce ethylene)	Acidification	19
	Global warming potential	29
	Ecotoxicity-water	29
	Human health non-cancer air	40

Table 3-9: Major adverse environmental impacts in the CEBC processes and their percentage contributions

Major Impacts	Impact Category	% Contribution relative to similar impacts from other sources
Fossil Fuel-based energy for ethylene production	Acidification	46
	Global warming Potential	48
	Ecotoxicity-water	69
	Human health non-cancer air	57

Major adverse environmental impacts in the Conventional Process:

Acidification Potential: The acid rain potential of the conventional process is primarily attributed to SO₂ and NO_x emissions associated with coal-based electrical power generation for compressing recycled gases and producing oxygen and to a lesser extent for natural gas-based

energy for producing ethylene (the endothermic cracking of ethane to produce ethylene).

Global Warming Potential: The carbon footprint associated with the production of 200,000 tonnes of EO by the conventional process is 1.54 billion kg CO₂ equivalent. Of this, the CO₂ produced as byproduct is 69.4 million kg. Of the total greenhouse gas (GHG) emissions in the process, coal-based electricity generation for gas compression is responsible for approximately 51%, fossil fuel-based energy used to make ethylene for 29%, and natural gas used to generate process steam for nearly 12%.

Eco-toxicity Water: Partitioning of the metal emissions (mercury, lead, chromium) into the water phase during the production of coal-based electricity is the primary cause of water contamination.⁶⁹

Human health non-cancer air: Metals (lead and mercury), inorganic and halogenated substances emitted during coal-based electricity generation needed for operating compression equipment (46%) and during natural gas-based steam generation (40%) contribute to 86% of the overall environmental impact in this category.

Major adverse environmental impacts in the CEBC Process

The major contributors and their environmental impacts for case 1 and case 2 of the CEBC process are similar to the base case and thus can be lumped together in this discussion.

Acidification Potential: The SO_x and NO_x emissions from the fossil fuel-based power generation steps needed to produce the raw materials (oxygen, ethylene, hydrogen and methanol) contribute the most to this impact. Such emissions during ethylene production alone contribute to 46% of this impact category. The other major source of SO₂ emissions is associated with the desulfurization of methane to less than 10 ppm to avoid poisoning of the reforming catalyst and

the production of oxygen by cryogenic separation of air.

Global Warming Potential: The carbon footprint associated with the production of 200,000 tonnes of EO by the CEBC processes is 1.16 billion kg CO₂ equivalent. Approximately 84% of this amount is attributed to the generation of fossil fuel-based energy required for the production of various raw materials (ethylene, hydrogen and methanol) with ethylene production contributing to 48% of this impact category. In contrast, the GHG emissions during process steam production from methane (i.e., natural gas) are significantly smaller (16% of this impact category). The elimination of ethylene burning and the non-requirement of additional feed gases (Ar, CH₄) and CO₂ absorbent (K₂CO₃) in the CEBC process results in reduced power consumption and a 25% reduction (approximately 291 million kg CO₂ equivalent) in the total GHG emissions compared to the conventional process.

Ecotoxicity-water: Partitioning of the heavy metal (cadmium, copper, lead and mercury) and inorganic chemicals into ground water contributes to this impact category. Fossil-fuel based energy for the recovery, transport and processing of natural gas (used to produce ethane, H₂ and methanol) contribute 28% of this impact category whereas phosphoric acid production (residual acids and heavy metals in calcium sulfate waste) contributes to 41% of this impact category.

Human health non-cancer air: Heavy metal (arsenic, cadmium, lead and mercury etc.) and halogenated organics from coal-based electricity generation needed for the production of raw materials (hydrogen, ethylene and oxygen) account for the bulk of these emissions. Approximately, 57% of the emissions in this impact category is attributed to the generation of fossil fuel-based process energy needed for recovery of natural gas and the production of ethylene.

3.7.2.2 Anthraquinone and Direct H₂O₂ Process

Cradle-to-Gate Life Cycle Assessment: Table 3-10 compares the cradle-to-gate environmental impacts of H₂O₂ production by the Anthraquinone and direct H₂O₂ processes.

Major adverse environmental impacts for the Anthraquinone Process

Acidification Potential: Fossil-fuel based energy for the transportation of crude oil across the ocean in tankers powered by bunker fuel needed for the production of raw material (2-ethylanthraquinone) has the greatest adverse environmental impact.

Global warming potential: The GHG emissions associated with the transportation of crude-oil by ocean going ships and the generation of natural-gas based process energy for H₂O₂ production.

Human health non-cancer air: Metal emissions associated with the generation of fossil-fuel based process for the production of H₂O₂.

Human health non-cancer water: The processing of crude oil is a highly water intensive process and introduces significant quantity of impurities in the waste-water stream and is the dominant impact in this category.⁷⁰

Table 3-10: Environmental impact (cradle-to-gate) analysis for producing 220,000 tonnes of H₂O₂ using Anthraquinone process and direct H₂O₂ process

Environmental Impact	Units	Anthraquinone Process, millions	Direct Hydrogen Peroxide Process, millions
Acidification	[mol H ⁺ Eq.]	145.6	113.4
Global Warming Potential	[kg CO ₂ Eq.]	798.2	722.6
Ecotoxicity-Air	[kg 2,4- DCP Eq.]	0.692	0.735
Ecotoxicity-Ground Surface Soil	[kg 2,4- Benzene Eq.]	0.004	0.0118
Ecotoxicity-Water	[kg 2,4- DCP Eq.]	6.59	25.8
Eutrophication	[kg N- Eq.]	0.116	0.059
Human Health Cancer-Air	[kg Benzene Eq.]	0.284	0.168
HHC-Ground Surface Soil	[kg Benzene Eq.]	0.14(10 ⁻⁴)	0.45(10 ⁻⁴)
HHC-Water	[kg Benzene Eq.]	0.038	0.080
Human Health Criteria-Air Point	[kg PM _{2,5} - Eq.]	0.92	0.716
Human Health Non Cancer-Air	[kg Toluene Eq.]	147.4	296.2
HHNC-Ground Surface Soil	[kg Toluene Eq.]	0.319	0.931
HHNC-Water	[kg Toluene Eq.]	1181	2694
Ozone Depletion Potential	[kg CFC-11 Eq.]	0.43(10 ⁻⁴)	0.25(10 ⁻⁴)
Smog Air Potential	[kg NO _x Eq.]	1.2(10 ⁻³)	0.946(10 ⁻³)

Major adverse environmental impacts of the Direct H₂O₂ Process

Acidification potential: The acid rain potential is primarily attributed to the SO₂ and NO_x emissions. Fossil fuel-based process energy for the production of raw material (methanol production, energy for various unit operations including, cryogenic separation of air etc.) has the largest impact in this category.

Global warming potential: The carbon footprint associated with the production of 220,000 tonnes of H₂O₂ by the direct H₂O₂ process is 722 million kg CO₂ equivalent. The green house gas (GHG) emissions resulting from the fossil fuel-based energy generation for the production of raw material (steam reforming of methane) is the dominant source.

Human health non-cancer air: Emission of metals and halogenated substances during the generation of fossil-fuel based energy for the production of raw material is the dominant source for this impact category.

Human health non-cancer water: Partitioning of the metal emissions during the generation of fossil-fuel based energy needed for raw material production.

3.7.2.3 Ethylene Production

Gate-to-gate analysis: The approach to estimate the environmental impact is assessed by first performing a *gate-to-gate* environmental impact assessment of an ethylene cracker. The potential emissions predicted in this simulation are compared against the emissions taken from the annual toxic release inventory data provided to United States Environmental Protection Agency (USEPA) by ExxonMobil for its olefins plant at Baytown, TX.⁷¹ and Total Petrochemicals USA Inc. for its facility at Port Arthur, TX⁷². The ethylene cracker capacity in both the plants is unknown. Ethane sourced from natural gas is the feedstock for the Total Petrochemicals facility⁷³ whereas naphtha is the feedstock source for the ExxonMobil olefin plant.⁷⁴ The data provided by the companies (Total Petrochemicals and ExxonMobil) only include fugitive emissions, stack emissions and emissions into the water stream at their facilities during the production of ethylene (*gate-to-gate* analysis). Table 3-11 compares the potential emissions predicted by GaBi[®] software to that reported by Exxon Mobil and Total Petrochemicals Inc. Hence, we can make

only qualitative comparisons on the actual and predicted emissions, and the relative amounts of these emissions. Thus, we can conclude only differences greater than an order of magnitude can be considered reliable for making safe conclusions about potential greenness of the competing feedstocks. The quantitative information generated by the cradle-to-gate environmental impact assessment is nevertheless useful in identifying potential adverse environmental impacts for the production of ethylene from corn, crude oil and natural gas.

Table 3-11: Qualitative comparison of the gate-to-gate environmental impacts associated with production of ethylene and that obtained from the toxic release inventory data submitted by Total Petrochemicals Inc. (unknown capacity) for their Port Arthur, TX facility and for the ethylene cracker operated by ExxonMobil (unknown capacity) for their Baytown facility to USEPA^{71,72}

Category	GaBi [®] gate-to-gate, millions	Crude Oil		Natural Gas	
		Exxon Baytown, millions	Mobil Treated Waste	Total Petrochemicals Port Arthur, millions	Treated Waste
		Released Waste		Released Waste	
Acidification, [mol H ⁺ Eq.]	24.2	11.4	11.9	4.77	18.49
Eco-toxicity Air, [kg 2,4-DCP Eq.]	0.561	0.94	0.94	0.02	0.03
Ecotoxicity-GSS, [kg Benzene Eq.]	0.00167	N/A	N/A	N/A	N/A
Eco-toxicity Water, [kg 2,4-DCP Eq.]	9	8.1	56.7	21.6	21.6
Eutrophication, [kg N-Eq.]	0.019	0.015	0.016	0.004	0.021
Global Warming Air, [kg CO ₂ -Eq.]	294	N/A	N/A	N/A	N/A
Human Health Cancer-Air, [kg Benzene Eq.]	0.018	0.078	1.09	0.089	0.20
Human Health Cancer-GSS, [kg Benzene Eq.]	6.61(10 ⁻⁶)	2.2(10 ⁻³)	0.08	N/A	N/A
Human Health Cancer Water, [kg Benzene Eq.]	0.012	0.029	1.5	0.013	0.12
Human Health Criteria Air Point Source, [kg PM _{2,5} - Eq.]	0.186	N/A	N/A	N/A	N/A
Human Health Non-Cancer Air, [kg Toluene Eq.]	36.4	13.9	27.8	0.325	2.4
Human Health Non-Cancer GSS, [kg Toluene Eq.]	0.134	N/A	N/A	N/A	N/A
Human Health Non-Cancer Water, [kg Toluene Eq.]	415	556	556	N/A	N/A
Ozone Depletion Potential, [kg CFC-11 Eq.]	2.49(10 ⁻⁶)	N/A	N/A	N/A	N/A
Smog Air, [kg NO _x Eq.]	4.08(10 ⁻⁴)	2.4(10 ⁻⁶)	1.8(10 ⁻⁴)	7(10 ⁻⁵)	8(10 ⁻⁵)

Eq.: Equivalent, DCP: Dichlorophenoxyace, N/A: Data not available at the toxic release inventory

Cradle-to-gate life cycle assessment: The cradle-to-gate environmental impacts of ethylene production from corn, crude oil and natural gas are compared in Table 3-12. The estimated cradle-to-gate impacts are generally one or two orders of magnitude greater than the predicted gate-to-gate emissions for similar production capacities (Table 3-11). The overall cradle-to-gate environmental impacts for ethylene production are of the same order of magnitude and the differences lie within prediction uncertainty. Of the results listed in Table 3-12, seven important categories are significant and are discussed.

Table 3-12: Environmental impact (cradle-to-gate) of manufacturing 400,000 tonnes/yr of ethylene from corn, crude oil and natural gas

Category	Corn (GaBi®), millions	Crude Oil (GaBi®), millions	Natural Gas (GaBi®), millions
Acidification, [mol H ⁺ Eq.]	467.3	531.0	376
Eco-toxicity Air, [kg 2,4- DCP Eq.]	1.1	2.48	0.07
Ecotoxicity-Ground Surface Soil, [kg Benzene Eq.]	0.016	0	0
Eco-toxicity Water, [kg 2,4- DCP Eq.]	30	51	78
Eutrophication, [kg N-Eq.]	1.4	0.3	0
Global Warming Air, [kg CO ₂ -Eq.]	268	198	167
Human Health Cancer-Air, [kg Benzene Eq.]	0.32	0.24	0.11
Human Health Cancer-Ground Surface Soil, [kg Benzene Eq.]	0.74	0	0
Human Health Cancer Water, [kg Benzene Eq.]	1.4	0.6	0.26
Human Health Criteria Air Point Source, [kg PM _{2.5} - Eq.]	2.0	3.5	1.8
Human Health Non-Cancer Air, [kg Toluene Eq.]	300	1130	20
Human Health Non-Cancer Ground Surface Soil, [kg Toluene Eq.]	29700	0	0
Human Health Non-Cancer Water, [kg Toluene Eq.]	46300	12100	5300

Ozone Depletion Potential, [kg CFC-11 Eq.]	47.6	27.4	0
Smog Air, [kg NO _x Eq.]	3.8(10 ⁻³)	5.9(10 ⁻³)	1.4(10 ⁻⁴)

Eq.: Equivalent, DCP: Dichlorophenoxyace

Major adverse environmental impacts for ethylene production from corn

Global warming potential: The greenhouse gas emissions associated with the production of natural gas-based steam generation needed for the dehydration of ethanol has the largest environmental impact in ethylene production from corn. The dehydration of ethanol (highly endothermic reaction that requires 1 kJ of energy producing 1 g of ethylene)⁷⁵ and fertilizer production (H₂ and NH₃ production) have the largest adverse environmental impacts. Further, CO₂ is a byproduct in the steam reforming reaction of CH₄⁷⁶ and the removal of CO₂ from the atmosphere during photosynthesis does not offset the additional emissions resulting from corn production.⁷⁷

Acidification: The acid rain potential of ethylene production is primarily attributed to SO_x and NO_x emissions associated with production of fossil fuel-based process energy for the dehydration of ethanol and raw material production (H₂ production for fertilizers).⁷⁸

Ecotoxicity-air: Emission of metals (Arsenic, Copper, Selenium and Zinc) and inorganic chemicals into the atmosphere causes ecotoxicity-air impact. Fossil-fuel based energy for the production of fertilizer and the dehydration of ethanol causes the greatest impact for this category.

Ecotoxicity ground surface soil: Contamination of soil with heavy metals (copper, zinc, nickel) contributes to this impact category. Extensive use of chemical fertilizers and pesticide for corn production results in the contamination of soil by metals such as zinc, copper and nickel which constitute approximately, 0.1 wt% of the fertilizer mass.⁷⁹ In 2009, the consumption of nitrogen,

phosphate, and potash based fertilizer was 4.8, 1.42 and 1.45 million nutrient tonnes, respectively, making corn production the most fertilizer intensive crop among all the crops grown in U.S.⁷⁸ Common agricultural practices such as conventional tilling (practice of turning or digging up soils) to prepare fields for new corn seeding removes organic residue from the top soil surface left by previous harvests or cover crops, further exacerbating the fertilizer requirement for cultivation. Ecotoxicity ground surface soil impact is negligible for ethylene production from crude oil and natural gas.

Ecotoxicity-Water: Extensive fertilizer usage and leaching of the fertile top soil introduces metals (arsenic, chromium, copper and nickel) into the water stream. The net water consumption in the production of ethanol from corn is 3-4 gallons of water per gallon of ethanol produced. The bulk of this make-up water is utilized to meet cooling tower and boiler water requirement resulting in an adverse impact on the water table of the process.⁷⁰

Eutrophication: Partitioning of the NO_x emission into the water phase and emission of ammonia, nitrates and phosphates to fresh water contribute to eutrophication. The USEPA reports increases in nitrogen and phosphorous concentration in the U.S. river system by 90% and 85%, respectively from 1960 to 2001. Agricultural practices for corn production such as tilling are the primary reason for soil erosion, the main causative factor for fertilizer runoff into the river system resulting in *eutrophication*. Loss of fertile soil due to leaching has adverse impacts on crop yields necessitating higher use of fertilizers. Some of the critical effects of eutrophication include turbidity, ecosystem and habitat disturbances and degradation of water quality.⁸⁰ Further, the wastewater discharged from an ethanol processing facility have a high biological oxygen demand (BOD) value of 18,000-37,000 mg/L.⁸¹

Human health non-cancer water and air: Heavy metal (lead, arsenic, chromium) and poly-

aromatic hydrocarbon emissions during the generation of fossil fuel-based energy for the raw material production and fertilizer run-off are the primary causative factors for the non-carcinogenic emissions. Attributes such as bioaccumulation and persistence are the measure of the toxicity of a substance. Unsustainable agricultural practices (fertilizer and pesticide usage) are the primary reason for the contamination of the air, ground surface soil and water. The utilization of DDGS, the byproduct during ethanol production as animal feed is an important route to human exposure for these toxins. Further, erosion of agricultural soil is a major source of heavy metal contamination of the river systems.⁸²

Major adverse environmental impacts for ethylene production from crude oil

Global Warming Potential: The major impact for ethylene production from crude-oil is the ocean-based transportation of crude oil in ships powered by bunker fuel and the generation of fossil fuel-based process energy for crude oil processing.

Acidification: The ocean-based transportation of crude oil in ships powered by bunker fuel (sulfur content 4.5%) and generation of fossil fuel-based process energy (causes significant SO₂ and NO_x emissions) are the major impacts.⁸³ Thus, if the environmental impacts associated with the tanker transportation of crude oil is discounted (in other words, if the crude oil for ethylene production is derived from U.S. reserves), the environmental footprint of ethylene production from crude oil is significantly lower.

Ecotoxicity-air: Majority of the U.S. crude oil imports consist of sour crude (high sulfur content) from Middle East, Africa and South America, and bitumen (oil sands) from Canada.⁸⁴ The energy investment for processing these fuels is higher in comparison to sweet crude (low sulfur content). Additionally, nickel an active metal in the hydrodesulfurization catalyst is extracted by

the roasting/smelting of nickel metal ore. Metal emission during the roasting process is the primary contributor to this impact category. This problem is further exacerbated by the large quantities of heavy fuel oil needed for the transportation of the crude oil across the ocean.

Ecotoxicity-Water: Petroleum refining industry consumes 65-90 gallons of water and produces 20-40 gallons of water waste for every barrel of crude oil processed. Approximately, 9.5 gallons of water are consumed per minute per megawatt of power produced and serving as source of water pollution.⁷⁰ Further, significant quantities of metals emitted during energy generation are partitioned into the water stream and considered as major adverse environmental impacts.⁷⁰

Eutrophication: Emission of nitrogen oxides during the generation of natural gas-based process energy (atmospheric distillation of crude oil and steam cracking of naphtha) is the greatest impact for crude oil feedstock.

Human health non-cancer water and air: Metals emitted during the generation of coal-based process energy has the major impact. The metal concentration in the flue-gas is arrested by scrubbing the flue gas stream in a venture-wet scrubber system. Thus, a portion of the metals emissions are introduced into the waste-water stream of a power plant.⁸⁵

Major adverse environmental impacts for ethylene production from natural gas

Global Warming Potential: Emissions associated with the generation of fossil-fuel based energy for the production of ethylene (recovery and processing) has the biggest impact.

Acidification Potential: Fossil fuel based energy production and the desulfurization of natural gas produce substantial emission of SO_x and cause the greatest impacts for the production of ethylene from natural gas.

Ecotoxicity water: Partitioning of metal emissions into the water phase during the generation of

fossil-fuel based energy is a major hot spot in this process.⁸⁶

3.7.2.4 Hydrogen Production

The *gate-to-gate* environmental impact assessment for the production of ethylene and ethylene oxide has established that differences that are greater than an order of magnitude can be only considered reliable for making safe conclusions about greenness of any process or feedstock. Thus, the quantitative information (shown in Table 3-13) generated by this cradle-to-gate environmental impact assessment will be utilized for the identification of major adverse environmental impacts in hydrogen production from various feedstocks. Of the results listed in Table 3-13, four important categories are significant and are discussed.

Table 3-13: Environmental impact (cradle-to-gate) of manufacturing 100,000 metric tonnes/yr of hydrogen from light gases (methane, ethane), naphtha and Chlor-Alkali plant.

Category	H ₂ from Methane, millions	H ₂ at Refinery, millions	H ₂ from Ethylene Cracker, millions	H ₂ from Chlor-Alkali Plant, millions	H ₂ production in Germany, millions
Acidification, [mol H ⁺ Eq.]	65.8	67.1	70.6	46.8	37.9
Eco-toxicity Air, [kg 2,4-DCP Eq.]	0.22	2.15	0.76	0.19	0.049
Ecotoxicity-Ground Surface Soil, [kg Benzene Eq.]	7(10 ⁻³)	12(10 ⁻³)	11(10 ⁻³)	0	71(10 ⁻³)
Eco-toxicity Water, [kg 2,4-DCP Eq.]	37.9	24.5	30.33	9.70	12.4
Eutrophication, [kg N-Eq.]	45(10 ⁻³)	32(10 ⁻³)	47(10 ⁻³)	12(10 ⁻³)	24(10 ⁻³)
Global Warming Air, [kg	1164	307	440	109	1070

CO ₂ -Eq.]						
Human Health Cancer-Air, [kg Benzene Eq.]	74(10 ⁻³)	52(10 ⁻³)	46(10 ⁻³)	54(10 ⁻³)	0.5(10 ⁻³)	
Human Health Cancer-Ground Surface Soil, [kg Benzene Eq.]	2.7(10 ⁻⁵)	4.1(10 ⁻⁵)	3.8(10 ⁻⁵)	0	22.5(10 ⁻⁵)	
Human Health Cancer Water, [kg Benzene Eq.]	50(10 ⁻³)	45(10 ⁻³)	56(10 ⁻³)	14(10 ⁻³)	19(10 ⁻³)	
Human Health Criteria Air Point Source, [kg PM 2,5-Eq.]	0.45	0.42	0.47	0.27	0.25	
Human Health Non-Cancer Air, [kg Toluene Eq.]	140	591	246	40.4	40.2	
Human Health Non-Cancer Ground Surface Soil, [kg Toluene Eq.]	0.56	0.93	0.87	0	5.3	
Human Health Non-Cancer Water, [kg Toluene Eq.]	1739	1054	1448	314	503	
Ozone Depletion Potential, [kg CFC-11 Eq.]	10.7(10 ⁻⁶)	6.8(10 ⁻⁶)	6.2(10 ⁻⁶)	12.2(10 ⁻⁶)	2.2(10 ⁻⁶)	
Smog Air, [kg NO _x Eq.]	8.08(10 ⁻⁴)	5.83(10 ⁻⁴)	7.52(10 ⁻⁴)	2.80(10 ⁻⁴)	4.73(10 ⁻⁴)	

Cradle-to-gate life cycle assessment

Acidification: Generation of natural gas-based process energy for raw material production (methane, cracking of ethane) and transportation of crude oil by bunker fuel powered by ocean going vessels has the largest impact for H₂ produced from fossil sources. Coal-based electrical power generation has the greatest impact for H₂ produced at a Chlor-Alkali plant. The potential emissions in all these routes are of the same order of magnitude. The relatively lower prediction for acidification potential for H₂ production in Germany is attributed to the comparatively lower

distance between Germany and the exporting nation.

Ecotoxicity water potential: Partitioning of metal emissions into the water phase during fossil-fuel based energy production and the generation of water waste during the processing of crude oil contributes to this impact category.⁷⁰ Further, the drilling mud employed in the production of oil in offshore rigs introduces arsenic, lead, mercury, cadmium, vanadium, chromium, zinc, aluminum and aromatic hydrocarbons into the underground water table thus causing significant water pollution in the vicinity of the oil rig.^{48, 87, 88}

Global warming potential: Generation of natural gas-based process energy and CO₂ emission during H₂ production in the case of methane feedstock contribute towards this impact category. The GHG emissions for H₂ produced at the refinery, chlor-alkali plant and ethylene cracker are comparable and substantially lower than that for hydrogen produced by the steam reforming of naphtha (in the case of Germany) or methane.

Human health non-cancer air: Metals emitted during the generation of fossil-fuel based energy for the production of raw material has the greatest impact for H₂ production. The distillation of crude oil is highly energy intensive and the net H₂ produced at a refinery is dependent on the quality of crude (sulfur content) and its naphthenic content. The bulk of the U.S. crude oil is sour translating to higher H₂ consumption for the upgrading of gasoline.⁸⁹ Thus, larger volumes of crude oil need to be transported and processed for producing the *100,000 tonnes of H₂*. Additionally, ships powered by bunker fuel (high sulfur content) and transporting crude oil across oceans results in air pollution. In contrast, natural gas for H₂ production in Germany is obtained via pipeline, resulting in substantially lower metal emissions.

3.7.2.5 Energy Production

As explained above, the production of ethylene, hydrogen, hydrogen peroxide and ethylene oxide involves highly energy intensive operations. The source of the energy required for various processing steps has a major influence on the overall environmental impacts. Coal is classified based on the carbon, ash and inherent moisture content. Hard coal, also known as anthracite, is the best quality coal with a high carbon content and calorific value. Lignite, commonly known as brown coal, has a relatively lower energy content due to high inherent moisture and ash contents.⁹⁰ The three major steps associated with the production of energy are: (i) extraction/production of energy source; (ii) transportation of energy source to power-plant; (iii) production of energy. Table 3-14 lists the potential impacts estimated by GaBi[®] for the mining of coal (*gate-to-gate analysis*) and cradle-to-grave analysis for producing energy. The emissions associated with the production of energy (difference between the impacts predicted by cradle-to-grave and gate-to-gate analyses) are compared to that reported by Lawrence Energy Center to the USEPA.⁹¹ The source and quality of coal used by the Lawrence energy Center for the production of energy is unknown. Based on the results in Table 3-14, the potential emissions associated with the mining of coal are highly dependent on the type of mine (surface mine or underground mine). The potential impact of mining coal from an underground mine is predicted to be higher than surface mine in most impact categories. As the differences in potential impacts lie within prediction uncertainty of this analysis we cannot conclusively establish the benignity of any particular type of mining.

Further, the global warming potential for energy production predicted by this analysis [76.5 kg CO₂ Equivalent] assuming that the coal is obtained from an underground mine is similar to the actual emissions reported by Lawrence Energy Center to USEPA [78 kg CO₂ Equivalent].⁹²

If the coal combusted in Lawrence Energy Center were to be obtained from a surface mine the predicted and reported GHG emissions are of the same order of magnitude. The similarity in the predicted and reported data lends certain level of credibility to our analysis and further identifies power generation (in the present case by the combustion of coal) has the greatest environmental impact in comparison to other activities such as mining and transportation of coal.

Table 3-14: Gate-to-gate analysis for the mining of coal to produce 1000 MJ of energy. Cradle-to-Grave environmental impact assessment for the producing 1000 MJ of energy from coal. Comparison of the emissions for the production of energy to that reported by the Lawrence Energy Center to USEPA.⁹¹

Category	Mining of Coal, (A)	Cradle-to-Grave Assessment for Energy Production, (B)	Potential Impact of Energy Generation, [B-A]	Lawrence Energy Center, TRI Data*			
	Hard Coal, mine	Lignite Coal, surface mine	Hard Coal	Lignite Coal			
Acidification, [mol H ⁺ Eq.]	17.2	1.84	39.36	30.97	22.16	29.13	7.35
Eco-toxicity Air, [kg 2,4-DCP Eq.]	0.386	0.0189	0.457	0.518	0.071	0.4991	0.00135
Eco-toxicity GSS, [kg Benzene Eq.]	-	-	4.8(10 ⁻⁵)	2.4(10 ⁻⁵)	-	-	N/A
Eco-toxicity Water, [kg 2,4-DCP Eq.]	0.3(10 ⁻⁴)	0.74(10 ⁻⁴)	2.3(10 ⁻⁴)	1.1(10 ⁻⁴)	1.99(10 ⁻⁴)	0.3(10 ⁻⁴)	1.5(10 ⁻⁴)
Eutrophication, [kg N-Eq.]	2.3(10 ⁻³)	8.24(10 ⁻⁴)	9.4(10 ⁻³)	9.5(10 ⁻³)	7.07(10 ⁻³)	8.7(10 ⁻³)	11.4(10 ⁻³)
Global Warming Air, [kg CO ₂ -Eq.]	20.8	7.72	97.32	100.31	76.5	92.6	78
Human Health Cancer-Air, [kg Benzene Eq.]	0.011	0.00323	0.099	0.0205	0.088	0.0172	0.031
Human Health Cancer-GSS, [kg Benzene Eq.]	-	-	1.5(10 ⁻⁷)	0.5(10 ⁻⁷)	-	-	N/A
Human Health Cancer Water, [kg Benzene Eq.]	0.00032	0.00126	0.011	0.002	0.01067	7.4(10 ⁻⁴)	N/A

Category	Mining of Coal, (A)	Cradle-to-Grave Assessment for Energy Production, (B)	Potential Impact of Energy Generation, [B-A]	Lawrence Energy Center, TRI Data*			
	Hard Coal, mine	Lignite Coal, surface mine	Hard Coal	Lignite Coal			
Human Health Criteria Air Point, [kg PM2.5- Eq.]	0.123	0.014	0.227	0.184	0.104	0.17	0.126
Human Health Non-Cancer Air, [kg Toluene Eq.]	24.099	5.39	49.9	32.44	25.80	27.05	N/A
Human Health Non-Cancer GSS, [kg Toluene Eq.]	-	-	0.0035	0.0014	-	-	N/A
Human Health Non-Cancer Water, [kg Toluene Eq.]	7.59	16.6	9.117	29.8	1.52	13.44	15
Ozone Depletion Potential, [kg CFC-11 Eq.]	3.77(10 ⁻¹¹)	1.47(10 ⁻¹¹)	5(10 ⁻⁸)	36(10 ⁻⁸)	4.99(10 ⁻⁸)	3.6(10 ⁻⁷)	N/A
Smog Air, [kg NO _x Eq.]	5.35(10 ⁻⁵)	1.91(10 ⁻⁵)	19(10 ⁻⁵)	21(10 ⁻⁵)	13.6(10 ⁻⁵)	19(10 ⁻⁵)	26(10 ⁻⁵)

Eq.: Equivalent, DCP: Dichlorophenoxyace

N/A: Data not available at the toxic release inventory

Natural gas, mixture of alkanes, predominantly methane, has a low sulfur content and high specific energy (MJ/kg) among all the sources compared in this analysis. Table 3-15 lists the impact of extracting natural gas (*gate-to-gate analysis*) and the cradle-to-grave environmental impact of producing energy from natural gas. The emissions predicted in this analysis are compared to the emissions reported by Astoria Generating Station to USEPA.⁹³ The potential global warming emissions predicted by GaBi[®] are of the same order of magnitude as reported by Astoria Generating Station the environmental impact with predictions being greater than that reported by the generating station to USEPA.⁹⁴ This analysis conclusively establishes energy production as the biggest hot spot even when natural gas is employed as energy source.

Heavy fuel oil (Number 6, residual fuel oil, bunker fuel oil) is mainly comprised of residues from cracking and distillation units in the refinery. These fuels have higher mass density and high carbon/hydrogen ratio compared to light fuel (Number 3 fuel oil).⁹⁵ Table 3-16 compares the potential impact associated with the production of fuel oil (high boiling fraction of crude oil) and emissions associated with the generation of energy from heavy fuel oil and light fuel oil, respectively. The impact of generating energy from heavy fuel oil and light fuel oil are similar and the differences lie within prediction uncertainty of this life cycle assessment. The environmental impact of producing energy from crude oil (*cradle-to-grave*) is greater than the impact of crude oil production (*gate-to-gate*) by one-or-two orders of magnitude.

Table 3-15: Gate-to-gate environmental impact assessment for extracting natural gas to produce 1000 MJ of energy and cradle-to-grave environmental impact for producing 1000 MJ from natural gas. Comparison of the predicted emissions for the production of energy to that reported by Astoria Generating Station to USEPA.⁹¹

Category	Extraction of Natural Gas, (GaBi [®]) (A)	Cradle-to-Grave Assessment for Energy Production, (B)	Potential Impact of Energy Generation [B-A]	Astoria Generating Station, TRI Data*
Acidification, [mol H ⁺ Eq.]	0.98	6.15	5.17	N/A
Eco-toxicity Air, [kg 2,4- DCP Eq.]	0.0031	0.013	9.9(10 ⁻³)	0.0016
Eco-toxicity-GSS, [kg Benzene Eq.]	-	-	-	N/A
Eco-toxicity Water, [kg 2,4- DCP Eq.]	5.4(10 ⁻⁴)	7.25(10 ⁻⁴)	1.85(10 ⁻⁴)	5.4(10 ⁻⁴)
Eutrophication, [kg N-Eq.]	2.14(10 ⁻³)	4.97(10 ⁻³)	2.83(10 ⁻³)	N/A
Global Warming Air, [kg CO ₂ -Eq.]	7.6	74.86	67.26	29.3
Human Health Cancer-Air, [kg Benzene Eq.]	0.000681	0.0045	0.0038	0.0017
Human Health Cancer-GSS, [kg Benzene Eq.]	-	-	-	N/A
Human Health Cancer Water, [kg Benzene Eq.]	0.00151	0.007	0.008	0.007
Human Health Criteria Air Point, [kg PM2.5- Eq.]	0.00539	0.0474	0.0420	N/A
Human Health Non-Cancer Air, [kg Toluene Eq.]	0.805	9.18	8.37	19.9
Human Health Non-Cancer GSS, [kg Toluene Eq.]	-	0.034	0.034	N/A
Human Health Non-Cancer Water, [kg Toluene Eq.]	105.52	163	57.4	39.7
Ozone Depletion Potential, [kg CFC-11 Eq.]	1.18(10 ⁻¹¹)	63(10 ⁻⁸)	6.29(10 ⁻⁷)	N/A
Smog Air, [kg NO _x Eq.]	4.49(10 ⁻⁶)	10(10 ⁻⁵)	9.5(10 ⁻⁵)	N/A

Eq.: Equivalent, DCP: Dichlorophenoxyace, N/A: Data not available at the toxic release inventory

Table 3-16: Gate-to-gate environmental impact assessment for the production of fuel oil to produce 1000 MJ of energy and the cradle-to-grave life cycle assessment for the production of 1000 MJ of energy from heavy fuel oil and light fuel oil.

Category	Gate-to-Gate Assessment Production of crude oil, (GaBi®)	Cradle-to-Grave Energy Production Heavy Fuel Oil (GaBi®)	Assessment for Light Fuel Oil (GaBi®)
Acidification, [mol H ⁺ Eq.]	1.23	24.18	9.58
Eco-toxicity Air, [kg 2,4- DCP Eq.]	0.004	0.356	0.054
Eco-toxicity Ground Surface Soil, [kg Benzene Eq.]	-	8.2(10 ⁻⁴)	9(10 ⁻⁴)
Eco-toxicity Water, [kg 2,4- Dichlorophenoxyace Eq.]	25.1(10 ⁻⁴)	80.4(10 ⁻⁴)	87.3(10 ⁻⁴)
Eutrophication, [kg N- Eq.]	2.26(10 ⁻³)	5.32(10 ⁻³)	5.16(10 ⁻³)
Global Warming Air, [kg CO ₂ -Eq.]	4.83	95.38	89.54
Human Health Cancer-Air, [kg Benzene Eq.]	0.000854	0.0835	0.0017
Human Health Cancer-GSS, [kg Benzene Eq.]	-	28(10 ⁻⁷)	30(10 ⁻⁷)
Human Health Cancer Water, [kg Benzene Eq.]	0.00252	0.0031	0.0031
Human Health Criteria Air Point, [kg PM2,5- Eq.]	0.0066	0.141	0.066
Human Health Non-Cancer Air, [kg Toluene Eq.]	0.89	91.67	17.04
Human Health Non-Cancer GSS, [kg Toluene Eq.]	-	0.0627	0.0679
Human Health Non-Cancer Water, [kg Toluene Eq.]	60	60.95	63.65
Ozone Depletion Potential, [kg CFC-11 Eq.]	8.25(10 ⁻¹⁰)	22(10 ⁻⁸)	21(10 ⁻⁸)
Smog Air, [kg NO _x Eq.]	5.59(10 ⁻⁶)	11(10 ⁻⁵)	11(10 ⁻⁵)

Eq.: Equivalent, DCP: Dichlorophenoxyace

Cradle-to-Grave life cycle assessment for energy production

Global Warming Potential (GWP) estimated for the various energy sources excluding natural gas are similar (the differences of 10% lie within predictable uncertainty), indicating that the deployment of a coal or fuel oil for energy production *does not* result in any significant decrease in carbon footprint. GaBi[®] predicts the carbon foot-print for the natural gas-based energy production to be of the same order of magnitude but lower by 25% primarily attributed to the low carbon content combined with high calorific value which makes energy production from natural gas comparatively cleaner as shown in Table 3-17.

Ecotoxicity-air: The potential metal emissions (copper and zinc) for energy production are of the same order of magnitude for all the energy sources. In coal, zinc is present in the sphalerite form which has a low melting point and is easily susceptible to vaporization resulting in metal emissions. Heavy metal emissions in fuels depend on the properties and concentration of metals and the technologies used for combustion and post-combustion clean-up.

Human health air-point source: The emission of NO_x, SO_x and dust particles during the production of energy contribute to this impact category. The emission of these pollutants are similar for the production of energy from coal and fuel oil and are an order of magnitude lower for energy production from natural gas and light fuel oil.

Table 3-17: Cradle-to-grave environmental impact assessment for producing energy from hard coal (anthracite), lignite coal, heavy fuel oil, light fuel oil and natural gas

Category	Coal		Fuel Oil		Natural Gas	
	Hard Coal (GaBi [®])	Lignite Coal (GaBi [®])	Heavy Fuel Oil (GaBi [®])	Light Fuel Oil (GaBi [®])	Natural Gas (GaBi [®])	Natural Gas
Acidification, [mol H ⁺ Eq.]	39.36	30.97	24.18	9.58	6.15	
Eco-toxicity Air, [kg 2,4-DCP Eq.]	0.157	0.518	0.356	0.054	0.013	
Ecotoxicity-Ground Surface Soil, [kg Benzene Eq.]	4.8(10 ⁻⁵)	2.4(10 ⁻⁵)	8.2(10 ⁻⁴)	9(10 ⁻⁴)	4.3(10 ⁻⁴)	
Eco-toxicity Water, [kg 2,4-DCP Eq.]	2.31(10 ⁻⁴)	1.1(10 ⁻⁴)	80.4(10 ⁻⁴)	87.3(10 ⁻⁴)	31(10 ⁻⁴)	
Eutrophication, [kg N-Eq.]	9.41(10 ⁻³)	9.51(10 ⁻³)	5.32(10 ⁻³)	5.16(10 ⁻³)	4.97(10 ⁻³)	
Global Warming Air, [kg CO ₂ -Eq.]	97.32	100.31	95.38	89.54	74.86	
Human Health Cancer-Air, [kg PM2.5- Eq.]	0.099	0.0205	0.0835	0.0017	0.0045	
Human Health Cancer-GSS, [kg Benzene Eq.]	1.5(10 ⁻⁷)	0.5(10 ⁻⁷)	28(10 ⁻⁷)	30(10 ⁻⁷)	17(10 ⁻⁷)	
Human Health Cancer Water, [kg Benzene Eq.]	0.011	0.0002	0.0031	0.0031	0.0031	
Human Health Criteria Air Point, [kg Benzene Eq.]	0.227	0.184	0.141	0.066	0.0474	
Human Health Non-Cancer Air, [kg Toluene Eq.]	24.099	32.44	91.67	17.04	9.18	
Human Health Non-Cancer Ground Surface Soil, [kg Toluene Eq.]	0.0035	0.0014	0.0627	0.0679	0.0341	
Human Health Non-Cancer Water, [kg Toluene Eq.]	9.117	16.36	60.95	63.65	105.52	
Ozone Depletion Potential, [kg CFC-11 Eq.]	5(10 ⁻⁸)	36(10 ⁻⁸)	22(10 ⁻⁸)	21(10 ⁻⁸)	63(10 ⁻⁸)	
Smog Air, [kg NO _x Eq.]	19(10 ⁻⁵)	21(10 ⁻⁵)	11(10 ⁻⁵)	11(10 ⁻⁵)	10(10 ⁻⁵)	

Eq.: Equivalent, DCP: Dichlorophenoxyace

Human health cancer air impact is primarily attributed to metal and organic emissions to air. Potential metal emissions for energy production from hard coal, lignite and heavy fuel oil are similar and an order of magnitude higher than that reported for natural gas and light fuel oil. Combustion of coal (anthracite and lignite) produces significant arsenic emissions, which has high toxicity and persistence.⁹⁶ The mobility of arsenic in the atmosphere during mining, combustion and storage of coal is dependent on its mode of occurrence. Arsenic concentration of coal produced in the U.S. can vary from 24 ppm to 71 ppm and is dictated by coal type and the location of the coal basin. Arsenic in hard coal and lignite is present in the pyrite organic phase. The storage facilities and waste material are major sources of arsenic mobilization. Coal cleaning technologies, employed to reduce sulfur content, are known to reduce arsenic concentration thus resulting in lower arsenic emissions during energy production from lignite. Significant quantities of SO₂, NO_x and particulate matter emissions are produced during mining and combustion operations. These emissions have been identified to have a great deleterious effect on humans.

The results from the foregoing analysis represent per capita environmental impacts from various energy sources and can therefore be utilized to quantify the environmental impact of energy utilization from various energy sources in general. At the present time we cannot conclusively establish the greenness of any particular energy source as the differences in the environmental impacts obtained by this cradle-to-grave analysis lie within the prediction uncertainty.

3.8 Conclusions

Comparative economic and environmental impacts assessments of the conventional and the CEBC processes for EO production were performed based on simulations of a 200,000

tonnes/year plant. Capital investments for both processes are estimated to be approximately \$120 million. The EO production cost in the conventional process is estimated to be 71.6 ¢/lb yielding a profit margin of 7.4 ¢/lb based on the 2009 EO market price. The estimated EO production cost in the CEBC process is 74.4 ¢/lb assuming a catalyst life of 1 year and leaching rate of 2.2 lb MTO/h (corresponding to a Re leaching rate of 10 ppm in the reactor effluent). The profit margin in the CEBC process increases to 13.6 ¢/lb EO if the catalyst is active for 1 year at a leaching rate of 0.11 lb MTO/h. The increased costs in the CEBC process due to the use of the more expensive oxidant (hydrogen peroxide compared to oxygen) and expensive catalyst (rhenium compared to silver) are clearly offset by the gains made from more effective ethylene utilization (total ethylene oxide selectivity at higher ethylene conversions). Further, higher utilization of H₂O₂ will increase the profit margin of the CEBC process. The relatively lower profit margin in case 1 of the CEBC process is attributed to the use of refrigeration, an expensive utility to remove the heat of reaction. The lower profit margin in case 2 of the CEBC process is attributed to the production of H₂O₂ by the anthraquinone process. The performance metrics established by this comparative analysis guide catalyst design for economic viability of the CEBC process.

Environmental emissions predicted by the *gate-to-gate* analysis of the simulated conventional process are greater but of the same order of magnitude compared to those reported by the BASF Corporation for a similar process at their Geismar, LA facility establishing credibility of this analysis method.⁶⁷ The cumulative environmental impacts estimated by the *cradle-to-gate* life cycle assessments of the conventional process and the various cases of the CEBC process are of the same order of magnitude in most of the impact categories such as acidification, global warming potential, soil pollution, eutrophication, and emissions of carcinogens. The main contributors to these adverse environmental impacts stem from coal-

based electricity generation (to power compressors) and fossil fuel-based energy for raw material production (used for ethylene, hydrogen and methanol). While the burning of ethylene to CO₂ constitutes only 4.4% of the total global warming potential of the conventional process, the lower GHG the emissions in CEBC process are attributed to lower ethylene feedstock and reduced energy requirement for separation and recycle of ethylene. A cradle-to-gate analysis reveals that the environmental impacts of conventional and all the cases of the CEBC processes lie within prediction uncertainty. A major fraction of the adverse environmental impacts for both processes stem mainly from sources outside the ethylene oxide plant. Further, the effective utilization of H₂O₂ will reduce the environmental impact proportionately. A major fraction of the environmental impacts for H₂O₂ production lie outside the boundaries of the plant.

The cumulative emissions estimated by the *cradle-to-gate* life cycle assessments of ethylene produced from corn, crude oil and natural gas are of the same order of magnitude in most of the impact categories such as acidification, global warming potential, eutrophication, and contamination of soil, air and water. The main environmental impact for ethylene production from corn stems from generation of fossil fuel-based energy for fertilizer production and dehydration of ethanol, and from the leaching of top surface soil. Absorption of carbon dioxide by plants due to photosynthesis does not totally offset the GHG emissions. For ethylene production from crude oil, the ocean-based transportation of crude oil and generation of fossil-fuel based process energy cause the greatest adverse environmental impact. Similar trends are observed for hydrogen production. The potential emissions associated with the production of coal-based energy (predicted by GaBi[®]) are similar in magnitude (~76 kg CO₂ Equivalent) to that reported by Lawrence Energy Center and Astoria Generating Station to USEPA. The predicted carbon footprints for all the energy sources (hard coal, lignite, heavy fuel oil, light fuel

oil and natural gas) is of the same order of magnitude. The environmental impact associated with the recovery and transportation of these fossil fuel-based energy sources is relatively small compared to the impact of energy generation from fossil fuels.

References

1. Rebsdatt, S.; Mayer, D., Ethylene Oxide. In *Ullmann's Encyclopedia of Industrial Chemistry*, 6th ed.; Hawkins, S.; Russey, W. E.; Pilkart-Muller, M., Eds. Wiley-VCH: New York, 2005; Vol. 13, p 23.
2. Weissermel, K.; Arpe, H.-J., *Industrial Organic Chemistry*. 4th ed.; Wiley-VCH: Washington D.C., 2003.
3. Buffum, J. E.; Kowaleski, R. M.; Gerdes, W. H. Ethylene Oxide Catalyst. US 5145824, 1992.
4. Zabetakis, M. G., *Flammability Characteristics of combustible gases and vapor*. 1st ed.; U.S. Department of Interior, US Bureau of Mines: 1939.
5. Hess, L. G.; Tilton, V. V., Ethylene Oxide - Hazards and Methods of Handling. *Industrial and Engineering Chemistry* **1950**, 42, (6), 1251-1258.
6. Lee, H. J.; Ghanta, M.; Busch, D. H.; Subramaniam, B., Towards a CO₂-free ethylene oxide process: Homogeneous ethylene oxide in gas-expanded liquids. *Chemical Engineering Science* **2010**, 65, (1), 128-134.
7. Lee, H. J.; Shi, T. P.; Busch, D. H.; Subramaniam, B., A greener, pressure intensified propylene epoxidation process with facile product separation. *Chemical Engineering Science* **2007**, 62, (24), 7282-7289.
8. Subramaniam, B.; Busch, D. H.; Lee, H. J.; Ghanta, M.; Shi, T.-P. Process for Selective Oxidation of Olefins to Epoxides. US 8080677 B2, 2011.
9. Ghanta, M.; Lee, H. J.; Busch, D. H.; Subramaniam, B., Highly Selective Homogeneous Ethylene Epoxidation in Gas (Ethylene)-Expanded Liquid: Transport and Kinetic Studies. *AIChE Journal (in press)* **2011**.

10. Dunn, J. B.; Savage, P. E., Economic and environmental assessment of high-temperature water as a medium for terephthalic acid synthesis. *Green Chemistry* **2003**, 5, (5), 649-655.
11. Fang, J.; Jin, H.; Ruddy, T.; Pennybaker, K.; Fahey, D.; Subramaniam, B., Economic and environmental impact analyses of catalytic olefin hydroformylation in CO₂-expanded liquid (CXL) media. *Industrial & Engineering Chemistry Research* **2007**, 46, (25), 8687-8692.
12. Gong, K. N.; Chafin, S.; Pennybaker, K.; Fahey, D.; Subramaniam, B., Economic and Environmental Impact Analyses of Solid Acid Catalyzed Isoparaffin/Olefin Alkylation in Supercritical Carbon Dioxide. *Industrial & Engineering Chemistry Research* **2008**, 47, (23), 9072-9080.
13. *Aspen HYSYS, 7.1*; Aspen Technologies: Calgary, Alberta, Canada, 2009.
14. Peters, M. S.; Timmerhaus, K. D., *Plant Design and Economics For Chemical Engineers*. Fourth ed.; McGraw Hill Inc.: New York, 1991; p 910.
15. Chilton, C. H.; Popper, H.; Norden, R. B., *Modern Cost Engineering: Methods and Data*. McGraw-Hill Publishing Company: New York, 1978; Vol. I, p 579.
16. Couper, J. R.; Penney, W. R.; Fair, J. R.; Walas, S. M., *Chemical Process Equipment: Selection and Design*. Second ed.; Butterworths: **Boston**, 1988.
17. Matley, J., *Modern Cost Engineering: Methods and Data* McGraw-Hill Publishing Company: New York, 1984; Vol. II, p 296.
18. US Energy Information Administration. <http://www.eia.doe.gov/>
19. U.S. Bureau of Labor Statistics. <http://www.bls.gov/cpi/> (Accessed June 10th, 2010),
20. Engineering News Record. www.enr.com (Accessed Jun 12th, 2010),

21. McCain, J.; Naumann, A. W.; Wang, W. Y. Thermal Process for Removal of Contaminants From Process Streams. US 5563282, 1996.
22. Markwordt, D. W. *Sources of Ethylene Oxide Emissions EPA-450/3-85-014*; Unoted States Department of Interior: Washington D. C., 1985; p 30.
23. Golubev, Y. D.; Dement'eva, L.; VLasov, G. M., The Solubility of ethylene oxide in C1-4 alcohols. *Soviet Chemical Industry* **1971**, (8), 3.
24. Kilty, P. A.; Sachtler, W. M. H., The mechanism of the selective oxidation of ethylene to ethylene oxide. *Catalysis Reviews Science and Engineering* **1974**, 10, (1), 1-16.
25. Fang, J.; Jana, R.; Tunge, J. A.; Subramaniam, B., Continuous homogeneous hydroformylation with bulky rhodium catalyst complexes retained by nano-filtration membranes. *Applied Catalysis A: General* **2011**, 393, 294-301.
26. Vora, B. V.; Pujado, P. R. Process For Producing Propylene Oxide. US 5599955, 1997.
27. Fischer, M.; Kaibel, G.; Stammer, A.; Flick, K.; Quaiser, S.; Harder, W.; Massonne, K. Process for the Manufacture of Hydrogen Peroxide. US 6375920 B2, 2002.
28. BASF Catalysts-Metal Prices. <http://www.catalysts.basf.com/apps/eibprices/mp/DPCharts.aspx> (Accessed June 5th, 2010),
29. Tosh, E.; Mitterpleininger, J. K. M.; Rost, A. M. J.; Veljanovski, D.; Herrmann, W. A.; Kuhn, F. E., Methyltrioxorhenium revisited: improving the synthesis for a versatile catalyst. *Green Chemistry* **2007**, 9, (12), 1296-1298.
30. Vezzosi, S.; Ferre, A. G.; Crucianelli, M.; Crestini, C.; Saladino, R., A novel and efficient catalytic epoxidation of olefins with adducts derived from methyltrioxorhenium and chiral aliphatic amines. *Journal of Catalysis* **2008**, 257, (2), 262-269.

31. Bracco, L. L. B.; Juliarena, M. P.; Ruiz, G. T.; Feliz, M. R.; Ferraudi, G. J.; Wolcan, E., Resonance energy transfer in the solution phase photophysics of $-\text{Re}(\text{CO})(3)\text{L}^+$ pendants bonded to poly(4-vinylpyridine). *Journal of Physical Chemistry B* **2008**, 112, (37), 11506-11516.
32. Zhou, B.; Rueter, M.; Parasher, S. Supported Catalysts Having a Controlled Coordination Structure and Methods For Preparing Such Catalysts. US 7011807 B2, 2006.
33. Haas, T.; Brasse, C.; Stochniol, G.; Glenneberg, J.; Woll, W. Aqueous Hydrogen Peroxide Solutions and Method of Making Same. US 7722847 B2, May 25th, 2010.
34. Fischer, M.; Butz, T.; Massonne, K. Preparation of Hydrogen Peroxide From Hydrogen and Oxygen. US 6872377 B2, 2005.
35. Goor, G.; Glenneberg, J.; Jacobi, S., Hydrogen Peroxide. In *Ullmann's Encyclopedia Of Industrial Chemistry*, 6th Edition ed.; Hawkins, S.; Russey, W. E.; Pilkart-Muller, M., Eds. Wiley VCH: New York, 2007; Vol. 18, p 35.
36. Pujado, P. R.; Hammerman, J. I. Integrated Process For The Production Of Propylene Oxide. US 5599956, 1997.
37. Durst, R. A.; Bates, R. G., Hydrogen Peroxide In *Kirk-Othmer Encyclopedia of Chemical Technology*, 5th ed.; Eul, W.; Moeller, A.; Steiner, N., Eds. Wiley: 2007; Vol. 14, p 32.
38. Rushmere, J. D. Process for Manufacturing Hydrogen Peroxide. 1987.
39. CEPCI Chemical Engineering Plant Cost Index. *Chem. Eng.* 2010, p 76.
40. ICIS. <http://www.icis.com/chemicals/channel-info-chemicals-a-z/> (Accessed June 15th, 2010),
41. U.S. Energy Information Administration-Crude Oil. <http://www.eia.doe.gov/> (Accessed June 5th,2010),

42. *GaBi*, 4.4; PE Solutions and Five Winds Corporation: United States, 2011.
43. Bare, J. C.; Norris, G. A.; Pennington, D. W.; McKone, T., TRACI: The Tool for the Reduction and Assessment of Chemical and Other Environmental Impacts. *Journal of Industrial Ecology* **2003**, 6, (3-4), 49-78.
44. Bare, J. C.; Hofstetter, P.; Pennington, D. W.; Udo de Haes, H. A., Life Cycle Impact Assessment Workshop Summary: Midpoint versus Endpoints: The Sacrifices and Benefits *International Journal of Life Cycle Assessment* **2000**, 5, (6), 319-326.
45. Allen, D. T.; Shonnard, D., *Sustainable Engineering Concepts, Design, and Case Studies*. 1st Edition ed.; Prentice Hall: New York, 2012; p 207.
46. Kalnes, T. N.; Koers, K. P.; Marker, T.; Shonnard, D., A Technoeconomic and Environmental Life Cycle Comparison of Green Diesel to Biodiesel to Biodiesel and Syndiesel. *Environmental Progress & Sustainable Energy* **2009**, 28, (1), 10.
47. Gujarathi, A. M.; Patle, D. S.; Agarwal, P.; Karemore, A. L.; Babu, B. V., Simulation and Analysis of Ethane Cracking Process. In CHEMCON: Vishakapatnam, 2009; p 8.
48. Kargbo, D. M.; Wilhelm, R. G.; Campbell, D. J., Natural Gas Plays in the Marcellus Shale: Challenges and Potential Opportunities. *Environmental Science & Technology* **2010**, 44, (15), 5679-5684.
49. Natural Gas. www.naturalgas.org (Accessed 23rd July),
50. Zimmermann, H.; Walzl, R., Ethylene. In *Ullmann's Encyclopedia of Industrial Chemistry*, Hawkins, S.; Russey, W. E.; Pilkart-Muller, M., Eds. Wiley-VCH: New York, 2009; Vol. 13, p 36.
51. Haussinger, P.; Lohmuller, R.; Watson, A. M., Hydrogen. In *Ullmann's Encyclopedia Of Industrial Chemistry*, 6th Edition ed.; Hawkins, S.; Russey, W. E.; Pilkart-Muller, M.,

- Eds. Wiley VCH: New York, 2007; Vol. 18, p 162.
52. Fiedler, E.; Grossman, G.; Kersebohm, D. B.; Weiss, G.; Witte, C., Methanol. In *Ullmann's Encyclopedia of Industrial Chemistry*, 6th Edition ed.; Hawkins, S.; Russey, W. E.; Pilkart-Muller, M., Eds. Wiley-VCH: New York, 2000; Vol. 23, p 14.
 53. Barron, R. F., Cryogenic Technology. In *Ullmann's Encyclopedia of Industrial Chemistry*, 6th Edition ed.; Hawkins, S.; Russey, W. E.; Pilkart-Muller, M., Eds. Wiley-VCH: New York, 2000; Vol. 10, p 46.
 54. Shimizu, S.; Watanabe, N.; Kataoka, T.; Shoji, T.; Abe, N.; Morishita, S.; Ichimura, H., Pyridine and Pyridine Derivatives. In *Ullmann's Encyclopedia of Industrial Technology*, Hawkins, S.; Russey, W. E.; Pilkart-Muller, M., Eds. Wiley VCH: 2000; Vol. 30, p 34.
 55. Muller, H., Sulfuric Acid and Sulfur Trioxide. In *Ullmann's Encyclopedia of Industrial Chemistry*, 6th Edition ed.; Hawkins, S.; Russey, W. E.; Pilkart-Muller, M., Eds. Wiley-VCH: 2000; Vol. 35, p 72.
 56. Schrodter, K.; Bettermann, G.; Staffel, T.; Wahl, F.; Klein, T.; Hofmann, T., Phosphoric Acid and Phosphates. In *Ullmann's Encyclopedia Of Industrial Chemistry*, 6th Edition ed.; Hawkins, S.; Russey, W. E.; Pilkart-Muller, M., Eds. Wiley VCH: 2008; Vol. 26, p 46.
 57. Freilich, M. B.; Petersen, R. L., Potassium Compounds. In *Kirk-Othmer Encyclopedia of Chemical Technology*, 5th ed.; Othmer, K., Ed. John Wiley and Sons: 2005; p 125.
 58. Rebsdatt, S.; Mayer, D., Ethylene Glycol. In *Ullmann's Encyclopedia of Industrial Chemistry*, 6th Edition ed.; Hawkins, S.; Russey, W. E.; Pilkart-Muller, M., Eds. Wiley-VCH: 2000; Vol. 13, p 16.
 59. Hussey, D. F.; Foutch, G. L.; Ward, M. A., Ultrapure Water. In *Ullmann's Encyclopedia*

- of Industrial Chemistry*, 6th ed.; Hawkins, S.; Russey, W. E.; Pilkart-Muller, M., Eds. Wiley-VCH: Weinheim, 2007; Vol. 39, p 41.
60. Austin, G. T., *Shreve's Chemical Process Industries*. 5th Edition ed.; McGraw Hill: Singapore, 1984; p 833.
 61. Sheldon, R. A.; Arends, I.; Hanefeld, U., Solid Acids and Bases as Catalysts. In *Green Chemistry and Catalysis*, Wiley-VCH: Delft, 2007; p 26.
 62. ICIS-Phthalic Anhydride. <http://www.icis.com/v2/chemicals/9076140/phthalic-anhydride.html> (August 2nd),
 63. Liptow, C.; Tillman, A.-M. *Comparative Life Cycle Assessment of Polyethylene based on sugarcane and crude oil*; Department of Energy and Environment, Division of Environmental System Analysis, Chalmers University of Technology: Goteberg, Sweden, 2009.
 64. Ruether, J.; Ramezan, M.; Grol, E. *Life-Cycle Analysis of Greenhouse Gas Emissions for Hydrogen Fuel Production in the United States from LNG and Coal*; National Energy Technology Laboratory: 2005; p 22.
 65. Kurt, C.; Bittner, J., Sodium Hydroxide. In *Ullmann's Encyclopedia Of Industrial Chemistry*, 7th Edition ed.; Hawkins, S.; Russey, W. E., Eds. Wiley-VCH: 2006; Vol. 33, p 12.
 66. Espenson, J. H.; AbuOmar, M. M., Reactions catalyzed by methylrhenium trioxide. *Electron Transfer Reactions* **1997**, 253, 99-134.
 67. Toxic Release Inventory-BASF Corporation. http://iaspub.epa.gov/triexplorer/release_fac_profile?TRI=70734BSFCRRIVER&year=2010&trilib=TRIQ1&FLD=&FLD=RELLBY&FLD=TSFDSP&OFFDISPD=&OTHDISP

- [D=&ONDISPD=&OTHOFFD=](#) (January 31st),
68. Greenhouse gas data publisher-BASF Corporation.
<http://ghgdata.epa.gov/ghgp/main.do#/facilityDetail/?q=Facility> or
[Location&st=LA&fid=526052&lowE=0&highE=23000000&&g1=1&g2=1&g3=1&g4=1&g5=1&g6=1&g7=1&s1=0&s2=0&s3=0&s4=0&s5=0&s6=0&s7=1&s8=0&s9=1&s301=1&s302=1&s303=1&s304=1&s305=1&s306=1&s401=1&s402=1&s403=1&s404=1&s701=1&s702=1&s703=1&s704=1&s705=1&s706=1&s707=1&s708=1&s709=1&s710=1&s711=1&ss=&so=0&ds=E](http://ghgdata.epa.gov/ghgp/main.do#/facilityDetail/?q=Facility) (February 5th),
69. Allen, D. T.; Shonnard, D., *Green Engineering: Environmentally-Conscious Design of Chemical Processes*. Prentice Hall: Upper Saddle River: New Jersey, 2002.
70. Aden, A. *Water Usage for Current and Future Ethanol Production*; National Renewable Energy laboratory: Denver, 2008; p 2.
71. Toxic Release Inventory-Exxon Mobil Chemical Company Olefins Plant
http://iaspub.epa.gov/triexplorer/release_fac_profile?TRI=77522XXNCH3525D&year=2010&trilib=TRIQ1&FLD=&FLD=RELLBY&FLD=TSFDSP&OFFDISPD=&OTHDISP
[D=&ONDISPD=&OTHOFFD=](#) (January 31st),
72. Toxic Release Inventory-Total Petrochemicals Inc. Port Arthur Refinery.
http://iaspub.epa.gov/triexplorer/release_fac_profile?TRI=70669CNCLKOLDSP&year=2010&trilib=TRIQ1&FLD=&FLD=RELLBY&FLD=TSFDSP&OFFDISPD=&OTHDISP
[PD=&ONDISPD=&OTHOFFD=](#) (January 31st),
73. Shell's new ethylene cracker in Appalachia may be the first of several.
<http://www.icis.com/Articles/2011/08/29/9488406/shells-new-ethylene-cracker-in-appalachia-may-be-the-first-of.html> (January 31st),

74. *Fact Sheet of ExxonMobil Complex Baytown Facility*; ExxonMobil: Baytown, Texas, 2012.
75. Morschbacker, A., Bio-Ethanol Based Ethylene. *Journal of Macromolecular Science, Part C: Polymer Reviews* **2009**, 49, 5.
76. Ahlgren, S.; Baky, A.; Bernesson, S.; Nordberg, A.; Noren, O.; Hansson, P. A., Ammonium nitrate fertiliser production based on biomass - Environmental effects from a life cycle perspective. *Bioresource Technology* **2008**, 99, (17), 8034-8041.
77. Tyner, W. E.; Taheripour, F.; Zhuang, Q.; Birur, D.; Baldus, U. *Land Use Changes and Consequent CO₂ Emissions due to US Corn Ethanol Production: A Comprehensive Analysis*; Department of Agricultural Economics, Purdue University: 2010; p 90.
78. Huang, W. Fertilizer Use and Price. <http://www.ers.usda.gov/Data/FertilizerUse/> (22nd July),
79. *Background Report on Fertilizer Use, Contaminants and Regulations*; National Program Chemicals Division, Office of Pollution Prevention and Toxics: Washington D.C., 1999; p 395.
80. Dodds, W. K.; Bouska, W. W.; Eitzmann, J. L.; Pilger, T. J.; Pitts, K. L.; Riley, A. J.; Schloesser, J. T.; Thornbrugh, D. J., Eutrophication of US Freshwaters: Analysis of Potential Economic Damages. *Environmental Science & Technology* **2009**, 43, (1), 12-19.
81. Pimentel, D.; Patzek, T. W., Ethanol Production: Energy and Economic Issues Related to U.S. and Brazilian Sugarcane. In *Biofuels, Solar and Wind as Renewable Systems*, Springer: 2008; pp 357-371.
82. Bennett, E. M.; Carpenter, S. R.; Caraco, N. F., Human impact on erodable phosphorus

- and eutrophication: A global perspective. *Bioscience* **2001**, 51, (3), 227-234.
83. Denton, J. E.; Mazur, L.; Milanes, C.; Randles, K.; Salocks, C. *Used Oil in Bunker Fuel: A Review of Potential Human Health Implications*; office of Environmental Health Hazard Assessment Integrated Risk Assessment Section (IRAS): 2004.
84. Crude Oil and Total Petroleum Imports ftp://ftp.eia.doe.gov/pub/oil_gas/petroleum/data_publications/company_level_imports/current/import.html (23rd July),
85. Pacyna, J. M., Atmospheric Emissions of Arsenic, Cadmium, Lead and Mercury from High Temperature Process in Power Generation and Industry. In *Lead, Mercury, Cadmium and Arsenic in teh Environment*, Hutchinson, T. C.; M., M. K., Eds. John Wiley & Sons: New York, 1987; p 20.
86. *Draft Plan to Study the Potential Impacts of Hydraulic Fracturing on Drinking Water Resources*; Office of Research and Development, U.S. Environmental Protection Agency: Washington D. C., February 7th, 2011; p 140.
87. Arthur, J. D.; Bohm, B.; Coughlin, B. J.; Layne, M. *Evaluating the Environmental Implications of Hydraulic Fracturing in Shale Gas Reservoirs*; San Antonio, Texas, 23-25 March, 2009; p 21.
88. Arthur, J. D.; Bohn, B.; Layne, M. *Hydraulic Fracturing Considerations for Natural Gas Wells of the Marcellus Shale*; Cincinnati, Ohio, 2008; p 17.
89. Bredeson, L.; Quiceno-Gonzalez, R.; Riera-Palou, X.; Harrison, A., Factors driving refinery CO₂ intensity, with allocation into products. *The International Journal of Life Cycle Assessment* **2010**, 15, (8), 817-826.
90. Kambara, S.; Takarada, T.; Yamamoto, Y.; Kato, K., Relation between Functional Forms

of Coal Nitrogen and Formation of No(X) Precursors during Rapid Pyrolysis. *Energy and Fuels* **1993**, 7, (6), 1013-1020.

91. Toxic Release Inventory-Lawrence Energy Center.
http://iaspub.epa.gov/triexplorer/release_fac_profile?TRI=66044LWRNC1250N&year=2010&trilib=TRIQ1&FLD=&FLD=RELLBY&FLD=TSFDSP&OFFDISPD=&OTHDISPD=&ONDISPD=&OTHOFFD= (January 30th),
92. Greenhouse Gas Emissions-Lawrence Energy Center.
<http://ghgdata.epa.gov/ghgp/main.do#/facilityDetail/?q=FacilityLocation&st=KS&fid=521954&lowE=0&highE=23000000&&g1=1&g2=1&g3=1&g4=1&g5=1&g6=1&g7=1&s1=1&s2=0&s3=0&s4=0&s5=0&s6=0&s7=0&s8=0&s9=0&s301=1&s302=1&s303=1&s304=1&s305=1&s306=1&s401=1&s402=1&s403=1&s404=1&s701=1&s702=1&s703=1&s704=1&s705=1&s706=1&s707=1&s708=1&s709=1&s710=1&s711=1&ss=&so=0&ds=E> (February 5th),
93. Toxic Release Inventory-Astoria Generating Station.
http://iaspub.epa.gov/triexplorer/release_fac_profile?TRI=11105STRGN18012&year=2010&trilib=TRIQ1&FLD=&FLD=RELLBY&FLD=TSFDSP&OFFDISPD=&OTHDISPD=&ONDISPD=&OTHOFFD= (January 31st),
94. Greenhouse Gas Emissions at Astoria Generating Station.
<http://ghgdata.epa.gov/ghgp/main.do#/facilityDetail/?q=FacilityLocation&st=NY&fid=520539&lowE=0&highE=23000000&&g1=1&g2=1&g3=1&g4=1&g5=1&g6=1&g7=1&s1=1&s2=0&s3=0&s4=0&s5=0&s6=0&s7=0&s8=0&s9=0&s301=1&s302=1&s303=1&s304=1&s305=1&s306=1&s401=1&s402=1&s403=1&s404=1&s701=1&s702=1&s703=1&s704=1&s705=1&s706=1&s707=1&s708=1&s709=1&s710>

=1&s711=1&ss=&so=0&ds=E (February 5th),

95. Goldstein, H. L.; Siegmund, C. W., Influence of Heavy Fuel Oil Composition and Boiler Combustion Conditions on Particulate-Emissions. *Environmental Science & Technology* **1976**, 10, (12), 1109-1114.
96. Kolker, A.; Palmer, C. A.; Bragg, L. J.; Bunnell, J. E. *Arsenic in Coal*; U.S. Geological Survey: Reston, 2005.

Chapter 4

Tungsten Incorporated Mesoporous Silicates as Epoxidation Catalysts

4.1 Introduction

Benchmarking of the CEBC-EO process against the conventional process identified the catalyst cost as a major economic driver. The performance metrics identified by this comparative analysis for the base case of the CEBC process are a minimum catalyst life of 1 year at a leaching rate of 2.2 lb MTO/h (10 ppm). The stringent performance metrics coupled with low abundance and exorbitant cost of rhenium metal (\$3,000/lb)¹ pose a significant challenge for the commercialization of any rhenium based technology.² Replacement of the expensive rhenium with highly active, selective and durable forms of heterogeneous catalysts based on relatively inexpensive tungsten (\$200/ton)³ has merit. Deployment of such catalysts will simplify catalyst separation and recycle steps, and make the process economics more favorable.

The syntheses of W-incorporated mesoporous materials have been reported extensively in literature. The epoxidation of higher molecular weight olefins (cyclohexene, 1-octene, geraniol, cyclopentene, and norbornene etc.) has been the probe reaction for establishing the catalytic activity of the synthesized material.⁴⁻⁸ Stucky *et al.*⁹ prepared and characterized tungsten-grafted MCM-48 material. In the presence of H₂O₂, the synthesized material formed mono-peroxo and diperoxo species which were confirmed spectrometrically (FTIR and Raman).⁹ The high olefin conversions and high epoxide selectivity provided justification for investigating W-based catalysts for the epoxidation of ethylene.

Recently, researchers at CEBC prepared new catalysts by incorporating tungsten into the framework of silica based mesoporous support KIT-6 (3-D ultra large cubic pore network)¹⁰ and KIT-5 (3-D close packed cage-type) with various tungsten loadings using either sodium tungstate or tungstic acid as the tungsten source.¹⁰ These materials were prepared *via* hydrothermal synthesis methods using a Pluronic triblock copolymer as the structure directing agent and *n*-butanol as an additive in the case of KIT-6. The synthesized materials showed a narrow pore size distribution of 5-7 nm with a large pore volume (~1.44 cm³/g). These materials were characterized by XRD, N₂ sorption, TEM and UV-Vis spectroscopy. In this chapter, the synthesized materials were evaluated for the selective epoxidation of ethylene using H₂O₂ as oxidant.

4.2 Experimental

4.2.1 Materials

Mesoporous W-KIT-6 catalytic materials used in the evaluation were synthesized as reported elsewhere.¹⁰ Similarly, W-KIT-5,¹¹ W-MCM-48,¹² W-MCM-41⁵ and W-SBA-15¹³ catalysts were prepared based on the procedure reported in the literature. All catalysts were synthesized at the CEBC and supplied for these studies. Ethylene was purchased from Matheson Tri-Gas Co. (Ultra high purity grade). The oxidant (50 wt% H₂O₂ in H₂O), methanol (HPLC grade, ≥ 99.99%), ferroin indicator solution, acetonitrile (HPLC grade ≥ 99.9%), anhydrous ethylene glycol, and tungsten (VI) oxide (powder, 99.995% trace metal basis) were purchased from Sigma-Aldrich and used without further purification. Ammonium meta tungstate hydrate was purchased from Fluka. Sodium tungstate and tungstic acid were purchased from Acros organics. Ceric sulfate (0.1 N) was purchased from Fischer Scientific. Trace metal grade sulfuric acid (99.9 wt%)

purchased from Fischer Scientific and diluted to 5% (V/V) H₂SO₄. Hydranal composite 5, a reagent used for volumetric titration of H₂O was purchased from Fluka. Ethylene oxide external standard was purchased from Supelco Analytical.

4.2.2 Catalyst Testing

The catalyst samples were activated by heat treatment at 500 °C for 6 h under a stream of air prior to reaction. The activities of the W-KIT-6 and W-KIT-5 catalysts for ethylene epoxidation was investigated in a stirred autoclave reactor following the same procedure as described in Chapter 2, except that the homogeneous catalyst and the PyNO are replaced with W-incorporated heterogeneous catalyst particles with an average size of less than 75 μm. The reaction mixture is analyzed chromatographically at the end of the reaction. Prior to depressurization the reaction mixture is cooled to -30 °C by immersing the Parr[®] reactor in the acetone + liquid nitrogen bath. Following which the reactor is depressurized to atmospheric pressure. Details of GC calibration, EO, H₂O and H₂O₂ are also discussed in Appendix B. Following the batch run the catalyst is recovered by filtration and reactivated by heat treatment at 500 °C under a stream of air. The stability of the catalyst is established by conducting recycling experiments. The catalyst samples utilized in the studies are from a single batch thus avoiding uncertainties associated with inter-batch variability.

4.3 Results and Discussion

4.3.1 Catalyst Characteristics

Detailed characterization may be found elsewhere.¹⁰ Briefly, low angle XRD revealed structural integrity of all prepared samples, with the incorporation of tungsten in the framework being

evident from a mild increase in unit cell parameter. The values of the textural parameters (surface area and pore volume) are consistent with those of typical mesoporous solids and decreases with an increase in tungsten content. The well-ordered pore structure and the narrow pore size distribution (around 6-7 nm) are evident from the narrow hysteresis loop of the nitrogen adsorption isotherms as well as from HR-TEM micrographs (shown in Figure 4-1). The presence of low nuclearity tungsten oxide at higher tungsten loadings was evident from high angle XRD, DR-UV-Vis spectroscopy and Laser Raman spectroscopy results. XPS studies suggest that the tungsten in the framework might be in the W^{6+} oxidation state.

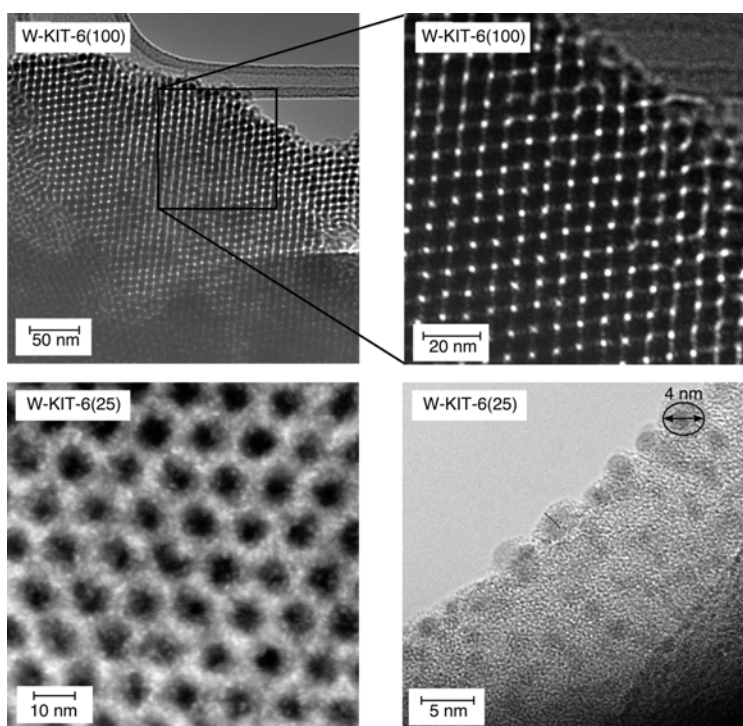


Figure 4-1: Representative Transmission Electron Microscopy of W-KIT-6.¹⁰

4.3.2 Ethylene Epoxidation

The catalyst performance studies were conducted in the absence of external and internal mass transfer limitations (details of the calculation provided in the Section E1 of Appendix E).¹⁴⁻¹⁶

Ethylene Epoxidation with W-KIT-6

The sample gas chromatogram of ethylene epoxidation products is shown in Figure 4-2. In addition to the reactant (ethylene), solvent (methanol), internal standard (acetonitrile) only ethylene oxide (product) is detected by the GC demonstrating the high selectivity and atom economy for the epoxidation of ethylene to EO by W incorporated catalysts.

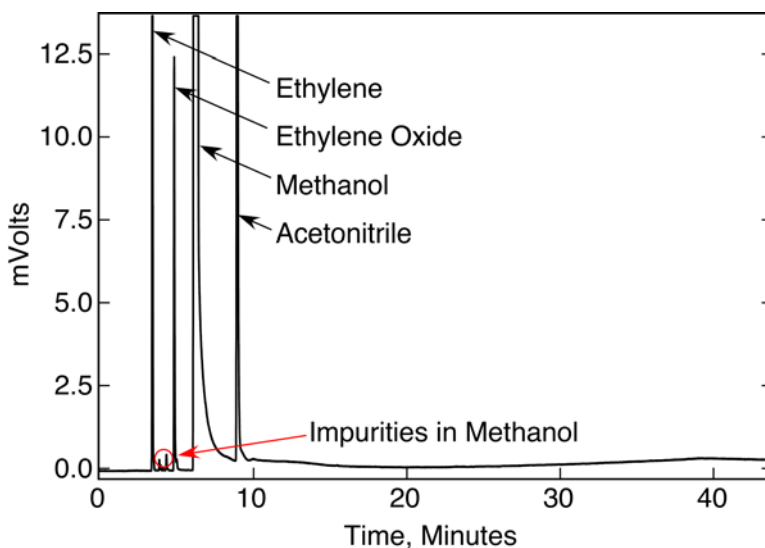


Figure 4-2: Sample gas chromatogram of the ethylene epoxidation products for W-catalyzed reaction.

Table 4-1 lists the catalyst performance metrics (EO yield and productivity, %H₂O₂ conversion) of the various W-KIT-6 catalyst samples synthesized using sodium tungstate as the tungsten metal source. The H₂O₂ conversion and EO yield increase with metal loading and are

commensurate with stoichiometry. The EO productivity (g EO/h/g W, based on moles of H₂O₂ consumed) is lower at higher W loading (Section E2 of Appendix E for methodology to estimate the EO productivity).

At higher W loadings (i.e. Si/W \leq 40), a significant quantity of the metal is present in the form of extra framework WO₃ crystallites which are catalytically inactive,^{5, 8, 9} thus resulting in lower EO productivity. At lower metal loadings (Si/W = 100) most of loaded tungsten is incorporated in the framework of the support (confirmed by XRD, Raman, and DR-UV-Vis) and appear to be in the catalytically active form. The EO productivity values of the recycled catalysts are similar to that of the fresh catalyst, suggesting long-term durability potential of these catalyst samples. The H₂O₂ conversions of the fresh and recycled catalysts are also similar when normalized with respect to catalyst loading and reaction time. The normalized H₂O₂ conversion for the fresh and recycled W-KIT-6 for the Si/W ratio of 10, 20, 40 and 100 are 2.8(10⁻³), 2.7(10⁻³), 4.6(10⁻³) and 6.6(10⁻³), respectively.

Table 4-1: Catalyst loading, %H₂O₂ conversion and EO Yield for W-KIT-6 catalyst (sodium tungstate) at various metal loadings. The initial reaction mixture contained 0.748 mol methanol + 0.134 mol H₂O₂ + 0.253 mol H₂O. Agitation speed = 1600 rpm, T = 35 °C, P = 50 bars, reaction time = 6 h.

W-KIT-6 S/W	Fresh Catalyst					(1 st Recycle)				
	Catalyst Amt., mg	H ₂ O ₂ Conv. (%)	EO mmol.	Yield, mmol.	Productivity, g EO/h-g W	Catalyst Amt., mg	H ₂ O ₂ Conv. (%)	EO mmol.	Yield, mmol.	Productivity, g EO/h-g W
10	696	8.52	8.76	0.36	0.36	452.8	5.65	6.00	0.36	0.36
20	1003	8.57	7.41	0.33	0.33	496	3.42	3.21	0.35	0.35
40	710	5.11	4.46	0.59	0.59	433	3.18	2.77	0.61	0.61
100	1003	5.04	4.40	0.86	0.86	665	2.29	1.95	0.83	0.83
WO ₃	107	1.62	0	0	0					

Table 4-2 lists the performance metrics of the W-KIT-6 catalyst prepared using tungstic acid as the tungsten metal source. The EO productivity of the W-KIT-6 catalyst synthesized using tungstic acid and sodium tungstate sources are of the same order of magnitude. At the Si/W ratio of 100, the EO productivity of the sample prepared using tungstic acid is greater compared to that prepared using sodium tungstate. Recycle studies show that all the catalyst samples prepared using sodium tungstate and tungstic acid retains their activity and selectivity. The normalized H₂O₂ conversion (g H₂O₂/h/g W) for fresh and recycled W-KIT-6 for the Si/W ratio of 10, 20, 40 and 100 are 2.63(10⁻³), 1.8(10⁻³), 6.4(10⁻³) and 1.62(10⁻³) g, respectively. Further, the EO productivity obtained with W-KIT-6 catalysts (0.3-3 g EO/h/g W) is of the same order of magnitude as the homogeneous Re-based (1.61-4.97 g EO/h/g Re)¹⁷ and Ag-based catalyst used in the conventional process (0.7-4.4 g EO/h/g Ag).¹⁸

Table 4-2: Catalyst loading, %H₂O₂ conversion and EO Yield for W-KIT-6 catalyst (tungstic acid) at various metal loadings. The initial reaction mixture contained 0.748 mol methanol + 0.134 mol H₂O₂ + 0.253 mol H₂O. Agitation speed = 1600 rpm, T = 35 °C, P = 50 bars, reaction time = 6 h.

W-KIT-6 Si/W	Fresh Catalyst					(1 st Recycle)				
	Catalyst Amt., mg	H ₂ O ₂ Conv. (%)	EO mmol.	Yield, EO/h-g W	Productivity, g EO/h-g W	Catalyst Amt., mg	H ₂ O ₂ Conv. (%)	EO moles	Yield, g W	Productivity, g EO/h-g W
10	711	7.93	8.43	0.34	0.34	312	4.51	4.78	0.35	0.35
20	708	3.42	2.89	0.23	0.23	338	1.83	1.58	0.21	0.21
40	501	4.68	3.96	0.85	0.85	355	2.93	2.65	0.83	0.83
100	711	6.16	5.28	2.18	2.18	314	2.86	2.39	2.16	2.16

Ethylene Epoxidation with W-KIT-5

Only ethylene oxide is detected as product by the GC, demonstrating the high selectivity afforded by the catalyst. Table 4-3, lists the catalyst performance metrics (EO yield and productivity, %H₂O₂ conversion) of the various W-KIT-5 catalyst samples synthesized using sodium tungstate as metal sources. The H₂O₂ conversions and EO yields increase with metal loading and are commensurate with stoichiometry. Similar, increase in EO yield was observed with catalyst loading. The EO productivity (g EO/h/g W, based on moles of H₂O₂ consumed) is lower at higher W loading (see Appendix E for methodology to estimate the EO productivity).

At higher W loadings (i.e. Si/W \leq 40), a significant quantity of the metal is present in the form of extra framework WO₃ crystallites which are catalytically inactive,^{5, 8, 9} thus resulting in lower EO productivity. At lower metal loadings (Si/W = 100), most of the loaded tungsten is incorporated into the framework of the support (confirmed by XRD, Raman, and DR-UV-Vis) and appears to be in the catalytically active form. The EO productivity values of the recycled catalysts are similar to that of the fresh catalyst, suggesting long-term durability potential of these catalyst samples. The H₂O₂ conversions of the fresh and recycled catalysts are also similar when normalized with respect to catalyst loading and reaction time. The normalized H₂O₂ conversion for the fresh and recycled W-KIT-5 at the Si/W ratio of 10, 20, 40 and 100 are 2.7(10⁻³), 2.3(10⁻³), 5.1(10⁻³) and 1.2(10⁻³), respectively.

Table 4-3: Catalyst loading, %H₂O₂ conversion and EO Yield for W-KIT-5 catalyst (sodium tungstate) at various metal loadings. The initial reaction mixture contained 0.748 mol methanol + 0.134 mol H₂O₂ + 0.253 mol H₂O. Agitation speed = 1600 rpm, T = 35 °C, P = 50 bars, reaction time = 6 h.

W-KIT-5 Si/W	Fresh Catalyst					(1 st Recycle)				
	Catalyst Amt, mg	H ₂ O ₂ Conv. (%)	EO moles	Yield, g	Productivity, g EO/h/g W	Catalyst Amt, mg	H ₂ O ₂ Conv. (%)	EO Yield, moles	Productivity, g EO/h-g W	
10	810	9.30	10.31	0.36	0.36	436	5.10	5.36	0.35	
20	804	7.11	6.12	0.30	0.30	388	2.33	2.20	0.29	
40	799	5.55	4.84	0.66	0.66	471	3.28	2.71	0.65	
100	803	4.80	4.16	3.16	3.16	472	6.48	5.63	3.26	

Table 4-4, lists the performance metrics of the W-KIT-5 catalyst prepared using tungstic acid as the tungsten metal source. The EO productivity of W-KIT-5 using sodium tungstate and tungstic acid metal sources are of the same order of magnitude. At higher metal loadings (Si/W= 10, 20 and 40) the EO productivity of the W-KIT-5 catalyst synthesized using tungstic acid and sodium tungstate as the metal sources are similar. At the Si/W ratio of 100, the EO productivity of the samples prepared using sodium tungstate is greater compared to that prepared using tungstic acid. Recycle studies show that all the catalyst samples prepared using sodium tungstate and tungstic acid retains their activity and selectivity. The normalized H_2O_2 conversion ($\text{g H}_2\text{O}_2/\text{h/g W}$) for W-KIT-5 at the Si/W ratio of 10, 20, 40 and 100 are $3.8(10^{-3})$, $3.0(10^{-3})$, $3.8(10^{-3})$ and $1.6(10^{-3})$, respectively. The EO productivity for the W-KIT-5 (0.3-3 g EO/h/g W) catalyst are of the same order of magnitude as that of the W-KIT-6 (0.35-2.18 g EO/h/g W), Re-based catalyst used in the CEBC-EO process (1.61-4.97 g EO/h/g Re)¹⁷ and Ag-based catalyst used in conventional process (0.7-4.4 g EO/h/g Ag)¹⁸.

Table 4-4: Catalyst loading, %H₂O₂ conversion and EO Yield for W-KIT-5 catalyst (tungstic acid) at various metal loadings. The initial reaction mixture contained 0.748 mol methanol + 0.134 mol H₂O₂ + 0.253 mol H₂O. Agitation speed = 1600 rpm, T = 35 °C, P = 50 bars, reaction time = 6 h.

W-KIT-5 Si/W	Fresh Catalyst					(1 st Recycle)				
	Catalyst Amt., mg	H ₂ O ₂ Conv. (%)	EO moles	Yield, g EO/h/g W	Productivity, g EO/h/g W	Catalyst Amt., mg	H ₂ O ₂ Conv. (%)	EO moles	Yield, g EO/h/g W	Productivity, g EO/h/g W
10	802	8.18	8.61	0.49	0.49	420	8.07	9.12	0.51	0.51
20	802	10.28	9.11	0.46	0.46	367	2.75	2.52	0.39	0.39
40	810	4.20	3.52	0.49	0.49	477	3.26	2.83	0.53	0.53
100	756	6.36	5.82	2.18	2.18	341	3.26	2.84	2.24	2.24
WO ₃	107	1.62	0	0	0					

Other Catalysts and Supports:

The effect of pore size and shape on the activity of the catalyst is explored by incorporating tungsten into the framework of the silica-based ordered mesoporous support such as MCM-41, MCM-48 and SBA-15. In addition to the thinner pore wall, the pore diameter of these supports is smaller compared to KIT-5 and KIT-6. As demonstrated for Pd incorporation in SBA-15,¹⁹ pore diffusion limitations caused by smaller pore dimensions may influence the incorporation of the metal into the framework and therefore, the metal dispersion in the support.

Table 4-5, lists the performance of these synthesized materials for ethylene epoxidation. For a fixed Si/W ratio, the H₂O₂ conversion and EO productivity are comparable for all the catalysts.

Table 4-5: Catalyst loading and EO Yield for W-incorporated support. The initial reaction mixture contained 0.748 mol methanol + 0.134 mol H₂O₂ + 0.253 mol H₂O. Agitation speed = 1600 rpm, T = 35 °C, P = 50 bars, reaction time = 6 h.

Support	Si/W	Catalyst Loading, mg	EO Yield, mmol.	Productivity, g EO/h/g W
SBA-15	20	255	2.12	0.40
MCM-41	20	500	4.15	0.40
MCM-48	20	251	0.91	0.18
MCM-48	10	252	4.15	0.45

For a fixed Si/W ratio of 20, the EO yield and productivity for the tungsten-incorporated catalysts such as W-MCM-41, W-MCM-48 and W-SBA-15 catalysts are similar to that observed for W-KIT-6 (0.3 g EO/h/g W) and W-KIT-5 (0.5 g EO/h/g W). The highly acidic synthesis conditions employed in the preparation of W-KIT-6 and W-KIT-5 result in the formation of the extra framework WO₃ species even at the low metal loading (Si/W = 40). In comparison, no

extra framework WO_3 species were found in W-MCM-41 (Si/W=31) and W-MCM-48 (Si/W=45) samples.¹⁹

Unsupported Catalysts:

Table 4-6 lists the H_2O_2 conversion, EO yield and productivity for unsupported catalysts. Tungstosilicic acid is present in the form of a suspension in the liquid phase (methanol + H_2O_2 + H_2O) compared to the other metal sources which are completely insoluble in the liquid phase (gas-liquid-solid reaction). The EO productivity and H_2O_2 conversion obtained with tungstosilicic acid and tungstic acid are significantly higher than those observed with sodium tungstate, ammonium meta tungstate and tungsten (VI) oxide.

Table 4-6: Catalyst loading, % H_2O_2 conversion and EO yield and productivity for unsupported catalysts. The initial reaction mixture contained 0.748 mol methanol + 0.134 mol H_2O_2 + 0.253 mol H_2O . Agitation speed = 1600 rpm, T = 35 °C, P = 50 bars, reaction time = 6 h.

Sample	Catalyst Amount, mg	H_2O_2 Conv. (%)	EO Yield, moles	Productivity, g EO/h/g W
Tungstosilicic Acid	125	9.28	8.21	0.52
Tungsten (VI) Oxide	107	1.62	1.32	0.02
Ammonium Meta Tungstate	114	1.13	1.1	0.08
Sodium Tungstate	50	0.60	-	0.08
Tungstic Acid	45	15.3	12.15	2.10

The EO productivity with sodium tungstate and ammonium metatungstate is found to be approximately 0.08 g EO/h/g W. In comparison, the EO productivity observed with W-KIT-6

[0.36-2.18 g EO/h/g W] and W-KIT-5 [0.36-3.16 g EO/h/g W] is substantially higher compared to the unsupported catalysts, demonstrating much superior catalytic performance of the metal incorporated support.

For the Si/W ratio of 100, the EO productivity and H₂O₂ conversion for W-KIT-6 (2.18 g EO/h/ g W) and W-KIT-5 (2.18 g EO/h/ g W) are comparable to that of unsupported tungstic acid (2.1 g EO/h/g W). At higher metal loadings (Si/W = 10, 20 and 40), the productivity of the supported catalysts is lower compared to unsupported tungstic acid. Furthermore, in the case of tungstosilicic acid, the EO productivity is of the same order of magnitude as that of the W-incorporated catalysts at higher metal incorporation (Si/W ratio of 10, 20 and 40). The obvious advantage of the supported W catalyst (compared to their unsupported counterparts) is that the metal leaching can be either minimized or totally avoided during continuous runs. The sparingly soluble tungstic acid undergoes decomposition during product separation.

In addition to the similarity in the EO productivity between the CEBC-EO process (1.61-4.97 g EO/h/g Re) with supported W catalyst and the conventional Ag-catalyzed EO process (0.7-4.4 g EO/h/g Ag), a number of similarities also exist between the CEBC-EO process and the Hydrogen Peroxide/Propylene Oxide (HPPO) process as follows.²⁰ (i) Methanol is employed as the co-solvent; (ii) H₂O₂ is the oxidant; (iii) a solid catalyst is used and the reactor is operated at a space velocity of 0.69 g PO/h/g Ti^{21, 22}, which is in the range of space velocities observed for EO productivity with supported tungsten catalysts; and (iv) the operating pressures (tens of bars) and temperatures (25-40 °C) are similar.^{21, 23, 24} Thus, there is substantial promise for commercializing the CEBC-EO process if the process economics based on catalyst performance is proven to be favorable.

4.4 Conclusions

The tungsten incorporated material epoxidized ethylene with near complete selectivity towards EO (99+%) under mild reaction conditions ($T= 40\text{ }^{\circ}\text{C}$, $P= 50\text{ bars}$). Similar EO productivity for the fresh and recycled catalysts suggests the long term durability potential of the catalyst. The EO productivity is greatest at the Si/W ratio of 100, where most of the tungsten is present in the catalytically active WO_4 form (confirmed elsewhere by UV-Vis and Raman studies). Further, the EO productivity observed with W-KIT-6 [0.3-3.16 g EO/h/g W] and W-KIT-5 [0.3-3.16 g EO/h/ g W] is of the same order of magnitude compared to the Re-based homogenous catalyst demonstrated in the CEBC-EO process and the Ag-catalyst used in the conventional process.

The complete utilization of ethylene to produce EO and the similarity of the CEBC-EO and the HPPO process provide a stimulus for identifying the major economic drivers and to establish performance metrics for economic viability of the process.

References

1. BASF Catalysts-Metal Prices.
<http://www.catalysts.basf.com/apps/eibprices/mp/DPCharts.aspx> (Accessed June 5th, 2010),
2. Ghanta, M.; Fahey, D.; Subramaniam, B., Is Ethylene Oxide from Ethylene and Hydrogen Peroxide More Economical and Greener Compared to Conventional Silver-Catalyzed Process? *Industrial & Engineering Chemistry Research (in preparation)* **2012**.
3. Shedd, K. B. *Tungsten*; United States Department of Interior: Washington D. C., 2011; p 20.
4. Somma, F.; Strukul, G., Oxidation of geraniol and other substituted olefins with hydrogen peroxide using mesoporous, sol-gel-made tungsten oxide-silica mixed oxide catalysts. *Journal of Catalysis* **2004**, 227, (2), 344-351.
5. Dai, W. L.; Chen, H.; Cao, Y.; Li, H. X.; Xie, S. H.; Fan, K. N., Novel economic and green approach to the synthesis of highly active W-MCM41 catalyst in oxidative cleavage of cyclopentene. *Chemical Communications* **2003**, (7), 892-893.
6. Shylesh, S.; Jia, M. J.; Thiel, W. R., Recent Progress in the Heterogenization of Complexes for Single-Site Epoxidation Catalysis. *European Journal of Inorganic Chemistry* **2010**, (28), 4395-4410.
7. Koo, D. H.; Kim, M.; Chang, S., WO₃ nanoparticles on MCM-48 as a highly selective and versatile heterogeneous catalyst for the oxidation of olefins, sulfides, and cyclic ketones. *Organic Letters* **2005**, 7, (22), 5015-5018.

8. Bera, R.; Koner, S., Incorporation of tungsten oxide in mesoporous silica: Catalytic epoxidation of olefins using sodium-bi-carbonate as co-catalyst. *Inorganic Chimica Acta* **2012**, 384, 5.
9. Morey, M. S.; Bryan, J. D.; Schwarz, S.; Stucky, G. D., Pore surface functionalization of MCM-48 mesoporous silica with tungsten and molybdenum metal centers: Perspectives on catalytic peroxide activation. *Chemistry of Materials* **2000**, 12, (11), 3435-3444.
10. Ramanathan, A.; Subramaniam, B.; Badloe, D.; Hanefeld, U.; Maheswari, R., Direct incorporation of tungsten into ultra-large-pore three-dimensional mesoporous silicate framework: W-KIT-6. *J. Porous Mater.* **2012**.
11. Kim, T. W.; Kleitz, F.; Paul, B.; Ryoo, R., MCM-48-like large mesoporous silicas with tailored pore structure: Facile synthesis domain in a ternary triblock copolymer-butanol-water system. *Journal of the American Chemical Society* **2005**, 127, (20), 7601-7610.
12. Boote, B.; Subramanian, H.; Ranjit, K. T., Rapid and facile synthesis of siliceous MCM-48 mesoporous materials. *Chemical Communications* **2007**, (43), 4543-4545.
13. Choi, M.; Heo, W.; Kleitz, F.; Ryoo, R., Facile synthesis of high quality mesoporous SBA-15 with enhanced control of the porous network connectivity and wall thickness. *Chemical Communications* **2003**, (12), 1340-1341.
14. Ramachandran, P. A.; Chaudhari, R. V., *Three-Phase Catalytic Reactors*. Gordon and Breach Science Publisher: New York, 1983; p 423.
15. Sano, Y.; Yamaguchi, N.; Adachi, T., Mass Transfer Coefficients for Suspended Particles in Agitated Vessels and Bubble Columns. *Journal of Chemical Engineering Japan* **1974**, 7, (4), 6.

16. Wan, H.; Chaudhari, R. V.; Subramaniam, B., Catalytic Hydroprocessing of *p*-cresol: Metal, Solvent and Mass-Transfer Effects. *Topics in Catalysis* **2012**.
17. Ghanta, M.; Lee, H. J.; Busch, D. H.; Subramaniam, B., Highly Selective Homogeneous Ethylene Epoxidation in Gas (Ethylene)-Expanded Liquid: Transport and Kinetic Studies. *AIChE Journal (in press)* **2011**.
18. Buffum, J. E.; Kowaleski, R. M.; Gerdes, W. H. Ethylene Oxide Catalyst. US 5145824, 1992.
19. Briot, E.; Piquemal, J. Y.; Vennat, M.; Brégeault, J. M.; Chottard, G.; Manoli, J. M., Aqueous acidic hydrogen peroxide as an efficient medium for tungsten insertion into MCM-41 mesoporous molecular sieves with high metal dispersion. *J. Mater. Chem.* **2000**, 10, (4), 953-958.
20. Vora, B. V.; Pujado, P. R. Process For Producing Propylene Oxide. US 5599955, 1997.
21. Pujado, P. R.; Hammerman, J. I. Integrated Process For The Production Of Propylene Oxide. US 5599956, 1997.
22. Nemeth, L. T.; P., M. T.; Jones, R. R. Epoxidation of Olefins using a Titania-Supported Titanosilicate. US 5354875, 1994.
23. Lee, H. J.; Ghanta, M.; Busch, D. H.; Subramaniam, B., Towards a CO₂-free ethylene oxide process: Homogeneous ethylene oxide in gas-expanded liquids. *Chemical Engineering Science* **2010**, 65, (1), 128-134.
24. Lee, H. J.; Shi, T. P.; Busch, D. H.; Subramaniam, B., A greener, pressure intensified propylene epoxidation process with facile product separation. *Chemical Engineering Science* **2007**, 62, (24), 7282-7289.

Chapter 5

Comparative Economic and Environmental Assessment of Propylene Oxide Production by the PO/TBA, HPPO and CEBC PO Processes

5.1 Introduction

Propylene oxide (PO) is the precursor of a wide variety of industrially important chemicals including propylene glycol and polyether polyols. The present commercial technologies generate significant amount of coproducts.¹ In 2007, researchers at the Center for Environmentally Beneficial Catalysis (CEBC) demonstrated the oxidation of propylene to propylene oxide by H_2O_2 with near complete selectivity based on converted propylene.^{2, 3} The process is catalyzed by methyltrioxorhenium (MTO) catalyst and pyridine-N-oxide promoter in solution. Propylene dissolves in the liquid phase under mild pressure (1 MPa) and temperature (20-40 °C) conditions. Because the reaction conditions are near propylene's critical pressure ($P_c = 4.5$ MPa) and in the vicinity of its critical temperature ($T_c=90$ °C), a propylene expands the liquid phase. The product PO remains dissolved in the liquid phase at the reactor conditions and can be recovered by simple distillation due to its low boiling point (34 °C).²

The CEBC-EO and CEBC-PO process concepts are very similar to the HPPO process. At a market price of 121 ¢/lb, PO is a more valuable product compared to EO which has a market price of 79 ¢/lb.⁴ To understand how the CEBC-PO process compares to the HPPO process, we perform comparative economic and environmental assessments of the two processes, and also the erstwhile PO/TBA process. This analysis identifies the major economic drivers in these

processes and establishes performance benchmarks (catalyst life, catalyst leaching rate, oxidant/catalyst ratio etc.) for economic viability of the CEBC-PO process. Similarly, comparative cradle-to-gate life cycle assessment (LCA) identifies the major adverse environmental impacts in these three technologies. The insights are clearly valuable to assess the practical viability of the companion CEBC-EO process.

5.2 Methodology

5.2.1 Simulation Package

Aspen HYSYS[®] 2009.7.1 software⁵ was employed to perform process simulations. The annual PO capacity for the plant scale simulations was set at 200,000 tonnes/year. Process information (mass and energy balances) obtained from the HYSYS[®] simulation were utilized in the design of process equipment.⁶⁻⁹ The UNIQUAC model was chosen to estimate the relevant thermodynamic properties since the reaction mixture contains polar, non-electrolytes at high pressures. Table 5-1 contains the list of specifications and assumptions. Medium-pressure steam is employed to meet the heating requirement in all three processes. Based on the operating temperatures, cooling water can be utilized to remove the heat of reaction in the PO/TBA process. The mild operating temperatures in the HPPO and CEBC processes require that chilled water be used to remove the heat of reaction.

Table 5-1: Assumptions made common to the simulations of the PO/TBA, HPPO and CEBC Processes⁹⁻¹³

PFD Specification	Description
Utility	Electricity is obtained from U.S. power grid which is a portfolio of sources. Steam is produced from natural gas
Catalysts and Solids	Estimated using the property estimator tool embedded in Aspen HYSYS [®] software
Catalyst Synthesis and Regeneration	Neglected in comparison to capital costs of unit operations
Thermodynamic Properties	Properties such as activity, compressibility, enthalpy, fugacity, and volume etc. are estimated using UNIQUAC model
Direct Costs ⁹	Installation (8.3%), Instrumentation and control (9.2%), Piping (7.3%), Electrical (4.6%), Building (4.6%), Land (1.5%), Yard (1.8%)
Indirect Costs ⁹	Engineering and Supervision (18-25%), Construction Expenses (17-20%), Legal Expenses (3%), Contractors Fees (6%)
Utility Costs ^{9, 11, 12}	Steam (\$ 10/1000 lbs), Electricity (\$ 0.0655/ KWh), Cooling Water (\$ 0.10/1000 gal), Refrigeration (-50 °C, \$ 60/GJ & -30 °C, \$ 30/GJ)
Labor Costs ^{10, 13}	Skilled Labor (46.9 \$/person/h), Unskilled Labor (35.6 \$/person/h)
Working Capital ⁹	18% of fixed capital investment
Miscellaneous Costs ⁹	Distribution, Marketing, research and development (10% of production cost), Depreciation Rate (10% per year), Tax Rate (25% of total fixed capital), Operating Supplies (10% of labor costs), Plant Overhead (80% of labor costs), Maintenance Material (3% of purchased cost)

5.3 Process Description

5.3.1 PO/TBA Process

This process may be viewed in two parts (Figure 5-1) *i*-butane oxidation and propylene epoxidation.

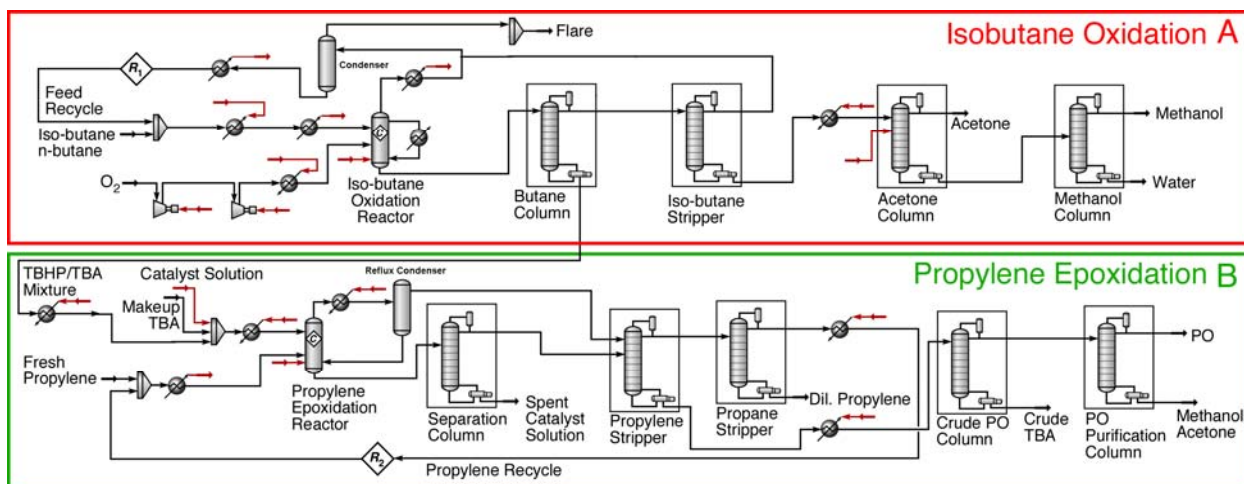


Figure 5-1: Process flow diagram for the PO/TBA process: (A) *i*-Butane oxidation; (B) Propylene epoxidation¹⁴⁻¹⁶

i-Butane oxidation reactor (Section A): Table 5-2 summarizes the simulation parameters and mass flow rates of the components entering and leaving the *i*-butane oxidation and propylene epoxidation reactors and the mass flow rates of components in the recycle streams. In section A, recycled gases (*i*-butane, butane) and make-up raw materials (*i*-butane and oxygen) are co-fed into six continuous stirred tank reactors (CSTR) in parallel (*total volume*=2143 m³).¹⁷ *i*-Butane undergoes non-catalytic liquid-phase oxidation to form the *t*-butyl hydroperoxide (TBHP). Typical reaction conditions are 3.0 MPa at 135 °C with an average residence time of 10 h. Under optimized conditions, the *i*-butane conversion is 37%, and the selectivity to TBHP is 53 mol% based on *i*-butane consumption. A major byproduct of this step is *t*-butyl alcohol, with a selectivity of 41 mol% (based on *i*-butane).¹⁴ The oxygen concentration in the liquid phase is kept below 4-7 mol% primarily for safety reasons.¹⁸ Temperature control in the TBHP reactor is achieved by re-circulating the liquid reaction mixture through a series of coolers.¹⁴ The liquid

phase containing TBHP, *t*-butanol and dissolved *i*-butane and *n*-butane exit the reactor from the bottom. The unreacted oxygen, nitrogen, undissolved *i*-butane and *n*-butane exit the reactor through the overhead stream (vent gases). The vent gases are partially condensed to recover the butanes (*i*-butane and *n*-butane) which are recycled (R_1) whereas the non-condensable gases (nitrogen and oxygen) are flared. The liquid effluent stream exiting the reactor is sent to the Butanes column (operated at $P = 0.2$ MPa, $T = 27$ °C) where the light ends (*i*-butane, *n*-butane) and byproducts (acetone and methanol formed by the photolytic or thermal decomposition of TBHP¹⁹) are separated from *t*-butanol and TBHP, which is sent to the propylene epoxidation reactor. The low concentration of methanol in the reactor effluent stream containing TBHP may pose a safety concern. By, preventing the build-up of methylhydroperoxide in the column we can minimize the risk associated with distillation of the mixture of TBHP+methanol+acetone+*i*-butane+*n*-butane.²⁰ The light ends recovered in the *i*-butane column are recycled whereas acetone and methanol are sent for further separation. *i*-Butane column is operated at $P = 0.6$ MPa, $T = 21$ °C. The low boiling point of butanes necessitates the use of lower column pressures thus requiring the use of chilled water. Acetone and methanol are separated by extractive distillation and water serves as the separation solvent.²¹ The acetone column is operated under vacuum (acetone column). The mixture of methanol and water are further separated by simple distillation. The condenser of the acetone column is cooled by refrigeration with propane and the methanol column is cooled with cooling water.

Propylene Epoxidation (Section B): In the second step, the oxidant (TBHP dissolved in TBA, from section A), make-up enriched propylene feedstock (propylene/propane ratio is 9:1) and

recycled gases (propylene/propane) are fed into four stirred tank reactors (*total volume=1080 m³*) in parallel.^{15, 16} Propylene is selectively epoxidized by TBHP in the presence of a homogeneous molybdenum-based catalyst at 121 °C and 3.5 MPa. For a residence time of 2 h, the reported conversion of TBHP is 98%, and the selectivity to PO product is 98.4% (based on converted TBHP).^{22, 23} Based on propylene the conversion is 29.3% and the selectivity towards PO is 100 mol%. The decomposition of TBHP is a side reaction and is minimized by controlling the temperature. Temperature control in the propylene epoxidation reactor is achieved by vaporizing and reflux condensing the reaction mixture.¹⁵ The non-condensable vapors from the reflux condenser are sent for product separation to the propylene stripper. The reactor effluent stream containing the unreacted reactants and products are recovered by a train of distillation columns. The spent catalyst solution is separated in the separation column (operated at $P= 0.5$ MPa, $T= 112$ °C). The overhead stream from the separation column is sent to a propylene stripper where propylene and propane are separated from PO, *t*-butanol and TBHP. The mixed propylene/propane is sent to a propane stripper (operated at $P= 0.6$ MPa, $T= 4$ °C). The enriched propylene stream is recycled back to the reactor (R_2). PO is separated from the *t*-butanol and TBHP in the crude PO column (operated $P= 0.2$ MPa, $T= 54$ °C). The crude PO is further purified by distillation (PO purification column, operated at $P=1.9$ MPa, $T=54$ °C). The condenser of the propylene column is cooled by refrigeration whereas the condensers in the separation, propane, crude PO and PO purification columns are cooled with cooling water. The byproduct/product ratio for the process is 2.4.

Table 5-2: Simulation parameters for the PO/TBA process obtained from literature.^{14, 22-24}

Input/Output stream flow rates (lb/h) from the TBHP and PO reactor obtained from HYSYS[®] simulation

TBHP production							
Reaction	Reactor: Six CSTR in parallel						
Conditions	P= 3 MPa, T= 135 °C; Conversion (<i>i</i> -butane)= 36.9 mol%, LHSV (Liquid Hourly Space Velocity)= 2.5 h ⁻¹						
Catalyst	Non-Catalytic						
Product Selectivity	TBHP= 53.4 mol%; TBA= 40.2 mol% (based on <i>i</i> -butane fed)						
Propylene Epoxidation							
Reaction	Reactor: Four CSTR in parallel						
Conditions	P= 3.5 MPa, T= 121 °C; Conversion (TBHP)= 98 %, Conversion (C ₃ H ₆)= 29.3% Liquid Hourly Space Velocity (LHSV)= 5 h ⁻¹ Feed Composition : Propylene/Propane: 9/1						
Catalyst	1.5% Mo Solution in TBA (165 ppm Mo in reaction mixture)						
Product Selectivity	PO= 98.4 mol% (based on TBHP fed), 100 mol% (based on C ₃ H ₆ consumed)						
<i>i</i> -Butane Oxidation			Propylene Epoxidation				
Mass Flow Rates	Input	Output		Input	Output	R ₁	R ₂
		Top	Bottom				
<i>i</i> -Butane	307340	757	193172	-	-	193930	-
<i>n</i> -Butane	2640	167	2406	-	-	2574	-
Oxygen	51700	440	-	-	-	-	-
Nitrogen	176	176	-	-	-	-	-
Methanol	33	-	3750	-	-	-	-
Acetone	66	-	6765	-	-	-	-
<i>t</i> -Butyl Alcohol	352	-	57590	136840	214940	350	-
<i>t</i> -Butyl Hydroperoxide	572	-	99770	99770	1995	570	-
Propylene	-	-	-	155980	110264	-	110200
Propane	-	-	-	18898	18898	-	15180
Propylene Oxide	-	-	-	1716	55200	-	-

Refer to Figure 5-1 for stream identification (R_j)

5.3.2 Hydrogen Peroxide/Propylene Oxide (HPPO) Process

New technologies for H_2O_2 production, by direct synthesis from H_2 and O_2 , have been reported separately by Headwaters Technology Innovation²⁵, Evonik Degussa²⁶ and BASF.^{27, 28} Because this technology appears to be more economically and environmentally favorable than the amylanthraquinone based process, we assume the H_2O_2 is produced directly from H_2 and O_2 using the technology developed by BASF.^{27, 28} The modified HPPO process (hereafter referred to as HPPO process) is a two-step process, H_2O_2 production and propylene epoxidation (Figure 5-2).

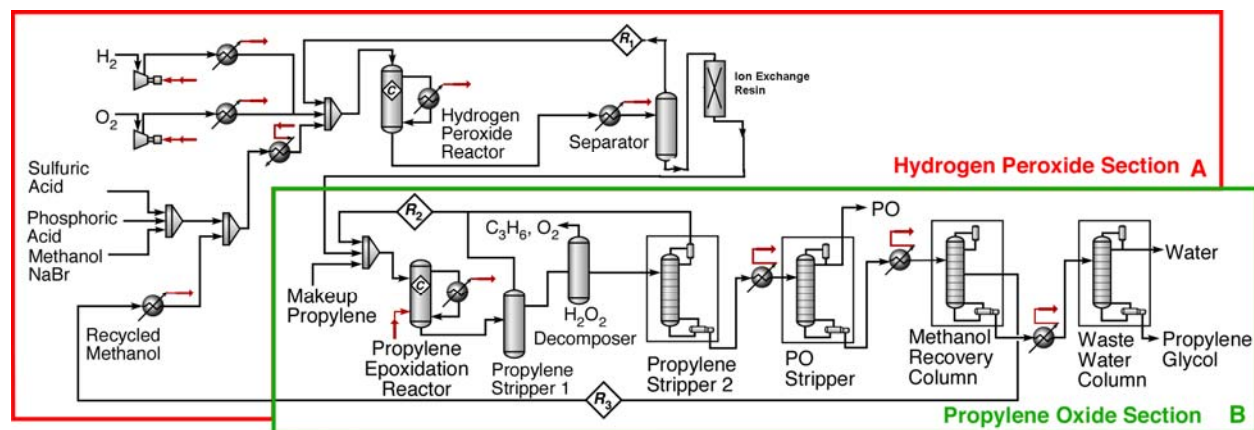


Figure 5-2: Process flow diagram for the HPPO process: (A) Hydrogen Peroxide production; (B) Propylene Oxide section.^{24, 28-30}

Hydrogen peroxide synthesis (Section A): H_2O_2 is assumed to be manufactured on-site directly from H_2 and O_2 . Along with recycled gases (H_2 , O_2), make-up reactants are compressed and sparged into a reactor ($volume=190 m^3$) flooded state with methanol.³⁰ The $Pd(NO_3)_2$ catalyst is impregnated on alloy-steel monoliths. Under optimized conditions of 40 °C and 5.1 MPa, the

reported H₂ conversion and selectivity towards H₂O₂ are 76% and 82%, respectively.^{27, 28} Unreacted hydrogen and oxygen are degassed from the liquid phase containing methanol, H₂O₂, H₂O and H₂O₂ stabilizers by simple depressurization. The recovered unreacted gases are recycled back to the reactor (R₁). The liquid stream is passed through an ion-exchange resin where the H₂O₂ stabilizers are absorbed. The liquid stream containing methanol, H₂O₂ and H₂O is sent to the propylene epoxidation reactor.²⁸

Propylene epoxidation (Section B): The mixture of H₂O₂/H₂O/methanol (from Section A), make-up reactants (propylene/propane feed ratio of 1.5:1)^{24, 31} and recycled gases (propylene/propane) are fed into three fixed-bed catalytic reactors connected in parallel (*total volume = 1020 m³*).³⁰ A titanium silicate (often referred to as TS-1) catalyzes propylene epoxidation by H₂O₂ at 40 °C and 2 MPa (Section B of Figure 5-2). During operation, the TS-1 catalyst activity gradually declines from an initial H₂O₂ conversion of 96% to 63% after two weeks, necessitating catalyst regeneration.²⁹ The total H₂O₂ conversion in the HPPO process is 100%. Of the 100%, the average H₂O₂ conversion in the reactor for epoxidation is 80% and the remaining 20% is safely decomposed. The selectivities toward the product PO and propylene glycol (PG) are 95.5% and 4.5%, respectively, based on converted H₂O₂. In addition to PG, trace quantities of acetone, acetic acid and formaldehyde are also formed as byproducts.²⁹ The bulk of the unreacted propylene and propane is recovered by simple depressurization in propylene stripper 1. The presence of unreacted H₂O₂ in the reactor effluent stream poses safety concerns during product separation and recovery by distillation as methanol and H₂O₂ mixtures in the vapor phase can form an explosive methylhydroperoxide in the distillation column. Hence, we assume that the

unreacted H_2O_2 (remaining 20%) is decomposed post-reaction at temperatures of 50 °C (below the boiling point of methanol) prior to a secondary recovery of the remaining unreacted propylene (propylene stripper 2), product PO and solvent methanol by distillation.³² Water and oxygen are produced by the decomposition of H_2O_2 . The effluent from the decomposer is a gaseous mixture of oxygen and propylene whose composition (1wt% propylene) lies below the lower flammability limit (LFL) of the mixture.¹⁸ The mass flow rates of components entering and leaving the reactor are summarized in Table 5-3. Temperature control in H_2O_2 and PO reactors is achieved by re-circulating the part of the reaction mixture through a series of heat exchangers.

Table 5-3: Simulation parameters for the Hydrogen Peroxide/Propylene Oxide (HPPO) process obtained from literature.^{24, 27, 28, 31} Input/Output stream flow rates (lb/h) for the H₂O₂ and PO reactor obtained from HYSYS[®] simulation.

H ₂ O ₂ production							
Reaction Conditions	Reactor: Fixed Bed Catalytic Reactor in parallel <i>P</i> = 5.1 MPa; <i>T</i> = 40 °C; Conversion (H ₂)= 76% Liquid Hourly Space Velocity (LHSV)= 5 h ⁻¹						
Catalyst	Palladium nitrate impregnated on alloy steel monoliths prepared from mesh						
Product Selectivity	H ₂ O ₂ selectivity= 82%; H ₂ O= 18% (based on H ₂ fed)						
Propylene Epoxidation							
Reaction Conditions	Reactor: Three Fixed Bed Catalytic Reactor in parallel <i>P</i> = 2.0 MPa; <i>T</i> = 40 °C; Conversion (H ₂ O ₂)= 80% (in the reactor), Conversion (C ₃ H ₆)= 48.8% Liquid Hourly Space Velocity (LHSV)= 5 h ⁻¹ Feed Composition : Propylene/Propane: 1.5/1						
Catalyst	Titanium Silicate (TS-1)						
Product Selectivity	PO= 95 mol%; PG= 4.5 mol% (based on H ₂ O ₂ fed) PO= 95.4 mol%; PG= 4.6 mol% (based on C ₃ H ₆ consumed)						
	Hydrogen Peroxide Synthesis		Propylene Epoxidation		Recycle Streams		
Mass Flow Rates	Input	Output	Input	Output	R ₁	R ₂	R ₃
Hydrogen	4070	880	-	-	880	-	-
Oxygen	209000	168740	4	-	168740	-	-
Nitrogen	95480	95480	1140	1140	1140	-	-
Hydrogen Peroxide (H ₂ O ₂)	-	42900	42900	8360	-	-	-
Water	-	10120	10120	31570	-	-	220
Methanol	256520	256700	25520	25520	-	-	256520
Sulfuric Acid	1030	-	-	-	-	-	-
Phosphoric Acid	260	-	-	-	-	-	-
Propane	-	-	51700	51700	-	51700	-
Propylene	-	-	85800	43920	-	43920	-
Propylene Oxide	-	-	-	55200	-	44	-
Propylene Glycol	-	-	-	3490	-	-	-

Refer to Figure 5-2 for stream identification (R_{*i*})

5.3.3 CEBC-PO Process

The CEBC-PO process also occurs in the liquid phase like the HPPO process. H_2O_2 is assumed to be manufactured on-site directly from H_2 and O_2 as in the HPPO process. (Section A of Figure 5-3). For additional process details refer to Section 5.3.2.

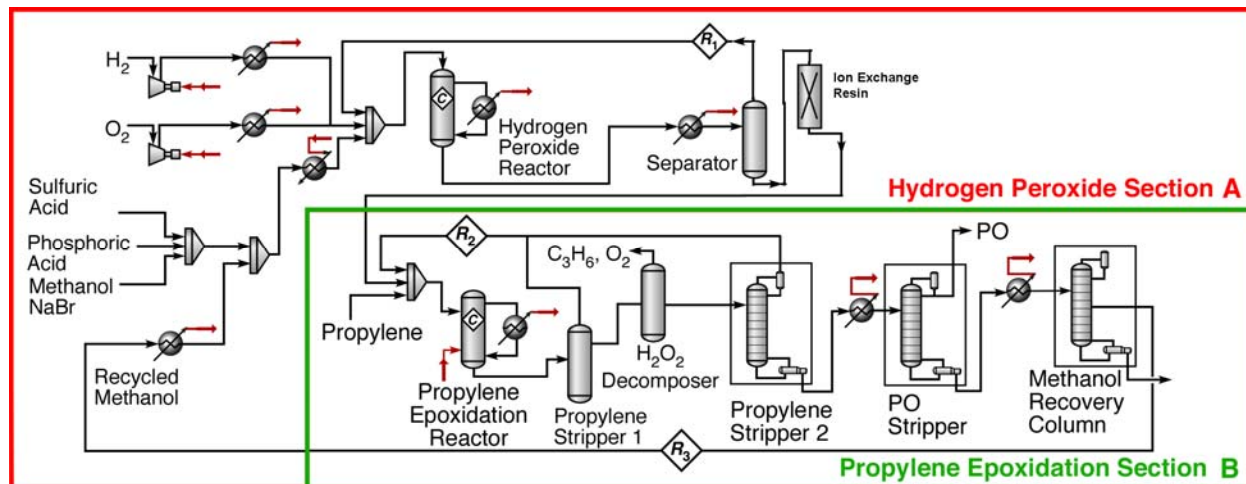


Figure 5-3: Process Flow Diagram for the CEBC-PO Process: (A) Hydrogen Peroxide production; (B) CEBC-PO Process.^{3, 28}

Propylene Epoxidation (Section B): Table 5-4 lists the simulation parameters and mass flow rates of components entering and leaving the reactor. Along with fresh (99.99%) and recycled propylene, aqueous H_2O_2 , make-up catalyst, promoter and methanol are co-fed into a continuous stirred tank reactor (*total volume = 1023 m³*) fitted with a nano-filtration membrane.³ Mass transfer studies clearly established the importance of adequate mixing in maintaining high PO productivity in the CEBC process.³³ The vigorous mixing in a CSTR enables maximum mixing thus alleviating mass transfer limitations. We assume the total volume is divided into four

reactors connected in parallel. Propylene (polymer grade, 99.99%) undergoes selective epoxidation in the liquid phase to form the product propylene oxide. The rhenium based catalyst is assumed to be immobilized onto a soluble polymer support. Further, the activity and selectivity of the immobilized catalyst is assumed to be similar to unbound MTO. The size exclusivity of the membrane will prevent the loss of the catalyst from the membrane reactor and allows the passage of only smaller components such as product (PO), unreacted propylene, unreacted H₂O₂ and methanol solvent. Based on the batch composition and conversion data, the liquid hour space velocity (LHSV) is estimated to be 5 h⁻¹ with the PO yield and selectivity (based on H₂O₂ conversion) values being 98+% and 99%, respectively.^{2, 3} The total H₂O₂ conversion in the CEBC-PO is 100%. Of the 100%, 71% of H₂O₂ is converted for the epoxidation of propylene. The remaining 29% is safely decomposed. Based on propylene the conversion 51.2% and the selectivity towards PO is 100 mol%.

The bulk of the unreacted propylene is recovered by simple depressurization from the reactor pressure of 2 MPa to 0.4 MPa in propylene stripper 1. Safety concerns associated with the presence of unreacted H₂O₂ in the reactor effluent stream necessitate the decomposition of the unreacted oxidant (remaining 29%) prior to secondary recovery of remaining unreacted propylene (in propylene stripper 2), product PO and solvent methanol. The unreacted H₂O₂ is decomposed post-reaction at temperatures of 50 °C (below methanol boiling point).³² The effluent from this decomposer is a gaseous mixture of oxygen and propylene whose composition (2 wt% propylene) lies below the lower flammability limit (LFL) of the mixture.¹⁸

Table 5-4: Simulation parameters for the CEBC process from literature^{2, 3, 27, 28, 34}

Input/Output stream flow rates (lb/h) for the H₂O₂ and PO reactor obtained from the HYSYS[®] simulation

H ₂ O ₂ production							
Reaction Conditions	Reactor: Fixed Bed Catalytic Reactor in parallel P= 5.1 MPa; T= 40 °C; Conversion (H ₂)= 76% Liquid Hourly Space Velocity (LHSV)= 5 h ⁻¹						
Catalyst	Palladium nitrate impregnated on alloy steel monoliths prepared from mesh						
Product Selectivity	H ₂ O ₂ selectivity= 82%; H ₂ O= 18% (based on H ₂ fed)						
Propylene Epoxidation							
Reaction Conditions	Reactor: Four CSTR in parallel P= 2.0 MPa; T= 40 °C; Liquid Hourly Space Velocity (LHSV)= 5 h ⁻¹ Conversion (H ₂ O ₂)= 71.9%, Conversion (C ₃ H ₆)= 51.2%						
Catalyst	Methyl Trioxorhenium (MTO)						
Product Selectivity	PO= 99+ mol% (based on H ₂ O ₂ fed), PO= 100 mol% (based on propylene consumed)						
	Hydrogen Peroxide Synthesis		Propylene Epoxidation		Recycle Streams		
Mass Flow Rates	Input	Output	Input	Output	R ₁	R ₂	R ₃
Hydrogen	3630	880	-	-	880	-	-
Oxygen	209000	164560	20	-	164560	-	-
Nitrogen	95480	95480	14960	14960	80520	14960	-
Hydrogen Peroxide (H ₂ O ₂)	-	47080	47080	13200	-	-	-
Water	880	20240	1760	18900	-	-	-
Methanol	248512	248512	250800	250800	-	-	250800
Sulfuric Acid	1030	-	-	-	-	-	-
Phosphoric Acid	260	-	-	-	-	-	-
Pyridine N-Oxide	-	-	8420	-	-	-	-
Propylene	-	-	81600	39800	-	39800	-
Propylene Oxide	-	-	-	55200	-	-	-
Methyltrioxorhenium	-	-	1866	-	-	-	-

Refer to Figure 5-3 for stream identification (R_j)

MTO catalyst synthesis and performance metrics: The high cost of rhenium (3,000 \$/lb)³⁵ necessitates the near complete recovery of MTO catalyst. Recently, a green and improved route for MTO synthesis was reported by Herrmann et al.³⁶ Based on this reported procedure, the cost

of the fresh catalyst and periodical reconstitution for this analysis are assumed to be \$5,000/lb and \$2,000/lb, respectively. Further, strategies for the immobilization of MTO have been reported by Saladino et al.³⁷ and Bracco et al.³⁸

5.4 Capital Costs

The capital investments are estimated based on standard methods⁹ and the costs are adjusted to 2010 dollars using Chemical Engineering Plant Index (CEPCI).³⁹ Reactor costs for the above processes is based on multiple reactors. Direct costs are estimated as a percentage of purchased equipment costs and installation costs and include all expenses for the purchase of piping, instrumentation and control, electrical and land use. Indirect costs are estimated as a percentage of direct costs and include engineering, supervision and expenses related to construction, legal and contractor's fee.⁹ The cost of *offsite* equipment such as water purification systems and refrigeration units are also considered. Table 5-1 lists the cost of utilities and the percentages utilized in the estimation of direct and indirect costs.

5.5 Production Costs

Production costs include raw materials, labor and utility expenses. The cost of raw material is obtained from Chemical Market Reporter.⁴ The energy balance information obtained from Aspen HYSYS[®] simulation serves as the basis for the estimation of utility expenses. The cost of utilities was obtained from Energy Information Administration and Department of Energy.^{11, 12} Operating labor expenses are dictated by plant capacity and principal operating steps. Average hourly wage

and monthly labor indexes for both skilled and unskilled labor are obtained from U.S. Bureau of labor and Engineering News Record and are listed in Table 5-1.^{10, 13}

5.6 Environmental Assessment

GaBi 4.4[®] software developed by PE solutions is employed to perform cradle-to-gate life cycle assessment of the PO/TBA, HPPO and CEBC processes. The software with its embedded U.S.-specific life cycle inventory enables us to perform a U.S.-specific life cycle analysis.⁴⁰ TRACI (Tools for the Reduction and Assessment of Chemical and Other Environmental Impacts), method developed by United States Environmental Protection Agency (USEPA) is employed to estimate the environmental impact of producing PO across the various impact categories listed in Table 3-4 (Chapter 3).⁴¹⁻⁴³ This analysis incorporates all the impact associated with raw material extraction, transport and processing. In the case of PO/TBA process, *t*-butanol is formed as the byproduct. Thus, a proportional allocation method based on the mass fraction of the products and byproducts is employed to estimate the environmental impact associated with PO production. The allocation is estimated as the quantity of the desired product (PO) to the total quantity of all the products produced in the process.

5.6.1 Basis

A U.S.-specific life cycle assessment (cradle-to-gate) is made to quantify the environmental impact of producing 55,200 lb/h (or ~200,000 tonnes/year) of PO by the PO/TBA, HPPO and the CEBC processes. The environmental impacts due to the mining of the molybdenum, titanium, palladium and rhenium metals are not considered in this analysis due to the lack of database

information regarding the metal losses incurred during processing of PO. Furthermore, the actual amounts of these metals used annually are relatively small compared to the usage of the other raw materials.

5.6.2 Raw Material Sourcing

The mass flow rates of raw materials consumed during the steady operation of the PO/TBA, HPPO and CEBC processes are shown in Figures 5-4, 5-5 and 5-6, respectively.

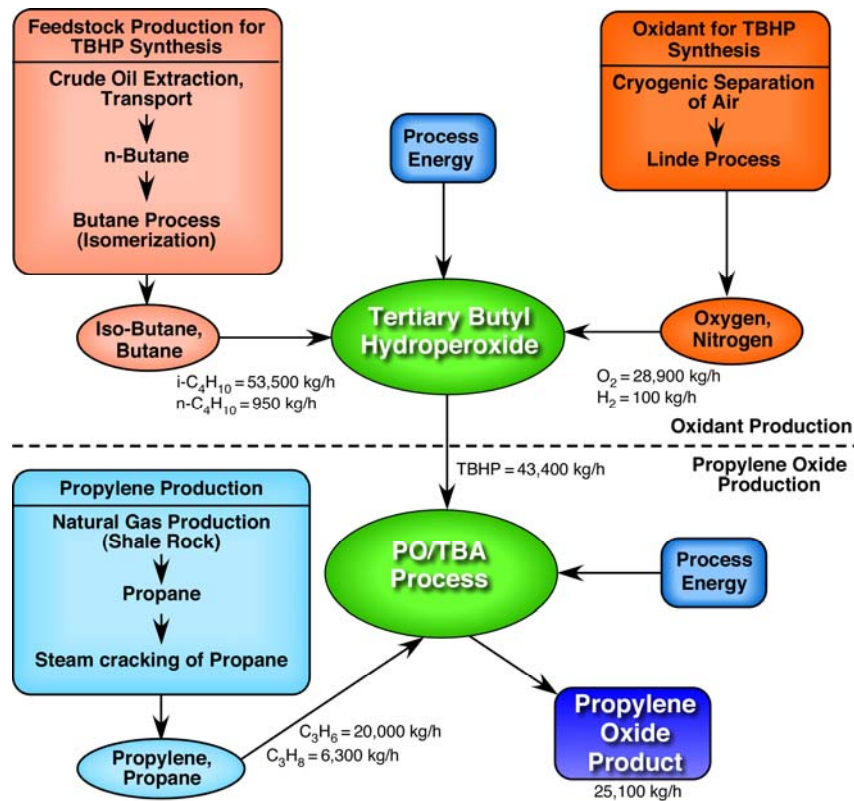


Figure 5-4: Boundaries of the cradle-to-gate LCA of the PO/TBA process.

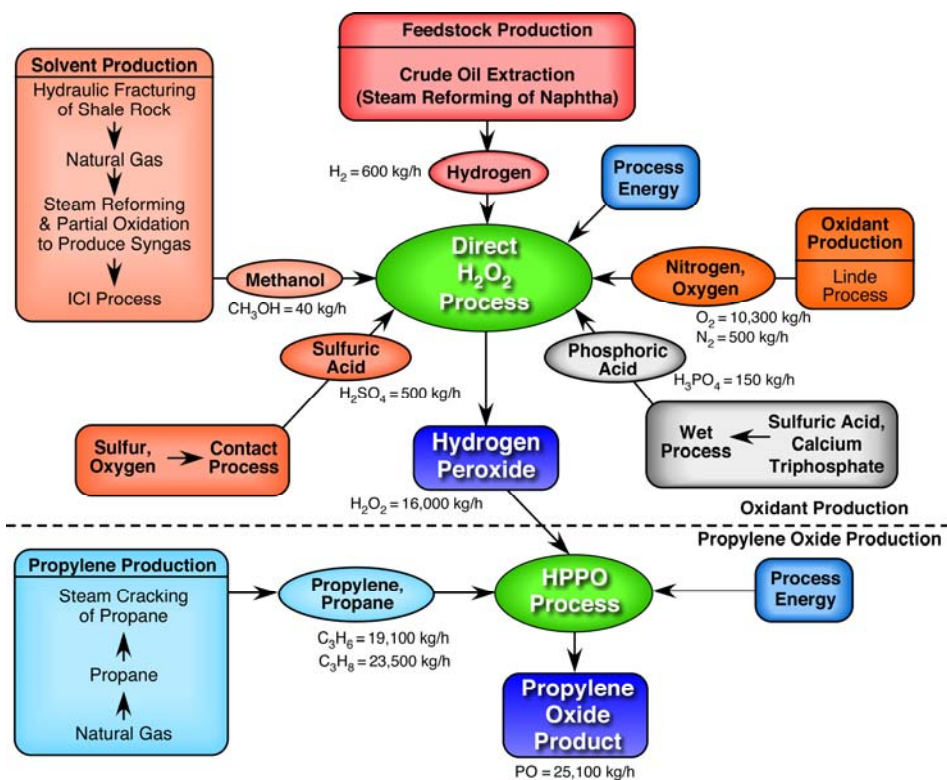


Figure 5-5: Boundaries of the cradle-to-gate LCA of the HPPO process

Bulk of the butane in the U.S. is sourced from natural gas and from naphtha. *i-Butane* is industrially produced by the isomerization of *n*-butane (Butamer[®] process). This equilibrium reaction favors the formation of *i*-butane (99%) at low temperature eliminating the need for product separation and recycle gas compression⁴⁴

Propylene is primarily produced in the U.S. as a byproduct of ethylene production from petroleum refinery processes, or by propane dehydrogenation. Propane dehydrogenation is an endothermic equilibrium reaction with an overall yield of 90%.⁴⁵ In the U.S. propane is obtained from natural gas and naphtha (a fraction of crude oil). This analysis incorporates the impact of transporting feedstock from the exporting nations to the U.S. Further, the energy required to

produce enriched or polymer grade purity propylene is considered in this environmental assessment.⁴⁵

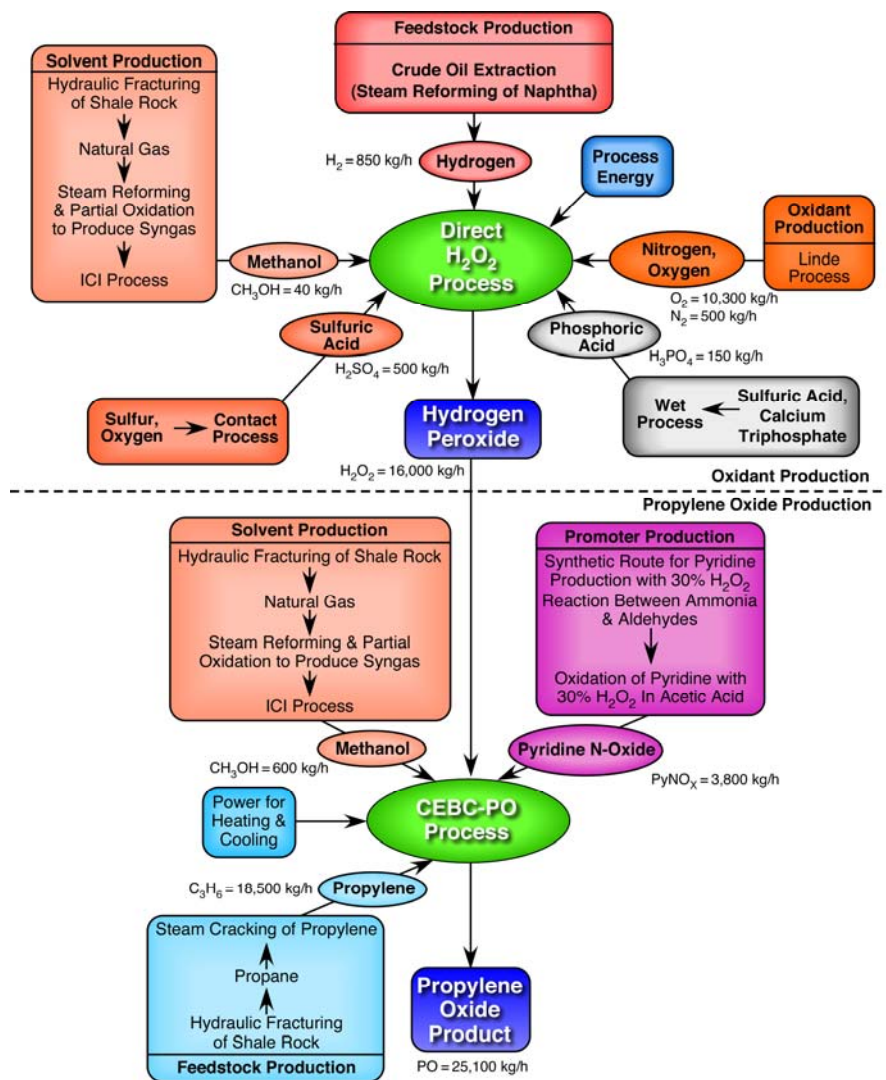


Figure 5-6: Boundaries of the cradle-to-gate LCA of the CEBC-PO process.

Hydrogen is primarily produced by the steam reforming of methane, cracking of ethane to ethylene or as a byproduct of chlor-alkali plants.⁴⁶ *Sulfuric acid* and *phosphoric acid* are

produced by Contact[®] process⁴⁷ and Wet[®] process,⁴⁸ respectively. *Pure oxygen* is produced by the cryogenic separation of air (LINDE[®] process).⁴⁹

Methanol is produced commercially by the ICI[®] process wherein methane is steam reformed to produce synthesis gas which is transformed to methanol.⁵⁰ *Pyridine-N-Oxide* is prepared by the oxidation of pyridine with 30% H₂O₂ in acetic acid. Industrially, pyridine is produced by the reaction of acetaldehyde and formaldehyde with ammonia in the presence of solid-acid catalysts at high temperatures and space velocity.⁵¹

5.7 Results and Discussion

5.7.1 Economic Assessment

5.7.1.1 Part I: Comparison of PO/TBA process and CEBC Process

Figure 5-7, compares the Total Capital Investment (TCI) and the expenses related to the purchase and installation of major process equipment for all the simulated PO processes. The expense categories are represented as checkered bars and the relative areas of the checkered bars reflect comparative costs. Dow-BASF reports the total capital cost for a PO plant based on the HPPO technology to be 25% lower compared to other conventional PO technologies such as PO/TBA process.⁵² The estimated capital cost for the HPPO process is lower than the PO/TBA process by 18%. As this is a comparative economic analysis and in order to maintain an even comparison we exclude the simulation of TBA purification sections for the PO/TBA process. If the capital costs for the installation of *t*-butanol purification section are considered then there would be a smaller deviation between the estimated and reported savings achieved by the

deployment of HPPO process. Thus, the prediction of the total capital cost is lower in comparison to the actual total investment.

A. Total Capital Investment

The estimated total capital investment for the PO/TBA and CEBC process are approximately \$116 million and \$95 million, respectively. As shown in Figure 5-7, the pump costs at approximately \$2 million are similar in both the processes. Similar volumes of unreacted material are recovered and recycled back to the reactor. At, \$5 million the cost of propylene separation columns is similar in both the processes. The low boiling point of propylene requires refrigeration of the propylene stripper to -37 °C to recover unreacted propylene. The major differences lie in the reactor, heat exchanger, and installation costs and are discussed in the following sections.

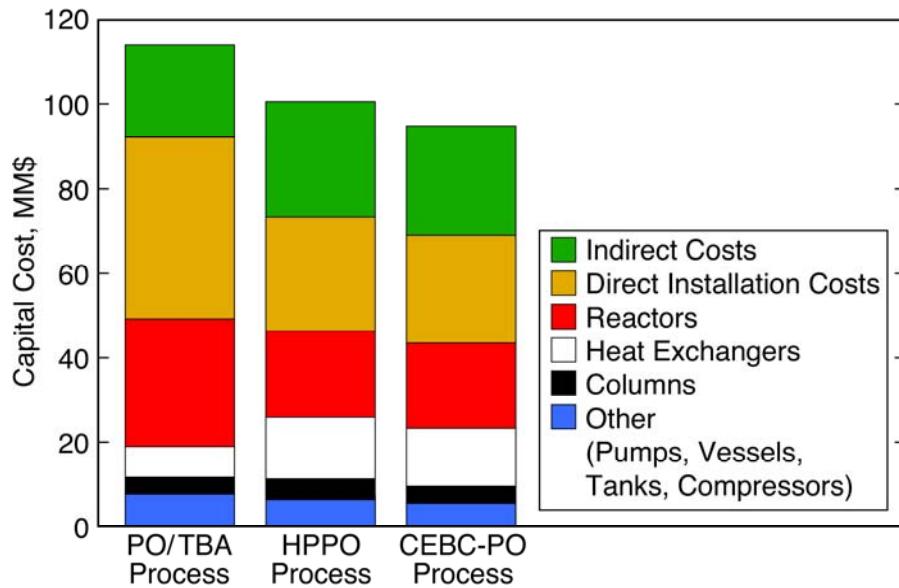


Figure 5-7: Comparison of the total capital investment for PO/TBA, HPPO and CEBC processes

Reactor cost in the PO/TBA and CEBC processes are approximately \$30 million and \$20 million, respectively. Propylene epoxidation and oxidant (TBHP and H₂O₂) synthesis reactors are constructed using stainless steel (SS-304) metal to minimize the metal catalyzed decomposition of the oxidants (TBHP and H₂O₂) in both the processes. The oxygen concentration in the TBHP synthesis reactor is maintained at 4-7 mol% to minimize the possibility of formation of flammable *i*-butane/air mixtures. This along with the longer residence times needed for TBHP (10 h) production compared to H₂O₂ (0.74 h) production necessitate the deployment of large reactor volume for TBHP synthesis to meet the production rate, translating into higher reactor costs for the PO/TBA process.

Heat Exchanger costs for the PO/TBA process are estimated at \$7.5 million compared to \$14 million for the CEBC process. Propylene epoxidation and H₂O₂ synthesis are highly exothermic reactions and both reactors are maintained at 40 °C in the CEBC process by employing chilled coolant. In contrast, the higher operating temperatures in the TBHP synthesis and propylene epoxidation steps of the PO/TBA process allow the use of cooling water to maintain temperature control, which reduces capital investment.

Direct Installation costs for the PO/TBA process are \$42 million compared to \$25 million for the CEBC process. The large reactor volumes in the PO/TBA process increases the direct costs associated with installation of instrumentation, control, piping and insulation. Indirect costs are estimated as a percentage of direct costs. The percentage is dependent on the complexity and safety concerns associated with the process.

B. Production Costs

Figure 5-8, compares the operating expenses incurred during PO production by the PO/TBA, HPPO and CEBC processes. Raw material and product costs are summarized in Table 5-5. Production costs include raw material, utilities, depreciation, R&D, taxes, insurance, overhead and labor.

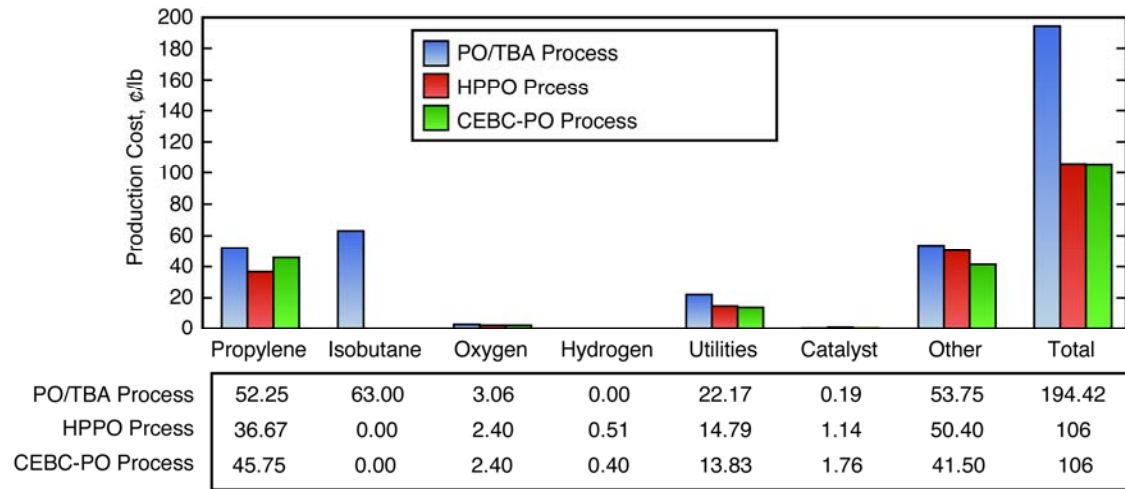


Figure 5-8: Comparison of the total production costs for PO/TBA, HPPO and CEBC processes. (*) The catalyst life and leaching rate are assumed to be 1 year and 0.018 lbs MTO/year; (#) “Other” includes costs for, research, plant overhead, materials and supplies for operation and maintenance, and labor

Table 5-5: Costs of raw material and products used in the analysis^{4, 35}

Commodity	Price, \$/lb
Hydrogen	0.088
Hydrogen Peroxide (Direct H ₂ O ₂ Process)	0.17
<i>i</i> -butane	0.30
Methanol	0.94
Methyl trioxorhenium	5,000
Molybdenum	450
Nitrogen	0.033
Oxygen	0.033
Palladium Nitrate Catalyst	7,924
Phosphoric Acid	0.204
Pure Propylene	0.55
Propylene Oxide	1.21
Pyridine <i>N</i> -Oxide	1.35
Sulfuric Acid	0.33
<i>t</i> -butanol	0.41
Titanium Metal	4.8
Steam	\$ 7/1000 lbs
Cooling Water	10 ¢/1000 gal
Electricity	6.55 ¢/KWH

As shown in Figure 5-8, the costs associated with the procurement of raw material and utilities are the dominant expenses in both the processes. The energy usage of the HPPO process is reported to be 35% low compared to existing PO technologies by Dow-BASF.⁵³ For a similar plant capacity, this comparative analysis estimates an energy savings of 28% for the HPPO process compared to PO/TBA process rendering credibility to this analysis. The utility cost

(steam, cooling water, electricity and refrigeration) for the PO/TBA, HPPO and CEBC processes are summarized in Table 5-6.

Table 5-6: The costs of utilizes in the PO/TBA, HPPO and CEBC processes

Utility	PO/TBA Process, (¢/lb PO)	HPPO Process, (¢/lb PO)	CEBC Process, (¢/lb PO)
Steam	9.6	3.24	3.9
Electricity	5.4	5.37	3.5
Refrigeration	6.6	5.57	5.9
Cooling Water	0.52	0.2	0.53

Oxidant: In the PO/TBA process, the oxidant TBHP is synthesized by the liquid phase oxidation of *i*-butane. At a market price of 30 ¢/lb⁴, the cost of *i*-butane is a major expense. The low selectivity and yield of TBHP increases the *i*-butane requirement and thus oxidant cost for a fixed PO plant capacity. Approximately 2.1 lbs of *i*-butane are consumed to manufacture the TBHP needed for the synthesis of one pound of PO. In contrast, the cost of manufacturing H₂O₂ is 17 ¢/lb, assuming a H₂ price of 8.8 ¢/lb.⁴ The high selectivity and yield of H₂O₂ in the direct route is the primary reason for the low oxidant cost. Only 0.05 lb of H₂ is consumed to synthesize the H₂O₂ (0.85 lb) needed for the production of 1 lb of PO. Based on this analysis the manufacturing cost of TBHP (oxidant) in the PO/TBA process is 62 ¢/lb PO, compared to the H₂O₂ (oxidant) cost of 14.4 ¢/lb PO in the CEBC process. Further, for the synthesis of 1 pound of PO, the PO/TBA process consumes 1.77 lb of oxidant TBHP compared to the 0.85 lb of oxidant H₂O₂ consumed in the CEBC process which further favors the use of H₂O₂ as oxidant.

Propylene: The cost of the propylene feedstock is based on its purity. Hence, there is an economic incentive if the process can tolerate a feedstock that also contains propane as impurity. The propylene purity in the feed stream of the PO/TBA process is 89%, with propane accounting for the remaining 11%. The cost of pure propylene is 55 ¢/lb⁴ and propylene feed cost for the PO/TBA process is assumed to cost 95% of the cost of pure propylene due to the non-availability of pricing information for enriched propylene in the public domain.

Utilities: The utility costs in the PO/TBA process (\$97 million) are higher compared to the (\$62 million) CEBC process. The high operating temperatures in the PO/TBA process allows the use of cooling water, a cheap and abundant resource in most locations. In contrast, chilled water (5 °C, a relatively expensive utility) is employed to remove the heat of reaction from the propylene epoxidation and H₂O₂ synthesis reactors in the CEBC process costing 4.7 ¢/lb PO. The steam requirement of the CEBC process is totally met by on-site steam generation equipment. In contrast, the cooling water absorbs the heat of reaction to form medium pressure steam which can be utilized to partially meet the steam requirement of the PO/TBA process. The net cost of process steam in the PO/TBA process is 9.6 ¢/lb PO compared to the 3.9 ¢/lb PO in the CEBC process. The large process steam requirement in the PO/TBA process is attributed to the separation of byproducts such as methanol, acetone, methyl formate, acids and other C5-C7 byproducts from the reaction mixture. The cost of cooling water in both the processes is similar at 0.52 ¢/lb PO. The separation of large quantities of *i*-butane and propylene result in higher refrigeration costs in the PO/TBA process, thus costing 6.6 ¢/lb PO. In contrast, in the CEBC process, the bulk of the unreacted propylene (93%) is recovered by depressurization and the remnants by simple distillation. Thus, the cost of propylene recovery in the CEBC process is 1.2

¢/lb PO. The electricity costs for operating compression and pumping equipment in the PO/TBA and CEBC process is 5.4 ¢/lb PO and 3.5 ¢/lb PO, respectively. The total utility costs for the PO/TBA and CEBC processes are 22.17 ¢/lb PO and 13.83 ¢/lb PO, respectively.

Effect of byproducts on the market value of PO: With a byproduct/product (TBA/PO) ratio of 2.4, the market price of TBA strongly influences the net profitability of PO synthesis by the PO/TBA process. Reduction in future demand for TBA due to a ban on MTBE as a gasoline additive across the world and high TBA capacity will have an adverse impact on the process economics of the PO/TBA process. The profit associated with the sale of PO reduces by 24 ¢ for every 10 ¢ reduction in the market price of TBA. This reduction in profit margin is proportional to the ratio of TBA/PO (byproduct/product). In contrast, water is the byproduct of the CEBC process, and the profitability of the CEBC process is independent of byproduct earnings.

Catalyst: In the PO/TBA process, the oxidant TBHP is synthesized by the non-catalytic liquid phase oxidation of *i*-butane. Further, propylene is epoxidized by a relatively inexpensive molybdenum catalyst. In contrast, the synthesis of H₂O₂ oxidant by the direct route requires the deployment of palladium catalyst (10,000 \$/lb).³⁵ Further, the deployment of rhenium metal (3,000 \$/lb)³⁵ catalyst in the CEBC process necessitates the near-quantitative recovery of the metal for the economic viability of the process.

5.7.1.2 Part II: Comparison of the HPPO and CEBC Process

A. Total Capital Investment

The total capital investment for the HPPO and CEBC process is approximately \$95 million, the difference being within the predictable uncertainty of this analysis. Capital costs for the

procurement and installation of reactor, heat exchanger, pump, compressor and columns are similar in both the processes. As shown in Figure 5-7, reactors, heat exchangers and installation costs dominate the capital costs.

Reactors for the HPPO and CEBC processes are constructed using stainless steel to minimize the metal catalyzed decomposition of the H_2O_2 oxidant. Further, similar residence time and PO yield in both the processes result in similar reactor volumes and thus capital costs. *Heat Exchanger* costs for HPPO and CEBC process is approximately \$14 million. Mild operating temperatures are employed in both the processes thus necessitating the installation of refrigeration equipment to remove the heat of reaction.

Direct installation costs for the HPPO and CEBC processes are approximately \$25 million due to the similarity of the instrumentation, piping, control and insulation costs in both the HPPO and CEBC processes. Indirect costs, are estimated as a percentage of direct costs, therefore demonstrate similar trend.

B. Production Costs

As shown in Figure 5-8, the total production costs for both the HPPO and CEBC processes are similar and within the estimable uncertainty. The raw material and utility expenses dominate the production costs in both the processes. The raw material cost for the synthesis of H_2O_2 oxidant needed for propylene epoxidation is identical for both the processes as H_2O_2 is manufactured using the technology adopted from the HPPO process. Further, the concentration of H_2O_2 in the reaction stream is similar in both technologies.

Propylene: In contrast to the HPPO process which utilizes a mixed stream of propylene (60%) and propane (40%), CEBC process employs pure propylene as feed. The cost of pure propylene is 55 ¢/lb⁴. Due to the non-availability of pricing information in the public domain, the cost of mixed propylene/propane feed stream is assumed to be 80% of the cost of pure propylene.

Utilities: Utility expenses for both the HPPO and CEBC processes are similar. Mild operating temperatures necessitate the deployment of chilled water, an expensive utility to remove the heat of reaction in both the processes thus resulting in high reactor cooling costs. Further, the low boiling point of propylene requires the refrigeration of propylene stripper 2 in both the processes to recover the remnants of the unreacted propylene. Propane refrigerated to a temperature of -30 °C is employed to cool the propylene strippers whereas the reactors are cooled with chilled water. Cooling water is employed for heat removal in the other separation columns in both the processes. The steam requirement in both the processes is approximately similar and is met by onsite steam generation units. The total cost of utilities in the HPPO and CEBC processes are 14.33 and 13.83 ¢/lb of PO. Table 5-5 lists the cost of utilities in both these processes.

Catalyst: The TS-1 catalyst employed in the HPPO process is relatively inexpensive compared to rhenium based catalysts used in the CEBC process. The deactivation of TS-1 catalyst requires regular regeneration resulting in higher operating expenses whereas the reaction rate of the MTO catalyst decreases in the presence of excess water and requires the use of excess oxidant to eliminate the decomposition of diperoxo form. The concentration of water in the reactor is controlled by performing the epoxidation in a stirred reactor fitted with a nanofiltration membrane. The membrane retains the polymer supported catalyst without causing any hindrance to the flow of other components (unreacted raw materials, products and solvent).

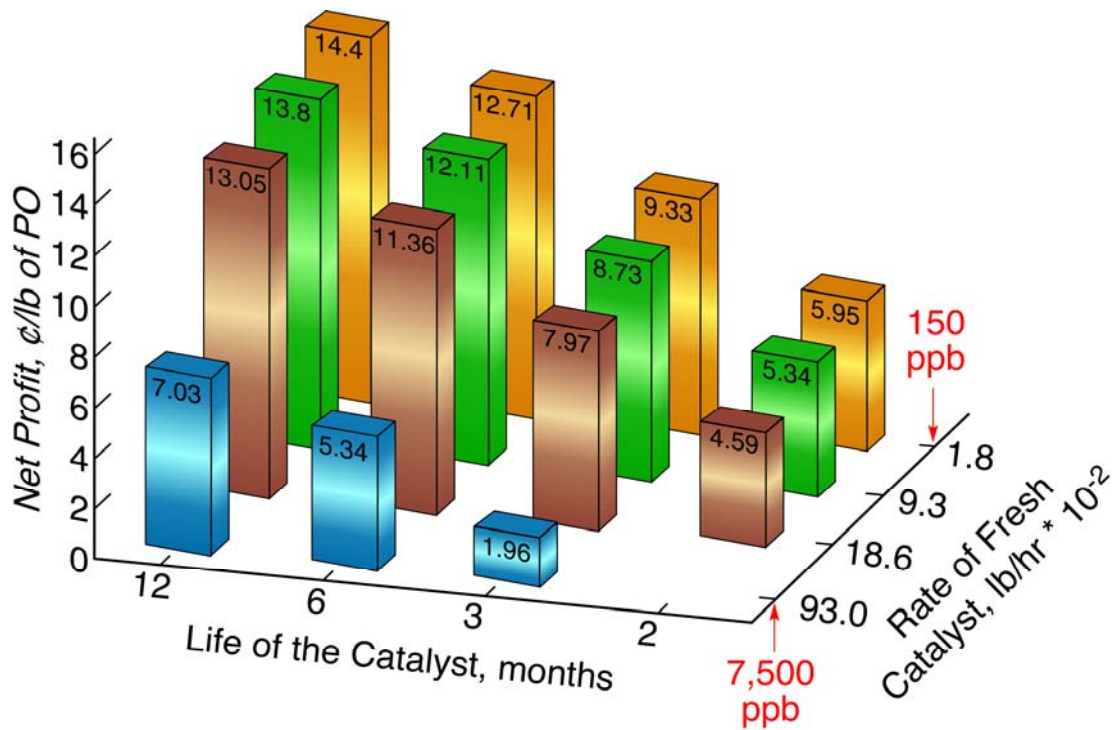


Figure 5-9: The effect of catalyst durability and leaching rate on the net profitability of the CEBC process

Effect of catalyst life and leaching rate on CEBC process economics: The cost of molybdenum metal is 450 \$/lb whereas the cost of titanium metal (sponge grade) is 4.8 \$/lb. At a market price of 3,000 \$/lb, rhenium is substantially expensive. Further, 1,866 lb of MTO catalyst is present dissolved in the epoxidation reactor. As shown in Figure 5-9, the CEBC process has the potential to be cost competitive with the HPPO process (production oxide cost: 106 ¢/lb PO, profit margin: 14.4 ¢/lb PO) provided the polymer bound MTO catalyst is active for 1 year and the rate of addition of fresh catalyst should be $1.8(10^{-2})$ lb/h or less. Further, we assume that 99% of the leached catalyst is recovered. The market price of PO is 121 ¢/lb PO.⁴ Sensitivity analysis identified catalyst lifetime and leaching rate to be major impact drivers impacting the net

profitability of the CEBC process. As shown in Figure 5-9, the economic feasibility of the CEBC process is dependent on the near quantitative recovery and recycling of the leached catalyst. Low leaching rates, high activity and durability over extended periods of times are desirable attributes for the immobilized catalyst. Clearly, the CEBC process has the potential to be commercially viable if the above performance metrics are met or surpassed. Hence, future research efforts should focus on the development of an active, stable and durable MTO catalyst.

5.7.2 Environmental Impact Assessment

Gate-to-gate analysis: The potential emissions estimated by the gate-to-gate environmental impact assessment of the simulated PO/TBA process are compared with that reported by LyondellBasell for their Bayport, Texas facility (Table 5-7). The LyondellBasell facility at Bayport produces PO by the propylene oxide/*t*-butyl alcohol (PO/TBA) route. Further, the production capacity of this facility is 227,272 tonnes of PO/yr which is comparable to that used in the simulation (200,000 tonnes/yr). The potential emissions are taken from the toxic release inventory data reported to the USEPA for both emitted and treated waste for this facility.⁵⁴ As shown in Table 5-7, the actual emissions from the LyondellBasell PO/TBA facility are an order of magnitude lower than that of the total waste treated. The potential emissions predicted by the software (ecotoxicity and impact on human health) are of the same order of magnitude as the total waste generated at the facility, with the predicted emissions being lower in most cases. This difference in the prediction of the potential emissions may be partially attributed to lower production capacity of the simulated PO/TBA process compared to that reported by the plant. Based on this gate-to-gate analysis, we only consider environmental impacts that differ by an

order of magnitude to be reliable for making conclusions about the relative impacts of the competing processes.

Table 5-7: Comparison of the environmental impact (gate-to-gate) estimated from the toxic release inventory data submitted by the LyondellBasell PO/TBA for their Bayport, Texas facility and that predicted by the GaBi[®] software.⁵⁴

Impact	GaBi [®] , million	LyondellBasell PO/TBA Process	
		Total Waste	Toxic Release Inventory EPA, millions Released
Acidification, [mol H ⁺ Eq.]	0	N/A	N/A
Ecotoxicity-Air, [kg 2,4- DCP Eq.]	1.29(10 ⁻³)	2.4(10 ⁻²)	0.35(10 ⁻³)
Ecotoxicity Ground Surface Soil, [kg Benzene Eq.]	0	0.27(10 ⁻⁶)	0.27(10 ⁻⁶)
Ecotoxicity Water, [kg 2,4-DCP Eq.]	1.72	2.73	0.49
Eutrophication, [kg N-Eq.]	0	N/A	N/A
Global Warming, [kg CO ₂ Eq.]	1.32(10 ⁻²)	N/A	N/A
Human Health Cancer-Air, [kg Benzene Eq.]	0.25	N/A	N/A
Human Health Cancer-GSS, [kg Benzene Eq.]	0	0.36	6.2(10 ⁻³)
Human Health Cancer-Water, [kg Benzene Eq.]	0.96	0.96	0.012
Human Health Criteria- Air Point Source [kg PM _{2.5} - Eq.]	0	N/A	N/A
Human Health Non-Cancer Air, [kg Toluene Eq.]	0.052	0.10	0.17(10 ⁻²)
Human Health Non-Cancer GSS, [kg Toluene Eq.]	0.94	0.71	0.012
Human Health Non-Cancer Water, [kg Toluene Eq.]	0.67	0.41	0.007
Ozone Depletion Potential, [kg CFC-11 Eq.]	0	N/A	N/A
Smog Potential, [kg NO _x Eq.]	0.0051	0.032	0.2(10 ⁻³)

N/A: Data not available in the toxic release inventory

Cradle-to-Gate Life Cycle Assessment: Table 5-8 compares the cradle-to-gate environmental impact of PO production across various impact categories in the PO/TBA, HPPO and CEBC processes. The estimated cradle-to-gate environmental impacts are generally one to two orders of magnitude greater than the gate-to-gate emissions (Table 5-7). The overall cradle-to-gate environmental impacts of the CEBC and HPPO processes are similar due to the similarity in raw material and process conditions in both the processes and thus can be lumped together in this discussion. The differences in the impact of CEBC and HPPO process is primarily attributed to the impact of coal-based energy production needed for the purification of propylene to polymer grade propylene. The predicted cradle-to-gate environmental impacts for the CEBC process is of the same order of magnitude as the PO/TBA process, with the predicted emissions being lower for the CEBC processes in most impact categories. The quantitative information generated by this analysis is utilized to identify potential impacts in the PO/TBA and CEBC processes as discussed in the section below. Tables 5-9 and 5-10 lists the major adverse environmental impacts and their percentage contribution relative to the overall impact for the PO/TBA, CEBC and HPPO processes.

Table 5-8: Comparative cradle-to-gate environmental impact assessment for producing propylene oxide by the PO/TBA, HPPO and CEBC processes

Impact	PO/TBA Process, millions	HPPO Process, millions	CEBC Process, millions
Acidification, [mol H ⁺ Eq.]	309	251	257
Ecotoxicity-Air, [kg 2,4- DCP Eq.]	5.16	1.4	1.4
Ecotoxicity Ground Surface Soil, [kg Benzene Eq.]	36(10 ⁻³)	8.7(10 ⁻³)	32(10 ⁻³)
Ecotoxicity Water, [kg 2,4- DCP Eq.]	107	32.4	31.5
Eutrophication, [kg N- Eq.]	0.175	0.096	0.10
Global Warming, [kg CO ₂ Eq.]	1525	1042	1125
Human Health Cancer-Air, [kg Benzene Eq.]	0.31	0.50	0.53
Human Health Cancer-GSS, [kg Benzene Eq.]	0.12(10 ⁻³)	0.3(10 ⁻⁴)	1(10 ⁻³)
Human Health Cancer-Water, [kg Benzene Eq.]	0.15	0.07	0.07
Human Health Criteria- Air Point Source, [kg PM _{2,5} - Eq.]	2.01	1.48	1.48
Human Health Non-Cancer Air, [kg Toluene Eq.]	1454	267	252
Human Health Non-Cancer GSS, [kg Toluene Eq.]	2.71	0.61	2.32
Human Health Non-Cancer Water, [kg Toluene Eq.]	4739	1945	1585
Ozone Depletion Potential, [kg CFC-11 Eq.]	0.4(10 ⁻⁴)	0.7(10 ⁻⁴)	0.8(10 ⁻⁴)
Smog Potential, [kg NO _x Eq.]	0.4(10 ⁻³)	0.5(10 ⁻⁵)	1.7(10 ⁻³)

Eq.: Equivalent, DCP: Dichlorophenoxyace

Table 5-9: Major adverse environmental impacts in the production of propylene oxide by the PO/TBA process

Pollution source	Impact Category	% Contribution relative to similar impacts form other sources
Coal-based energy production for compression	Acidification	42.3
	Ecotoxicity-water	81.5
	Global warming potential	25.5
Fossil-fuel based energy generation for raw-material production	Acidification	53.2
	Global warming potential	64.5
	Human health non-cancer air	83.2

Table 5-10: Major adverse environmental impacts in the production of propylene oxide by the HPPO and CEBC processes

Pollution source	Impact Category	% Contribution relative to similar impacts from other sources in the HPPO process	% Contribution relative to similar impacts from other sources in the CEBC process
Coal-based electrical power generation for refrigeration	Acidification	78.2	86
	Ecotoxicity-water	55	42
	Global warming potential	42	58
	Human health non-cancer air	57	56
Fossil fuel-based energy production for raw material production	Ecotoxicity-water	23	30
	Global warming potential	28	21
	Human health non-cancer air	27	28

Major adverse environmental impacts in PO/TBA Process:

Acidification Potential: The acid rain potential of the PO/TBA process is primarily attributed to SO_x and NO_x emissions associated with the generation of coal-based electrical power for

compressing recycled gases and fossil-fuel based energy for the production of *i*-butane and propylene raw material. The low yield of TBHP in the oxidant synthesis step and the wasteful decomposition of TBHP during propylene epoxidation translate into higher *i*-butane feedstock requirement. Significant quantities of SO_x and NO_x are emitted during energy production and also during the transportation of crude oil and natural gas via ocean-going vessels powered by bunker fuel.

Ecotoxicity Water Potential: Partitioning of the metal (cadmium, copper, chromium, lead and mercury) and inorganic chemical emissions into the water phase during the generation of coal-based electrical power contribute to this impact category. Energy for raw material production (*i*-butane and propylene) amounts to 81% of the impact in this category.

Global Warming Potential: The potential greenhouse gas (GHG) emissions associated with the production of 200,000 tonnes of PO by the PO/TBA process is 1.52 billion kg CO₂ equivalent. The greenhouse gas (GHG) emissions associated with the coal-based electrical power generation for compressing recycled gases and fossil fuel-based energy for the production of raw material (*i*-butane, propylene) in this process contribute approximately 25% and 65%, respectively, of the overall environmental impact in this category.

Human Health Non-Cancer Air Potential: Heavy metal emissions (arsenic, cadmium, and lead), inorganic (barium) and organic emissions (polychlorinated biphenyls) contribute to this impact category. Generation of fossil fuel-based energy for the production of raw material (*i*-butane and propylene) accounts for 83% of the impact in this category.

Major adverse environmental impacts in CEBC and HPPO Processes:

Acidification Potential: The deployment of refrigeration (chilled water), a highly energy intensive utility to remove the heat of reaction produced during H₂O₂ and PO synthesis have the largest adverse environmental impact. The coal-based electrical power generation for refrigeration in the CEBC and HPPO process contributes approximately 78% and 86%, respectively, of the overall environmental impact in this category.

Ecotoxicity Water Potential: Generation of coal-based electrical power for refrigeration and fossil-fuel based energy for raw material production (propane a component of natural gas is cracked to form propylene) contributes to approximately 42% and 30%, respectively of the overall impact in the CEBC process whereas for the HPPO process these impacts are 55% and 23%, respectively.

Global Warming Potential: The carbon footprint associated with the production of 200,000 tonnes of PO by the CEBC and HPPO processes is approximately 1.12 billion kg CO₂ equivalent. The estimated savings in GHG emissions is primarily attributed to the reduced environmental impact of H₂O₂ production compared to TBHP production employed in the PO/TBA process. Hydrogen needed for the production of H₂O₂ is produced by the steam reforming of methane (70-90 % of natural gas) whereas *i*-butane is produced by the isomerization of *n*-butane (0-20% of natural gas). The low yield of TBHP requires the extraction of large quantities of natural gas (for butane) needed to produce sufficient quantity of TBHP. Generation of coal-based electrical power for refrigeration and fossil fuel-based energy for the production of raw material (hydrogen) contribute to 58% and 21% of the overall impact in this

category for the CEBC process compared to 42% (refrigeration) and 28% (raw material production) in the HPPO process.

Human Health Non-Cancer Air Potential: Metal emissions associated with the generation of coal-based energy for refrigeration and fossil fuel-based energy for propylene production contribute to approximately 56% and 28% of the overall impact in the category for the CEBC process. For, the HPPO process the environmental impact is 57% and 27%, respectively.

5.8 Conclusions

Aspen HYSYS[®] based plant scale simulations of the PO/TBA, HPPO and CEBC processes were utilized to perform comparative economic and environmental assessment. The capital costs for the HPPO and CEBC process are similar but lower than PO/TBA process by 18%. The manufacturing cost of PO by the PO/TBA process is 96 ¢/lb and yields a profit margin of 24.98 ¢/lb PO assuming a TBA market price of 41 ¢/lb. The similarities in operating conditions in both the HPPO and CEBC process results in similar production costs. PO production cost synthesized by the HPPO process is 106 ¢/lb and yields a profit margin of 14.4 ¢/lb based on the 2009 PO market price. For the CEBC process to be as profitable as the HPPO process the catalyst MTO has to be active for a minimum of 1 year [at a leaching rate of $1.8(10^{-2})$ lb/h]. However, the loss of revenue stream from the sale of TBA for MTBE production makes the economics of the CEBC process more favorable than the PO/TBA process [based on the assumption that the MTO catalyst is durable for 1 year and has a leaching rate $1.8(10^{-2})$ lb/h or less]. Further, the use of a mixed feed containing propylene and propane (without propane separation) will also make the CEBC process more competitive with HPPO process as well.

Environmental emissions predictable by the *gate-to-gate* analysis of the simulated PO/TBA process is of the same order of magnitude compared to those reported by LyondellBasell to USEPA for their Bayport facility, TX. The cumulative cradle-to-gate environmental impacts estimated by GaBi[®] for the PO/TBA, HPPO and CEBC processes are of the same order of magnitude in all the impact categories, with the predicted emissions being higher for PO/TBA process. The environmental impact of TBHP production is greater than H₂O₂ production. Coal based electrical power generation for compression and fossil fuel based energy for raw material production (*i*-butane, propylene) have the greatest adverse environmental impact in the PO/TBA process. In the case of CEBC and HPPO processes the greatest adverse environmental impact is the coal-based electrical power generation for the refrigeration of reactors (H₂O₂ and PO). A reduction of 26% in GHG emissions is observed for the production of PO by H₂O₂-based processes. The greenness of the CEBC process cannot be conclusively established at the present time as the savings lie within prediction uncertainty of this analysis. This analysis shows traces the environmental impacts for all the processes to sources outside the plant boundaries.

References

1. Kahlich, D.; Wiechern, U.; Lindner, J., Propylene Oxide. In *Ullmann's Encyclopedia of Industrial Chemistry*, 6th ed.; Hawkins, S.; Russey, W. E.; Pilkart-Muller, M., Eds. Wiley-VCH: New York, 2012; Vol. 30, p 20.
2. Lee, H. J.; Shi, T. P.; Busch, D. H.; Subramaniam, B., A greener, pressure intensified propylene epoxidation process with facile product separation. *Chemical Engineering Science* **2007**, 62, (24), 7282-7289.
3. Busch, D. H.; Subramaniam, B.; Lee, H. J.; Shi, T. P. Process for Selective Oxidation of Olefins to Epoxides. US 7649101 B2, 2010.
4. ICIS. <http://www.icis.com/chemicals/channel-info-chemicals-a-z/> (Accessed June 15th, 2010),
5. *Aspen HYSYS*, 7.1; Aspen Technologies: Calgary, Alberta, Canada, 2009.
6. Chilton, C. H.; Popper, H.; Norden, R. B., *Modern Cost Engineering: Methods and Data*. McGraw-Hill Publishing Company: New York, 1978; Vol. I, p 579.
7. Couper, J. R.; Penney, W. R.; Fair, J. R.; Walas, S. M., *Chemical Process Equipment: Selection and Design*. Second ed.; Butterworths: **Boston**, 1988.
8. Matley, J., *Modern Cost Engineering: Methods and Data* McGraw-Hill Publishing Company: New York, 1984; Vol. II, p 296.
9. Peters, M. S.; Timmerhaus, K. D., *Plant Design and Economics For Chemical Engineers*. Fourth ed.; McGraw Hill Inc.: New York, 1991; p 910.
10. U.S. Bureau of Labor Statistics. <http://www.bls.gov/cpi/> (Accessed June 10th, 2010),

11. U. S. Energy Information Administration-Electricity. http://www.eia.gov/energyexplained/index.cfm?page=electricity_in_the_united_states (Accessed October 24th, 2011),
12. U. S. Energy Information Administration-Natural Gas. (Accessed October 24th, 2011),
13. Engineering News Record. www.enr.com (Accessed Jun 12th, 2010),
14. John C. Jubin, J. Oxidation of Isobutane to Tertiary Butyl Hydroperoxide. US 5149885, 1992.
15. Preston, K. L.; Wu, C.-N. T.; Taylor, M. E.; Mueller, M. A. Staged Epoxidation of Propylene with Recycle. US 5349072, July 6th, 1994.
16. Wu, C.-N. T.; Taylor, M. E.; Mueller, M. A. Controlled Epoxidation of Propylene. 5410077, April 25th, 1995.
17. Thomas, K. A.; Preston, K. L. Reaction of Isobutane with Oxygen. US 5436375, July 25th, 1995.
18. Zabetakis, M. G., *Flammability Characteristics of combustible gases and vapor*. 1st ed.; U.S. Department of Interior, US Bureau of Mines: 1939.
19. Wang, Y. W.; Duh, Y. S.; Shu, C. M., Characterization of the Self-Reactive decomposition of tert-Butyl hydroperoxide in three different diluents. *Process Safety Progress* **2007**, 26, (4), 299-303.
20. Arai, M.; Kobayahi, M.; Tamura, M. *Explosion of Methanol Distillation Column of Detergent Manufacturing Plant*; Ichihara, Chiba, Japan, 1991; p 12.
21. Botia, D. C.; Riveros, D. C.; Ortiz, P.; Gil, I. D.; Sanchez, O. F., Vapor-Liquid Equilibrium in Extractive Distillation of the Acetone/Methanol System Using Water as

- Entrainer and Pressure Reduction. *Industrial & Engineering Chemistry Research* **2010**, 49, (13), 6176-6183.
22. Issacs, B. H. Preparation Of Soluble Molybdenum Catalysts for Epoxidation of Olefins. US 4590172, 1986.
 23. Stein, T. W.; Gilman, H.; Bobeck, R. L. Epoxidation Process. US 3849451, 1974.
 24. Vora, B. V.; Pujado, P. R. Process For Producing Propylene Oxide. US 5599955, 1997.
 25. Zhou, B.; Rueter, M.; Parasher, S. Supported Catalysts Having a Controlled Coordination Structure and Methods For Preparing Such Catalysts. US 7011807 B2, 2006.
 26. Haas, T.; Brasse, C.; Stochniol, G.; Glenneberg, J.; Woll, W. Aqueous Hydrogen Peroxide Solutions and Method of Making Same. US 7722847 B2, May 25th, 2010.
 27. Fischer, M.; Butz, T.; Massonne, K. Preparation of Hydrogen Peroxide From Hydrogen and Oxygen. US 6872377 B2, 2005.
 28. Fischer, M.; Kaibel, G.; Stammer, A.; Flick, K.; Quaiser, S.; Harder, W.; Massonne, K. Process for the Manufacture of Hydrogen Peroxide. US 6375920 B2, 2002.
 29. Teles, J. H.; Rehfinger, A.; Berg, A.; Rudolf, P.; Rieber, N.; Bassler, P. Method For Producing An Epoxide. US 7026493 B2, Feb 6th, 2006.
 30. Brocker, F. J.; Haake, M.; Kaibel, G.; Rohrbacher, G.; Schwab, E.; Stroezel, M. Isothermal Operations of Heterogeneously Catalyzed Three Phase Reactions. US 7576246 B1, July 31st, 2000, 2009.
 31. Pujado, P. R.; Hammerman, J. I. Integrated Process For The Production Of Propylene Oxide. US 5599956, 1997.

32. Personal communication with Dr. Yucel Onal. In Evonik Degussa GmbH, Marl, Germany, 2011.
33. Ghanta, M. Modeling of the phase behavior of light (C2 & C3) olefins in liquid phase epoxidation systems and experimental determination of gas/liquid mass transfer coefficient. University of Kansas, Lawrence, 2008.
34. Goor, G.; Glenneberg, J.; Jacobi, S., Hydrogen Peroxide. In *Ullmann's Encyclopedia Of Industrial Chemistry*, 6th Edition ed.; Hawkins, S.; Russey, W. E.; Pilkart-Muller, M., Eds. Wiley VCH: New York, 2007; Vol. 18, p 35.
35. BASF Catalysts-Metal Prices. <http://www.catalysts.basf.com/apps/eibprices/mp/DPCharts.aspx> (Accessed June 5th, 2010),
36. Tosh, E.; Mitterpleininger, J. K. M.; Rost, A. M. J.; Veljanovski, D.; Herrmann, W. A.; Kuhn, F. E., Methyltrioxorhenium revisited: improving the synthesis for a versatile catalyst. *Green Chemistry* **2007**, 9, (12), 1296-1298.
37. Vezzosi, S.; Ferre, A. G.; Crucianelli, M.; Crestini, C.; Saladino, R., A novel and efficient catalytic epoxidation of olefins with adducts derived from methyltrioxorhenium and chiral aliphatic amines. *Journal of Catalysis* **2008**, 257, (2), 262-269.
38. Bracco, L. L. B.; Juliarena, M. P.; Ruiz, G. T.; Feliz, M. R.; Ferraudi, G. J.; Wolcan, E., Resonance energy transfer in the solution phase photophysics of $-\text{Re}(\text{CO})(3)\text{L}^+$ pendants bonded to poly(4-vinylpyridine). *Journal of Physical Chemistry B* **2008**, 112, (37), 11506-11516.
39. CEPCI Chemical Engineering Plant Cost Index. *Chem. Eng.* 2010, p 76.

40. *GaBi*, 4.4; PE Solutions and Five Winds Corporation: United States, 2011.
41. Bare, J. C., Developing a Consistent Decision-Making Framework by Using the U.S. EPA's TRACI. *AIChE Journal* **2002**.
42. Bare, J. C.; Hofstetter, P.; Pennington, D. W.; Udo de Haes, H. A., Life Cycle Impact Assessment Workshop Summary: Midpoint versus Endpoints: The Sacrifices and Benefits *International Journal of Life Cycle Assessment* **2000**, 5, (6), 319-326.
43. Bare, J. C.; Norris, G. A.; Pennington, D. W.; McKone, T., TRACI: The Tool for the Reduction and Assessment of Chemical and Other Environmental Impacts. *Journal of Industrial Ecology* **2003**, 6, (3-4), 49-78.
44. Griesbaum, K.; Behr, A.; Biedenkap, D.; Voges, H.-W.; Garbe, D.; Paetz, C.; Collin, G.; Mayer, D.; Hoke, H., Hydrocarbons. In *Ullmann's Encyclopedia of Industrial Chemistry*, 6th ed.; Hawkins, S.; Russey, W. E.; Pilkart-Muller, M., Eds. Wiley-VCH: New York, 2012; Vol. 18, p 48.
45. Eisele, P.; Killpack, R., Propene. In *Propene*, 6th Edition ed.; Hawkins, S.; Russey, W. E.; Pilkart-Muller, M., Eds. Wiley-VCH: New York, 2012; Vol. 30, p 11.
46. Haussinger, P.; Lohmuller, R.; Watson, A. M., Hydrogen. In *Ullmann's Encyclopedia Of Industrial Chemistry*, 6th Edition ed.; Hawkins, S.; Russey, W. E.; Pilkart-Muller, M., Eds. Wiley VCH: New York, 2007; Vol. 18, p 162.
47. Muller, H., Sulfuric Acid and Sulfur Trioxide. In *Ullmann's Encyclopedia of Industrial Chemistry*, 6th Edition ed.; Hawkins, S.; Russey, W. E.; Pilkart-Muller, M., Eds. Wiley-VCH: 2000; Vol. 35, p 72.

48. Schrodter, K.; Bettermann, G.; Staffel, T.; Wahl, F.; Klein, T.; Hofmann, T., Phosphoric Acid and Phosphates. In *Ullmann's Encyclopedia Of Industrial Chemistry*, 6th Edition ed.; Hawkins, S.; Russey, W. E.; Pilkart-Muller, M., Eds. Wiley VCH: 2008; Vol. 26, p 46.
49. Barron, R. F., Cryogenic Technology. In *Ullmann's Encyclopedia of Industrial Chemistry*, 6th Edition ed.; Hawkins, S.; Russey, W. E.; Pilkart-Muller, M., Eds. Wiley-VCH: New York, 2000; Vol. 10, p 46.
50. Fiedler, E.; Grossman, G.; Kersebohm, D. B.; Weiss, G.; Witte, C., Methanol. In *Ullmann's Encyclopedia of Industrial Chemistry*, 6th Edition ed.; Hawkins, S.; Russey, W. E.; Pilkart-Muller, M., Eds. Wiley-VCH: New York, 2000; Vol. 23, p 14.
51. Shimizu, S.; Watanabe, N.; Kataoka, T.; Shoji, T.; Abe, N.; Morishita, S.; Ichimura, H., Pyridine and Pyridine Derivatives. In *Ullmann's Encyclopedia of Industrial Technology*, Hawkins, S.; Russey, W. E.; Pilkart-Muller, M., Eds. Wiley VCH: 2000; Vol. 30, p 34.
52. Dow and BASF receive Presidential Green Chemistry Challenge Award for HPPO Technology.
http://www.flexpack.org/INDUST/PRESS_RELEASES/2010/201007/Dow_and_BASF_receive_Presidential_Green_Chemistry_Challenge_Award.pdf (February 23rd),
53. New BASF and Dow HPPO Plant in Antwerp Completes Start-Up Phase.
<http://www.basf.com/group/pressrelease/P-09-154> (February 23rd),
54. Toxic Release Inventory-LyondellBasell Chemical Company Bayport Facility.
http://iaspub.epa.gov/triexplorer/release_fac_profile?TRI=77507RCCHM10801&year=2

010&trilib=TRIQ1&FLD=&FLD=RELLBY&FLD=TSFDSP&OFFDISPD=&OTHDISP
D=&ONDISPD=&OTHOFFD= (January 31st),

Chapter 6

Conclusions and Recommendations

6.1 Conclusions

Researchers at the Center for Environmentally Beneficial Catalysis (CEBC) had previously reported a novel ethylene epoxidation process that produces EO selectively (i.e., eliminating the formation of CO₂ as byproduct) in a methanol/water liquid phase containing dissolved H₂O₂ (oxidant) and methyltrioxorhenium (catalyst).¹ The reaction is performed in an *ethylene-expanded liquid phase* at pressures that also allows the substrate (ethylene) to be dissolved in substantial amounts. This dissertation has addressed several relevant issues related to the practical viability of the aforementioned CEBC-EO process concept including (a) fundamental engineering studies related to mass transfer, thermodynamics and intrinsic reaction kinetics; (b) economic analysis benchmarked against conventional silver-catalyzed EO process to identify catalyst and other performance metrics for practical viability of the CEBC-EO process; (c) cradle-to-gate environmental impact analysis to evaluate overall greenness; and (d) evaluation of heterogeneous tungsten-based epoxidation catalysts as cost-effective alternatives to Re-based catalysts. The results from these studies, summarized below, have not only contributed to advancing fundamental knowledge in the area of gas-expanded liquids but also to a clear understanding of the sustainability aspects (both economic as well as environmental) of the new process concept.

Fundamental Engineering Studies

The CEBC-EO process was characterized with respect to the underlying thermodynamics, mass transfer and intrinsic kinetics. Volumetric expansion studies revealed that the liquid reaction phase (methanol+ H₂O₂/H₂O) was expanded by up to 12% by compressing ethylene to 50 bars. Mass transfer studies confirmed the absence of external mass transfer limitations beyond an agitation speed of 1200 rpm. Intrinsic kinetic parameters estimated from fixed semi-batch reactor studies disclosed moderate activation energy (+57±2 kJ/mol).² The knowledge of these critical engineering data has enabled the pressure intensification of the CEBC-EO process. Under these optimized conditions, the productivity of the H₂O₂-based CEBC-EO process (1.61-4.97 g EO/h/g Re) is comparable to that of the O₂-based conventional process (0.7-4.4 g EO/h/g Ag).³

Economic Analysis

Comparative economic and environmental impact assessments were performed based on plant scale simulations (200,000 tonnes/yr plant capacity) of the CEBC-EO and conventional processes using Aspen HYSYS[®]. The capital costs for both the processes were estimated to be \$120 million. The EO production cost for the conventional process was calculated to be 71.6 ¢/lb, yielding a profit margin of 7.4 ¢/lb based on the 2009 EO market price of 79 ¢/lb EO. The estimated EO production cost for the CEBC-EO process was estimated to be 74.4 ¢/lb assuming a catalyst life of 1 year and leaching rate of 2.2 lb MTO/h, resulting in a profit of 4.6 ¢/lb EO. The process has the potential to yield a profit of 13.6 ¢/lb EO provided the catalyst is active for 1 year at a leaching rate of 0.11 lb MTO/h.

Environmental Assessment

Environmental emissions predicted by the *gate-to-gate* analysis of the simulated conventional process were larger but of the same order of magnitude compared to those reported by BASF Corporation for a similar process at their Geismar, LA facility rendering credibility to the analysis.⁴ Thus, only those differences that are greater than an order of magnitude can be considered significant.

The cumulative environmental impacts estimated by the cradle-to-gate LCA were of the same order of magnitude in most impact categories. Further, a major fraction of the adverse environmental impacts for both the processes stem mainly from sources outside the ethylene oxide plant. The generation of fossil fuel-based energy for ethylene production was the major hot spot in all the impact categories for the CEBC-EO process. For the conventional process, generation of fossil fuel-based energy for ethylene production and coal-based electrical power generation for compression of recycled gases were the major hot spots in all the impact categories. The burning of feedstock in the conventional process contributed only 4.4% to the total global warming potential of the conventional process. The cumulative emissions by the cradle-to-gate LCA for ethylene production from naphtha, natural gas and corn were estimated to be of the same order of magnitude. The predicted emissions were found to be similar for the production of H₂ and energy from fossil fuel sources.

Heterogeneous Tungsten-based Epoxidation Catalyst

Catalyst evaluation studies identified W-incorporated mesoporous silicas (KIT-6 and KIT-5) as promising cost-effective alternatives to Re-based catalysts for ethylene epoxidation. The W-based catalysts epoxidized ethylene with near complete EO selectivity (99+%, based on H₂O₂

consumed) at mild reaction conditions, similar to the homogeneous Re-based catalytic process. Further, the EO productivity [(0.3-3.16 g EO/h/g W)] was found to be of the same order of magnitude as displayed by the homogeneous Re-based catalyst (1.61-4.97 g EO/h/g Re) and the Ag-based catalyst (0.7-4.4 g EO/h/g Ag) used in the conventional O₂-based EO process.³ The highest EO productivity value in the abovementioned range was observed at low tungsten loadings (Si/W ratio = 100) where most of the tungsten is present in the catalytically active WO₄ (tungsten tetraoxide) form. Similar EO productivities were exhibited by fresh and recycled catalysts, suggesting long term durability potential of the W-incorporated catalysts. Furthermore, the tungsten source (sodium tungstate or tungstic acid) and support did not have any appreciable influence on the activity of the catalyst.

Economic and Environmental Assessment of CEBC-PO process

Because of the similarity of the CEBC-EO and CEBC-PO process concepts with the commercial HPPO process, economic analysis of the CEBC-PO process was performed and benchmarked against the PO/TBA and HPPO processes. The capital cost for the PO/TBA process was estimated to be \$116 million compared to \$95 million for CEBC-PO and HPPO processes. The PO production cost for the PO/TBA process is 96 ¢/lb and yields a profit margin of 24.9 ¢/lb PO assuming a TBA market price of 41 ¢/lb. The PO production cost for the HPPO process is 106 ¢/lb and yields a profit margin of 14.4 ¢/lb based on the 2009 PO market price. For the CEBC-PO process to be as profitable as the HPPO process, the MTO catalyst should be active for a minimum of 1 year at a leaching rate of $1.8(10^{-2})$ lb/h. The environmental impact for all the processes were of the same order of magnitude with the predicted emissions being higher

for PO/TBA process. Furthermore, the major impacts for all the processes are traced to sources outside the plant boundaries for raw material production and generation of process energy.

In summary, the results from this dissertation research have led to rational process intensification of the CEBC-EO process. Furthermore, the guidance provided by economic analysis prompted catalyst evaluation studies resulting in the identification of cost-effective W-incorporated mesoporous silicas as highly selective ethylene epoxidation catalysts, a major breakthrough. The EO productivity on these catalysts is comparable to those observed with Re- and Ag-catalysts. The many process similarities between the HPPO and CEBC-EO process minimize the risk associated with the commercialization of this new ethylene epoxidation technology.

7.2 Recommendations

The key findings in this dissertation point to the following recommendations for future research:

- The presence of methyl trioxorhenium in the highly active and stable diperoxo form necessitates the deployment of excess H_2O_2 (oxidant/catalyst of 10).^{5, 6} Safety considerations require that any unreacted H_2O_2 present in the reactor effluent stream must be decomposed prior to the recovery of the products by distillation. The oxidant/catalyst ratio in the Re-catalyzed epoxidation reaction is maintained at 143. The effect of oxidant/catalyst ratios and on EO yield and catalyst lifetime needs to be established. The economic analysis must be updated to quantify the impact of these cost savings.
- Immobilize Re onto a soluble polymer support and establish the activity of the synthesized catalyst for the epoxidation of ethylene.⁷⁻⁹ Demonstrate the durability of the catalyst by conducting continuous reactions in a CSTR fitted with a nano-filtration membrane and

establish the economic viability of the process. The successful demonstration provides an opportunity to extend this concept to other feedstocks such as propylene, butylene and to the epoxidation of olefins in streams containing mixed olefins and paraffin's (*e.g.*: mixed streams of ethane + ethylene and propane + propylene).

- Perform intrinsic kinetic studies for the epoxidation of ethylene using immobilized methyltrioxorhenium catalyst. Develop a reactor model for the rational design and scale-up of the membrane reactor.
- Measure the temporal EO yields for the tungsten catalyzed ethylene epoxidation by online sampling of the reaction mixture and independently establish quantitative EO productivity.
- Update the economic analysis for the CEBC-EO process with tungsten catalysts, and establish performance benchmarks for the economic viability of the proposed process.
- Investigate the oxygen transfer mechanism at the heterogenized active metal site and design catalysts that are highly active and selective toward the epoxidation of ethylene. Further establish the true heterogeneity of W-KIT-5 and W-KIT-6 catalysts and by conducting hot filtration tests and by analyzing the reaction mixture for W leaching by ICP.
- Incorporate the active metal species (tungsten and other metals such as cerium) in other silica-based mesoporous supports (amorphous and ordered) such as TUD-1, MCM-41, MCM-48 and SBA-15. Perform systematic studies to investigate the impact of catalyst loading and textural properties on the catalyst performance metrics. Establish the true heterogeneity of the synthesized catalysts.
- Perform continuous ethylene epoxidation runs using heterogeneous catalysts in a trickle bed reactor or a CSTR fitted with a nanofiltration membrane, and establish their performance (activity, selectivity and durability) over extended period of times. Extend this concept to

develop technologies for the epoxidation of olefins (propylene) and in streams containing mixed olefins and paraffins (as in refinery off-gases). The selective epoxidation of olefins in the mixture of olefin and paraffin lower feedstock costs resulting in higher profit margins. The deployment of highly active solid catalysts for ethylene epoxidation may introduce mass transfer limitations (gas-liquid, liquid-solid or pore resistances) which may limit EO yields. Systematic mass transfer studies must be performed to optimize reaction conditions to alleviate pore resistances. Intrinsic kinetic parameters for ethylene epoxidation using solid catalysts must be established and suitable reactor models developed for rational reactor design and scale-up.

References

1. Subramaniam, B.; Busch, D. H.; Lee, H. J.; Ghanta, M.; Shi, T.-P. Process for Selective Oxidation of Olefins to Epoxides. US 8080677 B2, 2011.
2. Ghanta, M.; Lee, H. J.; Busch, D. H.; Subramaniam, B., Highly Selective Homogeneous Ethylene Epoxidation in Gas (Ethylene)-Expanded Liquid: Transport and Kinetic Studies. *AIChE Journal (in press)* **2011**.
3. Buffum, J. E.; Kowaleski, R. M.; Gerdes, W. H. Ethylene Oxide Catalyst. US 5145824, 1992.
4. Toxic Release Inventory-BASF Corporation.
http://iaspub.epa.gov/triexplorer/release_fac_profile?TRI=70734BSFCRRIVER&year=2010&trilib=TRIQ1&FLD=&FLD=RELLBY&FLD=TSFDSP&OFFDISPD=&OTHDISP D=&ONDISPD=&OTHOFFD= (January 31st),
5. Espenson, J. H.; AbuOmar, M. M., Reactions catalyzed by methylrhodium trioxide. *Electron Transfer Reactions* **1997**, 253, 99-134.
6. Abu Omar, M. M.; Hansen, P. J.; Espenson, J. H., Deactivation of methylrhodium trioxide-peroxide catalysts by diverse and competing pathways. *Journal of the American Chemical Society* **1996**, 118, (21), 4966-4974.
7. Bracco, L. L. B.; Juliarena, M. P.; Ruiz, G. T.; Feliz, M. R.; Ferraudi, G. J.; Wolcan, E., Resonance energy transfer in the solution phase photophysics of $-\text{Re}(\text{CO})_3\text{L}^+$ pendants bonded to poly(4-vinylpyridine). *Journal of Physical Chemistry B* **2008**, 112, (37), 11506-11516.

8. Vezzosi, S.; Ferre, A. G.; Crucianelli, M.; Crestini, C.; Saladino, R., A novel and efficient catalytic epoxidation of olefins with adducts derived from methyltrioxorhenium and chiral aliphatic amines. *Journal of Catalysis* **2008**, 257, (2), 262-269.
9. Saladino, R.; Neri, V.; Peliccia, A. R.; Mincione, E., Selective epoxidation of monoterpenes with H₂O₂ and polymer-supported methylrhenium trioxide systems. *Tetrahedron* **2003**, 59, 7403-7408.

Appendix A-Volumetric Expansion of Liquid Phase by Propylene

In the CEBC-PO process, propylene is reacted with H_2O_2 in the presence of a catalyst. To improve, the solubility of propylene in methanol is employed as a co-solvent. The high solubility of propylene in the liquid phase results in the swelling of the liquid phase resulting in the formation of gas-expanded liquid (GXL's). Volumetric expansion studies were conducted to quantify the volumetric expansion of the liquid phase with increasing pressure at various temperatures using the experimental procedure described in Chapter 2.

A-1. Volumetric Expansion Studies

The volumetric expansion of the liquid phase containing either methanol alone or ternary mixtures (methanol + H_2O_2 + H_2O or *t*-butyl alcohol + H_2O_2 + H_2O) is shown in Figure A1-3. At a fixed temperature, the solubility of propylene in the liquid phase increases with increasing pressure (Figure A1). Propylene is a condensable gas and these gases have a unique property when pressurized to its critical pressure near the vicinity of their critical temperature, i.e. $T = (0.8-1.2) \cdot T_c$ K they liquefy significantly swelling the liquid phase. Propylene when pressurized to 12 bars in the temperature range of 20-40 °C liquefies and significantly expands the liquid phase. The maximum volumetric expansion ratios for propylene + methanol system at approximately 12 bars and at 20, 30 and 40 °C are 1.91, 1.53 and 1.34, respectively. This signifies a substantial increase in the liquid phase volume upon propylene addition. The corresponding mole fractions (x_E) of propylene in the liquid phase are 0.27, 0.185 and 0.12 respectively. These values are consistent with the reported VLE behavior of this binary system

and previously predicted values. Chapter 2-29 In comparison the propylene mole fraction in methanol phase at 20 °C and 1 bar is almost negligible.

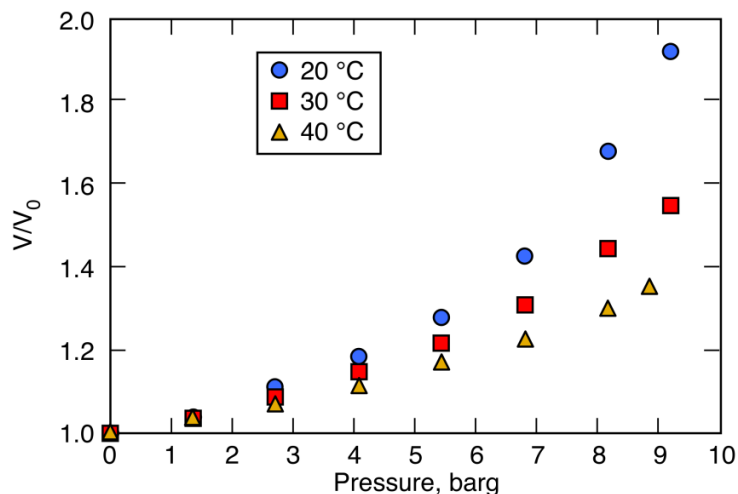


Figure A1: Volumetric expansion ratios of propylene+methanol binary system upon pressurization by propylene. The size of the plotted data point represents the experimental uncertainty

Though, the volumetric expansion ratios in the ternary mixture (containing methanol, H₂O₂ and H₂O) at similar conditions are comparatively lower compared to pure methanol (Figure A2). The expansion ratios at 20, 30 and 40 °C are 1.17, 1.12 and 1.08, respectively. The low volumetric expansion of propylene in the pressure range reflects the fact that propylene is less soluble in the presence of water. The corresponding mole fractions of propylene are 0.046, 0.032 and 0.026. In comparison, the propylene mole fraction in water at 20 °C and 10 bars is 9.48(10⁻⁴). Chapter 2-30

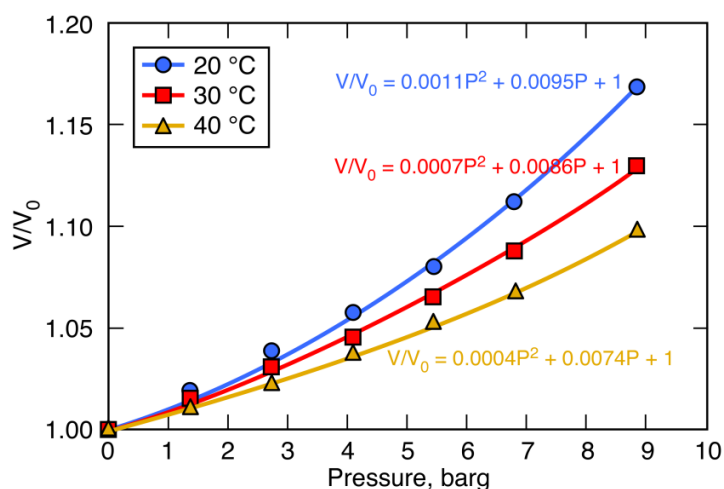


Figure A2: Volumetric expansion of propylene+methanol+50 wt% H₂O₂/H₂O system upon pressurization by propylene. Initial composition of liquid phase: 0.748 mol methanol + 0.134 mol H₂O₂ + 0.253 mol H₂O. Initial volume = 15 mL. The size of the plotted data point represents the experimental uncertainty.

Figure A3 shows the volumetric expansion of a mixture containing 0.21 mol *t*-butyl alcohol + 0.08 mol H₂O₂ + 0.11 mol H₂O by propylene. At a fixed pressure, the volumetric expansion of the liquid phase decreases with increasing temperature primarily attributed to lower gas solubility in the liquid phase. The maximum volumetric expansion at 10 bars and at 20, 30 and 40 °C are 1.49, 1.33 and 1.20, respectively. The corresponding mole fractions of propylene are 0.28, 0.20 and 0.143, respectively. The solubility of propylene in the ternary mixture of *t*-butyl alcohol + H₂O₂ + H₂O is greater than that of methanol + H₂O₂ + H₂O.

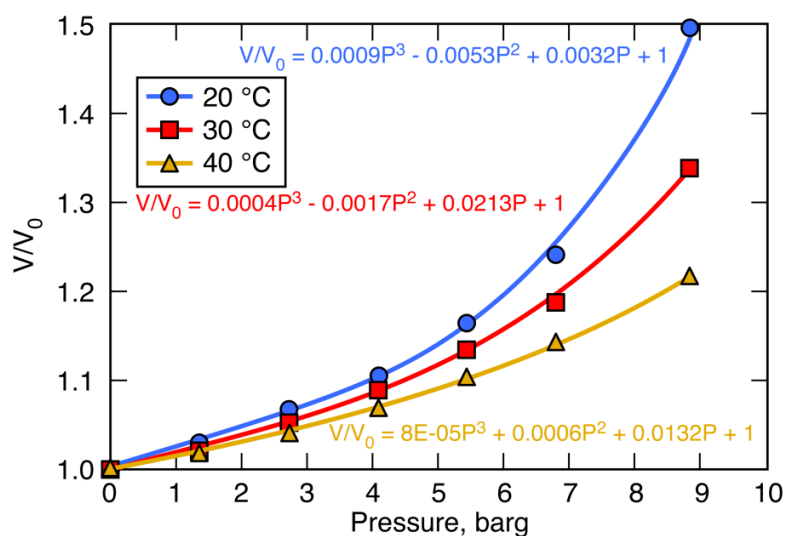


Figure A3: Volumetric expansion of propylene+*t*-butyl alcohol+50 wt% H₂O₂/H₂O system upon pressurization by propylene. Initial composition of liquid phase: 0.21 mol *t*-butyl alcohol + 0.08 mol H₂O₂+ 0.11 mol H₂O. Initial volume = 15 mL. The size of the plotted data point represents the experimental uncertainty.

Appendix B-Analytical Procedure

B-1. Sampling procedure, GC method and sample chromatogram

The reaction mixture is sampled at regular intervals of time through a Valco four-port liquid internal sample injector and the products were analyzed with an Agilent 6890N GC (see data in Chapter 2). The 1 μL internal sample passage is filled with the circulating liquid, and upon injection, the components are swept by the He carrier gas into a capillary column [CP-Wax 58(FFAP) CB, 25 m x 0.32 mm x 0.2 μm]. The GC oven temperature is maintained at 30 $^{\circ}\text{C}$ for the first 5 min following which the temperature is raised from 30 $^{\circ}\text{C}$ to 220 $^{\circ}\text{C}$ at a ramp rate of 5 $^{\circ}\text{C}/\text{min}$ and finally the oven is held at 220 $^{\circ}\text{C}$ for 5 min. The Agilent software is programmed to collect samples at regular intervals of time (1 h). In addition to the reactant (ethylene), solvent (methanol), internal standard (acetonitrile) only ethylene oxide (product) is detected by the GC, demonstrating the high selectivity of the CEBC EO process. The absence of CO_2 and O_2 in the gas and liquid phase is established by analyzing the gas phase by GC in our previous publication.^{Chapter2-2}

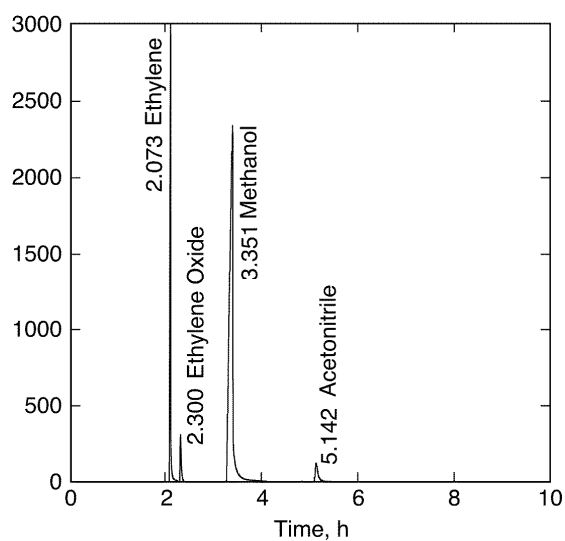


Figure B1: Sample gas chromatogram of ethylene epoxidation products

Calibration of the Gas Chromatogram

Figure B2 shows the calibration curve for the EO. The concentration ranges chosen for the calibration correspond to EO yield of 0 to 50%. As shown in the figure, a linear correlation is observed between the moles of EO/moles of acetonitrile vs. area of EO/area of acetonitrile.

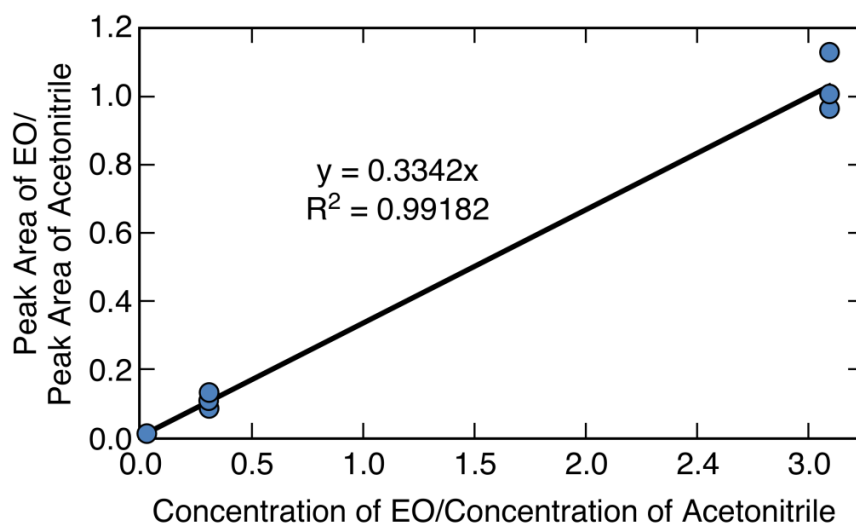


Figure B2: Calibration of the product concentrations for Agilent GC

B-2. H₂O₂ determination by ceric sulfate titration

Hydrogen peroxide content is determined by titrating the standardized ceric sulfate to a pale blue endpoint using ferroin indicator. ^{chapter 2-26, 27} Ferroin indicator (pink color) is added to the conical flask containing 150 mL of sulfuric acid (5% (v/v)) cooled to below 5 °C. This mixture is titrated with ceric sulfate till pale blue and, serves as the baseline. A predetermined amount of sample is added to this solution and swirled to mix. In the presence of excess H₂SO₄, H₂O₂ oxidizes the ferrous 1,10-phenanthroline to its corresponding ferric derivative giving the solution a pink tinge. This pink color solution is rapidly titrated with ceric sulfate solution. The presence of strong acids enables the reduction of ceric sulfate to cerous sulfate. The free electron needed for this reaction is produced by the oxidation of ferrous 1,10-phenanthroline indicator to its corresponding ferric ion.

B-3. H₂O content determination by Karl-Fischer titration

Volumetric Karl Fischer (KF) titration ^{Chapter 2-28, 29} was used to quantitatively establish the water produced in the epoxidation reaction. The KF titration involves the reaction of iodine with water in an alcoholic solution in the presence of sulfurous acid and base. The KF reaction is pH dependent and performs reliably only in the range of 5 and 7. A predetermined amount of the sample is dissolved in the methanol solvent. The water content of the sample is established by titrating the dissolved sample with hydranal composite 5, a mixture of iodine, sulfur dioxide and imidazole. The iodine in the titrant reacts with water. The end point of the titration is the detection of free iodine in the solution, recorded by the voltametric indicator. The mass of water formed in the reaction is determined by measuring the water concentration in the liquid phase before and after the reaction.

Appendix C-Economic Analysis

Table C1. The costs of various utilities in the Conventional and CEBC-EO processes are

Utility	Conventional Process (ϕ /lb EO)	CEBC-EO Process (ϕ /lb EO)
Steam	13.4	5.7
Electricity	14	2
Refrigeration	2.75	1.8
Cooling Water	0.52	0.55

Table C2. Capital costs of the various unit operations in the conventional process and the various cases of the CEBC-EO process

Unit Operations	Conventional Process, US\$	Base Case CEBC-EO Process, US\$		
		Base Case	Case 1	Case 2
Reactors	11,289,812	15,636,959	22,556,111	15,636,959
Columns	4,479,682	2,540,573	2,540,573	1,436,990
Vessels and Tanks	759,822	2,930,890	2,930,890	1,563,722
Heat Exchangers	15,349,351	44,000,000	44,000,000	6,321,600
Compressors	6,244,422	4,605,348	4,605,348	1,116,383
Pumps	1,980,892	1,208,980	1,208,980	1,054,024

C3. Estimation of the Reactor Cost

The reactor cost is dictated by the thickness of the reactor shell and the fabrication cost both which are dependent on the operating pressure and the material of construction (Chapter 3). The operating pressure in the conventional vapor-phase process is 30 bars and the thickness of the

reactor shell is 3.7 cm. The thickness of the reactor is the basis for estimating the weight of the steel needed for the construction of the reactor. The cost of the carbon steel is estimated using an empirical equation that gives the cost of the steel in 2001 dollars. The cost of the carbon steel for constructing the three reactors is \$3.7 million. The factor for estimating the fabrication cost of the unit operation operating at 30 bars and 200-260 °C is 1.4. The total cost of fabrication for the three reactors is \$5.1 million. Thus, the total reactor cost is based on 2001 dollars is \$8.8 million and \$11 million based on 2010 pricing. The cost of the reactors employed in the CEBC-EO process is estimated using similar methodology. Further, thickness of metal serves as the basis for estimating the cost of various distillation columns used in both the processes. ^{Chapter 3-13, 18-20}

Appendix D- Estimation of Allocation Factors for Environmental Assessment

D1. Estimation of the Allocation Factor for Environmental Impacts

ISO-14040 standards require proportional allocation of the environmental impacts whenever coproducts are formed. The proportional allocation method to estimate these environmental impacts is based on energy. The calorific values of all the products and co-products formed are listed in the Table A1.

Table D1: Calorific values of all the products and co-products

Component	Net Calorific Value (MJ/kg)
Hydrogen	141.80
Methane	55.50
Ethane	51.90
Propane	50.35
Butane	49.50
Gasoline	47.30
Kerosene	46.20
Diesel	44.80
Light Fuel Oil	44
Heavy Fuel Oil	42
Coke	29
Basic Oil	41
Waxes	7.53
Asphalt	15
LPG	46.1
Ethylene	50.50
Propylene	49.159
Butadiene	44.61
Ethanol	29.2
Dried Distillers Grain	29.7

Allocation factor for the production of ethylene from naphtha

Allocation factor for ethylene produced from naphtha is the ratio of the net calorific value of ethylene (desired product) to the sum of the net calorific value of all the products formed during the production of ethylene.

$$\text{Allocation factor for ethylene from naphtha} = 50.50/856.24 = 0.058$$

Allocation factor for the production of ethylene from natural gas

Along with ethane, other hydrocarbons such as methane, propane, n-butane are also present in natural gas. Further, hydrogen is formed as coproduct during the thermal cracking of ethane.

$$\text{Allocation factor for ethylene from natural gas} = 50.50/382.57 = 0.125$$

Allocation factor for the production of ethylene from corn

Dried distillers grain is the coproduct for ethylene production from corn.

$$\text{Allocation factor for ethylene from corn} = 50.50/79.7 = 0.633$$

Allocation factor for the production of hydrogen from methane

Methane, ethane, propane and n-butane are the coproducts of hydrogen production from methane.

$$\text{Allocation factor for hydrogen from methane} = 141.80/349.50 = 0.40$$

Allocation factor for the production of hydrogen at a refinery

The coproducts of hydrogen are ethane, propane, n-butane, gasoline, kerosene, diesel, wax, coke, asphalt, basic oil, light fuel oil and heavy fuel oil.

Allocation factor for hydrogen production at a refinery = $141.80/856.24 = 0.165$

Allocation factor for the production of hydrogen from ethylene cracker

The feedstock ethane is sourced from both crude oil and natural gas. Thus, the coproducts of this route are methane, ethane, propane, n-butane, gasoline, kerosene, diesel, light fuel oil, heavy fuel oil, coke, basic oil, waxes, asphalt, LPG, ethylene, and butadiene.

Allocation factor for hydrogen production at an ethylene cracker = $141.80/856.24 = 0.165$

Allocation factor for the production of hydrogen at a Chlor-Alkali plant

A proportional allocation based on the mass of products and coproducts is basis used for the estimation of allocation factor.

Allocation factor for hydrogen production at a Chlor-Alkali plant = $0.025/1.905 = 0.131$

Appendix E- Estimation of Transport Limitations

E1. Confirmation of the Absence of Interphase and Inter-particle Limitations

In the absence of EO yield vs. time data or H₂O₂ conversion vs. time data for ethylene epoxidation in the presence of heterogeneous catalyst, we assume the initial reaction rate for both homogeneous and heterogeneous catalysts are of the same order of magnitude.^{Chapter 5-14} This assumption is justified given that the overall productivity for the heterogeneous process (0.35-2.18 g EO/h/g W) is of the same order of magnitude as the MTO-based homogeneous catalytic process (1.61-4.97 g EO/h/g Re).

Liquid-Solid Mass Transfer Limitations

Volumetric *gas-liquid* mass transfer coefficient (k_{la}) = 0.0082 s⁻¹.

Catalyst amount = 700 mg

Volume of the reaction mixture = 31 ml

Catalyst concentration = (700/31) = 0.022 g/cm³

Moles of H₂O₂ consumed = 0.006 mol

Reaction rate $r_{EO} = 1.77(10^{-6}) \text{ mol} / \text{cm}^3 \text{ s}$

Diffusivity $D_{C_2H_4} = 22.7(10^{-5}) \text{ cm}^2/\text{s}$

Diameter of the particles (d_p) = 0.0075 cm

Density of particle (ρ_p) = 0.27 g/cm³

Liquid-solid interfacial area = $\left(\frac{6w}{\rho_p d_p} \right) = \left(\frac{6 * 0.022}{0.27 * 0.0075} \right) = 81 \text{ cm}^{-1}$

The liquid-solid mass-transfer coefficient (K_s) for particles with the diameter of 0.075 cm and agitated at speed of 23 rps is $4(10^{-2})$ obtained from correlation developed by Sano et al. *Chapter 5-*

15,16

$$\alpha_2 = \frac{R_{EO}}{K_s a_p C_A^*} = \frac{1.77(10^{-6})}{4(10^{-2}) * 81 * 6.83(10^{-3})} = 7.99(10^{-5}) < 0.1$$

The value of this factor suggests that the liquid-to-solid mass transfer resistance is practically absent.

Intraparticle Diffusion

The intraparticle diffusion resistances can be inferred from estimations of the Thiele parameter as follows. *Chapter 5-14*

Tortuosity of the particle (τ)^{1,2} = 3

Porosity of the catalyst particle (ε)^{1,2} = 0.5

$$\text{Effective diffusivity } (D_e) = \left(\frac{D\varepsilon}{\tau} \right) = \frac{5.96(10^{-6}) * 0.5}{3} = 9.93(10^{-7}) \text{ cm}^2 / \text{s}$$

$$\begin{aligned} \text{Concentration of ethylene at the catalyst surface} &= C_A^* - \frac{R_{C_2H_4}}{\left(\frac{1}{k_l a_b} + \frac{1}{k_s a_p} \right)^{-1}} \\ &= 6.83(10^{-3}) - \frac{1.77(10^{-6})}{\left(\frac{1}{0.0082} + \frac{1}{4(10^{-2})81.1} \right)^{-1}} \\ &= 6.82(10^{-3}) \end{aligned}$$

$$\phi_{\text{exp}} = \frac{d_p}{6} \left(\frac{\rho_p R_A}{D_e w A_s} \right)^{1/2} = \frac{0.0075}{6} \left(\frac{0.27 * 1.77(10^{-6})}{9.93(10^{-7}) * 0.022 * 6.83(10^{-3})} \right)^{1/2} = 0.07 < 0.2$$

As ϕ_{exp} is less than 0.2, it can be concluded that intraparticle diffusional gradients are insignificant. Hence the conversion studies on the heterogeneous W-KIT-5 and W-KIT-6 catalysts were performed under kinetic control.

E2. Sample calculation for the estimation of productivity

Composition of the reaction mixture:

Methanol (solvent) = 24 ml

50% H₂O₂/H₂O = 6 ml

Acetonitrile (internal standard) = 1 ml

Theoretical concentration of hydrogen peroxide = 6 ml * 0.5 * 1.21 (g/ml) = 3.63 g

Mass of the reaction mixture = 26.687 g

Reaction Pressure = 750 psig

Reaction Temperature = 35 °C

Reaction Time = 6 h

Catalyst

Catalyst Amount = 504.9 mg

Si/W ratio = 10

Tungsten Loading = 0.306 g/g of catalyst

Mass of active metal = 452 * 0.306 = 138.3 mg

Hydrogen Peroxide Concentration

Before Reaction

The concentration of H₂O₂ in the reaction obtained from ceric sulfate titration = 13.53%

Mass of H₂O₂ in the reaction mixture = (13.53/100) * 26.68 = 3.61 g

Moles of H_2O_2 in the reaction mixture = 0.106 moles

After Reaction

The concentration of H_2O_2 in the reaction obtained from ceric sulfate titration= 13.21%

Mass of H_2O_2 in the product mixture = $(13.21/100)*26.68*(0.86/0.89) = 3.40 \text{ g}$

Moles of H_2O_2 in the product mixture = 0.10 moles

Moles of H_2O_2 consumed = 0.006 moles

% $\text{H}_2\text{O}_2 = (0.006/0.106) = 3.42$

Moles of H_2O_2 consumed = Moles of ethylene oxide formed = 0.006 moles

Mass of ethylene oxide product = $0.006*44 = 0.264 \text{ g}$

Productivity = $(0.264*1000)/(6*138.3) = \mathbf{0.381 \text{ g EO/h/g W}}$